University of Southampton

Quaternary History of the Polar Front in the Scotia Sea, Antarctica: Foraminiferal and Stable Isotope Evidence.

Ruth Elisabeth Hale

A dissertation submitted for the degree of Doctor of Philosophy

School of Ocean and Earth Science

May 2001

UNIVERSITY OF SOUTHAMPTON

ABSTRACT

FACULTY OF SCIENCE

SCHOOL OF OCEAN AND EARTH SCIENCE

Doctor of Philosophy

QUATERNARY HISTORY OF THE POLAR FRONT IN THE SCOTIA SEA, ANTARCTICA: FORAMINIFERAL AND STABLE ISOTOPE EVIDENCE

by Ruth Elisabeth Hale

The Polar Front is contained within the Antarctic Circumpolar Current which flows through the Drake Passage into the Scotia Sea before continuing eastwards around Antarctica. The Polar Front separates Antarctic waters to the south and Subantarctic water to the north and is also a boundary across which there are major changes in biological productivity and carbonate production and preservation. In the Scotia Sea the position of the Polar Front axis is controlled by submarine topography and therefore this area provides a means of studying the movement of this feature over the last glacial cycle. Mixed biogenic-terrigenous deposition occurs and cores contain a high-resolution late Quaternary record of the last glacial-interglacial transition. Glacial sediments are diatom-bearing clayey silts and Holocene interglacial sediments are foraminifera-bearing diatom muds in the south, muddy diatom-bearing foraminifera oozes in the north. The aim of this study is to analyse the benthic foraminiferal assemblage and stable isotope record of the north Scotia Sea and Falkland Trough through the last glacial transition.

Benthic and planktonic foraminifera were picked and counted to identify changes in assemblages and productivity. Palaeoproductivity increased considerably from the glacial to the interglacial stage. A small number of benthic foraminifera species dominate the assemblage and the abundance of these species increases during the deglaciation. At this point warmer water planktonic species appear in the cores. Foraminiferal abundance continues to increase during the interglacial with a mid-Holocene productivity maximum identified in a number of the cores between approximately 7.5 and 4 ka. This period is represented by an increase in the benthic species *Eilohedra weddellensis* and *Epistominella exigua* and may indicate a time of phytodetritus deposition in the Scotia Sea. Following the warm period, abundance decreases to the present day and may represent a time of cooling. Carbon and oxygen stable isotope analysis was carried out on the species *Neogloboquadrina pachyderma* and *Oridorsalis tener* and the results show higher ^{18}O and lower ^{13}C during the glacial stage. The oxygen isotope data suggest that at the end of the last glacial stage warming may have started at approximately 14ka in the north and was marked by a meltwater event at around 11.3ka. This deglacial warming was interrupted by a return to cooler conditions centred at 10.5ka for a period of about 1,000 years before resuming warming. Changes in biogenic productivity are accompanied by water mass changes during this time. There was a decrease in the flux of North Atlantic Deep Water into the Scotia Sea during the glacial stage and the area was instead dominated by southern-source bottom water. Antarctic Bottom Water formation did not stop during the glacial stage but was much reduced. These deglacial events have also been recorded from other sectors of the Southern Ocean at a similar time. The carbon isotope data record a maximum in productivity during the mid-Holocene as identified by the increase in foraminifera abundance, which may correspond to a climatic optimum identified in a number of other studies from Antarctica and the Southern Ocean.

It can be suggested from this study that the distribution of both planktonic and benthic foraminiferal productivity is controlled by movements of the Polar Front in the Scotia Sea. It occupied a more northerly position during the last glacial stage, lying at least as far north as 52°S and possibly farther. This was also accompanied by a northward extension of the sea-ice edge and of carbonate under-saturated polar waters and hence productivity and preservation of carbonate were reduced at the core sites. At the end of the glacial stage when the climate began to warm the ice cover began to melt back, the Polar Front migrated south across the core sites, and productivity was enhanced. There is a general increase in productivity from south to north and an increase in dissolution from north to south in the Scotia Sea, and the Polar Front is a boundary across which there is a large change in these properties.

The cores all seem to respond similarly at surface and deep water levels to environmental change during the last glacial transition and therefore it can be concluded that they were influenced by the same water mass and any small scale variations may be due to localised organic carbon flux to the sea floor. Comparing this study to other research from the Southern Ocean and Antarctica, the events identified here during the transition from glacial to interglacial stage seem to be at least circumpolar in extent. The connection with the northern hemisphere and therefore the global synchroneity of this transition is still not certain and would benefit from more study, particularly to the south of the Polar Front. The last glacial transition therefore seems to be a time of significant change in foraminiferal distribution and productivity in the surface and deep waters of the Scotia Sea. However, the Holocene period also shows evidence of some fluctuation in climate, perhaps on a more localised scale in the Southern Ocean.

CONTENTS

AKNOWLEDGEMENTS

I would like to thank my supervisors Prof. John W. Murray and Dr. Carol J. Pudsey for their guidance, support and encouragement throughout. This PhD was funded by NERC as a CASE studentship with the British Antarctic Survey. I would also like to thank Carol for taking me on the JR48 BAS Antarctic Geoscience cruise, it was an experience of a lifetime! Thanks also to Dr. C. Bryant at the NERC Radiocarbon Facility in East Kilbride for help with the AMS radiocarbon analyses and to Steve Cooke at the Southampton Oceanography Centre who ran the stable isotope analyses for me. Thanks to Tracey Crawshaw for her diatom results and to Carol for supplying sedimentological and diatom data. The basic framework for the Scotia Sea maps were drawn at BAS.

Many people have helped to keep me sane over the last few years including a number of friends near and far afield, without whom life would have been a lot more difficult, they know who they are. Lastly, thanks to my family for their love and encouragement and for no doubt putting up with the worst of me, and for making me keep going.

LIST OF FIGURES

LIST OF TABLES

LIST OF ABBREVIATIONS

PF	Polar Front
PFZ	Polar Frontal Zone
SAZ	Subantarctic Zone
ACC	Antarctic Circumpolar Current
SAF	Subantarctic Front
STF	Subtropical Front
SACCF	Southern Antarctic Circumpolar Current Front
S bdy	Southern boundary of the ACC
AASW	Antarctic Surface Water
SASW	Subantarctic Surface Water
AAIW	Antarctic Intermediate Water
NADW	North Atlantic Deep Water
CDW	Circumpolar Deep Water
UCDW	Upper Circumpolar Deep Water
LCDW	Lower Circumpolar Deep Water
MCDW	Modified Circumpolar Deep Water
AABW	Antarctic Bottom Water
WSBW	Weddell Sea Bottom Water
WSDW	Weddell Sea Deep Water
ACR	Antarctic Cold Reversal
YD	Younger Dryas
MW	Meltwater event
LGM	Last Glacial Maximum
CCD	Carbonate Compensation Depth
IRD	Ice Rafted Debris

Chapter One

INTRODUCTION

1.1. Aim of the study

The British Antarctic Survey HIgh LATitude palaeoenvironments (HILATS) project (1995-2000) includes investigation of the response of deep ocean sediments to Quaternary glacial-interglacial cycles. Work is at present focused on the Scotia Sea and Falkland Trough, influenced by the Antarctic Circumpolar Current (ACC) during the last 30-40 Ma. Sediments deposited below the ACC contain a record of changing biogenic productivity, water chemistry, movement of water masses and oceanic fronts, terrigenous sediment sources, as well as the strength of current flow.

Microfaunal and stable isotope data have been collected from the Scotia Sea (Fig.1.1), Antarctica in order to study the palaeoceanography of the region through the last glacial-interglacial cycle (isotope stages 2-1). A number of cores from north and south of the Polar Front (PF) have been collected by the British Antarctic Survey (BAS) and the results from seven of these cores will be presented in this study.

The principal aims of the study are to identify the benthic foraminiferal assemblages present downcore and relate these to specific oceanographic conditions within the Scotia Sea, including any movements of the PF within the Late Quaternary period. Results from stable isotope studies using planktonic foraminifera will also be used to interpret the surface

palaeoceanographic record. Benthic stable isotopes will be used to examine changes in the deep-water masses and circulation of the Scotia Sea. Diatoms will also be studied in two cores, one from north of the PF and the other from the south, and these data will be used in the study of the timing of the deglaciation within the Scotia Sea. AMS Radiocarbon dating will be carried out on samples from four of the cores in this study which should then provide a stratigraphic framework, allowing the cores to be compared to other studies.

1.2. The role of the Southern Ocean in global climate change

The palaeoclimatic and palaeoceanographic records of the Southern Ocean around Antarctica are basic components for understanding the important role this continent plays in the world climate system. However despite increased interest in this subject over recent years, our knowledge of Antarctica's role in the global system still suffers from inconsistency and a lack of correlatable data.

The Antarctic continent is fundamental in driving the global atmospheric regime due to its strong negative radiation budget (Drewry *et al.*, 1993). The Southern Ocean plays two important roles in world climate, firstly the massive flow of water transported by the Antarctic Circumpolar Current provides the only deep-water linkage between the Atlantic, Pacific and Indian Oceans, allowing the efficient transport of heat, salt, nutrients and freshwater around the globe (Nowlin and Klinck, 1986). The southern Indian and Pacific Oceans export heat southwards whereas the South Atlantic carries heat northwards (Macdonald and Wunsch, 1996), with the Southern Ocean providing a link. It also plays an influential, but poorly understood role as a major sink for atmospheric carbon dioxide (Nowlin and Klink, 1986; Drewry *et al.*, 1993; Whitworth *et al.*, 1998). During the Quaternary period the climate of our planet has been subject to a succession of cold periods in which large parts of the northern hemisphere were covered in ice. The majority of scientists believe that these ice ages were driven by variations in the distribution of insolation (Hays *et al.*, 1976; Imbrie *et al.*, 1984), but insolation alone cannot explain the amplitude and hemispheric synchroneity of the temperature changes (Short *et al.*, 1991). Other feedback mechanisms must therefore play a role, and evidence from ice-core studies has shown that at

least part of the cooling was probably due to lower atmospheric CO_2 contents. The oceans are the largest active carbon reservoir and a key component as a sink and a transfer mechanism for the motion of carbon through the world system, and therefore the origin of the glacial CO_2 decrease must lie in the ocean.

Secondly, the Southern Ocean is the major source of both intermediate and deep waters which ventilate the World Ocean. The formation and sinking of these water masses results in a significant exchange of heat, freshwater and gases such as CO_2 between low and high latitudes and is therefore an important component of the Earth's ocean-climate system. Water from the Southern Ocean is largely responsible for keeping the rest of the deep sea cold, and 55-60% of the oceanic volume is cooled around Antarctica before being transported north (Gordon, 1988). It is this cold, dense bottom water formed in the seas around Antarctica, which is largely responsible for driving the global thermohaline circulation system, and this activity is believed to be the cause of fluctuations of Quaternary climate (Broecker *et al.*, 1985, 1990).

An interesting recent discovery in palaeoclimate research is that abrupt climate changes have occurred repeatedly for the past several hundred thousand years or more, and therefore our stable climate of the last 10,000 years is more of an anomaly than normal. Current ideas link these abrupt changes in climate to reorganisation of the global patterns of oceanic and atmospheric circulation. If abrupt climate changes involve a reorganisation of circulation patterns in the ocean and atmosphere, it is important to study records from the Southern Ocean, both to understand changes in the process of deep-water formation that occur there, and to describe more fully the climate patterns that are transmitted globally by thermohaline circulation via the Antarctic Circumpolar Current (ACC) (Anderson, 1998a).

1.3. The Study Region

The Southern Ocean can be defined as the region to the south of the Subtropical Convergence or Subtropical Front (STF) and can be divided into two zones: the Subantarctic Zone, lying between the STF and the Polar Front (PF), and the Antarctic Zone to the south of the PF (Fig.2.2). Within the Atlantic sector of the Southern Ocean, the STF lies at approximately 40°S and the PF at about 50°S (Anderson *et al.*, 1998b).

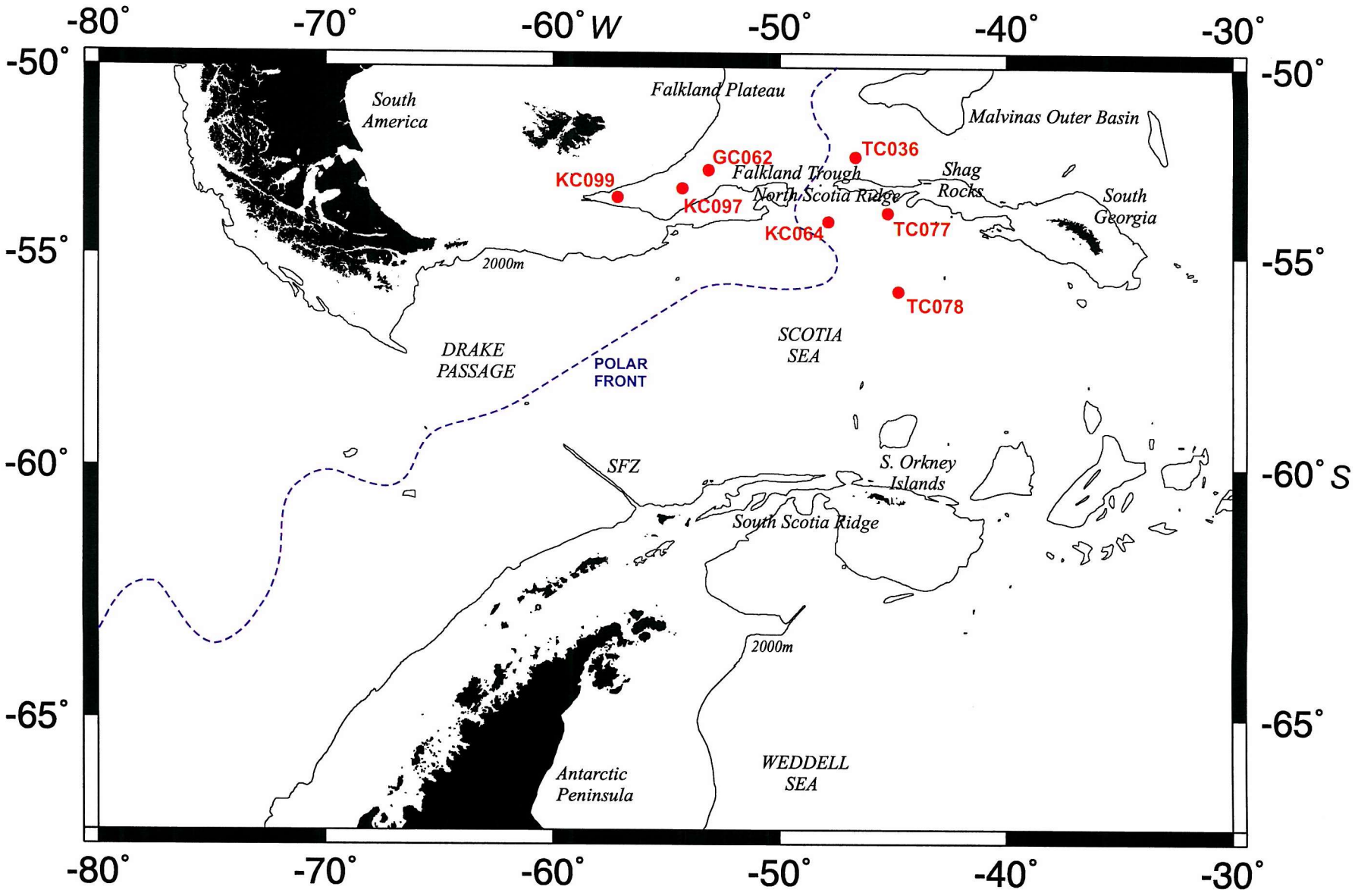

Figure 1.1. Map of the Scotia Sea showing core locations and position of Polar Front (SFZ = Shackleton Fracture Zone).

The Scotia Sea extends from the southernmost tip of South America at 56°S 65°W to the Antarctic Peninsula and lies within the Antarctic zone of the South Atlantic. It is bounded on three sides by the North Scotia Ridge at 54°S, the South Scotia Ridge at 60°S and to the east by the South Sandwich Island Arc at 27°W (Fig.1.1). Both the North and South Scotia Ridges are discontinuous, reaching sea level only at Shag Rocks, South Georgia and the South Orkney Islands but there are deep gaps within the ridges that reach depths of approximately 3000m. To the west is the narrow Drake Passage that connects the Scotia Basin to the Pacific Ocean. Generally depths within the Scotia Sea Basin reach an average of 3000-4500m (Tectonic Map, 1985).

The Falkland Trough consists of an east-west bathymetric deep extending 1300km from the South American continental margin to the Malvinas Outer Basin in the western South Atlantic. It is bordered to the north by the Falkland Plateau and to the south by the North Scotia Ridge. The topographic relief of the North Scotia Ridge strongly influences the flow of Circumpolar Deep Water across the western Falkland Trough. Shallower components of the ACC flow directly across the North Scotia Ridge and Falkland Trough, with increased flow along the Antarctic Polar Front (PF). It is thought that the ACC flows directly across the western Falkland Trough as the Falkland (Malvinas) Current, and then continues northward into the western Argentine Basin (Peterson and Whitworth, 1989; Piola and Gordon, 1989; Peterson, 1992).

1.4. Tectonic development / Isolation of Antarctica

The Scotia Sea is an area of complex tectonic development. Its present configuration has evolved since about 40Ma, with the breakup of Gondwana and the resulting movement of South America relative to Antarctica. This led to the opening of Drake Passage, which formed a deep water sea-way between South America and the Antarctic Peninsula (Barker *et al.*, 1991).

The earliest identified marine magnetic anomalies in the western Scotia Sea are dated at 28.7Ma (Mid Oligocene) (Barker and Burrell, 1977; LaBrecque and Rabinowitz, 1977), and therefore this could suggest that coherent sea-floor spreading in Drake Passage began at about 29Ma (Barker and Burrell, 1977). Some ocean floor had already formed by 29Ma, probably during initial disruption of the continuous continental connection between South America and

west Antarctica. Fragments of that original connection, such as South Georgia, Shag Rocks and the South Orkney blocks, now make up the north and south Scotia Ridge (Fig.1). However a complete barrier was still intact at the western end of Drake Passage in the form of two submarine ridges. These were shallow continental fragments that subsided slowly. Therefore although water at continental shelf depths could have passed between the Pacific and Atlantic Oceans across the Shackleton Fracture Zone as early as 28-29Ma, a deep gap was not in existence until the ridges cleared, estimated at about 23.5 ± 2.5 Ma (Oligocene/Miocene boundary) (Barker and Burrell, 1977). At this point the onset of the Antarctic Circumpolar Current occurred and is broadly confirmed by the widespread introduction of a siliceous biofacies in Southern Ocean sediments of early Miocene age. This facies today dominates sedimentation between the Polar Front and the Antarctic Divergence (Fig.2.4) (Barker and Burrell, 1982). The opening of the last gateways separating Antarctica from the other continental blocks resulted in the isolation of Antarctica in the south polar region for the remainder of the Cenozoic (Lawver *et al.*, 1992). This makes the Southern Ocean unique among the world's oceans in having a continuous band of water flowing around the Antarctic Continent with circulation almost unlimited by landmasses.

The Scotia Sea basin itself is the result of a series of back-arc and oceanic spreading episodes on the boundary between the South American Plate and the Antarctic Plate (Barker and Hill, 1981), and the relative eastward migration of the evolving South Sandwich arc and trench (Barker *et al.*, 1991).

Chapter Two

OCEANOGRAPHIC SETTING

2.1. The Antarctic Circumpolar Current (ACC)

The Antarctic Circumpolar Current or West Wind Drift is the only zonal current encircling the globe, constricted only at Drake Passage (Fig.2.2). The axis of the ACC is constrained in the Scotia Sea as it flows out of the Drake Passage, and hence this area is useful in the study of the palaeoflow of the ACC (Pudsey and Howe, 1998). The ACC flows east around Antarctica between 40° and 65°S, extending from the surface to about 4000m and contributes significant amounts of circumpolar water to all deep ocean basins (Corliss, 1983). The ACC is the world's strongest oceanic current system with a transport of 127 ±24 x $10^6 m^3 s^{-1}$ (Fandry and Pillsbury, 1979). The transport of the ACC through Drake Passage and into the Scotia Sea has received much attention after the initiation of the International Southern Ocean Studies (ISOS) program in the early 1970s. Nowlin and Klinck (1986) reviewed the observational and theoretical progress from the first 10 years of the study and reported a mean transport of 134 Sv through Drake Passage (see also Whitworth and Peterson, 1985). In a model study of the same transport the predicted value is 96 Sv which shows reasonable agreement with that cited by Nowlin and Klinck (1986) (Johnson and Bryden, 1989). More

recent studies have estimated the transport through Drake Passage to be closer to 161 Sv (K. Heywood, ALBATROSS cruise; www.mth.uea.ac.uk/ocean/ALBATROSS) or 140 ±6 Sv throughout the whole water column (Ganachaud and Wunsch, 2000). On leaving the confines of Drake Passage and entering the Scotia Sea, the ACC is deflected north and west by the submerged ridge of the Scotia Arc, before it turns east again to flow around South Georgia and across the Atlantic sector of the Southern Ocean (Deacon, 1933, 1937; Gordon and Goldberg, 1970). The Scotia Sea is dominated by the eastward or north-eastward flow of the ACC and the main flow path is parallel to the PF and the SAF (Pudsey and Howe, 1998) (Fig.2.1). Although the ACC is primarily a wind-driven current, which is forced at the surface but with flow extending to the seabed, oceanographic measurements provide adequate evidence for significant ACC bottom flow (Howe *et al.*, 1997). Flow speed decreases with depth and near the seabed it is strongly modified by local topography (Gordon *et al.*, 1978). Near surface velocities of 20-60cms^{-1} were measured between Drake Passage and 0°W using current meters and drift buoys (Nowlin and Clifford, 1982; Hofmann, 1985; Grose *et al.*, 1995). There are few near bottom measurements of deep flow except in Drake Passage where Bryden and Pillsbury (1977) and Whitworth *et al.* (1982) recorded unsteady flow with speeds up to 10cm/s at a depth of 2700m.

The northern extent of the ACC is marked by the Subantarctic Front (SAF) and the southern ACC boundary marks the change between the ACC and subpolar circulation (East Wind Drift) to the south. Flow within the ACC is therefore concentrated at three fronts - the Subantarctic Front, the Polar Front and to a lesser extent at the Southern ACC Front (Fig.2.1), and all have been described in detail in the literature (Deacon, 1933, 1937, 1982, 1984; Gordon, 1967; Gordon *et al.*, 1977a,b; Nowlin *et al.*, 1977; Nowlin and Clifford, 1982; Whitworth and Nowlin, 1987; Orsi *et al.*, 1995). The fronts are permanent circumpolar bands of large horizontal density gradients, superimposed on the southward rise of isopycnals. All three ACC fronts appear as maxima in geostrophic volume transport relative to a deep common level (Orsi *et al.*, 1995). Flow within the ACC is concentrated in narrow jets coinciding with the principal fronts, which are interspersed with broader zones of reduced or even reversed flow (Smith *et al.*, 2000) creating large shear within the water column (Daly *et al.*, 2001). From drift buoy data, Hofmann (1985) calculated the mean current flow within the PF and SAF was 40cms^{-1} compared to mean speeds in non-front regions of 23-35cms^{-1}.

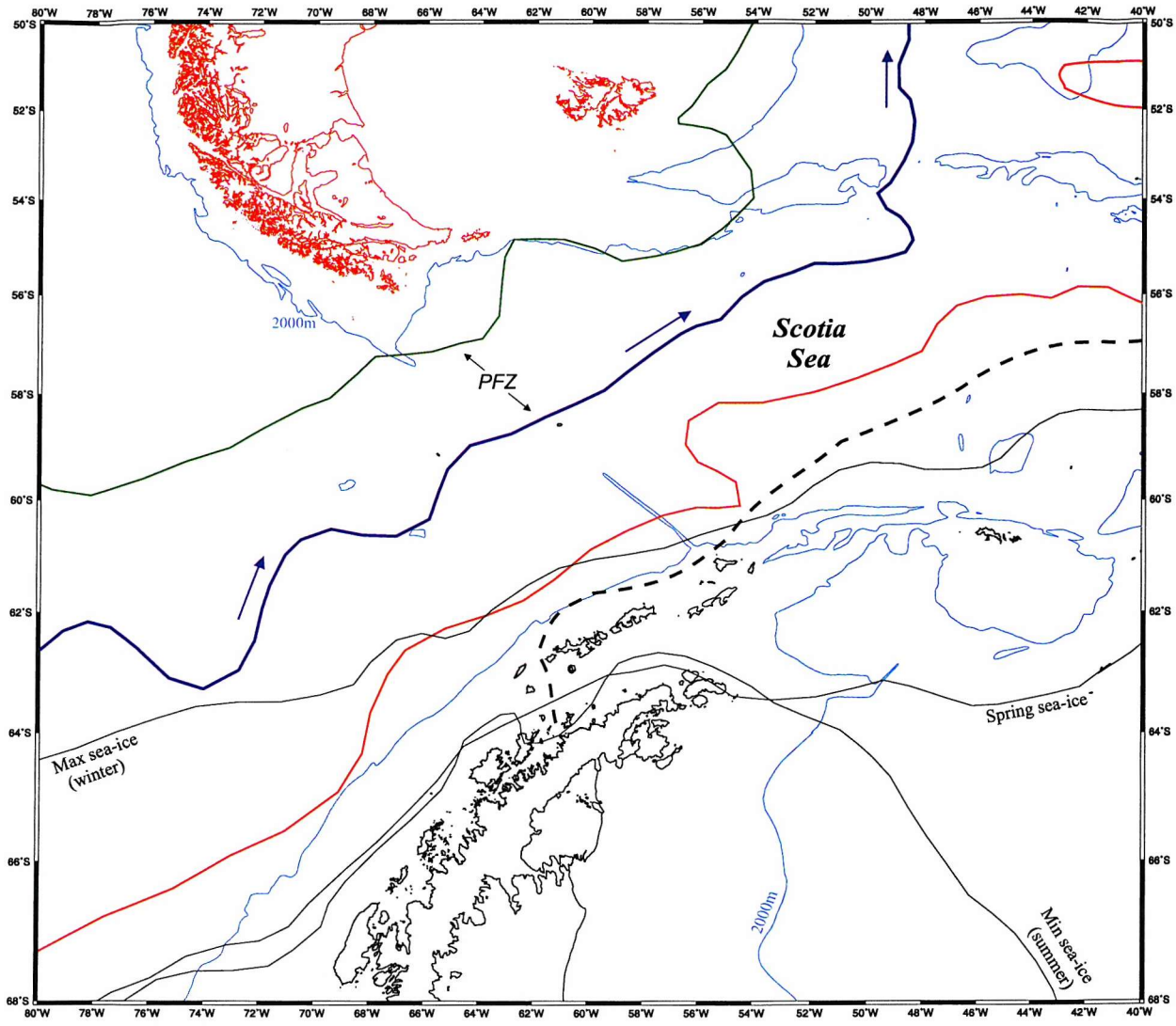

Figure 2.1. Position of the Antarctic Circumpolar Current (ACC) and its associated fronts in the Scotia Sea.

The positions of the fronts are mainly determined by topographic (e.g. mid-ocean ridge system) steering of the ACC as a whole (Gordon *et al.*, 1978) in combination with the global spatial pattern of the wind fields, in particular the distribution of the curl of the wind stress (Nowlin and Klinck, 1986).

A major study of the hydrography and currents of the Atlantic sector of the Southern Ocean was undertaken during the UK WOCE A23 cruise during the austral autumn of 1995 (www.mth.uea.ac.uk/ocean/a23/welcome.html). The section roughly lies along 35°W, although the southern end was moved east due to heavy sea-ice cover. Relative to major oceanographic features, A23 sampled the water masses and ocean currents of the Weddell Gyre, the ACC and the southern half of the South Atlantic Subtropical Gyre.

2.1.1. The Antarctic Polar Front (PF)

The Polar Front or Antarctic Convergence is an important oceanic boundary that separates cold, nutrient-rich Antarctic Surface Water (AASW) to the south from warmer, less nutrient-rich Subantarctic Surface Water (SASW) to the north. It is at the PF that AASW is overridden by the slightly less dense SASW (Gordon, 1971) (Fig.2.4). North of the PF surface waters have a winter temperature warmer than 2.0°C, whereas to the south, they are below 1.0°C and have a lower salinity than waters to the north of the PF (Orsi *et al.*, 1995). The mean temperature change across the PF has been estimated by Moore *et al.* (1999) as 1.44°C across an average width for the PF of 43km (see also Gille, 1994).

The PF passes through the centre of Drake Passage and turns north at 50°W to pass through Shag Rocks Passage in the North Scotia Ridge (Pudsey and Howe, 1998) (Fig.1.1). This is the only gap in the North Scotia Ridge with depths greater than 2000m. The mean path of the PF through the Scotia Sea was determined by Moore *et al.* (1997) using satellite SST data over a two year period (1987-88). The estimated position of 58.7°S along 64°W agrees with the position of the subsurface expression measured during the International Southern Ocean Studies (ISOS) Drake 79 experiment, where it ranged between about 58.5° and 59.5°S (Hoffman and Whitworth, 1985). The s-shaped bend of the PF in the Scotia Sea seems likely to be due to the northern arm of the Scotia Ridge (Deacon, 1982). The PF is intensified (increased width and temperature change across it) at major bathymetric features such as Drake Passage, but the surface expression weakens over deep ocean basin areas (Moore *et al.*, 1999).

The surface expression of the PF is marked by a strong Sea Surface Temperature (SST) gradient (Deacon, 1933, 1937; Mackintosh, 1946) and by a steepening of the meridional gradients of temperature, silicate and other nutrients, by transitions in phytoplankton and zooplankton, and by a noticeable difference in climate. There is much eddying and mixing of cold and warm water (Gordon *et al.*, 1977; Georgi, 1978; Joyce *et al.*, 1978), but the sustained presence of a weak temperature minimum below the warmer water north of the front is a clear indication of continued sinking (Deacon, 1982). It is the surface expression of the front which is known to have moved latitudinally in response to climate change (Hays *et al.*, 1976; Williams, 1976; Morley and Hays, 1979; Dow, 1978). The subsurface expression of the PF is located where Antarctic Surface Water descends rapidly, such as the point where the minimum potential temperature layer sinks below 200m depth (Deacon, 1933, 1937, 1982; Orsi *et al.*, 1995), or where subsurface salinities at approximately 200m reach minimal values (34.0-34.1 PSU) (Gordon *et al.*, 1978; Taylor *et al.*, 1978). The mean paths of the surface and subsurface expressions of the PF are closely coupled over much of the Southern Ocean, and where they do split the surface expression usually lies to the south of the subsurface expression (Moore *et al.*, 1999). The PF is thought to extend to the ocean floor (Gordon, 1967) as indicated by a nearly circumpolar zone of current ripples, manganese nodules and scour zones corresponding to the PF (Goodell, 1973). This is also supported by hydrographic data which indicate that the all of the ACC fronts are perceptible throughout the water column (Veth *et al.*, 1997).

Hydrographically the PF is the northern boundary to cold near-surface water formed by winter cooling. The northern extent of the 2.0°C isotherm in the AASW near 200m water depth is widely used as an indicator for the location of the PF, but it is probably not a distinct line (Botnikov, 1963; Peterson and Stramma, 1991). The PF is also thought to be the northern termination of the temperature minimum layer of the AASW (Gordon, 1967). Other indicators of the position of the PF in the Scotia Sea are given in Table 2.1. The PF shows highest variability in the northern Scotia Sea with considerable meandering and ring formation (Moore *et al.*, 1997) which was also reported by Gordon *et al.* (1977). In fact the Polar Frontal jet crosses the Mid-Atlantic Ridge almost perpendicular, therefore there is no topographic steering and consequently instability and meandering are more likely (Veth *et al.*, 1997). The wide variation in the position of the PF determined from repeated transects has long been known (Mackintosh, 1946). The maximum recorded displacement of the PF

being 70km to the north and 120km to the south of its mean position in the Drake Passage (Whitworth, 1980). The PF divides into two parts at 56°S, 140°W over the USARP Fracture Zone. The southern branch, the secondary polar front, extends eastward to at least 108°W where it then weakens (Gordon, 1967).

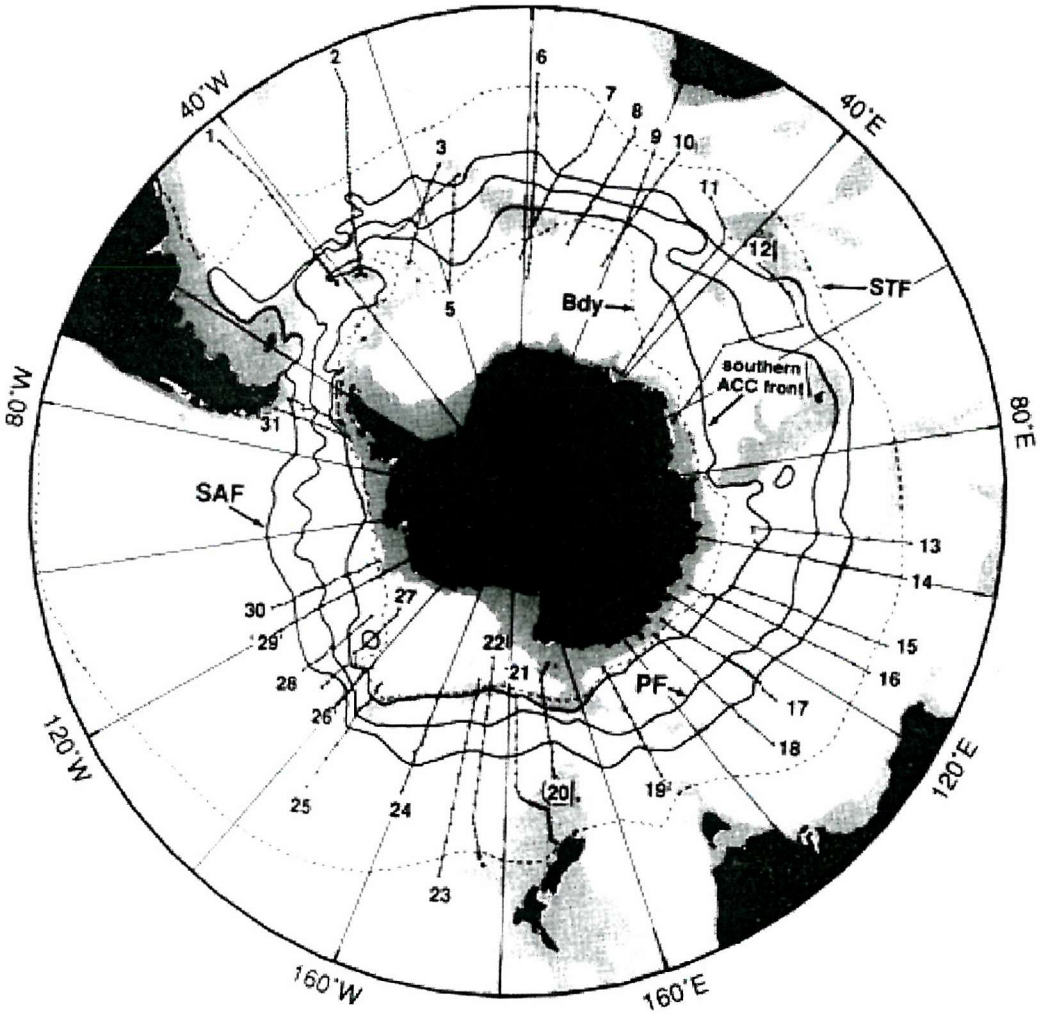

Figure 2.2. Circumpolar distributions of the Subantarctic Front (SAF), Polar Front (PF) and the southern ACC front; the Subtropical Front (STF) and southern boundary of the ACC (Bdy) are shown as dashed lines. The numbered lines refer to vertical sections (see Table 4 in Orsi et al., 1995) on which transports and property distributions were examined, depths less than 3000m are shaded (from Orsi et al., 1995).

2.1.2. The Polar Frontal Zone (PFZ)

The PF forms the southern boundary of the Polar Frontal Zone but is probably not a distinct line, rather an eddy-populated region of transition between Antarctic and Subantarctic surface waters (Peterson and Stramma, 1991). The PFZ is bound to the north by the Subantarctic Front (SAF) which is more well defined than the PF to the south (Whitworth, 1980) (Fig.2.1). In water temperature the frontal zone is identified in two ways: (1) by a sharp north-south surface gradient and (2) by a sudden increase in the north slope of the Tmin layer from depths of between 200-300m to depths of 500-600m, where it mixes with the warmer south-flowing water. A number of records show a steplike pattern of the surface temperature across the PFZ, making it difficult to determine which of the steps is the most likely frontal position (Gordon, 1967). The PFZ, like other frontal systems is a geographically meandering feature (Ikeda *et al.*, 1989). Mackintosh (1946) wrote about the PFZ, "At the surface the junction of Antarctic and Sub-Antarctic water seldom lies in a straight line, probably because it is an unstable boundary. It forms twists and loops that may extend as much as 100 miles north or south, and it possibly even forms isolated rings." The PFZ can vary in width by 2-4° latitude and is entirely contained within the eastward flowing Antarctic Circumpolar Current (ACC) (Gordon, 1967). In the eastern part of the South Atlantic the PFZ is quite broad, stretching latitudinally between about 45°S and 53°S, whereas in the western part it is much narrower extending roughly between 49°S and 51°S (Lutjeharms, 1985). See Figure 2.3 for temperature, salinity and oxygen profiles within the PFZ.

2.1.3. The Subantarctic Front (SAF)

The Subantarctic Front separates Subtropical Surface Water (STSW) from Subantarctic Surface Water (SASW) and runs through the north side of Drake Passage. On leaving Drake Passage the SAF turns abruptly northward, passing just south-east of the Falkland Islands and forms the Falkland Current (Fig.2.1). Following the work of Whitworth and Nowlin (1987) the position of the SAF is indicated by the rapid northward sinking of the salinity minimum associated with the Antarctic Intermediate Water (AAIW), from near the surface in the PFZ ($S<34$ PSU) to depths greater than 400m in the Subantarctic zone ($S<34.30$ PSU). It is marked by a zone of closely spaced, nearly vertical isotherms (Sievers and Emery, 1978; Lutjeharms, 1985) (see Table 2.1).

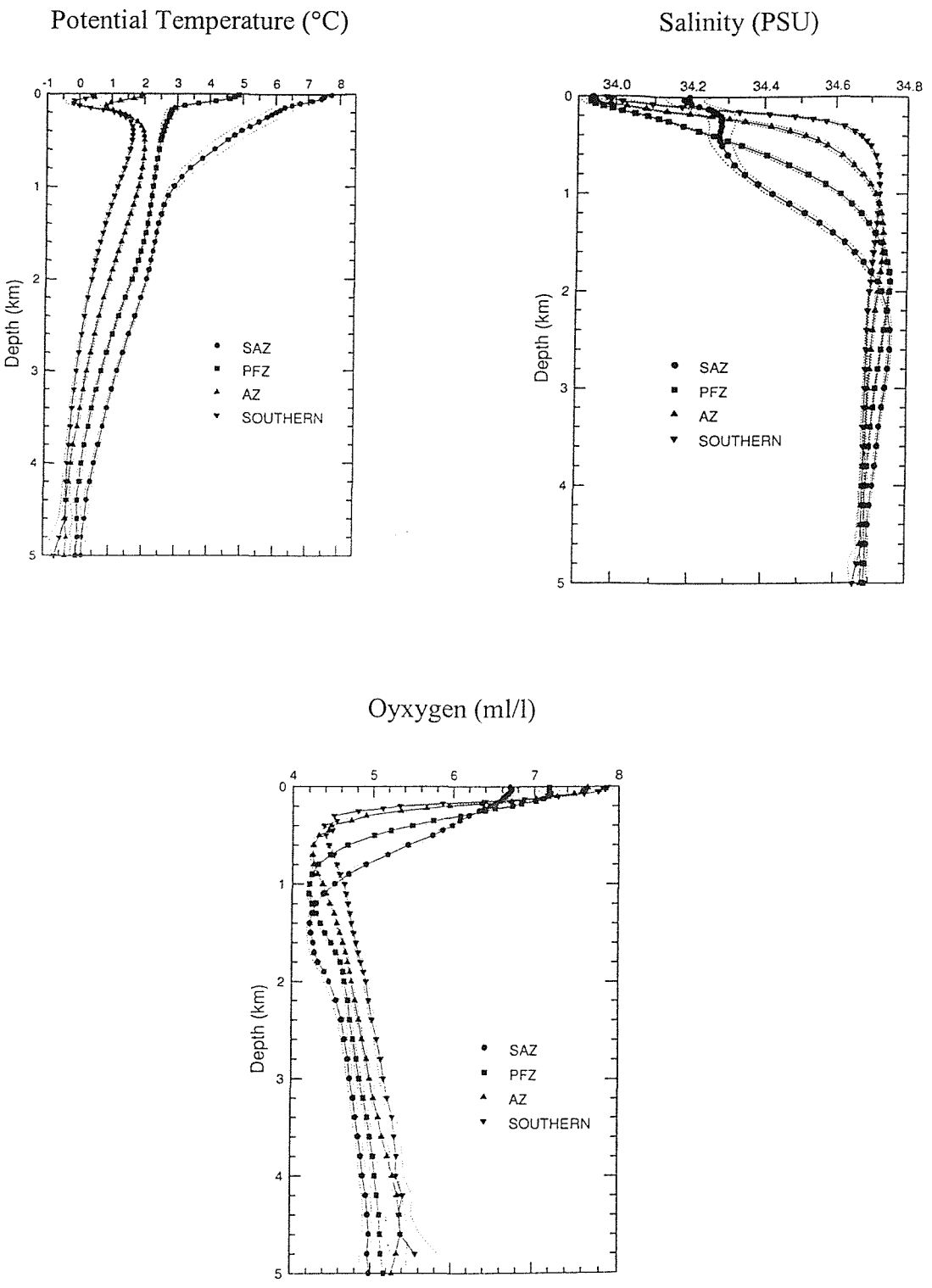

Figure 2.3. Average vertical profiles for a) potential temperature (°C), b) salinity (PSU) and c) dissolved oxygen (ml l^{-1}) computed at standard depths for stations shown in Figure 2.2. Averages are shown for each zone (no. of stations): SAZ (94), PFZ (111), AZ (113) and southern ACC zone (63); dotted envelopes indicate the 95% confidence intervals (from Orsi *et al.*, 1995).

2.1.4. The Southern ACC Front (SACCF)

The Southern ACC Front is a deep reaching current core, but is the only front within the ACC that does not separate distinct surface water masses. Instead, it is considered to be more of an interruption in the Antarctic Zone (Veth *et al.*, 1997). It lies on the south side of Drake Passage and crosses the Scotia Sea at about 58°S (Locarnini *et al.*, 1993), following a more zonal route along the northern edge of the South Scotia Ridge (Fig.2.1).

SAF:	$S < 34.20$ PSU at $Z < 300$m, farther south
	$\theta > 4$-5°C at 400m, farther north
	$O_2 > 7$ml l^{-1} at $Z < 200$m, farther south
PF:	$\theta < 2$°C along the θ-min at $Z < 200$m, farther south
	θ-min (if present) at $Z > 200$m, farther north
	$\theta > 2.2$°C along the θ-max at $Z > 800$m, farther north
southern:	$\theta > 1.8$°C along θ-max at $Z > 500$m, farther north
	$\theta < 0$°C along θ-min at $Z < 150$m, farther south
	$S > 34.73$ PSU along S-max at $Z > 800$m, farther north
	$O_2 < 4.2$ ml l^{-1} along O_2-min at $Z > 500$m, farther north

Table 2.1. Property indicators of the three ACC fronts (from Orsi *et al.*, 1995). (S = salinity, Z = depth, θ = potential temperature).

2.1.5. The Southern Boundary of the ACC

The southern boundary of the ACC marks the poleward extent of the Upper Circumpolar Deep Water (UCDW) signal and it is at this point that the core of UCDW is entrained into the mixed layer of the subpolar regime. It coincides with the boundary between the ACC and the Weddell Gyre and marks a change in geostrophic shear between the ACC and subpolar circulation (Orsi *et al.*, 1995) (Fig.2.2). The large northward bend of the southern boundary of the ACC and the Southern ACC Front at 30°W represents the intrusion of Weddell Sea Deep Water (WSDW) into the southern Scotia Sea (Locarnini *et al.*, 1993).

The location of the principal fronts as described by Orsi *et al.* (1995) were confirmed during the AESOPS study (Antarctic Environment and Southern Ocean Process Study), September 1996 – March 1998, which took place in the southwest Pacific sector of the Southern Ocean

spanning the ACC at 170°W. Fronts in the ACC were found to extend to the bottom (>3000m) and the locations of the fronts were confirmed by the high-velocity jets evident in shipboard ADCP measurements (Barth *et al.*, submitted). The increased meridional gradients in deep isopycnals were also observed which were thought to be indicators of the ACC fronts by Orsi *et al.* (1995) (Anderson, unpublished).

This study also incorporated the JGOFS study (Joint Global Ocean Flux Study) which was designed to evaluate the magnitude of the organic matter flux from the ocean's surface to depth, and the controls on the processes that regulate this flux (see Smith *et al.*, 2000 for more details of this study).

2.2. Other Southern Ocean Fronts

2.2.1. The East Wind Drift or Continental Counter Current

The ACC is bound to the south by subpolar circulation in the form of a smaller wind-driven current flowing in the opposite direction to the ACC, known as the East Wind Drift. The signature of this current is a general downsloping of isotherms toward the continental slope (Whitworth *et al.*, 1998). This current occurs close to the Antarctic continent south of about 65°S, where winds from the east and south-east blow off the ice sheet, and produce a surface current which flows westward (Deacon, 1937). The East Wind Drift is classically supposed to start in the Bellingshausen Sea and circulate anti-clockwise around the continent into the Weddell Sea. The results of iceberg studies showed that the bergs began between the continent and the Antarctic Divergence, showing westward movement close to the coastline in the East Wind Drift; they then turned through a great semicircular bend or retroflection to end up north of the Divergence in the ACC (Tchernia, 1980). Three tracks of this type have been identified: from the Weddell Sea to Enderby Land, Enderby Land to Adelie land and in the Ross Sea region. This circulation may be important in transferring water from close to the continent to the ACC (Tchernia and Jeannin, 1984).

The obstruction of the East Wind Drift by the Antarctic Peninsula and its permanent ice shelves cause it to broaden, forming a large and sluggish clockwise circulation within the Weddell Sea called the Weddell Gyre. Surface waters within the Weddell Sea and Scotia Sea therefore have differing origins and properties, the former having lower temperatures

(Deacon, 1982) and higher silicate concentrations (Michel, 1984). The cyclonic Weddell Gyre in the south extends to the seabed (Reid, 1989) and is separated from the anticyclonic Subtropical Gyre in the north by the ACC (Peterson and Whitworth, 1989).

2.2.2. The Weddell-Scotia Confluence

The boundary between the surface waters of the Weddell Sea and the ACC is known as the Weddell-Scotia Confluence (Gordon, 1967; Patterson and Sievers, 1980). It extends from a western limit near the northern tip of the Antarctic Peninsula (~55°W) to 20°W (Patterson and Sievers, 1980). In the south-eastern Scotia Sea, around 60°S, weak mid-depth potential temperature and salinity maxima reveal the Weddell-Scotia Confluence signal (Locarnini *et al.*, 1996). It is a semi-permanent frontal system, determined partly by bottom topography, whose position follows the curve of the Scotia Arc (Fig.2.1). It is best defined in the western Scotia Sea between the South Shetland Islands and the South Orkneys (Foster and Middleton, 1984) where the Scotia Ridge tends to prevent outflow of Weddell water into the Scotia Sea (Carmack and Foster, 1975), and is indicated here by a strong temperature gradient. To the west of the South Orkneys, this front gradually loses its structure due to a progressive increase in mixing of the two water types and is characterised in the east by an extensive eddy system (Deacon and Moorey, 1975; Maslennikov and Solyankin, 1979; Patterson and Sievers, 1980; Foster and Middleton, 1984).

2.2.3. The Subtropical Front (STF)

The Subtropical Front to the north of the ACC (Fig.2.2) separates waters of the Southern Ocean from the warmer and saltier waters of the subtropical circulations. It occurs between 33° and 42°S with the mean position located at about 37.55°S in the Southern Indian Ocean (Morley, 1989). It marks the southern boundary of the subtropical gyres of the southern hemisphere and is distinguished by large meridional surface gradients in temperature and salinity (Stramma and Peterson, 1990). Deacon (1937) called this hydrographic boundary the Subtropical Convergence, but this was later replaced by the term Subtropical Front (Clifford, 1983; Hofmann, 1985). Deacon (1937) noted that surface temperature changes as large as 4-5°C mark the location of the STF. Its approximate position is now thought to lie within a band across which temperatures increase northward from 10°C to 12°C, and salinities from 34.6 PSU to 35.0 PSU at 100m (Deacon, 1982). Northward from the STF, temperature and

salinity both continue to increase rapidly (Peterson and Whitworth, 1989). The STF is the northern limit of Subantarctic Surface Water (SASW) and probably the southern limit of many warm-water faunal species (Deacon, 1982).

2.3. Hydrography

Waters from the North Atlantic, the Antarctic Circumpolar Current and the Weddell Sea enter the South Atlantic and are caught up in a circulation system imposed by winds, thermohaline and geostrophic processes. The near-surface, wind-driven circulation in the southernmost Atlantic and the Weddell Sea is dominated by a system of gyres and the circumpolar current systems (Peterson and Stramma, 1991).

Due to the prevailing climatic conditions in the Southern Ocean, an intense transfer of heat from the sea to the atmosphere takes place (Gordon and Taylor, 1975), and this heat loss from the ocean must be replaced by poleward ocean heat fluxes to the Southern Ocean. One mechanism which achieves this is abyssal western boundary currents (Stommel and Arons, 1960a, b) which transport cold waters formed at high latitudes equatorward, resulting in an opposing poleward heat flux. See review by Warren (1981) of the spreading of bottom waters from their source regions to the rest of the world ocean basins.

2.3.1. The Antarctic Divergence

One of the most important oceanographic processes in the seas around Antarctica is the wind-driven upwelling of deep-water which occurs at the Antarctic Divergence (average latitude 65°S) (Fig.2.4). This process is fundamental to biology and allows deep-water contact with the surface layers and air-sea interactions to occur (Gordon, 1971). Clockwise winds develop around low-pressure areas which causes a westward flowing coastal current called the East Wind Drift, while to the north of the lows the winds are westerlies and the resultant eastward circulation is the West Wind Drift. Ekman transport in the southern hemisphere is to the left of the wind and therefore the East Wind Drift has southward transport and the West Wind Drift has northward transport. The Antarctic Divergence is found between them; it allows southward upwelling of Circumpolar Deep Water (CDW) in response to the northward and downward flow of Antarctic Surface Water (AASW). At the zone of upwelling, an oxygen minimum and temperature maximum occur, accompanied by a high nutrient concentration

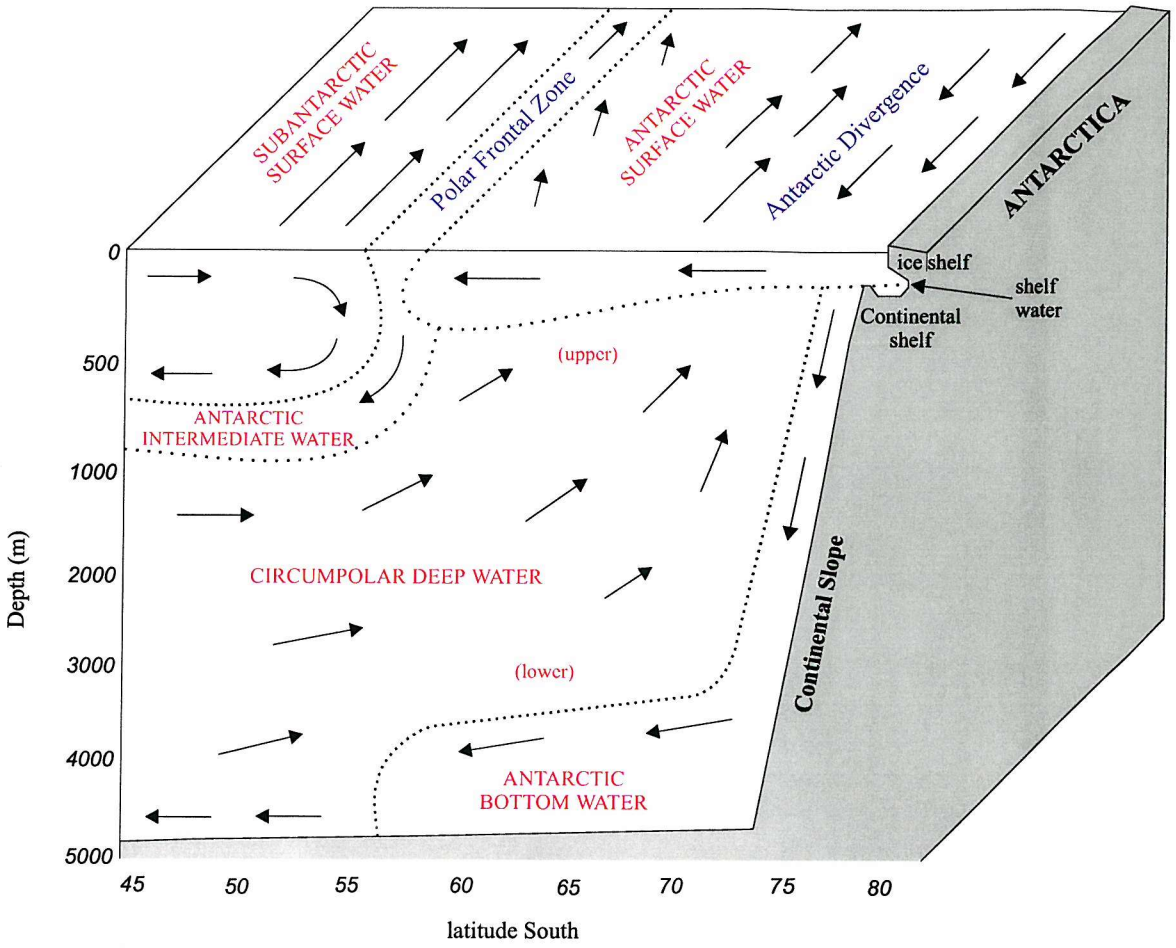

Figure 2.4. Schematic representation of the water masses in the Antarctic and sub-Antarctic (after Gordon and Goldberg, 1970). The reality of an organised meridional circulation pattern (ie. north-south transport) has been questioned, and the meridional components are now best visualised as intermittent transports associated with eddy and ring type structures (Bryden, 1983; Nowlin and Klinck, 1986).

(Gordon and Molinelli, 1982). There are sometimes lower ice concentrations observed at the Antarctic Divergence in winter due to the warmer water that is reaching the surface from below, which may be a mechanism for the formation of polynas like in the Weddell Sea (Wadhams, 2000). The upwelling also necessitates a southward flow of deep water (Gordon, 1971). The polar waters represent a net heat source for the atmosphere and therefore in the Southern Ocean this heat loss is partly compensated for by the poleward motion and upwelling of warm deep water (Foldvik and Gammelsrod, 1988).

2.3.2. Circulation and Water Masses in the Scotia Sea

The environments of the waters of the Scotia Sea are particularly complex. Waters of the ACC, the Weddell Gyre and the East Wind Drift intermingle within an area of complex topography, to produce complicated mixtures of water masses (Stein and Heywood, 1994). The general character of the water circulation is fairly well known (Fig.2.4). It is a three-layer system in which water that is cooled and diluted in high latitudes spreads outwards at the surface and bottom of the ocean, while warm water which replenishes the salt as well as the heat moves inward in the intervening deep layer (Deacon, 1977). The surface and bottom water masses are Antarctic in origin, in that their characteristics are attained south of the PF. Their northward and downward component motion is compensated by a southward and upward flowing deep-water mass. The result of this important meridional exchange is that heat and nutrients are supplied to the surface of Antarctic waters from lower latitudes, and the oxygen content of the deep water of the world is replenished. Such a process allows a steady heat flux from ocean to atmosphere and a high biological productivity rate in the photic zone. This helps to maintain the proper environment for life in the deep water and the low temperatures of the deep ocean (Gordon, 1971).

- **Surface Water Masses**

Antarctic Surface Water (AASW)

Antarctic Surface Water extends from the Polar Front to the continental margins of Antarctica (Fig.2.4) where shelf waters are at near freezing temperatures (Table 2.2). The most conspicuous feature of this water mass is its very low temperature, presumably the result of winter cooling (Gordon, 1967). The low salinity of AASW is maintained by the melting of

icebergs and ice shelves and by the excess of precipitation over evaporation in the Southern Ocean (Wadhams, 2000). The surface waters therefore form a relatively thin layer of cold, low salinity, highly oxygenated water reaching only to about 250m, and extend north to the PF where it sinks below the slightly less dense Subantarctic Surface Water to form the bulk of Antarctic Intermediate Water. Antarctic Surface Water is subdivided into the surface water of the Weddell Sea and that of the Scotia Sea by the Weddell-Scotia Confluence. The surface water of the Weddell Sea is colder and spans a greater salinity range than the Scotia Sea surface water (Gordon, 1971).

Subantarctic Surface Water (SASW)

Subantarctic Surface Water extends north with increasing thickness from the Polar Front to the Subtropical Front (Sievers and Nowlin, 1984). It is marked by a higher temperature and salinity than AASW (Table 2.2).

- **Intermediate Water Masses**

Antarctic Intermediate Water (AAIW)

This water mass is nutrient-poor, oxygen-rich and has a low salinity (Table 2.2) with a characteristic subsurface salinity minimum, which appears immediately north of the PF (Sievers and Nowlin, 1984). Because AAIW properties are similar to surface waters near the PF, the traditional mechanism of formation proposed involved a significant component of AASW sinking below SASW at the PF (Deacon, 1933, 1937; Wüst, 1935) (Fig.2.4). More recently, mixing across the PF by small-scale processes in the Scotia Sea and Drake Passage are proposed (Gordon *et al.*, 1977; Joyce *et al.*, 1978). Molinelli (1978, 1981) proposed that AAIW in the ACC results from the mixing along an isopycnal (density) surface of cool, fresh AASW and warm, salty water from the North Indian Ocean. Antarctic Intermediate Water then spreads north above Circumpolar Deep Water and influences most of the oceans of the southern hemisphere (Gordon, 1971). It forms a layer of low salinity below the thermocline in all three southern hemisphere oceans reaching depths of 1000m in the subtropical gyres (Piola and Gordon, 1989). It follows a predominantly anticyclonic flow in the South Atlantic consistent with recent chlorofluorocarbon data (Warner and Weiss, 1992; Gordon *et al.*,

1992), but there is also some weak equatorward transport along the western boundary in the South Atlantic (Wüst, 1935).

Water Mass	Potential Temperature (θ) (°C)	Salinity (PSU)
AASW	< 0.5	34.40
	(Orsi *et al.*, 1995)	
SASW	summer > 7	≤ 34.1
	(Sievers and Nowlin, 1984)	
AAIW	3.8 - 4.8	34.2
	(Piola and Gordon, 1989)	
CDW	0.0 - 1.0	34.7 - 34.73
	(Sievers and Nowlin, 1984)	
NADW	2.0	>34.9
	(Labeyrie *et al.*, 1987)	
AABW	-0.4	34.66
	(Foster and Carmack, 1976)	
WSDW	-0.7 - 0.0	< 34.67
	(Locarnini *et al.*, 1993)	
WSBW	< -0.7	> 34.65
	(Carmack and Foster, 1975a)	

Table 2.2. Properties of the water masses within the Southern Ocean.

- **Deep Water Masses**

The deep South Atlantic is ideal to study changes in the depth distribution of deep water properties because it reveals the mixing zone between North Atlantic Deep water (NADW) and southern-source deep water masses (e.g. Reid, 1996). The present day circulation in the deep western South Atlantic, is dominated by interactions between NADW flowing towards the south and Weddell Sea Deep Water (WSDW) and Circumpolar Deep Water (CDW) flowing to the north.

Circumpolar Deep Water (CDW)

This southward flowing water mass is warm, salty, low in oxygen but high in nutrients and occupies most of the deep layers (Table 2.2). Circumpolar Deep Water is the most voluminous water mass within the ACC and is a mixture of waters formed in the Antarctic region and warm deep water flowing from the North Atlantic, Pacific and Indian Oceans. This water is converted into AASW at the Antarctic Divergence sea-air interface (Fig.2.4).

CDW moves east as part of the ACC and re-circulates around Antarctica. As it does it loses water to the surface and bottom waters and is re-supplied around the entire continent including an important contribution of highly saline, warm, oxygen-rich NADW (Gordon, 1971). Whitworth and Nowlin (1987) showed that waters from the Weddell Gyre are also incorporated into CDW as it flows east through the South Atlantic, resulting in ventilation of the ACC. This mixing in the Scotia Sea establishes a connection between changes in WSDW production in the Weddell Sea and the abyssal water characteristics of the World Ocean, via the ACC (Locarnini *et al.*, 1993).

Circumpolar Deep Water flowing below ~2000m is confined within the northern Scotia Sea by the North Scotia Ridge but can pass through a deeper gap (~3000m) at Shag Rocks Passage further to the east along the ridge. Most CDW flows through this gap and continues to flow east along the southern edge of the eastern Falkland Plateau (Howe *et al.*, 1997).

North Atlantic Deep Water (NADW)

Beneath the surface waters, the warm, saline, highly-oxygenated but nutrient-poor NADW enters the Southern Ocean from the north and extends southward into the circumpolar water, where it separates the CDW into an upper and lower layer, and then turns eastward as part of the ACC (Reid, 1989). The influence of NADW to CDW is circumpolar and it provides the maximum in salinity and minima in nitrate and phosphate of Lower Circumpolar Deep Water. The maximum in oxygen and minimum in silica of NADW are overwhelmed by stronger sources from the south and are not distinguishable in CDW east of the Greenwich Meridian (Whitworth and Nowlin, 1987). The major components of NADW come from the mixing of cold Norwegian Sea bottom water with warm, saline North Atlantic intermediate water while overflowing through the Denmark and Faeroe sills to the North Atlantic basins (Labeyrie *et al.*, 1987).

Upper and Lower Circumpolar Deep Water (UCDW and LCDW)

North of about 55°S CDW encounters NADW in intermediate depths and is divided into an upper and lower water mass (Gordon, 1967) (Fig.2.4). These two distinct layers can be distinguished using certain criteria (Whitworth and Nowlin, 1987): Upper Circumpolar Deep Water (UCDW) which is indicated by a temperature maximum, oxygen minimum and nutrient maximum (about 400m deep, Meredith *et al.*, 2000); Lower Circumpolar Deep Water (LCDW) which is indicated by a salinity maximum and nutrient minimum (about 1200m deep, Meredith *et al.*, 2000). At the southern boundary of the ACC and hence the boundary with the Weddell Gyre, UCDW shoals to the level of the AASW where it is entrained in the surface layer and is not present in the Weddell Gyre (Orsi *et al.*, 1995). Lower Circumpolar Deep Water is dense enough to penetrate south of the ACC into the subpolar regime underneath AASW. Its poleward spread often reaches the Antarctic continental shelves (Deacon, 1982), where it mixes with shelf waters to form denser water that sinks downslope (Foster and Carmack, 1976; Jacobs *et al.*, 1970). The resulting mixture spreads northward into the ACC, cooling and freshening the CDW, and eventually fills most of the World Ocean abyssal layers through a series of deep western boundary currents that branch off the ACC (Mantyla and Reid, 1983).

Modified Circumpolar Deep Water (MCDW)

This water type lies between the two isopycnals that separate CDW from AASW above and from AABW below, and for a given density is colder and fresher than regional CDW. It may be formed by a number of processes: vertical mixing with overlying AASW (Winter Water) or underlying Shelf Water (Newsom *et al.*, 1965; Foster and Carmack, 1976a), or by isopycnal mixing with Shelf Water (Carmack and Killworth, 1978; Jacobs *et al.*, 1985; Whitworth *et al.*, 1994). It is thought to be involved in the formation process of deep water within the Weddell Sea (section 2.3.3) (see review in Whitworth *et al.*, 1998).

Antarctic Bottom Water (AABW)

There are two deep-water masses in the Scotia Sea, namely CDW in the north and AABW in the south (Locarnini *et al.*, 1993). Antarctic Bottom Water is formed in the Weddell Sea and originates from Weddell Sea Bottom Water (WSBW). As Weddell Sea Bottom Water spreads from its site of formation in the southern and south-western Weddell Sea it mixes with

warmer and more saline Weddell Sea Deep Water above to form AABW, which then cascades north into the southern Scotia Sea (Gordon, 1971). The water which has upwelled from the deep circumpolar current near the Antarctic coast is further cooled by heat exchange with the atmosphere and sea-ice and becomes more saline due to sea-ice formation, and hence sinks rapidly. Its residence time at the surface is so short that neither phytoplankton utilisation nor gas exchange with the atmosphere significantly reduces its CO_2 content (Weiss *et al.*, 1979), and as a result the newly formed AABW is strongly undersaturated with respect to carbonate (Duplessy *et al.*, 1988).

Weddell Sea Deep Water (WSDW)

This is the deep-water mass south of the Weddell-Scotia Confluence. Weddell Sea Deep Water influences the thermohaline circulation of the world's oceans directly as a component of the deep western boundary current in the South Atlantic and indirectly by cooling and freshening of CDW (Mantyla and Reid, 1983). Wüst (1933) proposed what has historically been considered the main outflow route for WSDW from the Weddell Sea to the Argentine Basin. He thought that waters from the Weddell Sea passed through a gap in the mid-ocean ridge and flowed north as a deep boundary current against the eastern slope of the South Sandwich Arc. There may also be some return poleward flow of the coldest WSDW and Weddell Sea Bottom Water (WSBW) above the South Sandwich Abyssal Plain due to restriction by the ACC (Locarnini *et al.*, 1993). Weddell Sea Deep Water also leaves the Weddell Sea through deep narrow passageways in the South Scotia Ridge. The deepest gap is the narrow Orkney Passage (3500m) (LaBrecque *et al.*, 1981), although there are shallower gaps through which some WSDW may flow (Gordon, 1966; Nowlin and Zenk, 1988). On entering the Scotia Sea WSDW flows in a westward abyssal current along the northern side of the South Scotia Ridge (Wüst, 1933; Nowlin and Zenk, 1988; Locarnini *et al.*, 1993). This current is then blocked by bathymetric features and turns cyclonically to follow the predominant eastward flow of the ACC, and hence distributes WSDW throughout the rest of the Scotia Sea (Locarnini *et al.*, 1993). It is also possible that WSDW may spill over the entire length of the South Scotia Ridge at shallower depths (Weiss and Bullister, 1984).

Three possible routes have been proposed for WSDW to leave the Scotia Sea and contribute to the deep western boundary current of the Argentine Basin: Wittstock and Zenk (1983) report a small north-eastward flow of cold bottom water from the northern Scotia Sea through

Shag Rocks Passage; Nowlin and Zenk (1988) propose a westward flow (25% WSDW) into the southern Drake Passage through the Shackleton Fracture Zone; Locarnini *et al.* (1993) suggest that a more likely route is through the Georgia Passage at 3200m depth (LaBreque, 1986) into the Georgia Basin, with a resultant westward flow of WSDW along the Falkland Trough.

Circumpolar Deep Water is ventilated by the cold and fresh WSDW of the Weddell Gyre immediately upstream of being modified by the salty NADW. This stresses the importance of the southwestern Atlantic Ocean in determining the characteristics of the most voluminous water mass in the Southern Ocean.

Weddell Sea Deep Water is believed to be renewed via vertical mixing between Weddell Sea Bottom Water (WSBW) and CDW, and is therefore thought of as old, upwelled, re-circulated WSBW. In a recent study by Meredith *et al.* (2000), however, a CFC data set was used to present evidence of renewal of WSDW by direct contributions from the Antarctic continental shelf (see paper for full review).

Weddell Sea Bottom Water (WSBW)

Weddell Sea Bottom Water is the coldest and densest of all the Southern Ocean deep waters (Table 1.2). It is derived from the mixing of CDW and shelf waters that then flow down slope. It is recognised by a lower potential temperature than other deep water masses and larger near-bottom temperature gradients, suggesting recent formation in the south-western and western Weddell Sea (Carmack, 1973). Under the action of the Coriolis force the cold bottom water follows the perimeter of the Weddell Sea in a clockwise direction as the Weddell Gyre (Gill, 1973; Killworth, 1973; Deacon, 1979). These dense waters are confined to the Weddell Sea Basin, both topographically by the Southern Ocean ridge system and dynamically by the ACC (Mantyla and Reid, 1983).

Both AASW and AABW flow north compensating for southward flowing CDW (Fig.2.4). These northward flowing Antarctic water masses are eventually altered as they move from their source regions; their characteristics are changed through interaction with the overlying water column and with the bottom sediments. Silica in the bottom water is increased by dissolution of biogenic silica from the ocean floor (Edmond *et al.*, 1979), and oxygen is

consumed by respiration (Mantyla and Reid, 1983). They enter the deep water and flow south to start the cycle over again which results in an overturning process.

The temperatures and salinities of the main water masses contrast strongly and their cores are clearly revealed in TS profiles (Fig.2.5). In the Antarctic Zone the presence of AASW is indicated by low salinity and, in summer, by a temperature minimum within the top 200m. Below this layer temperatures and salinities increase within the CDW, whose upper and lower levels are indicated respectively by temperature and salinity maxima. Temperature decreases again towards the seabed, indicating the presence of AABW (Sievers and Nowlin, 1984).

All of the major water masses surrounding Antarctica reflect the nature of its source region and contains a "core" layer in which the original characteristics are strongest (Table 2.3). Core layers are identified by either maximum or minimum (extrema) values of salinity, temperature or oxygen. However not all extrema layers are true core layers in the sense that their characteristics are those attained at the source region. Extremes may be induced by local conditions or acquired in transit from the source region. The water between the core layers is a mixture, blending the characteristics of the layers above and below (Gordon, 1967).

Core Layer	Water Mass
Temperature minimum	AASW
Temperature maximum	CDW (upper)
Oxygen minimum	CDW (upper)
Salinity maximum	CDW (lower)
Deep potential temperature minimum	AABW
Deep oxygen maximum	AABW

Table 2.3. Extrema layers found in the Southern Ocean.

a)

b)

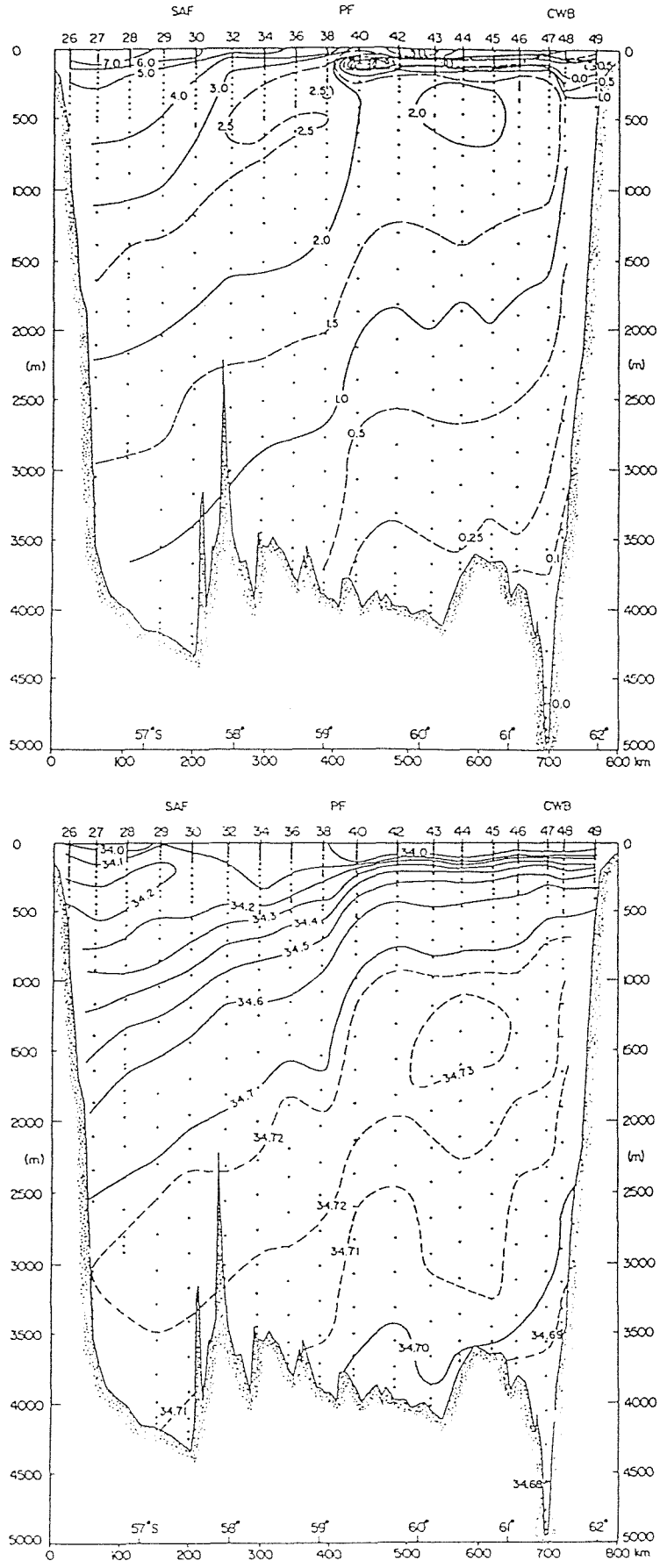

Figure 2.5. Profiles of a) potential temperature (°C) and b) salinity (PSU) along a transect across Drake Passage (from Sievers and Nowlin, 1984).

2.3.3. Formation of Bottom Water

A study by Brennecke (1921) first showed that the very cold bottom water in the Atlantic could be traced back to the Weddell Sea. A number of years later observations from the Discovery Expeditions published by Deacon (1937) also clearly pointed to the Weddell Sea as the main source of deep water in the world ocean. Further studies of the Weddell Sea (Seabroke *et al.*, 1971; Gill, 1973; Carmack and Foster, 1975; Foster and Carmack, 1976; Killworth, 1977; Carmack, 1977) have confirmed the dominant influence of Weddell Sea Bottom Water (WSBW) in the formation of classically defined Antarctic Bottom Water (AABW) (Table 1.2). The Weddell Sea probably accounts for approximately 80% of the total production today (Foldvik and Gammelsrod, 1988) with minor sources being the Ross Sea (Jacobs *et al.*, 1970, 1985) and off the coast of Adélie Land (Gordon and Tchernia, 1972; Rintoul, 1998).

The method of production of Antarctic Bottom Water is not fully understood, but it is generally accepted that the characteristics of the bottom water are attained by a mixture of surface water and deep water (Brennecke, 1921; Mosby, 1934; Defant, 1961). The surface water temperature must decrease to near freezing and the salinity must increase, creating a surface density high enough to initiate sinking (Gordon, 1971). These conditions are reached during periods of ice formation when brine is released and a large reservoir of cold, high salinity shelf water is produced (Brennecke, 1921; Mosby, 1934).

The proposed methods for the formation of bottom water have been reviewed in Whitworth *et al.* (1998). The pioneering modern study of bottom water formation was carried out by Gill (1973). He explained it as a two stage process: first, water from "above the salinity maximum" mixes with saline shelf water to produce the water seen at the bottom of the shelf edge; this water then sinks along the slope, entraining the warmer, saltier CDW to produce bottom water. Gill also refers to the water from above the salinity maximum as "downwelled water from above the pycnocline", which could refer to Whitworth's Modified CDW.

A more widely cited review is Foster and Carmack (1976), which again proposes a two-stage process, first of which is the formation of Modified Warm Deep Water from a mixture of Winter Water and Warm Deep Water "over the deep ocean basin". The second stage is similar to Gill's first, the mixing of Modified Warm Deep Water with Western Shelf water at the shelf to produce WSBW. Modified Warm Deep Water is also within the domain of Whitworth's Modified CDW. However as explained by Whitworth *et al.* (1998), when

employing this mixing method it should be understood that "deep ocean" can only refer to depths of less than 1500m where Winter Water salinities of 34.5 PSU necessary for this process to occur, are possible. The process of a warm high-salinity water mass mixing with a cold low-salinity water mass to produce a third water mass which is more dense than either of its constituents was first noted by Fofonoff (1956) and is known as "cabelling" (Wadhams, 2000).

Foldvik *et al.* (1985b) theorise that Ice Shelf Water from the Filchner Ice Shelf in the south-west Weddell Sea spills over the edge of the continental shelf and mixes directly with CDW offshore. Whitworth *et al.* (1998) summarise that the vertical mixing of CDW with Shelf Water can contribute to AABW but this type of mixing requires the simultaneous presence of Shelf Water and unmodified CDW at the shelf break, which is a situation that is probably not widespread around Antarctica. Therefore as Smith *et al.* (1984) concluded, although Ice Shelf Water has been proven to have a role in AABW formation near the Filchner Depression, it has only a marginal influence on large-scale oceanography.

Whatever the method for the formation of bottom water may be, as Gill (1973) pointed out, the front near the upper continental slope and shelf is the primary site for these processes. Ainley and Jacobs (1981) described a similar front in the Ross Sea and named it the Antarctic Slope Front. Therefore on a large scale, there are just two places around Antarctica (the Weddell and Ross Seas) where CDW from the ACC approaches the continental margin.

During glacial times WSDW and WSBW formation was probably reduced (see Fütterer *et al.*, 1988; Grobe and Mackensen, 1992; Pudsey, 1992). Today, as described above, significant parts of WSBW originate from underneath the ice shelves and spills over the shelf edge as a supercooled plume, cascading down the slope to contribute to WSBW. During glacial times however, sea level was lowered and the grounding line of the west Antarctic ice cap coincided with the shelf break at most of the continental shelves, and the supply of warm and saline northern borne deep water into the Weddell Sea was greatly reduced (e.g. Anderson *et al.*, 1980; Oppo *et al.*, 1990; Grobe and Mackensen, 1992; Mackensen *et al.*, 1994). Therefore, because of the smaller ice shelves and the reduced amount of saline deep water, the amount of bottom water generated by supercooling beneath ice was reduced (Mackensen *et al.*, 1996).

2.4. Sea-Ice Distribution

Sea-ice is a critical part of the climate system with respect to rapid climate change (Peltier, 1993). Sea-ice influences climate by reflecting solar radiation, altering deep-oceanic convection in high latitudes, decreasing heat exchange between the ocean and atmosphere, cooling the adjacent continent, altering surface-ocean productivity by photosynthetic algae, and changing atmosphere-ocean carbon fluxes (Wadhams, 2000).

The areal extent of sea-ice around Antarctica is roughly twice the size of the Antarctic Ice Sheet and experiences a five-fold increase annually during winter (Mullan and Hickman, 1990). This seasonal variability in the sea-ice coverage is one of the most significant factors regulating the energy balance of the southern hemisphere atmosphere and ocean (Mullan and Hickman, 1990; Martinson and Iannuzzi, 1998). The extent of sea-ice around Antarctica also regulates the penetration of light in surface waters and therefore primary productivity (Anderson, 1999).

Antarctic sea-ice undergoes a vast change in area from roughly 2-4 x 10^6 km^2 in the austral spring to a maximum of 20 x 10^6 km^2 (60% of the Southern Ocean) in the austral autumn. The maximum ice cover is circumpolar in extent. Most of the pack-ice is newly formed each year and therefore only reaches a thickness of 1-2m (Foldvik and Gammelsrod, 1988), but some multi-year ice occurs in the Weddell Sea. Seasonal sea-ice in the south-west Atlantic sector varies between a winter maximum position north of South Georgia and a winter minimum position of 60°S (Gloersen *et al.*, 1992) (Fig.2.1). South of the spring (mid-January) sea-ice edge there is only 3 months of open water a year (Pudsey and Howe, 1998). This feature is coincident with the southern boundary of the circum-Antarctic diatom ooze belt (Burckle and Cirilli, 1987). The absence of boundaries to the north enhances the ice melt in summer and approximately 85% of the sea-ice melts each year (Mullan and Hickman, 1990). Upwelling of relatively warm, saline CDW continually supplies heat to the base of the sea-ice, and therefore the sea-ice is linked to deep-water circulation. Observational and model studies suggest that the heat supplied by CDW, combined with spring solar radiation increases, is critical to the spring melt-back of the sea-ice (Gordon and Huber, 1990; Martinson, 1990). The region covered by the seasonal advance and retreat of sea-ice, while overlapping with the Antarctic Zone, is sometimes classified separately as the Seasonal Ice Zone (SIZ; Tréguer and Jacques, 1992). This separation is made because the stabilisation effect of freshwater added by melting sea-ice often leads to phytoplankton blooms as well as

to distinct species assemblages (Smith and Nelson, 1985; Mitchell *et al.*, 1991; Tréguer and Jacques, 1992; Arrigo *et al.*, 1999). This is similar to the term Marginal Ice Zone (MIZ) as described in Wadhams (2000) as the region of ice which lies close to an open ocean boundary. A true MIZ has its character permanently determined by abutting on to a rough ocean with a climate of long, high waves. The Antarctic circumpolar ice edge is one of only four MIZs in the world and is the longest and widest of these (Wadhams, 2000). Satellite observations show large fluctuations in the seasonal distribution of the Antarctic pack ice including larger polynas and leads. Floating ice shelves, several hundred metres thick cover more than 1 million km^2 in the Southern Ocean (Foldvik and Gammelsrod, 1988).

2.5. Nutrients

The Southern Ocean and the ACC south of the Polar Front comprise about 10% of the world's ocean surface and contain significant concentrations of surface macronutrients (i.e. NO_3, PO_4, SiO_3) (El Sayed. 1978). The surface layer is characterised by a ubiquitous abundance of these macronutrients with complete exhaustion of nutrient availability being seldom observed. The available nutrients are not removed by the primary producers and therefore the general scenario is of limited nutrient uptake and corresponding oligotrophy (Goeyens *et al.*, 1998).

In general the concentration of nutrients in surface waters south of the Polar Front are much higher than those found in other oceanic waters (Knox, 1970; El-Sayed, 1978). Nutrient rich water upwells at the Antarctic Divergence spreading out to ultimately downwell at the PF (Knox, 1994). The PF separates the Antarctic Zone to the south, where high winter Si concentrations result from upwelling of CDW, from the PFZ to the north, where Si-depleted AAIW sinks and begins its northward transit. Stratification varies seasonally and the biological response to summer stratification is evident in the reduction of nutrient concentrations (Smith *et al.*, 2000). Concentrations of major inorganic nutrients are high in both the Antarctic and Subantarctic Zones, although the northward decrease in the concentration of dissolved silicate occurs more abruptly at the PF than is the case for nitrate and phosphate (Lutjeharms *et al.*, 1985). In the Southern Ocean the concentration of nutrients is lowest in the surface waters and greatest in the Warm Deep Layer for nitrate and phosphate. Phosphate and nitrate remain fairly constant in the upper waters, whereas silicate

shows a near continuous increase with depth south of about 55°S. High surface silicate is presumed to result from remineralisation of diatoms (Nelson and Gordon, 1982; Edmond *et al.*, 1979) and/or upward mixing of deep waters. Approximately 18-58% of silicate is re-dissolved in the upper 100m (Nelson and Gordon, 1982).

Results from the INAEX III cruise along a track between 11° to 53°E (3-6 March, 1984) in the Indian sector of the Southern Ocean showed that the concentration of NO_3, PO_4 and SiO_3 were 28.6, 2.04 and 61.9 μM, respectively near the Antarctic Divergence (68°S); 24.6, 1.71 and 12.42 μM, respectively near the PF (53°S); 19.2, 1.36 and 2.8 μM, respectively south of the STC (42°S); 1.1, 0.2 and 1.6 μM, respectively north of the STC (38°S). This showed that that NO_3 and PO_4 remain high up to south of the STC, but Si concentration reduces rapidly north of the PF (Verlencar and Dhargalkar, 1992). Similarly, data from studies by Kuramoto and Koyama (1982) and Watanabe and Nakajima (1982) from a transect along 45°E longitude showed that silica concentration in the surface waters was relatively high (57μmol/kg) at 67°S and it decreased sharply to 15μm/kg at 60°S, then dropped to very low values (~ 1μmol/kg) just north of the PF, reflecting its assimilation by diatoms and silicoflagellates. Nitrate however, only decreased from 27μmol/kg at 60°S to 22μmol/kg at the PF.

Therefore the nutrient pool in the Southern Ocean exhibits a unique feature of the interaction with physical and biological processes. Although strong physical mixing actively replenishes the surface layers with nutrients, the high biological demand for these nutrients quickly removes these elements from the surface waters. Ultimately those elements with higher mineralisation capacity (N and P) retain their richness in the surface waters, whereas Si mineralises at a much slower rate and so is lost from the surface waters to the deeper layers and to the bottom sediments as biogenic material (Verlencar and Dhargalkar, 1992).

During the INAEX I cruise (18 Jan - 8 Feb, 1982) along the same track, chlorophyll and primary productivity were measured to distinguish the biologically active regions. A maximum chlorophyll value of 0.7 mgm^{-3} was recorded at 58°S, and other locations in the region between 69° to 30°S showed chlorophyll and primary productivity of <0.32 mgm^{-3} and <0.43 mgC $m^{-3}h^{-1}$, respectively in the surface water. Water column values of chlorophyll and primary productivity showed elevated values at 58°S and another peak of primary productivity at 68°S, while the rest of the values were low (Verlencar and Dhargalkar, 1992).

During the European leg of the JGOFS (AESOPS) cruise (Oct/Nov. 1992) to the South Atlantic sector of the Southern Ocean large phytoplankton blooms were recorded in the PFZ (0.7 to >4 $mgChlam^{-3}$) but not in either of the retreating ice-cover area (0.3 $mgChlam^{-3}$) or within the Weddell Gyre (southern section of the ACC). They concluded that frontal regions are therefore major production sites in the Southern Ocean and that the input of meltwater and its associated algae from the retreating ice-edge is by itself an insufficient condition to promote phytoplankton blooms. The reason for the development of the bloom may be a combination of shallow mixed layers, high iron concentrations and low grazing pressure. They also noted a clear drawdown of CO_2 in the PFZ (Bathmann *et al.*, 1997; Peeken, 1997; Veth *et al.*, 1997; Smetacek *et al.*, 1997).

In the southwest Pacific sector of the Southern Ocean at 170°W as part of the JGOFS cruise (Sept-March, 1998), Smith *et al.* (2000) measured average concentrations of chlorophyll within the mixed layer to the north and south of the PF spanning the ACC. To the north of the PF (56°50.4'S) the concentration was 0.19 μgl^{-1} during December whereas to the south (64°9'S) they were an order of magnitude greater with a mean value of 2.90 μgl^{-1} during the same time period. By late February chlorophyll levels at this same location had decreased to 0.44 μgl^{-1}. Early signs of a developing bloom were first observed at the PF in this sector during November 1997 (Landry *et al.*, submitted). Peak bloom conditions at the PF in December were subsequently recorded by an array of bio-optical moorings (Abbott *et al.*, 2000), by remote sensing (Moore *et al.*, 1999), and by ship-based observations. It is thought that stratification created by interleaving water masses, together with local upwelling induced by meanders in the PF, contributed to favourable growing conditions early in the season (Smith *et al.*, 2000).

Therefore due to high nitrate levels and low but stable chlorophyll concentrations on average measured throughout the year (Banse, 1996), the PFZ is part of the high-nitrate, low-chlorophyll (HNLC) region of the Southern Ocean that may be iron limited (Martin *et al.*, 1990; DeBaar *et al.*, 1995; Banse, 1996).

Surface ρCO_2 (partial pressure of CO_2) and TCO_2 (total carbonate) were measured in a transect heading south from New Zealand along 170°W, and was found to increase gradually across the Polar Frontal Zone and then increase sharply on reaching the pack ice (Purkerson and Millero, 1996).

Chapter Three

REVIEW OF SEDIMENTS AND MICROPALAEONTOLOGICAL STUDIES OF THE SCOTIA SEA

3.1. Sediments

Changing oceanography as a consequence of changing climate produces temporal variability in the sediment record, especially over the last glacial-interglacial cycle. In the Scotia Sea and other parts of the Southern Ocean there are extensive areas of Quaternary deposition consisting mainly of hemipelagic and muddy contourite facies. These have been mapped and described by Pudsey *et al.* (1988), Pudsey (1992), Howe *et al.* (1997) and Pudsey and Howe (1998). Much of the Scotia Sea floor is isolated from major continental-margin sources of sediment with only the southern tip of South America and the west coast of the Antarctic Peninsula having near-continuous downslope pathways to the Scotia Sea. Sediment supply, both terrigenous and biogenic, is controlled by oceanic circulation in the form of the Antarctic Circumpolar Current and to a lesser extent the Weddell Gyre (Pudsey and Howe, 1998).

Antarctic surface waters of the present time are recorded in the sediment as a broad biosiliceous facies that extends north to the position of the Polar Frontal Zone, reflecting the

high productivity of the surface waters between the Antarctic Divergence and the Polar Front (Fig.2.4). Within this facies diatom ooze and muddy diatom ooze are the most common surface sediment (Demaster, 1981; Defelice and Wise, 1981; Wefer and Fischer, 1991). The low carbonate content of these sediments is due to the corrosive nature of the bottom water (AABW/WSDW) in the southern Scotia Sea (Harloff and Mackensen, 1997). North of this zone, calcareous biogenic sediment dominates at water depths above the Carbonate Compensation Depth (CCD), and red clay is found below it (Lisitsyn, 1972; Goodell, 1973). In ocean depths the south-to-north transition from mainly siliceous ooze to calcareous ooze occurs at the Polar Front, and the interbedding of these two sediment types is used to study changes in palaeoclimate (Deacon, 1982). One of the main characteristics of the PFZ therefore, is that it is a zone of high surface water biosiliceous production which is reflected by the predominantly biosiliceous composition of the sediments deposited beneath it (Goodell, 1973). Burckle and Cirilli (1987) recognised this phenomenon and used it to define the diatom ooze sediment belt in the Southern Ocean in terms of the position of the PFZ. They related poorly-preserved diatom assemblages north of the PF to reduced phytoplankton activity in warmer surface waters, and poor preservation to the south of the belt to the effects of winter and spring sea-ice on primary production. The presence of sand-sized ice-rafted debris (IRD) may also help to determine the position of the PFZ as it is in this region that the sediment-laden icebergs melt on contact with warmer SASW. Therefore biosiliceous sediments at the northern edge of the PFZ may be diluted by high concentrations of IRD (Westall and Fenner, 1991). South of the biosiliceous belt near the Antarctic continent is an area of terrigenous sediment deposition composed predominantly of silty diatom clay with terrigenous component derived from the continent. Variations in the terrigenous sediment-biogenic silica belts near Antarctica have been related to fluctuations in sea-ice cover (Lazarus and Caulet, 1993), and the boundary between terrigenous sediments and siliceous ooze at 60°S is equal approximately to the mean position of Antarctic sea ice (Hays *et al.*, 1976; Cooke and Hays, 1982).

North of the South Orkney Islands sedimentation rates are slow in the centre of the Scotia Sea and increase towards the north and the south (Echols, 1971). Bottom water flow controls sedimentation: in the Weddell Sea flow is relatively slow and sedimentation is continuous (Pudsey *et al.*, 1988). In the northern Scotia Sea however, towards the axis of the ACC, deep

flow is much faster and hiatuses in sedimentation are common (Ledbetter and Ciesielski, 1986).

The cores from the Western Falkland Trough (KC099, KC097 and GC062) are taken from across a sediment drift and contain three different lithofacies. Foraminiferal sands at the core tops contain 60% biogenic material and 40% from a terrigenous source, and are sandy contourites. All three of these cores from deeper water areas on the western trough contain diatom muds below the sandy unit at the core top. Poor sorting, fine grain size and high biogenic diatom content suggest deposition within a low energy, hemipelagic environment with weak current flow. At the base of cores KC097 and GC062 there is a sandy mud unit showing more input of fine terrigenous sand. From magnetic susceptibility records it can be seen that GC062 is more condensed with expanded sections as you move west (Howe *et al.*, 1997). Core TC036 is found to the east in the Falkland Trough, also located on a sediment drift and shows a similar lithology to the other Falkland Trough cores. Within this core however there are thin horizons of foraminifera-bearing muddy diatom ooze found at various depths within the core down to the base.

The cores from the northern Scotia Sea (KC064, TC077 and TC078) show a biogenic-terrigenous cyclicity, with biogenic sediment at the seabed passing down into a more terrigenous unit and eventually into another biogenic unit. The upper biogenic unit is between 0.5-2m thick and consists of dark greyish-brown foraminifera-bearing diatom mud, overlying olive grey to greenish-grey diatom mud or muddy diatom ooze. The terrigenous unit attains a maximum thickness of 2m in KC064, and consists of diatom-bearing mud (Fig.4.1). The contact with the upper biogenic unit is gradational. The lower biogenic unit is not seen in this study (Pudsey and Howe, 1998).

3.1.1. Holocene Sediments

In Holocene surface sediments (Fig.3.1) biogenic carbonate is present only at sites in the northern Scotia Sea and to the north in the Falkland Trough. In KC097 to the north of the PF, carbonate content is as high as 70% in the top samples. KC064 to the south of the PF however, contains only approximately 6% carbonate[1] in the upper part, preservation is poor and most carbonate is in the fine fraction. The dominance of the silt-sand size fraction is due

[1] $CaCO_3$ was measured by acid dissolution method (weigh dry sample, dissolve in dilute HCl,rinse,dry, re-weigh), diatom % measured by point counting (Pudsey, 1993) - data provided by C.J.Pudsey.

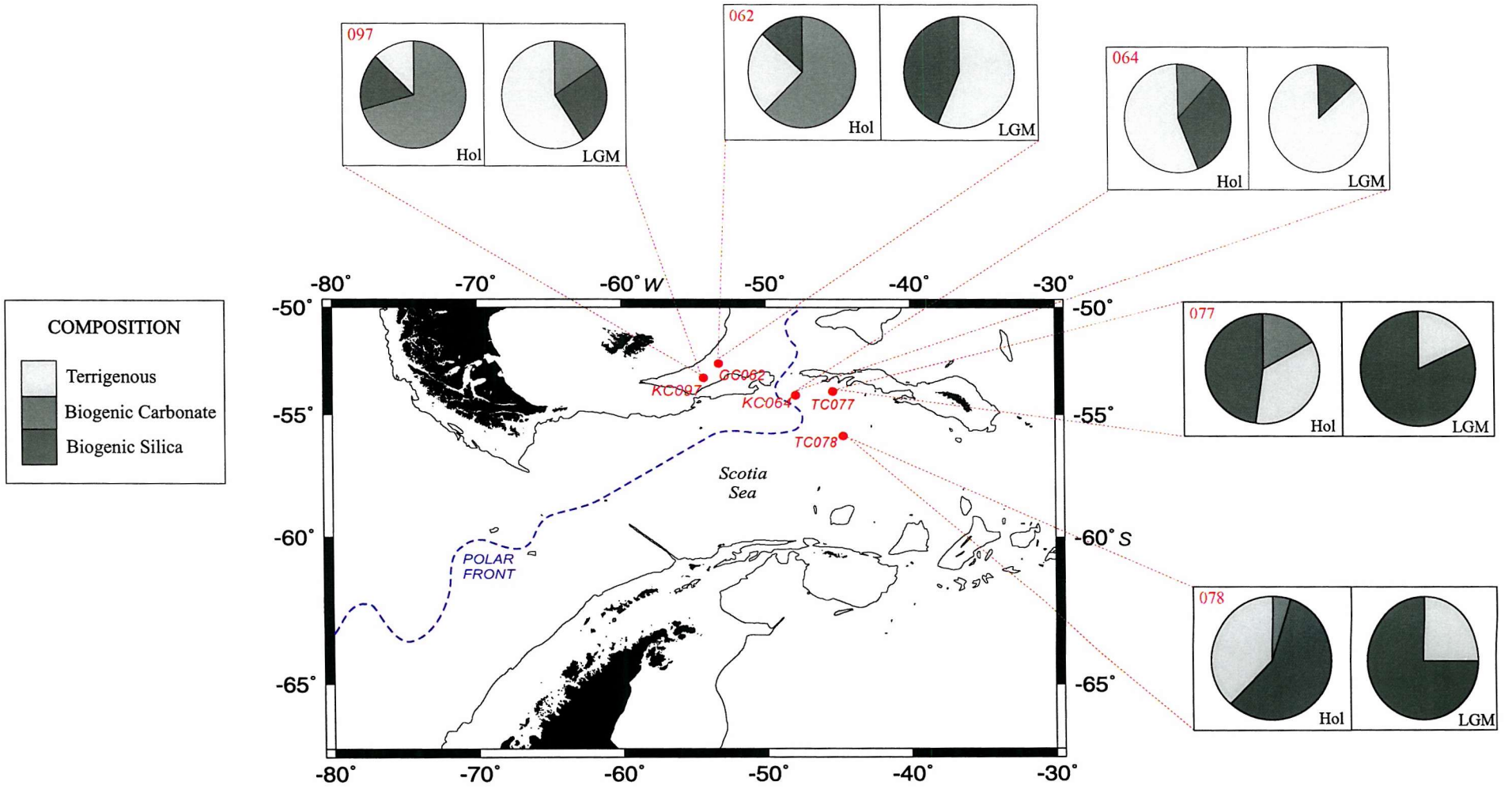

Figure 3.1. Composition of Holocene and LGM sediments at core sites. No data was available for TC036 and KC099. Holocene compositions are from core top data. Data for TC077 and TC078 is from the piston cores at those sites. Data from BAS.

to an increased flux of planktonic foraminifera (*Neogloboquadrina pachyderma*) (Mackensen *et al.*, 1993a). Modern sediments of the Subantarctic Zone are similar to those found in the oligotrophic subtropical gyres and reflect the predominance of carbonate-secreting plankton (80% carbonate, 15% terrigenous, 5% biogenic silica, Charles *et al.*, 1991). Recent sediments within and south of the PF are siliceous oozes (75% biogenic silica, 20% terrigenous, 5% carbonate, Charles *et al.*, 1991) reflecting the prominence of diatoms in Antarctic waters (Anderson *et al.*, 1998a). Biogenic silica, composed of diatoms and some radiolarians and silicoflagellates, dominate the sediments in the central and southern Scotia Sea although preservation becomes poor south of 61°S. Terrigenous material forms up to half of the sediment in the northern Scotia Sea and is the main constituent of the cores near the South Scotia Ridge, but in the deeper, more central parts of the Scotia Sea it is still not as important as biogenic silica. The texture of Holocene sediments at the core-top show a general fining trend from NW to SE, seen as a decrease in sand and silt content and an increase in clay. The sand is mainly of terrigenous origin and most of the carbonate is in the fine fraction (Pudsey and Howe, 1998).

3.1.2. Last Glacial Maximum (LGM) Sediments

Sediments from the Last Glacial Maximum (Fig.3.1) contain much less biogenic and more terrigenous material with no biogenic carbonate and a uniform content of about 20-25% biogenic silica over most of the Scotia Sea. Diatom preservation is good in the north, but poor in the southern Scotia Sea. Over the entire area of the Scotia Sea, terrigenous supply predominated over biogenic input at the LGM, in contrast to the Holocene (Pudsey and Howe, 1998). As the percentage of carbonate decreases downcore the amount of biogenic silica increases in KC097 from 17% at the top to 25% at 60cm depth. Terrigenous material predominates and is as high as 60% in KC097 and 80% in KC064 in glacial sediments. There is no carbonate present due to lower surface productivity and higher carbonate dissolution (Howe *et al.*, 1997). In the Subantarctic Zone, to the north of the PF biogenic silica accumulation rates increased several-fold during glacials (Mortlock *et al.*, 1991; Charles *et al.*, 1991) whereas carbonate accumulation rates declined sharply (Howard and Prell, 1994; Kumar, 1994). Carbonate is virtually absent from glacial sediments south of the PF in the Antarctic Zone, and this is accompanied by a decline in biogenic silica (Mortlock *et al.*, 1991) and excess barium accumulation rates (Shimmield *et al.*, 1994; Frank, 1995). This is

interpreted to reflect lower productivity south of the PF during glacial periods (Anderson *et al.*, 1998). The increasing influence of sea-ice cover during the last glacial period restricted productivity in the surface waters of the southern Scotia Sea and hence the underlying sediments were not supplied with carbonate from the surface. In the northern Scotia Sea the increased terrigenous input and lower biogenic carbonate levels at the LGM may be accounted for by an increased supply of suspended sediment from the Antarctic Peninsula, to the benthic nepheloid layer. The LGM sediments all contain less sand grade sediment than in the Holocene and almost all the sand is terrigenous. This is accompanied by increased amounts of clay compared to the Holocene samples (Pudsey and Howe, 1998).

3.1.3. Dating the Sediments

The cores used in this study have been dated using a number of different methods. The relative abundance of the diatom *Cycladophora davisiana* has been used, which was first described by Hays *et al.* (1976). They recognised that in the Southern Ocean it is present in low numbers (1-2 %) at core tops and early interglacial stage, but abundant (10-25 %) in the glacial stage. Therefore the first downcore abundance peak can be used to indicate the LGM at 18ka. Late Quaternary *C. davisiana* abundance stratigraphy has also been correlated to oxygen isotope stratigraphy in the subantarctic (Hays *et al.*, 1976) and in the North Atlantic (Morley and Hays, 1979).

The abundance of the trace element barium was first thought to be significant as an indicator of palaeoproductivity by Dymond *et al.* (1992). They suggested that barite precipitation takes place on sinking biogenic particles and is associated with organic matter decomposition. Once deposited in the deep-sea sediments it is insoluble as long as sulphate is present within pore waters (Shimmield, 1992). It is thought to be a more stable tracer of palaeoproductivity than organic carbon, biogenic carbonate or biogenic silica particularly where bottom waters are corrosive. The use of biogenic barium as a palaeoproductivity indicator has now been demonstrated in several areas of the Southern Ocean (Shimmield *et al.*, 1994; Bonn, 1995; Nürnberg *et al.*, 1997). Shimmield *et al.* (1994) and Bonn (1995) found that in the Scotia and Weddell Seas barium was high in the warm isotope stages, therefore high at core tops and showed a downcore decrease. The highest Ba/Al ratio is found at the core top in all the cores from the Falkland Trough and Scotia Sea indicating high palaeoproductivity corresponding to the carbonate-bearing interval (Dymond *et al.*, 1992). Therefore following Shimmield *et al.*

(1994) the downward decrease in the biogenic barium signal can be used to indicate the base of the Holocene, which marks the stage 1/2 boundary at about 12ka (SPECMAP age). The influence of any lithogenic barium probably from the East Scotia Sea spreading centre at 30°W, was subtracted from the total using a Ba/Al ratio (see text in Pudsey and Howe, 1998). Where available AMS radiocarbon dates from this and other studies have also been used to date the sediments.

3.2. Productivity

Variation in surface ocean productivity is considered to be an important factor controlling changes in atmospheric CO_2 and studies of deep-sea sediments have revealed large changes in productivity over the last glacial-interglacial cycle (Müller and Suess, 1979; Berger, 1989; Mix, 1989; Herguera and Berger, 1991, 1994). During the process of photosynthesis in surface waters, dissolved CO_2 is converted to organic carbon. Part of this organic carbon is transferred to the deep ocean where it is decomposed and oxidised back to CO_2. This is called the "biological pump" and it continually transfers CO_2 from the atmosphere to the deep-sea at a rate of approximately 5 x 10^6 gyr^{-1} (Martin *et al.*, 1987). The storage and transportation of CO_2 in the ocean plays an important role in the climate system (e.g. Broecker, 1982; Knox and McElroy, 1984; Wenk and Siegenthaler, 1985; Boyle, 1988; Keir, 1988, 1990; Mix, 1989).

Global ocean productivity is 26.9 $GtCm^{-2}y^{-1}$ and 13% of this total occurs in the Southern Ocean around Antarctica (south of 50°S) (Berger *et al.*, 1988). Ocean surface productivity is generally enhanced along oceanographic fronts (Yoder *et al.*, 1994) such as the SAF and PF within the ACC (Wefer and Fischer, 1991; Laubscher *et al.*, 1993; De Baar *et al.*, 1995), and the STF further to the north (Laubscher *et al.*, 1993). Surface productivity then decreases north-eastwards to the centre of the subtropical gyre (Berger, 1989). Areas closer to the Antarctic continent which are covered by winter sea ice are characterised by seasonal productivity with strong organic matter pulses associated with the spring sea ice melt (Goeyens *et al.*, 1991; Comiso *et al.*, 1993).

High productivity in the Scotia Sea occurs in a belt just south of the PF and north of the average winter sea-ice limit. This is where high accumulation rates of biogenic silica occur (DeMaster, 1981; Defelice and Wise, 1981; DeMaster *et al.*, 1991; Mortlock *et al.*, 1991;

Wefer and Fischer, 1991). Recently there have been a number of studies into the silica cycle and productivity in the Southern Ocean (Honjo *et al.*, 2000; Pondaven *et al.*, 2000; Ragueneau *et al.*, 2000), which have all shown that the PFZ is an area of significant silica and carbon primary production compared to the Marginal Ice Zone (MIZ) and the Permanently Open Ocean Zone (POOZ) (Quéguiner *et al.*, 1997). The fluxes and accumulation rates of biogenic material in the PFZ and Antarctic Zone are also higher than previously estimated. Organic carbon fluxes at 1km depth within these zones at 170°W in the Western Pacific sector of the Southern Ocean were relatively uniform (1.7-2.3 $gm^{-2}yr^{-1}$), and about twice the estimated ocean-wide average (ca. 1 $gm^{-2}yr^{-1}$). The large biogenic silica flux in this area (57 $gm^{-2}yr^{-1}$) helps to explain the high silica accumulation found south of the PF. However unlike the biogenic material, lithogenic particles were among the lowest measured in the open-ocean reflecting a low input of dust (Honjo *et al.*, 2000b). During the AESOPS cruise maximum export fluxes along 170°W were collected by a sediment trap at 63°S (221 $mgm^{-2}d^{-1}$ at 1031m; Honjo *et al.*, 2000a). Fluxes were lower at 57°S (92 $mgm^{-2}d^{-1}$ at 982m), and intermediate fluxes were collected at the PF (60°S, 156 $mgm^{-2}d^{-1}$ at 1003m). In a global context, the annual opal flux at 63°S is the largest ever measured (Smith *et al.*, 2000) and greater than that measured in the highly productive Arabian Sea upwelling system (48 $mgm^{-2}d^{-1}$ at 828m; Honjo *et al.*, 1999). Therefore despite its reputation as a region of low annual productivity, the Southern Ocean clearly generates a substantial annual flux of biogenic material which is exported to the deep sea (Smith *et al.*, 2000). Much of this high productivity is fuelled by the upwelled supply of nutrients associated with CDW (Shimmield *et al.*, 1994).

Forty percent of organic carbon exported from the photic zone of the Southern Ocean into the deep sea is synthesised in coastal zones and on continental shelves and in the PFZ, even though these zones occupy only 10% of the surface ocean area. Annual primary productivity in the PFZ is $83gCm^{-2}$ compared to an average annual primary productivity in the Southern Ocean of about $26gCm^{-2}$ (Wefer and Fischer, 1991). In the Antarctic and Polar Frontal Zones values of up to 0.8% Total Organic Carbon (TOC) content of surface sediments are measured below 2km water depth. North of the SAF down to depths of 4km TOC values vary around 0.2% but exceed 0.5% on the abyssal floor. The flux of organic carbon to the seabed exerts a strong influence on the community structure and taxonomic composition of the deep-sea benthos (Thiel, 1983; Caralp, 1984; Altenbach and Sarnthein, 1989; Loubere, 1994). The

seasonality of that flux will also influence the benthic community (Gooday, 1988; Gooday and Lambshead, 1989; Thurston *et al.*, 1994), which may show a rapid response to the increased supply of organic matter (Linke *et al.*, 1995). In recent years primary productivity and the resulting flux rates of organic carbon to the seabed have been used as a quantitative measure of food supply to benthic foraminifera (Altenbach, 1988; Altenbach and Sarnthein, 1988; Loubere, 1996; Schmiedl *et al.*, 1997).

The annual downward carbon flux at 100m water depth, a measure for the amount of carbon reaching the sediment surface may be about one sixth of the primary production in the study area (Mackensen *et al.*, 1993a). Different mathematical equations have been used to quantify these flux rates, each derived from different concepts. These empirical equations can stress either flux rates themselves (Suess, 1980; Sarnthein *et al.*, 1992) or the decrease of the fluxes with increasing water depth (Betzer *et al.*, 1984; Berger *et al.*, 1988). The equations are based on primary production, export rate, and flux rate data from sediment traps (Altenbach *et al.*, 1999). Berger *et al.* (1988) have summarised an equation for estimating this downward carbon flux by converting primary production to export production, in simple form after Suess (1980), for the top 1000m of the water column:

$$J(z) = 0.2\ PP / Z$$

where: Z = depth in units of 100m

PP = primary production

At depths greater than 1000m a term representing more slowly decomposing organic matter is needed:

$$J(z) = 0.17\ PP / Z + r^*\ PP$$

where: r = near 1%

In all locations, the flux of material reaching the seabed at depths greater than 1000m is only a few percent of the euphotic zone production, indicating that efficient recycling of production occurs in the upper few hundred meters of the water column (Loubere and Fariduddin, 1999). In some areas, like the northwest Indian Ocean and the northeast Atlantic, surface-ocean biological productivity is highly seasonal and organic matter reaches the seabed in pulses, sometimes as fresh phytodetritus (e.g. Smith *et al.*, 1996). The accumulation

of phytodetritus has been loosely related to major flux events as a result of spring/summer phytoplankton blooms. In a recent study by Mackensen *et al.* (1995) of core top samples in the South Atlantic, they recognise the presence of a "phytodetritus assemblage" to the north of the PF as indicated by the opportunist benthic foraminifera *Epistominella exigua.*

Berger *et al.* (1988) suggest that the coastal and subpolar regions account for one half of the total production and for more than 80% of the flux to the seafloor. Another important factor is the seasonality of the carbon flux that will be important in areas such as the Southern Ocean, which are ice-covered for long periods of the year. Lampitt and Antia (1997) calculated that the deep water flux and seasonal variability of organic carbon flux, with data normalised to 2000m, in polar regions is between 0.01 - 5.9 $g/m^2/y$.

Recent studies from the Southern Ocean have shown that during glacial stages, palaeoproductivity was lower south of the PF than during interglacial times (Mackensen *et al.*, 1989; Grobe *et al.*, 1990; Mortlock *et al.*, 1991; Charles *et al.*, 1991; Francois *et al.*, 1992; Kumar *et al.*, 1993; Shimmield *et al.*, 1994). Francois *et al.* (1992) suggest that the Southern Ocean polar water did not suffer major nitrate uptake during glacial times and therefore productivity was not a major influence on lowering glacial atmospheric CO_2. Glacial productivity was weaker and displaced to the north. The extent of glacial sea ice is thought to be of high importance in determining the productivity of the surface waters, and therefore the supply of biogenic detritus to Southern Ocean sediments (Shimmeild *et al.*, 1994). There is also some evidence for a decrease in productivity during a cooling event between approximately 12,000-11,000 years BP (Labracherie *et al.*, 1989; Shimmield *et al.*, 1994).

3.3. Benthic Foraminifera

The earliest account of recent benthic foraminifera from the Antarctic region was by Brady (1884) on material from the H.M.S. Challenger Expedition during 1873-1876, but this was mainly a taxonomic study (reviewed by Jones, 1994).

Much of the pioneering work was done by Earland (1933, 1934, 1936) and Heron-Allen and Earland (1932) on material from the Scottish National Antarctic Expedition and the Discovery Expedition, and also by Heron-Allen and Earland (1922) on the Terra Nova Expedition of 1910. Foraminifera collected by the British Antarctic Expedition were studied

by Chapman (1916a, b) and from the Australasian Antarctic Expedition by Chapman and Parr (1937). Another important expedition for the collection of foraminifera was the BANZ Antarctic Research Expedition studied by Parr (1950).

The next stage of research focused more on quantitative faunal studies of Antarctic benthic foraminiferal assemblages in relation to the water depth and reviewed the early taxonomic work. These studies include, among others Uchio (1960), Saidova (1961), McKnight (1962), Bandy and Echols (1964), Pflum (1966), Echols (1971), Herb (1971), Douglas and Woodruff (1981). Echols (1971) and Herb (1971) both discussed foraminiferal ecology regarding species and assemblages in the Scotia Sea and Drake Passage respectively. They both established faunal provinces (biofacies) and bathymetric zonations, recognising the importance of the PF as a division between faunas and bathymetric zones. Echols distinguished five foraminiferal biofacies associated with water depth and sediment composition. Both studies found calcareous assemblages present only at relatively shallow depths, <1600m in the southern Scotia Sea and 3500m in the Drake Passage south of the PF, as opposed to 4200m north of the PF.

During the 1970s it was recognised that the distribution of benthic faunas was not controlled by depth alone, but by hydrographic parameters which are generally correlated with depth. Numerous studies have described foraminiferal assemblages from Antarctic surface sediments and have linked their distribution to environmental parameters such as the Carbonate Compensation Depth (CCD) (Kennett, 1968; Milam and Anderson, 1981; Ward *et al.*, 1987), bottom-water masses (Lohmann, 1978; Corliss, 1979a,c, 1983b; Mead, 1985; Mead and Kennett, 1987; Jones and Pudsey, 1994; Ishman and Domack, 1994; Schmiedl *et al.*, 1997), substrate-type, productivity, oxygen content and food supply (Osterman and Kellogg, 1979; Asioli, 1995) or to a combination of these parameters (Mackensen *et al.*, 1990, 1993a, 1995; Schnitker,1994; Violanti, 1996; Harloff and Mackensen, 1997). A synthesis by Murray (1991) provided ecological information about foraminifera in environments from nearshore to the deep sea within the Southern Ocean.

However the majority of benthic foraminiferal studies from the Southern Ocean have focused on the spatial distribution of foraminifera and their relation to the present day environmental conditions using surface sediment samples, rather than examining down-core trends over a given time period. There are only a handful of studies describing the change in foraminiferal assemblage in the Southern Ocean over the last glacial-interglacial cycle, and these include

by region from the South Atlantic sector (Mackensen *et al.*, 1994; Schmiedl and Mackensen, 1997), the Weddell Sea (Mackensen and Douglas, 1989), the Southeast Indian Ocean sector (Corliss, 1979b, 1983; Corliss *et al.*, 1986; Wells *et al.*, 1994), the Ross Sea (Pflum, 1966; Fillon, 1974; Kellogg *et al.*, 1979).

Mackensen *et al.* (1994) studied the glacial-interglacial contrasts in foraminifera and stable isotopes at 69°S in the Atlantic sector of the Southern Ocean. They found that glacial stages were indicative of low biogenic silica accumulation, moderate carbonate accumulation, a benthic fauna representing low productivity, different benthic and planktonic $\delta^{13}C$ values consistent with reduced primary productivity and stratification of the water column and therefore suppressed water generation. Schmeidl and Mackensen (1997) studied cores from the northern Cape Basin in the south-east Atlantic using $\delta^{13}C$ to show that NADW flow into the Southern Ocean was restricted to interglacial periods.

3.4. Distribution of Foraminifera in the Scotia Sea

Benthic foraminifera are found in abundance in deep-sea sediments and the assemblages present are generally associated with the overall circulation pattern of the area. However, in areas of high productivity where high fluxes of organic matter occur, the faunal composition may be changed. Consequently the recorded signal represents a combination of both the bottom water mass signal and the local surface ocean productivity signal (Mackensen and Douglas, 1989; Mackensen *et al.*, 1990). In the Atlantic sector of the Southern Ocean the distribution pattern of benthic foraminiferal assemblages is generally related to bottom water mass properties (e.g., Schnitker, 1974; Lohmann, 1978; Corliss, 1979; Douglas and Woodruff, 1981), and the flux of organic matter from the surface ocean (e.g., Lutze and Coulbourn, 1984; Mackensen *et al.*, 1985; Gooday, 1988; Corliss and Chen, 1988; Loubere, 1991). Studies of foraminiferal distribution by Pederson *et al.* (1988), Altenbach and Sarnthein (1989), Herguera and Berger (1991), Altenbach (1992) concluded that food supply is a primary control on the overall abundance of benthic foraminifera at the sea floor. The organic matter flux to the sediments, and therefore the food supply to the benthos, is driven by surface ocean productivity. Therefore the adaptation of certain foraminifera to different rates of food supply may be correlated to surface ocean productivity (Loubere, 1991). In the deep sea the benthos is entirely dependent on imported organic carbon from the surface for

their energy requirements. However the flux of material reaching the seabed at depths greater than 1000m is only a few percent of the euphotic zone productivity indicating efficient recycling of production occurs in the upper few hundred metres (Loubere and Fariduddin, 1999). A review of the relationship between non-calcareous taxa and organic carbon flux is given in Gooday *et al.* (1997), and of agglutinated and calcareous taxa in Gooday (1994).

The distribution of foraminifera is also influenced by other factors including temperature, oxygen, substrate and importantly the rate of solution of calcium carbonate ($CaCO_3$) (Fig.3.2). In general, calcareous foraminifera are found in sediments above the Carbonate Compensation Depth (CCD) where water is saturated with $CaCO_3$. Agglutinated foraminifera are found in greater abundance in sediments below the CCD where water is under saturated with $CaCO_3$.

The solution of calcareous tests, shown by severely corroded specimens, occurs throughout the study area, but the rate of solution of $CaCO_3$ is apparently much higher in areas of non-calcareous assemblages in the southern and eastern Scotia Sea, than in areas of calcareous assemblages to the north. The distribution of calcareous tests and of evidence of solution of calcareous tests may be explained by the CCD rising southward from greater than 4000m on the northern Scotia Ridge to less than 500m on the southern and eastern Scotia Ridge (Echols, 1971). In the South Atlantic preservation will also correlate with changing water masses (AABW/NADW) (Loubere and Fariduddin, 1999). South of the PF organic carbon contents of greater than 0.5% at a depth of less than 4000m occur in sediments with high biogenic silica content and rapid deposition rates. Due to the decay of organic matter and carbon dioxide formation at the sediment surface, most foraminifera become dissolved forcing the lysocline up to only a few hundred metres (Mackensen *et al.*, 1993a). Therefore on the North Scotia Ridge typically 60-99% of foraminifera are calcareous at depths of 360-3400m, while on the South and East Scotia Ridges only 0-53% are calcareous at similar depths. This means that there is a concentration of planktonic and calcareous benthic foraminifera to the north and a concentration of agglutinants to the south and east (Echols, 1971).

The PF therefore serves as a limit between spatial and depth distributions of associations north and south of it. Some associations seem to be restricted to regions north of the PF while others occur in much shallower depths south of the front than north of it (Harloff and Mackensen, 1997).

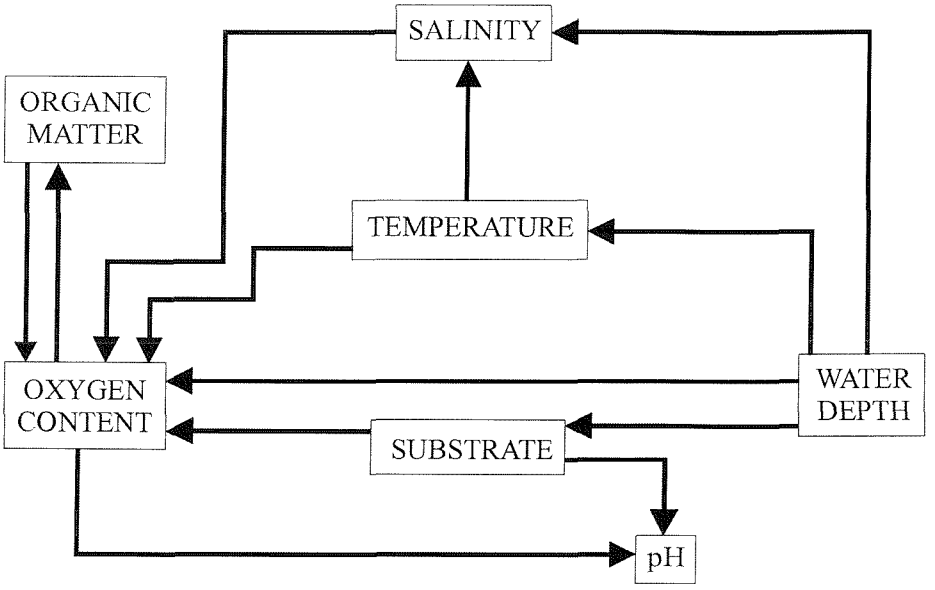

Figure 3.2. Common variables in the physical environment affecting benthic foraminifera distributions. Arrows indicate interrelationships of variables. After Van der Zwaan (1982).

3.5. Other Micropalaeontological Studies

Planktonic foraminifera from core top sediments from north and south of the PF in Drake Passage and the South Pacific sector of the Southern Ocean have been studied by Blair (1965). Chen (1966) studied live planktonic foraminifera from water samples in the Scotia Sea and Drake Passage in relation to ocean currents at various depths. Other planktonic foraminifera studies from cores in the south-east Indian Ocean (Williams, 1976) and east of New Zealand (Weaver *et al.*, 1997) refer to Quaternary fluctuations of the PF. The results of these studies will be discussed in Chapter 6.0.

Jordan and Pudsey (1992) carried out a study of the diatoms in the Scotia Sea and their record through the Quaternary. They found that the diatom content increased towards the north and that diatom-rich and diatom-poor sediments alternated downcore. The local stratigraphy was

based on the relative abundance of 6 prominent species that were assigned as environmental indicators. The changes in species composition were found to be related to the N-S movement of the winter ice edge and PF.

A recent study by Harland *et al.* (1998) reviewed the dinoflagellate cysts in a transect of core tops from the Falkland Trough to the Weddell Sea. They found a clear latitudinal trend in cyst distribution that could be divided into two domains. First, to the south of 60°S, there are low numbers of cysts and low diversity and second, to the north of 60°S, there are richer assemblages and higher species diversity. Each domain is also characterised by specific dinoflagellate species. The division between the two domains is thought to coincide with the northern limit of sea-ice.

Radiolaria from the Scotia Sea have been reviewed by T. Crawshaw (2000) in her thesis, also supported by BAS.

3.6. Stable Isotopes

Prior to a study by Grobe *et al.* (1990) in the eastern Weddell Sea, sediments from south of the present day PF were not included in the reconstruction of Quaternary stable isotope stratigraphy due to the paucity of biogenic carbonate (Hays *et al.*, 1976; Shackleton, 1977; Imbrie *et al.*, 1984; Pisias *et al.*, 1984; Prell *et al.*, 1986; Martinson *et al.*, 1987; Williams *et al.*, 1988). All interpretations of southern high latitude glacial and interglacial palaeoenvironments before this study have therefore suffered from a lack of detailed worldwide correlatable stratigraphic data. In recent years however, there has been increased interest in stable isotope records from north and south of the PF in the Southern Ocean for benthic and planktonic foraminifera, especially through the last glacial-interglacial cycle (Mackensen *et al.*, 1989, 1993b, 1994; Charles and Fairbanks, 1990; Mackensen and Bickert, 1999; Niebler *et al.*, 1999).

Grobe *et al.* (1990) found evidence for a meltwater spike at the beginning of interglacials within the oxygen isotope record, and a synchronous planktonic and benthic $\delta^{13}C$ signal indicated continuous bottom water formation during glacials. Primary productivity was also restricted during glacials due to continuous ice coverage. Mackensen *et al.* (1989) have also presented a stable isotope stratigraphy for both planktonic and benthic foraminifera from 69°S in the Weddell Sea which has been correlated with the global isotope stratigraphy. The

benthic and planktonic $\delta^{18}O$ records are thought to reflect global continental ice volume changes and the influence of a meltwater lid respectively. Peak values of planktonic and benthic $\delta^{13}C$ in warm periods suggest increased surface productivity during interglacials within the Southern Ocean.

Only a few isotope records from Subantarctic and South Atlantic cores have been published (Hays *et al.*, 1976; Curry and Lohmann, 1982; Labeyrie and Duplessy, 1985; Labeyrie *et al.*, 1987; Oppo and Fairbanks, 1987; Curry *et al.*, 1988; Mulitza *et al.*, 1999).

3.6.1. Background to Stable Isotopes

Oxygen ($^{18}O/^{16}O$) and carbon ($^{13}C/^{12}C$) are included in probably the most important family of palaeoclimatic tools used to reconstruct past climates. The ratio of two isotopes of a particular element is expressed using the following convention, taking carbon as an example:

$$\delta^{13}C = \frac{(^{13}C/^{12}C)\ \text{sample} - (^{13}C/^{12}C)\ \text{standard}}{(^{13}C/^{12}C)\ \text{standard}} \times 1000$$

The principal rationale behind stable isotopes as proxies is that the ratio of heavy to light isotopes of an element in any material is a function of many variables, including climate-related variables such as sea surface temperature (SST), salinity, ice volume, atmospheric temperature and moisture source (Cronin, 1999).

All modern calcareous foraminifera are calcitic with the exception of the suborder Robertinina. Biogenic calcite should be secreted in isotopic equilibrium with the ambient seawater, however often this does not happen and disequilibrium is caused. The observed offsets must be due to fractionation processes during the uptake of carbon into calcite, the so-called vital effects (Grossman, 1987; Ravelo and Fairbanks, 1995). These include:

1. Uptake of metabolic CO_2 during calcification,
2. Growth or calcification rate,
3. Physiological changes with ontogeny,
4. Kinetic isotope effects in the transport of carbonate ions to the site of calcification,
5. Photosynthetic utilization of light carbon by symbionts which increases the available ^{13}C for calcification.

Vital effects may lead to carbonates being depleted in ^{18}O relative to equilibrium (Williams *et al.*, 1981; Grossman, 1987). Other influences on the isotopic composition of ^{18}O include changes in ambient water temperature, changes in the evaporation/precipitation at the site of formation of the water mass under study, differential dissolution, sediment transport, bioturbation and stratigraphic disturbance (Imbrie *et al.*, 1984).

Variations in the proportions of ^{13}C and ^{12}C in biogenic carbonates are caused by (Murray, 1991):

1. Global and regional changes in surface-water productivity,
2. Different water masses and circulation patterns,
3. Vital effects,
4. Microhabitat effects,
5. Postdepositional dissolution.

3.6.2. Oxygen Isotopes

Ice sheets lock up huge amounts of freshwater and prevent normal recirculation of this water back into the oceans. Freshwater is enriched in ^{16}O, and increased growth of ice caps draws more water from the oceans, leading to a drop in sea level and relatively higher concentrations of ^{18}O (the heavier isotope) in the remaining seawater. When Emiliani pioneered the use of oxygen isotopes for studies of deep-sea cores in the 1950s, he recognised the isotopic signal is due to two main factors: growth temperature and isotopic composition of seawater. It is now accepted that the dominant signal is due to change in seawater composition, and oxygen isotopic ratios are now used as a "continental global ice-volume" signal, with temperature playing a secondary role (Shackleton and Opdyke, 1973). Lighter values of the oxygen isotope indicate periods with less continental ice and conversely during glacial periods, ice preferentially stores the light isotope (^{16}O) and seawater is enriched in ^{18}O (Kennett, 1982). The "glacial effect" (Olausson, 1965; Shackleton, 1967) is believed to dominate the isotopic signal in foraminifera in regions with relatively small temperature and salinity variability or deep-sea abyssal environments.

Each distinct isotopic event over the last 1 million years has been assigned a stage number by Emiliani (1955; 1966) and Shackleton and Opdyke (1973). These isotopic stages represent alternating interglacial and glacial episodes, with the present interglacial stage being referred to as isotope stage 1 and the last glacial as stage 2.

3.6.3. Carbon Isotopes

Shackleton (1977) showed the use of $\delta^{13}C$ and its potential significance in studying water mass movement and palaeoproductivity, and suggested a connection between climatically induced changes in the terrestrial biosphere with observed carbonate dissolution cycles and the flux of dissolved CO_2 in the oceans. Biological and chemical processes that fractionate carbon isotopes in the ocean provide one of the most useful tracers for reconstructing past distributions of water masses and their properties. The present distribution of $\delta^{13}C$ of ΣCO_2 delineates the general distribution of water masses in the oceans, and the gradients in $\delta^{13}C$ between locations record the net flow direction between ocean basins (Curry *et al.*, 1988).

The distribution of $\delta^{13}C$ in the ocean is controlled principally by photosynthesis and remineralisation of organic carbon, and by the mixing between water masses of different isotopic composition. Photosynthesis in surface water preferentially extracts ^{12}C from seawater, causing the enrichment of the surface water ΣCO_2 in ^{13}C (Curry *et al.*, 1988). The value of $\delta^{13}C$ in seawater, after primary producers have removed all nutrients, is controlled by the mean $\delta^{13}C$ and the mean nutrient concentration of the ocean (Broecker, 1982; Broecker and Peng, 1982). Deep waters of the oceans typically exhibit higher concentrations of nutrients and CO_2 compared with surface waters as a result of organic processes involving photosynthesis, sinking of organic debris, and respiration by bottom dwelling organisms. As deep water remains near the ocean floor for longer periods, nutrients and CO_2 continue to accumulate and O_2 content decreases. Because of the close relationship between accumulation of $\delta^{13}C$ and CO_2, the $\delta^{13}C$ can represent a valuable tracer of nutrient flow through the World Ocean. The $\delta^{13}C$ of deep-water CO_2 is lower than in surface water due to accumulation of metabolic carbon. Therefore any major change in the cycling of nutrients and CO_2 in the deep ocean is reflected in $\delta^{13}C$ and thus recorded in microfossils (Kennett, 1982).

In most oceans a linear correlation is seen between $\delta^{13}C_{\Sigma CO2}$ values and nutrient contents of deep and bottom water masses because the distribution of both are controlled by the interaction of biologic uptake at the sea surface and decomposition in deeper water masses, with the general circulation of the ocean (Kroopnick, 1980; Kroopnick, 1985). This $\delta^{13}C$ signal of the water masses is recorded in the shells of benthic foraminifera and is therefore used as a nutrient proxy to explain deep water palaeocirculation (see Duplessy *et al.*, 1984;

Curry *et al.*, 1988; Oppo *et al.*, 1990; Raymo *et al.*, 1990; Boyle, 1992; Sarnthein *et al.*, 1994).

Chapter Four

MATERIALS AND METHODS

4.1. Core Sites

A series of kasten, gravity and trigger cores were collected by BAS from the Scotia Sea during the RRS *James Clark Ross* cruises JCR04 (1993) and JCR09 (1995) and the RRS *Discovery* cruise D172 (1987-88). The seven cores studied here were chosen based on their position relative to the modern-day Antarctic Polar Front and form a transect across the Polar Front (PF) from north-west to south-east in the northern Scotia Sea (Fig.1.1) The cores contain a relatively high proportion of carbonate material throughout the top section or at least in the core top. Core locations and water depths are given in Table 4.1 and complete core logs and magnetic susceptibility curves can be seen in Figures 4.1, 4.2 and 4.3.

The kasten cores were opened and subsampled on board ship before being stored horizontally at +4°C, first on board ship and subsequently at BAS. Piston cores were split and described, then sampled for micropalaeontological, geochemical and grain size analysis. Each half of a split core was encased in (i) cling film; (ii) layflat tubing, and stored horizontally in a cold room maintained at +3°C to +6°C. Radiolarian species counts were made on sand-fraction

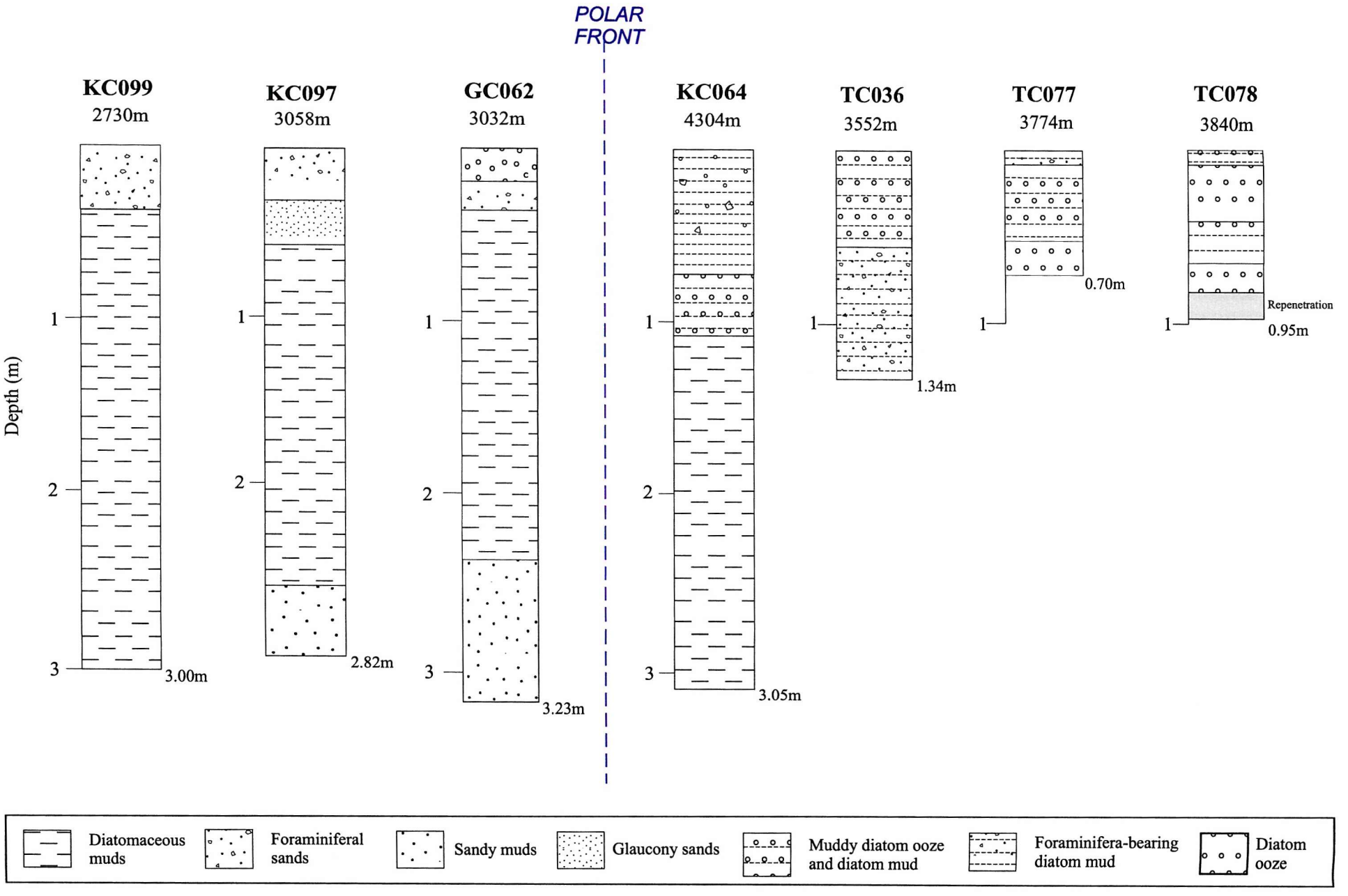

Figure 4.1. Core logs.

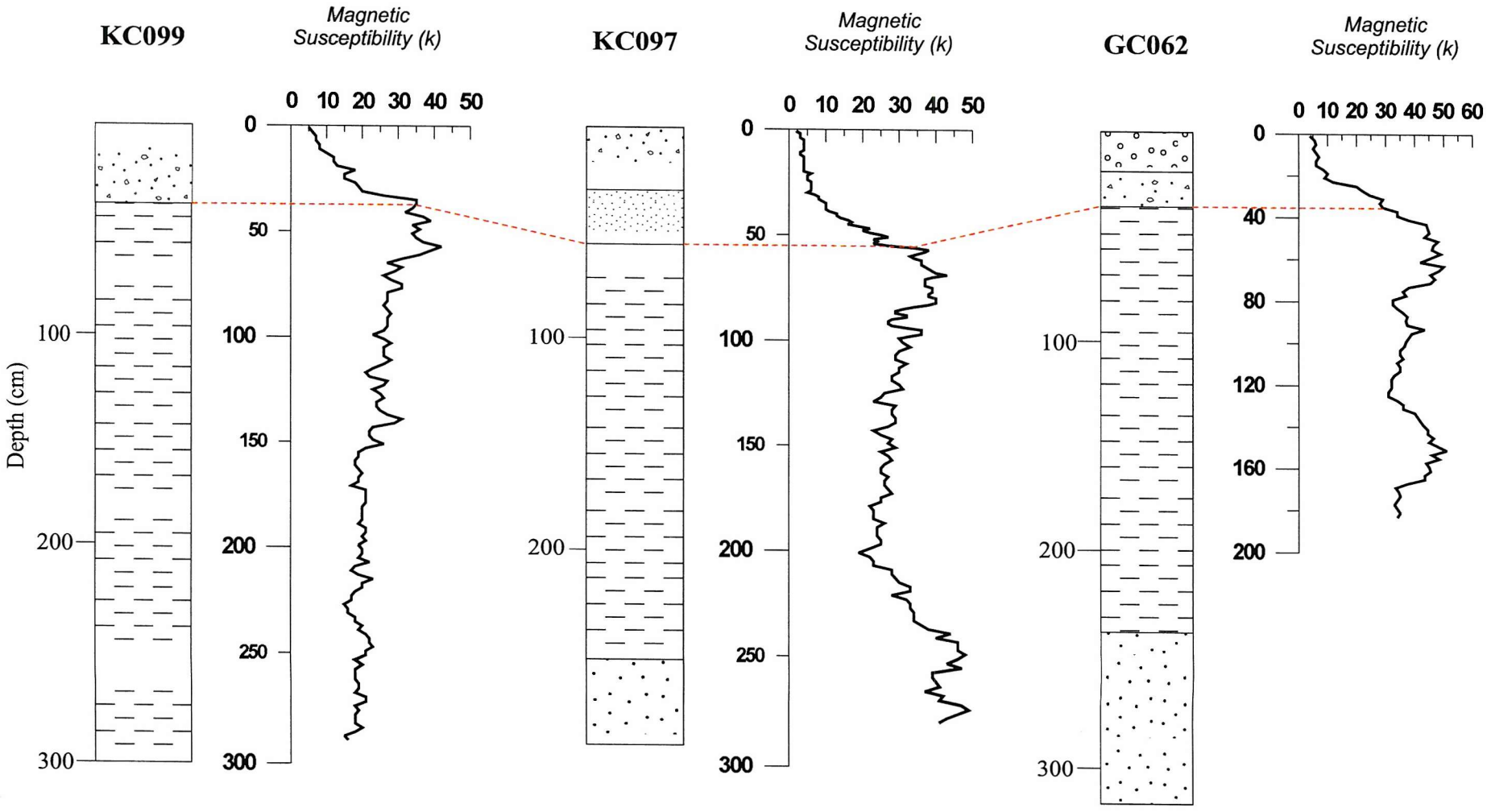

Figure 4.2. Magnetic susceptibility for cores from North of the Polar Front (see Fig. 4.1 for lithological key). The magnetic susceptibility corresponds to the lithological cyclicity, with very low susceptibility in the upper biogenic unit and high susceptibility in the terrigenous unit. The red line is the change from the biogenic unit to the terrigenous unit correlated between the cores.

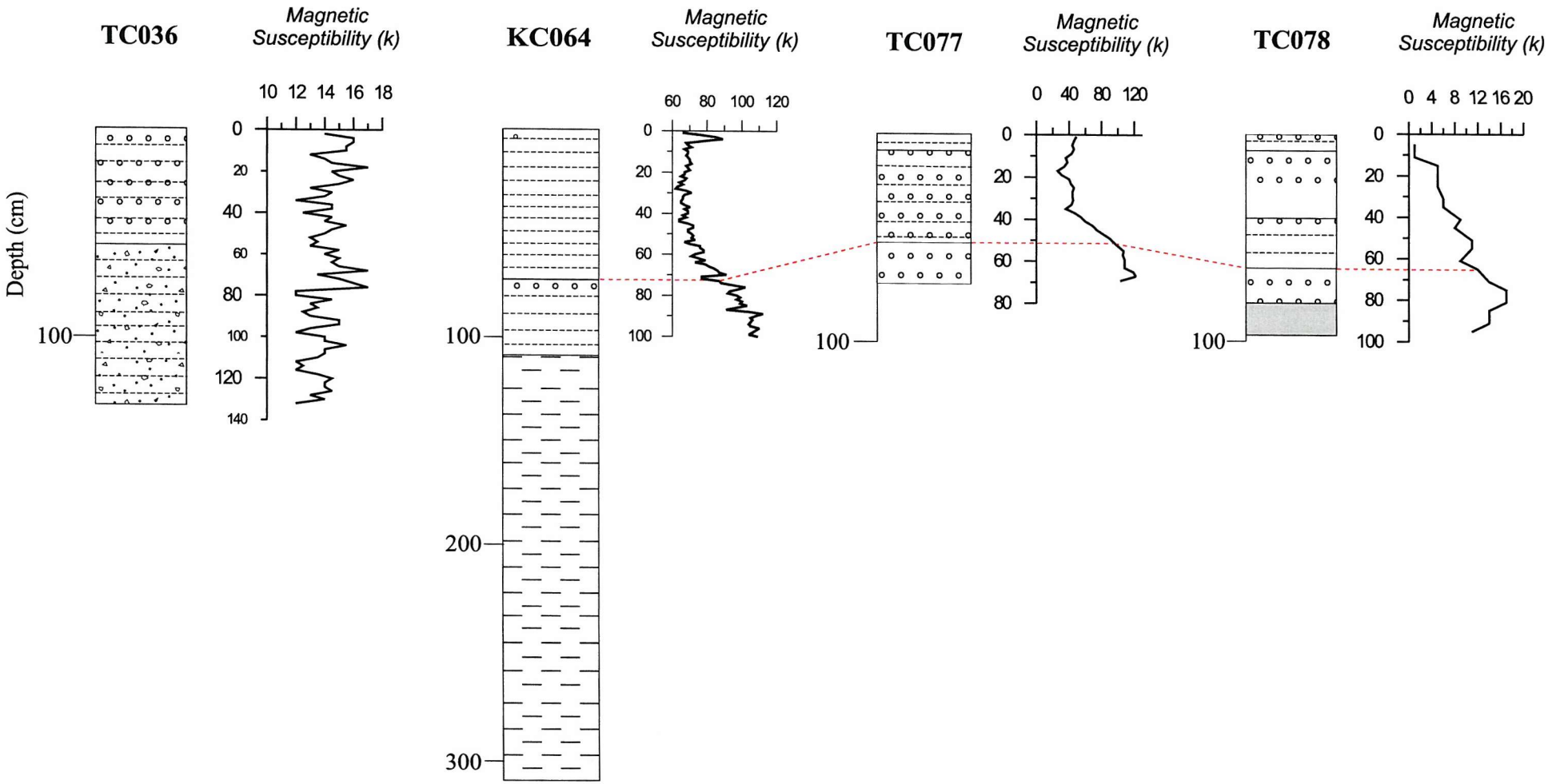

Figure 4.3. Magnetic susceptibility for cores from South of the Polar Front..

slides prepared by a random-settling method. Major and trace element geochemistry was determined by x-ray fluorescence on powdered bulk sediment samples. All these procedures were carried out by BAS.

Core	Depth (m)	Latitude (°S)	Longitude (°W)	Core length (cm)
KC097	3058	53°21.0′	54°41.0′	282
KC099	2727	53°30.0′	57°02.8′	300
GC062	3000	52°55.5′	53°41.0′	323
KC064	4304	53°52.1′	48°20.3′	305
TC077	3774	53°55.0′	45°28.0′	70
TC078	3840	55°33.0′	45°00.9′	95
TC036	3552	52°36.2′	46°52.7′	134

Table 4.1. Core details.

The distance of each core from the PF was determined as the PF is a sinuous frontal feature and therefore longitude and latitude may not be a realistic x-axis for plots of geographical variation. The cores were measured perpendicular to the PF and the distance was converted to nautical miles and kilometres using the map in Text-Fig. 2 in Harland *et al.* (1998).

Core	Distance from Polar Front (km)
KC099	444 N
KC097	296 N
GC062	222 N
KC064	88 S
TC036	185 S
TC077	267 S
TC078	282 S

Table 4.2. Distance of core sites from the present day position of the Polar Front.

4.2. Sampling

Samples were taken from the working half of each core initially at 5cm intervals in the top 1m and then every 20cm from 1m downcore to the base. This strategy was used as there appeared to be a change in sediment character from more foraminiferal-rich sand and mud to purely diatom mud with few foraminifera, through the cores (Fig.4.1). In cores TC077 and TC078 only core top samples were picked as there was no carbonate observed below about 20cm. For cores GC062 and TC036 samples were taken at more irregular intervals in some sections and this was dependent on the raw material that had been available at BAS to sample.

After initial results had been obtained, some sections of the cores were re-sampled at closer intervals where greater fluctuations in foraminiferal abundance were observed. This was either a sample taken between the 5cm gaps or as in KC064 and KC097, samples were then taken every 1cm in some sections.

4.3. Processing

4.3.1. Foraminifera

Approximately $1cm^3$ of sediment was taken form the core and dried overnight in an oven at no greater than 60°C to remove excess water. The sample was then allowed to cool and weighed to provide the dry weight. For foraminiferal analysis the sample was then left for 24 hours to soak in warm water containing 5% Calgon (sodium hexametaphosphate) until it had disaggregated. Each sample was washed gently through a 63μm mesh sieve and dried, the greater than 63μm fraction was then weighed when dry. The fine fraction (<63μm) was collected on filter paper for possible coccolith study. A 63μm mesh sieve was used in order to retain any small benthic foraminifera which may be important constituents of the assemblage. Other benthic foraminifera studies from the area have used either a 63μm or 125μm mesh sieve and it can be noted that the larger sieve size did not retain some of the foraminifera found in high abundance in this study.

For benthic foraminiferal counts a split was made and the weight recorded to enable the number of foraminifera per gram of sediment to be calculated. Approximately 250

individuals were counted, picked and identified (full taxonomic list in section 11.0); planktonic foraminifera were also counted for absolute abundance and Planktonic/Benthic foraminifera ratios, from the same >63μm size fraction sample and the different species present were noted. The identification of the species *Eilohedra weddellensis* follows that of Echols (1971) from a study of benthic foraminifera in the Scotia Sea. Classification of planktonic foraminiferal distributional zones is based on Blair (1965) and Bé (1969, 1977). In some samples fewer than 250 benthic foraminifera were counted, as the abundance was lower. Duplicate counts of planktonic foraminifera were also carried out on certain samples in one of the cores to test the accuracy of the counting method. This reproducibility data can be seen in Appendix 1.

4.3.2. Diatoms

A smear slide was made of each sample using standard preparation techniques and these were used to look at the general faunal and lithological composition and for identifying any diatoms present. The slides were examined using an Olympus BH-2 light microscope under normal illumination for the presence of the diatoms *Nitzschia curta* and *Nitzschia cylindrus* (sea-ice indicator species), *Thalassiothrix antarctica* (Antarctic open ocean species) and *Eucampia antarctica* (glacial ice indicator species). Their abundance was estimated by indicating whether they were absent, rare, common or abundant in the sample. Diatom results from cores KC064 and KC097 only will be presented here in Appendix 18 and discussed in Chapter 6.0.

4.3.3. Stable Isotopes

Stable isotopes are analysed by mass spectrometric determination of the mass ratios of carbon dioxide (CO_2) obtained from the sample, with reference to a standard CO_2 of known composition. The CO_2 is produced by reaction of the carbonate with 100% orthophosphoric acid at 70°C. During each run a reference carbonate (H1) of known composition is analysed as a standard for each carousel run. Each sample is analysed sequentially using the individual acid dosing or 'drip' method, in which a small amount of acid is allowed to drip onto the sample, the product being frozen out (S. Cooke pers. comm., 1999). Such a method is employed by the Europa Scientific Geo 20-20 Stable Isotope Ratio Mass Spectrometer (IRMS) based at the Southampton Oceanography Centre operated by Steve Cooke, and is a

fully automated, memory free, preparation device for determining $\delta^{13}C$ and $\delta^{18}O$ in carbonate samples.

Isotope data are reported in conventional per mil (‰) deviations from the Vienna Pee Dee Belemnite (PDB) standard, which is a Cretaceous belemnite from the Pee Dee formation of South Carolina, PDB having $\delta^{18}O = 0$ and $\delta^{13}C = 0$ by definition (Epstein *et al.*, 1953). However, the PDB standard is now unavailable and instead two additional standards with known δ values relative to the PDB standard are used to calibrate this method to the Vienna PDB scale. These are NBS-18 (carbonatite) and NBS-19 (limestone). The composition of the H1 standard was calculated using NBS-19, and checked periodically against NBS-18.

All results are given in the standard δ notation and have an analytical precision of better than +/- 0.02‰ for $\delta^{13}C$ and +/- 0.04‰ for $\delta^{18}O$. More positive values indicate enrichment of the heavy isotope relative to the standard. These δ values are for the sample gas and not for the carbonate. A fractionation effect occurs during the reaction due to the temperature at which this is taking place, resulting in an offset from the isotopic composition of the carbonate. The offset or fractionation factor for oxygen for the Geo 20-20 is $\alpha = (\delta^{18}O)_{carbonate} / (\delta^{18}O)_{CO2} = 1.00844$. The $\delta^{18}O$ is corrected for the α-fractionation factor and both $\delta^{18}O$ and $\delta^{13}C$ are normalised to the H1 standard and so to the PDB scale.

Samples from five of the cores studied were submitted for carbon and oxygen stable isotope analysis. Measurements were made on planktonic foraminifera from cores KC064, KC097, KC099 and GC062. Results were also available from TC036 (pers. comm. C.J.Pudsey, measurements made by Caroline Bertram at BAS and the University of Cambridge). The planktonic foraminifer *Neogloboquadrina pachyderma* sinistral was used, and samples for analysis contained on average 15 specimens picked from the 150-250μm size fraction. This required dry sieving the processed sediment at 125μm to remove any small material. Where possible, foraminifera without signs of partial dissolution were selected for isotope analysis.

Measurements were carried out on benthic foraminifera in samples from cores KC064, KC097 and TC036. The benthic species *Oridorsalis tener* was used as it was found to occur persistently throughout the core, although in very low numbers at certain depths. On average 15 specimens were picked from the 125 - 250μm size fraction for each sample. In a study by Graham *et al.* (1981), *O.tener* was found to have a deviation from ^{18}O equilibrium of about -

0.4‰ (*Uvigerina* spp. and *Pyrgo murrhina* also have similar values). Woodruff *et al.* (1980) carried out a study on a number of different benthic foraminifera species from the East Pacific Ocean and found that they all probably deposited calcite out of equilibrium with the growth environment. The $\delta^{13}C$ value of dissolved HCO_3^- in deep Pacific equatorial waters is quite uniform at +0.13 ±0.5‰ (Kroopnick, 1974) and therefore using the fractionation factor of Emrich *et al.* (1970), the $CaCO_3$ in equilibrium with that HCO_3^- at 1.5°C has a value of +1.19‰. All of the foraminifera were found to be depleted in ^{13}C relative to the equilibrium value and Woodruff *et al.* (1980) calculated that *Oridorsalis umbonatus* had a deviation from ^{13}C equilibrium of between -1 and -1.5‰. Disequilibrium values between species are often not constant and this has important consequences for downcore isotope curves (Belanger *et al.*, 1981), and it is therefore useful to use a single species rather than a mix of different species.

4.3.4. Radiocarbon Dates

Accelerator Mass Spectrometry (AMS) ^{14}C dating was carried out on 16 samples from cores KC064, KC097, KC099 and GC062 and consisted of foraminiferal carbonate and bulk organic carbon samples. The aim of the radiocarbon age analysis was to determine whether a glacial meltwater event identified from the stable isotope records in two of the cores was synchronous through all 4 cores from the northern Scotia Sea. Also, to date the core top samples in order to determine the completeness of the stratigraphic record and the reservoir effect. A sample list and the reason for each analysis is shown in Appendix 2.

Two dates for the core top were requested for KC097 and KC064, one on foraminiferal carbonate and one on bulk organic carbon. The request was made in light of interesting results obtained under allocation 650/0596 for Scotia Sea material (see Howe and Pudsey, 1999). That study included two such pairs of dates, one for a core top and one for a sediment trap at the same site. The results showed that there was a bigger offset at the core top than in the trap (about 1000 years difference), which may indicate that in the long term there is more reworking of "old" fine-grained organic carbon than foraminifera tests. The results from the radiocarbon dating in this study may help to support this idea, although there are no other sediment traps available for analysis at this time.

The samples for radiocarbon dating were chosen based on the oxygen and carbon stable isotope records and the foraminiferal abundance curves from all four cores. Dates were

already available from BAS for core 063[2] - PC063 and TC063, which is located close to KC064 in the North Scotia Sea. Using magnetic susceptibility curves for KC064 and core 063 it was possible to correlate between them and estimate some dates at points in KC064. These dates could then be correlated to KC097, KC099 and GC062, again using magnetic susceptibility to estimate dates for all the samples being submitted for analysis. In all these cores magnetic susceptibility is generally variable downcore even though the sediment appears homogenous, and this provides a powerful tool for correlation. Susceptibility depends on the concentration and grain size of ferri-magnetic minerals (review in Robinson, 1990), which are related to the terrigenous source composition and dilution by biogenic material. In the Scotia Sea susceptibility generally decreases from NW to SE (Pudsey and Howe, 1998).

The foraminiferal carbonate samples consisted of specimens of *Neogloboquadrina pachyderma* (s) picked from the greater than 125μm size fraction. For most samples at least 15mg was submitted, but the samples from KC064 to the south of the PF contained fewer foraminifera so smaller samples were picked (at least 2mg). For the core top bulk organic carbon samples, more than 1 gram of sediment was supplied for analysis. All samples were sent to the NERC Radiocarbon Laboratory in East Kilbride for preparation to graphite. The larger samples were then sent to the University of Arizona National Science Foundation-AMS facility, and the smaller samples to the Centre for Accelerator Mass Spectrometry, Lawrence Livermore National Laboratory, University of California, for ^{14}C analysis.

The bulk organic carbon samples required pre-treatment to remove any carbonate inclusions. The sediment was digested in 2M HCl (80°C, 10 hours) washed free of mineral acid with distilled water then dried and homogenised. The total carbon in a known weight of the pre-treated sample was recovered by combusting to CO_2 by heating with CuO in a sealed quartz tube. The gas was then converted to graphite by Fe/Zn reduction. The foraminiferal carbonate samples did not require any pre-treatment. The samples were hydrolysed to CO_2 using 85% orthophosphoric acid at 25°C. The gas was converted to graphite by Fe/Zn reduction.

In keeping with international practice the results are reported as conventional radiocarbon years BP (relative to AD 1950) and % modern ^{14}C, both expressed at the +/- 1σ level for overall analytical confidence. The dates have not been converted to calendar years for discussion in this study (see Bard *et al.*, 1990).

[2] Core 063: latitude - 53°56.00'S, longitude - 48°02.60'W, depth - 3956m.

4.3.5. Scanning Electron Microscope (SEM)

Benthic and planktonic foraminifera were picked and mounted on SEM stubs and viewed using the Cambridge Instruments S360 SEM at BAS. These plates can be seen in section 11.0.

4.4. Statistical Methods

4.4.1. Absolute and Relative Abundance

Absolute abundance refers to the number of individuals in a certain volume of sediment. This was calculated for planktonic and benthic foraminifera by:

$$N = \frac{\text{no. foraminifera counted}}{\text{wt. foraminifera counted (g)}} \times \frac{\geq 63\mu\text{m fraction wt. (g)}}{\text{sample wt. (g)}}$$

where N = number of foraminifera in 1gram of dry sediment.

Relative abundance is the proportion of a species of the entire assemblage, e.g. percentage:

$$(N / N_{TOTAL}) \times 100$$

where N = number of individuals in a certain species.

N_{TOTAL} = total number of individuals in a sample.

All species with a relative abundance of greater than 5% were considered as significant, as this was considered to be the point at which the species became statistically important. At abundances lower than 5% the error bar may be greater than the occurrence of the species in certain samples.

4.4.2. Planktonic : Benthic Ratio

To record the planktonic : benthic ratio the proportions of each need to be determined:

$$(P / P+B) \times 100$$

where P = number of planktonic foraminifera in dry weight.
B = number of benthic foraminifera in dry weight.

There are a number of generally accepted indexes of dissolution in deep-sea sediments including planktonic/benthic foraminiferal ratio, percentage of calcium carbonate and percentage of fragmentation of tests (Berger, 1973; Gardner, 1975; Thunnell, 1976). In this study the planktonic/benthic ratio and the percentage of carbonate will be used to indicate the occurrence of dissolution, and the general state of preservation of the foraminiferal test will also be noted.

The planktonic/benthic ratio (P:B) is commonly used as a generalised palaeobathymetric indicator. Phleger (1964) noted that planktonic foraminifera are found in greater densities in open ocean environments than benthic foraminifera, which show higher productivity in neritic environments than in the deeper ocean. Therefore as the depth of water and distance from shore increases in an open ocean, the P:B ratio should also increase (Gibson, 1989). However in this study the P:B ratio is more useful as an indicator of dissolution down core through the last glacial-interglacial cycle.

4.4.3. Sediment Accumulation Rate

The mass accumulation rate for sediments (Prell *et al.*, 1982) and benthic foraminifera (Herguera and Berger, 1991; Herguera, 1992) have been determined as follows:

$$\underset{(g/cm^2/kyrs)}{\text{Sediment Accumulation Rate (SAR)}} = \underset{(cm/kyrs)}{\text{Sedimentation Rate}} \times \underset{(g/cm^3)}{\text{Dry Bulk Density (DBD)}}$$

$$\text{Benthic Foraminiferal Accumulation Rate (BFAR) (BF/ cm}^2\text{/kyrs)} = \text{SAR} \times \text{no. foraminifera per gram dry sediment}$$

Dry bulk density had not been previously measured for all cores and so was calculated as follows, using a water content of 40% as an example:

water density = 1.00 x 0.4 = 0.4

quartz density = 2.65 x 0.6 = 1.59

wet density = 1.99 g/cc

When the same sample is dry:

air density = zero (nearly) x 0.4 = 0

quartz density = 2.65 x 0.6 = 1.59

DBD = 1.59 g/cc

The number of foraminifera produced per unit area per unit time depends on the supply of organic matter to the sea floor, and this is a reflection of the productivity within the photic zone (Herguera, 1992). This assumption appears to be reasonable in light of earlier studies of foraminifera (see full list of studies in Herguera, 1994). However, one factor which may affect the reliability of this calculation is the constancy of the sedimentation rate throughout the core (Herguera, 1992).

Therefore the BFAR may be used to estimate the palaeoflux of organic matter to the seabed and in turn surface water palaeoproductivity (Herguera, 1992; Berger and Herguera, 1992). It is important to quantify the export of organic carbon from the uppermost water layer as this export affects the partial pressure of the CO_2 in the surface waters and hence the partial pressure of CO_2 within the atmosphere (Herguera, 1992).

4.4.4. Species Diversity

It is known that the diversity of foraminiferal assemblages depends on macroenvironmental factors such as the latitude and depth in which the assemblage is found. Therefore this is the basis for using the diversity of fossil foraminiferal assemblages as palaeoenvironmental indicators (Pielou, 1979).

In simple terms, the diversity of a community is a measure of the number of species and the evenness with which the individuals are apportioned among them (Pielou, 1975). There are a number of available indices for calculating diversity (Peet, 1974) but only two of the more commonly used methods are discussed here.

(i) *The Information Function*

The Shannon-Weaver formulation based on the information theory (H) is often used as an index of heterogeneity (see Pielou, 1974 for a full overview). It is valuable as it takes into account the number of species and the distribution of individuals between the species. The role of evenness in the abundance of species was termed 'equitablility' by Peet (1974).

$$H(S) = -\sum_{i=1}^{s} p_i \ln p_i$$

where s = number of species.

p_i = the proportion of the ith species (p = percent divided by 100).

A low value of H(S) indicates that most individuals of an assemblage are concentrated in a few species, whereas a higher number indicates that they are more equally distributed among a larger number of species (Echols, 1971).When all species have equal abundances the maximum value of H is attained:

$$H(S)_{max} = \ln S.$$

There are problems with using the information function, which should be taken into consideration. The function strongly depends on the sample size and is usually an underestimate for a given sample. This is due to the problem of inadequate sample size and the need to recognise every species present. Also microenvironmental factors influence diversity as well, making it impossible to determine the properties of the macroenvironment from the diversities of only one or a few sample assemblages (Pielou, 1979).

(ii) *Fisher Alpha Index* (α)

The most frequently used measure of species richness is the α index first described by Fisher *et al.* (1943). The index assumes that the number of individuals of each species follow a logarithmic series and it also takes the rarer species into account.

$$\alpha = \frac{n^1}{x}$$

where x = constant of value <1.

$n^1 = N(1-x)$, where N = number of individuals.

An advantage of this index is that values can be read directly from a base graph by plotting the number of species against the number of individuals in a sample. Ideally it should be applied only to samples where the number of foraminifera exceeds 100 as this is the lowest acceptable value (Murray, 1973). A high value for α indicates increased foraminiferal diversity within the assemblage. The index is a useful method for comparing samples of different sizes and to see whether the difference between samples is due to the size or some ecological factor.

4.4.5. PRIMER V5.0 and 5.1 (Plymouth Routines In Multivariate Ecological Research)

Three types of analyses have been used and are described from Clarke and Warwick (1994).

(i) ***Cluster Analyses***

This uses a similarity matrix based on the Bray-Curtis Coefficient, which results from a terrestrial application (Bray and Curtis, 1957), and measures the similarity of species abundance/biomass between samples. A view in which most emphasis is on the pattern of occurrence of the rare species may be different from one which the emphasis is wholly on the handful of species that numerically dominate most of the samples. Therefore the answer may be to restrict the analysis to a single similarity coefficient (i.e. Bray-Curtis Coefficient) but allow a choice of transformation of the data. There is a transformation continuum which ranges through none, square root, fourth root, logarithmic to recording only the presence or absence for each species. At the former end of the spectrum all attention will be focused on the dominant counts, at the latter end the rarer species. The data have been used either with no transformation or a 4th root transformation. The 4th root transformation of the data has a fairly severe effect in down-weighting the importance of the very abundant species, so that the less dominant and even the rare species play some role in determining the similarity of two samples.

In this analysis a hierarchical clustering method is used where the samples are grouped and the groups themselves form clusters at lower levels of similarity. The aim is to find «natural groupings» of samples. All samples with fewer than 60 benthic foraminifera have been excluded from the analysis to allow interpretable clustering.

(ii) *MDS (non-metric Multi Dimensional Scaling)*

The starting point for this analysis is the similarity matrix from the cluster analysis. MDS constructs a "map" or configuration of the samples, in a specified number of dimensions, which attempts to satisfy all the conditions imposed by the rank similarity matrix. Each configuration may show some "stress" between the similarity rankings and the corresponding distance rankings in the ordination plot. Therefore the principle of the MDS algorithm is to chose a configuration of points which minimises this degree of stress. Stress will increase with reducing dimensionality of the ordination but also with increasing quantity of data, and a rough guide to the interpretation of the level of stress is shown below:

< 0.05 = an excellent representation with no prospect of misinterpretation.
< 0.1 = good ordination with no real prospect of a misleading interpretation.
< 0.2 = still potentially useful 2-D picture, though not too much reliance should be placed on the detail of the plot, and a cross-check should be made using an alternative technique.
> 0.3 = indicates the points are close to being arbitrarily placed in the 2-D ordination space.

(iii) *Principal Components Analysis (PCA)*

A primary problem in studies of relative frequency data is the need to reduce a large data-set by using a multivariate statistical technique into a few, palaeontologically meaningful variables (principal components), which contain the essential information about the complex interrelations among the species. These variables are often interpretable in terms of the underlying environmental causes to which associated species may have responded in a similar manner (Malmgren and Haq, 1982). There are two types of principal components analysis, Q-mode and R-mode, and this study uses Q-mode PCA to highlight assemblage changes down-core. In Q-mode PCA (Imbrie and Purdy, 1962; Imbrie and Kipp, 1971) the

objective is essentially the assessment of relations among the samples where the coordinate axes are represented by *N* samples (Malmgren and Haq, 1982). R-mode techniques (Blanc *et al.*, 1972; Malmgren and Kennett, 1976b; Thunell *et al.*, 1977) aim to examine interrelations among taxa and operate in the so-called "taxon space". This is a multivariate space with *p* orthogonal axes (*p* is the number of taxa or groups of taxa), and each sample represents a point in this space; its location is a function of the percentage values of each of the *p* taxa.

The starting point of a PCA is the original data matrix. The data array is thought of as defining the positions of samples in relation to axes representing the full set of species, one axis for each species. Typically, there are many species (maximum 50) so the samples are points in a very high-dimensional space.

Principal Components Analysis attempts to portray/resolve the similarities or differences between entities (samples, species, etc) in terms of placement in a multidimensional space. The dimensions of this new space are determined by converting the original or transformed data into some measurement of similarity between entities, and factoring the matrix of similarities into eigenvectors (mutually perpendicular axes defining the coordinate system of the new space) and eigenvalues (a measure of how "important" each new axis is to the data) (Parker and Arnold, 1999).

It may be necessary to reduce the size of the data set and eliminate some species from the analysis. However the necessity of making an arbitrary decision about which species to exclude is one of the problems with applying PCA to biological community data. In this study only those species which make up more than 3% of the absolute abundance in at least one of the samples has been included in the analysis (although species abundance are entered as raw data counts rather than as a percentage of the total abundance). It may also be necessary to make an initial transformation (none, square root, fourth root, logarithmic) of the data to avoid over-domination of the analysis by the very common species (see section 4.4.5.(i) for explanation of transformations).

The data matrix can also be normalised. For each species abundance, subtract the mean count and divide by the standard deviation over all samples for that species. This makes the variance of samples along all species axes the same so all species are of potentially equal importance in determining the principal components. Normalised analysis is termed correlation-based PCA and not normalised analysis is covariance-based PCA. It is suggested

that covariance-based PCA and transformation of the data is better for species abundance matrices, as in this study.

An ordination map of the samples is produced, usually in two or three dimensions, in which the placement of samples, rather than representing their simple geographical location, reflects the similarity of their biological communities.

Chapter Five

RESULTS

This chapter will be split into sections with the results from cores to the north of the Polar Front presented first, followed by the results from cores to the south of the Polar Front. Multivariate analysis results from three of the cores have been grouped together and will be presented at the end of this chapter.

CORES FROM NORTH OF THE POLAR FRONT

5.1. KC097

This core lies approximately 296 km to the north-west of the Polar Front in the western Falkland Trough and has been sampled down to a depth of 282cm below the surface. Using the radiocarbon dates obtained for this core (Fig.5.6a) it can be estimated that the sample interval is approximately 300-350 years and a total of 36 samples were picked from this core. The lithology of this core shows an upward change from sandy muds at the base through diatom muds into a foraminiferal sand unit at the top. The carbonate content shows an overall increase up-core with the largest change occurring between 50-60cm which corresponds to

the change in lithology from diatom muds to foraminiferal sands (Fig.4.1). The magnetic susceptibility corresponds to the lithological record, with higher susceptibility in the diatom muds (terrigenous) unit (Fig.4.2).

5.1.1. Benthic Foraminiferal Abundance

The absolute abundance data are shown in Figure 5.1 and the raw data counts are included in Appendix 3.

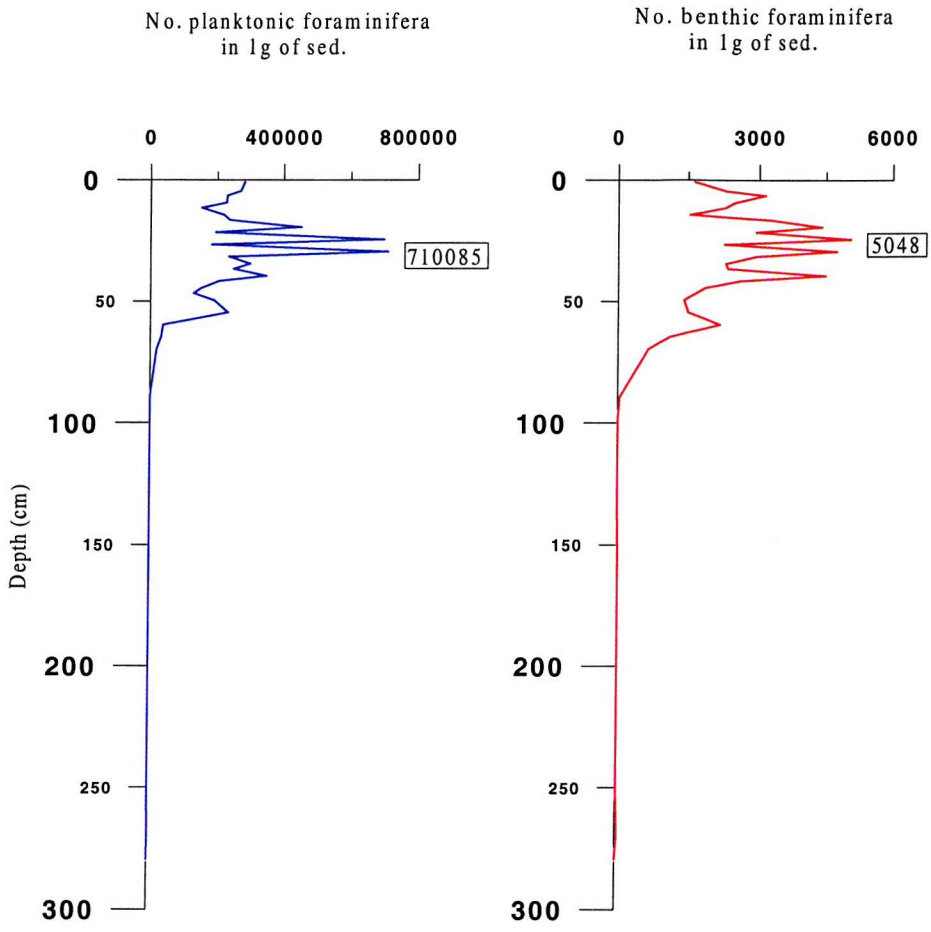

Figure 5.1. Planktonic and benthic foraminiferal absolute abundance for KC097.

Absolute abundance is high, up to 5048 foraminifera per gram with the abundance maximum occurring at 25cm below the sediment surface. Benthic foraminifera are absent from the base sample and occur only in low numbers in the lower section of the core. They completely disappear again between 150-110cm and do not re-appear until 100cm where there is a rapid

increase in abundance up through the core followed by a decline in numbers at the top. The greatest variation in abundance occurs in the top 50cm of the core (Fig.5.1).

Plots of the relative abundance of individual species can be seen in Figure 5.2 and individual species counts are shown in Appendix 4. In Figure 5.2 each species is shown as a percentage of the total assemblage. Samples with fewer than a total of 60 benthic foraminifera have been excluded from the graphs as they would be statistically unreliable. However, these samples are indicated on the graphs as a circle at the depth at which they contain a representative of the particular species. It should be noted that the graphs have different percentage scales.

There are 82 species from 44 different genera identified in this core with 6 unidentified taxa. The dominant taxa are shown below with the number of samples in which the species formed more than 5% of the assemblage and the benthic ranking with percentage means in brackets:

Eilohedra weddellensis	32	(27.1)
Gyroidinoides spp.	26	(7.03)
Epistominella exigua	19	(6.54)
Cassidulina crassa	19	(5.68)
Globocassidulina subglobos	18	(5.6)
Nonionella iridea	10	
Fissurina spp.	7	
Lagena spp.	7	
Oridorsalis tener	5	

Other species that are common in most samples, but are not abundant, are *Angulogerina angulosa* and *Bolivinellina translucens*. *Eilohedra weddellensis* is the dominant species and the most persistent throughout the core, being absent from only 3 samples where there were no foraminifera found and at 100cm.

The relative abundance of the individual species follows the general pattern of increased abundance up-core, as seen in the benthic absolute abundance record described above. *Eilohedra weddellensis, Gyroidinoides* spp., *E. exigua* and *G. subglobosa* all show the similar trend of a sharp initial increase at 100cm (60cm for *E. exigua*) followed by high numbers throughout the rest of the core, with some fluctuations (Fig.5.2). *Eilohedra weddellensis* shows a large decrease at 60cm and decreases at the core top along with *E.*

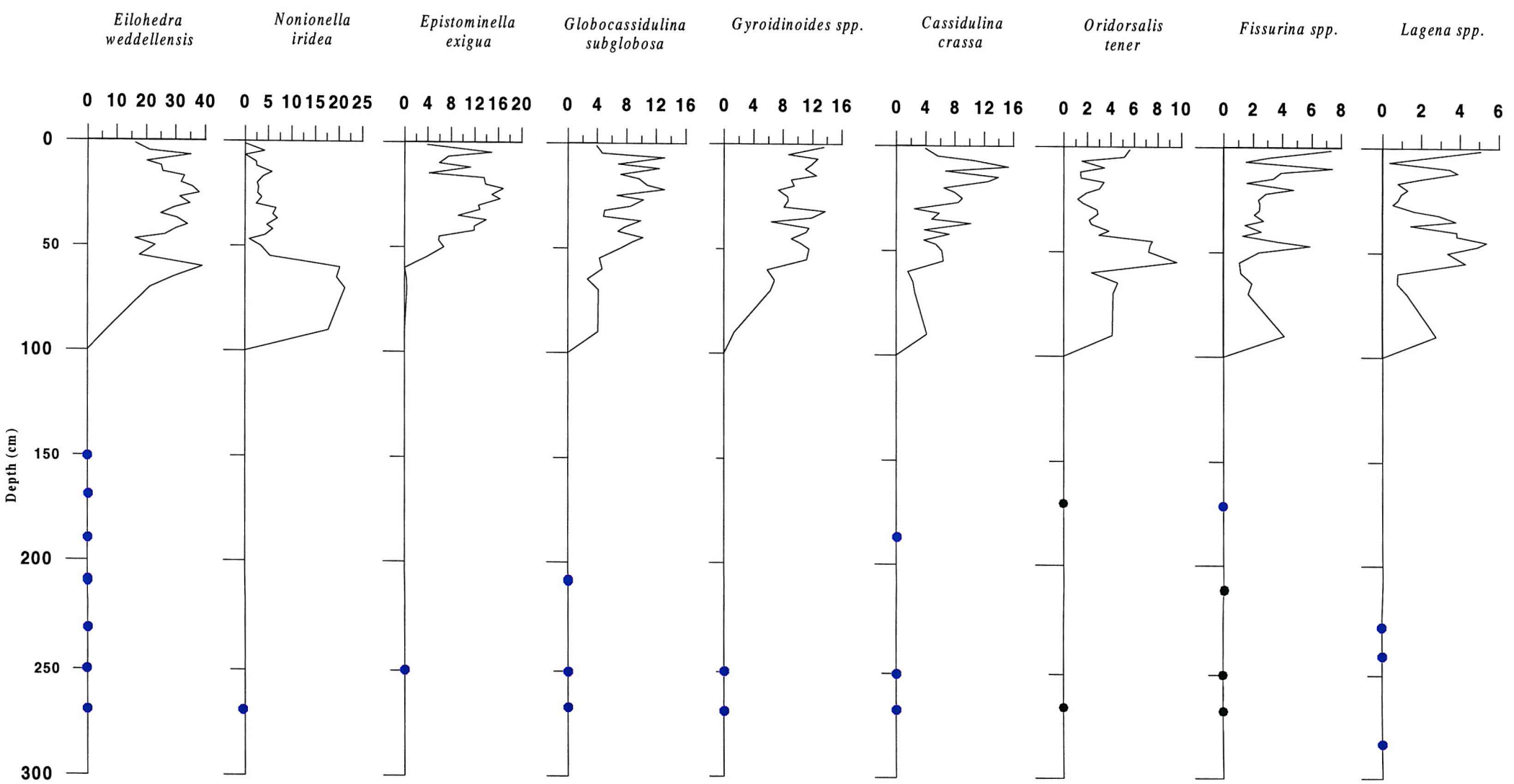

Figure 5.2. Relative abundance (%) of dominant benthic foraminifera for KC097.

● species present but foraminiferal abundance is statistically too low to calculate %.

exigua and *G. subglobosa*, whereas *Gyroidinoides* sp. is increasing at the core top. However, as species diversity generally increases up core the decline in relative abundance of *E. weddellensis*, *E. exigua* and *G. subglobosa* at the core top may be as a result of an increase in some rarer species.

Cassidulina crassa, O. tener, Fissurina spp. and *Lagena* spp. all show a similar abundance record with an initial increase at 100cm followed by a subsequent decrease shortly after to an abundance minimum at 60cm (Fig.5.2). There then follows a sharp rise in numbers to a peak value at 50cm which is again followed by a decline in numbers in the top part of the core. All these species show a slight increase at the core top, except for *C. crassa* that is decreasing. The only exception appears to be *N. iridea* which shows an initial large increase in abundance at 90cm until 50cm when the numbers decline from 20 to 5% and remain low to the top of the core.

Agglutinated taxa occur in low abundance and diversity with only 11 species from 9 different genera being identified throughout the whole core. The most persistent species is *Eggerella bradyi* that occurs in most samples down to a depth of 65cm, but usually only forms less than 2% of the total abundance.

5.1.2. Species Diversity

5.1.2.1. The Information Function H(S)

H(S) and H(S)max were computed for each sample where the population exceeded 60 individuals to avoid misleading results from small sample size (Appendix 5). The H(S) value ranges from 0.94 at 17cm to 3.01 at 90cm. Below 90cm there were not enough foraminifera present for the samples to be included in the analysis, except at 270cm below the surface which is marked on the plot (Fig.5.3). There is an initial decrease between 90-70cm then H(S) values tend to fluctuate between 1.0 and 2.0 up through the rest of the core. There is a peak at about 55cm and the values are high at the core top.

A low H(S) number indicates that most of the individuals are concentrated into a few dominant species, whereas a higher number indicates that they are more equally distributed among a larger number of species (Echols, 1971). Therefore a greater H(S) value indicates greater species diversity. Some assemblages with low diversity may indicate that few species have adapted to the environment but those few may occur in great abundance.

5.1.2.2. The Fisher Alpha Index (α)

The α value ranges from 7 to 15 (Appendix 5). Again there are no values for α below 70cm due to low foraminiferal abundance. Alpha values are high between 55-35cm below the surface, and then lower between 35-10cm with an increase again at the core top (Fig.5.3).

The third graph in Figure 5.3 shows that the number of species in each sample increases up core to maximum values within the top 50cm which may also indicate that diversity is higher in this top section.

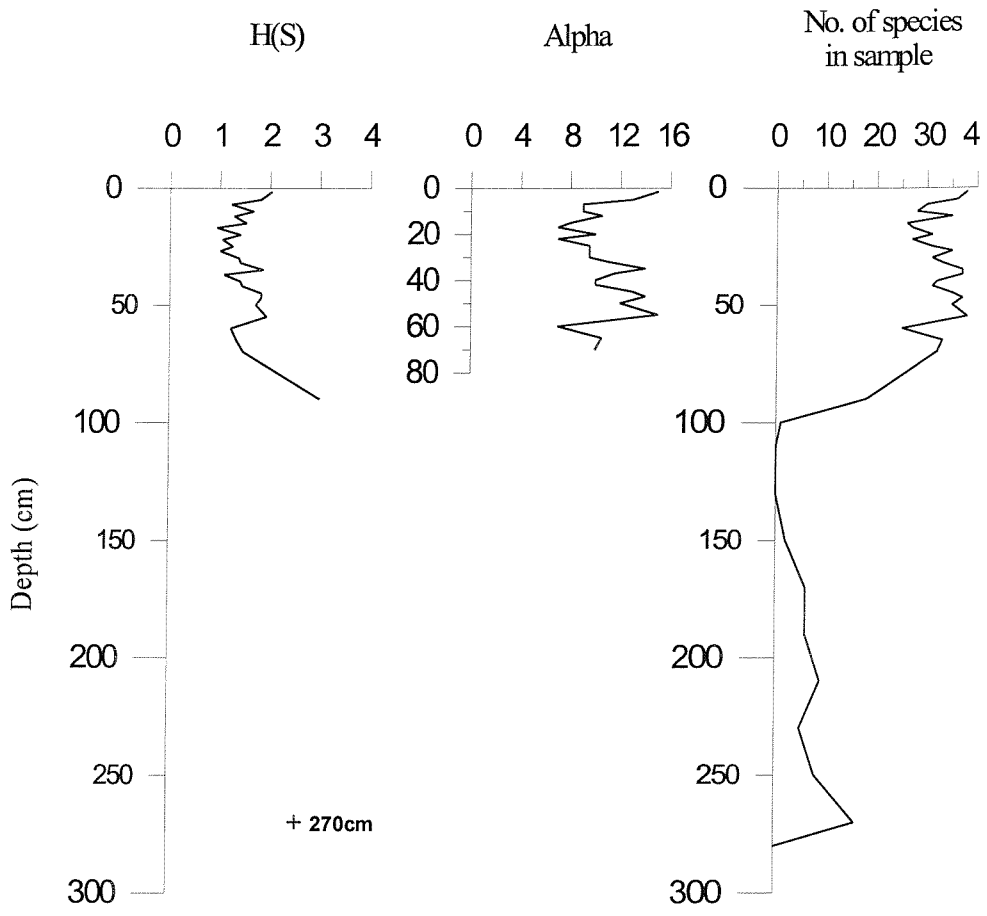

Figure 5.3. Species Diversity functions for KC097.

5.1.3. Planktonic Foraminiferal Abundance

Absolute abundance data are shown in Figure 5.1 and raw data counts are included in Appendix 3.

The dominant foraminifer is the left-coiling (sinistral) *Neogloboquadrina pachyderma*. It occurs in almost every sample throughout the core and usually comprises over 95% of the total planktonic assemblage.

The absolute abundance is generally very high, up to 710085 foraminifera per gram with the abundance maximum occurring at 30cm below the sediment surface. Planktonic foraminifera are absent from the base sample and occur only in low abundance in the lower section of the core. They completely disappear again between 150-110cm and re-appear in low abundance at 90cm below the surface. The number of foraminifera then begins to increase rapidly and continues up through the core until abundance starts to decrease just below the surface. The greatest variation again appears to be occurring in the top 50cm of the core. This pattern complements the benthic foraminiferal absolute abundance record.

Seven other species of planktonic foraminifera also occur but in very low abundance and not in all samples, and therefore were not counted, but their presence was noted (Table 5.1). These are listed below with the number of samples in which they were:

Globorotalia truncatulinoides	25
Globorotalia crassaformis	19
Globorotalia inflata	16
Globigerina bulloides	14
Globigerinita uvula	8
Globigerinita glutinata	2
Turborotalita quinqueloba	1

The subtropical/transition species *G. truncatulinoides* appears in many of the samples in the top 1m of the core. *Globigerina bulloides* and *G. uvula* occur in fewer samples than *G. truncatulinoides* but are more abundant within those samples than the other five species listed above.

Assemblage	Planktonic species	1.5 - 3 cm	5 - 6 cm	7 - 8 cm	10 - 11 cm	12 - 13 cm	15 - 16 cm	17 - 18 cm	20 - 21 cm	22 - 23 cm	25 - 26 cm	27 - 28 cm	30 - 31 cm	32 - 33 cm	35 - 36 cm	37 - 38 cm	40 - 41 cm	42 - 43 cm	45 - 46 cm	47 - 48 cm	50 - 51 cm	55 - 56 cm	60 - 61 cm	65 - 66 cm	70 - 71 cm	90 - 91 cm	100 - 101 cm	150 - 151 cm	170 - 171 cm	190 - 191 cm	210 - 211 cm	230 - 231 cm	250 - 251 cm	270 - 271 cm
Subtropical	*Globorotalia crassaformis*	*	*	*	*	*	*		*	*	*	*	*		*	*	*	*	*	*	*	*	*	*										
Subtropical / Transition	*Globorotalia truncatulinoides*	*	*	*	*	*	*	*	*	*	*	*	*	*	*	*	*	*	*		*	*	*	*	*	*								
Transition / cold-temperate	*Globorotalia inflata*		*	*	*				*	*	*		*	*	*		*		*				*	*		*								
Transition / cold-temperate	*Globigerinita glutinata*			*		*																									*			*
Subantarctic / upwelling	*Globigerina bulloides*			*		*			*	*			*		*	*		*	*		*	*				*			*			*	*	*
Subantarctic	*Turborotalita quinqueloba*																																	
Subantarctic	*Globigerinita uvula*	*	*		*	*	*	*		*			*		*	*															*			
Antarctic	*Neogloboquadrina pachyderma*	*	*	*	*	*	*	*	*	*	*	*	*	*	*	*	*	*	*	*	*	*	*	*	*	*	*	*	*	*	*	*	*	*

Table 5.1. Planktonic foraminifera species found in KC097 (based on Blair, 1965; Be, 1969, 1977).

5.1.4. Calcium Carbonate Dissolution

In the modern ocean, carbonate dissolution increases with depth and is high in regions with high sedimentation rates of organic matter. Carbonate dissolution is a process that selectively removes thinner, less resistant foraminifera before thicker, more resistant ones. It selectively alters the planktonic foraminiferal fauna and causes test fragmentation and therefore increased relative abundance of benthic foraminifera. Benthic foraminifera, being much more resistant, are therefore useful indexes of dissolution intensity, assuming that benthic productivity has not changed over the time interval.

Where there is no value for the P:B ratio shown foraminifera were completely absent from the sample (Appendix 6 and gap in curve in Fig.5.4). The P:B ratio remains high throughout most of the core (Fig.5.4) with a slight decrease between 50-100 cm below the surface. On average the percentage of planktonic foraminifera is about 98%. Therefore it would appear that as the P:B ratio decreases down core the effects of dissolution must also increase down core leading to an increase in the relative abundance of benthic foraminifera. This can also be seen in the carbonate record which shows a decreasing percentage of carbonate within the sediment down core from 70% in the top sample down to 12% at 70cm below the surface (Fig.5.4).

Foraminiferal test fragmentation increases down core and is accompanied by a decrease in test preservation. In the samples from the lower section of the core the planktonic foraminifera often show evidence of holes in the walls of the individual chambers (see plate – section 12).

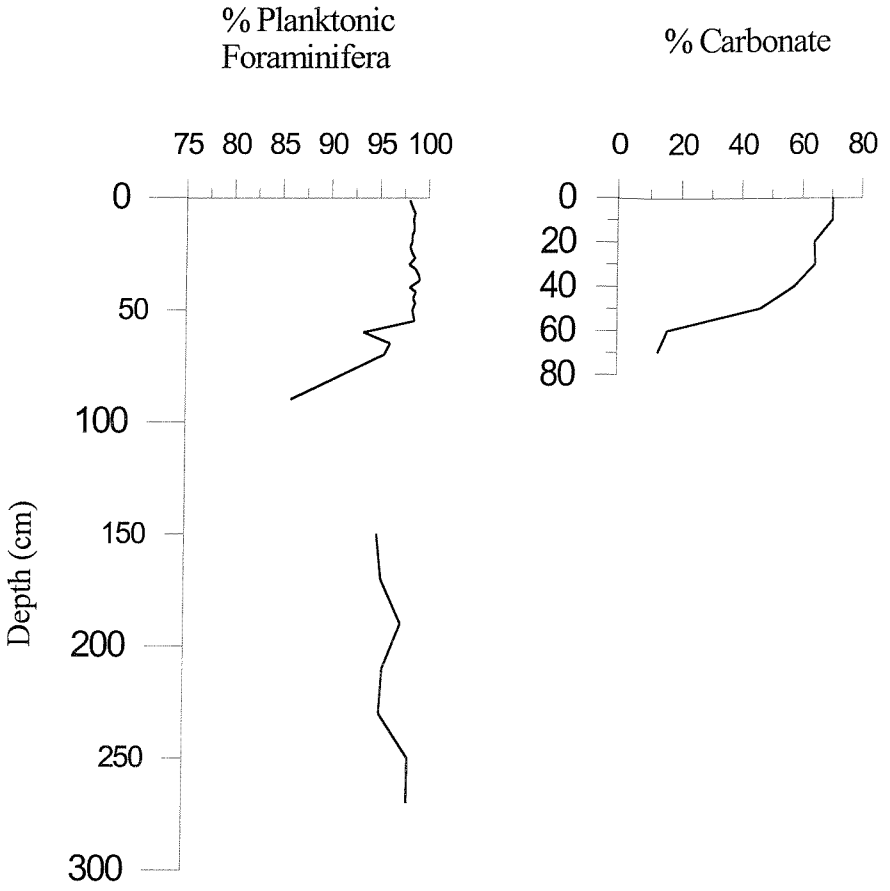

Figure 5.4. Dissolution indices for KC097 (gap in record = no foraminifera in sample)

5.1.5. Stable Isotopes

Carbon and oxygen stable isotope analysis was carried out for planktonic and benthic foraminifera in this core. The results are shown in Tables 5.2 and 5.3, and isotope curves can be seen in Figure 5.5. The results have not been adjusted to take into account vital effects.

Depth (cmbsf)	$\delta^{13}C$ (‰ PDB) *N. pachyderma*	$\delta^{18}O$ (‰ PDB) *N. pachyderma*
1.5-3	1.04	2.26
10-11	0.93	2.06
20-21	0.99	2.23
25-26	0.62	2.18
30-31	0.29	2.37
50-51	0.58	2.72
70-71	0.46	3.01
90-91	0.41	2.94
150-151	0.57	2.68
170-171	0.47	2.56
190-191	0.58	2.66
210-211	0.66	2.61
230-231	0.51	2.69
250-251	0.70	2.22
270-271	0.55	2.43

Table 5.2. Planktonic foraminiferal carbon and oxygen stable isotope data for KC097.

Depth (cmbsf)	$\delta^{13}C$ (‰ PDB) *O. tener*	$\delta^{18}O$ (‰ PDB) *O. tener*
1-2	-1.01	3.01
10-11	-1.35	2.73
20-21	-1.42	2.38
25-26	-1.32	3.11
30-31	-1.29	3.32
35-36	-1.26	3.22
40-41	-1.19	3.29
50-51	-1.29	3.35
60-61	-1.67	4.02
70-71	-1.75	4.20

Table 5.3. Benthic foraminiferal carbon and oxygen stable isotope data for KC097.

The planktonic isotope values based on *N. pachyderma* range from 0.29 to 1.04‰ for $\delta^{13}C$ and from 2.06 to 3.01‰ for $\delta^{18}O$. The carbon isotope curve shows a general increasing trend up-core with values becoming more positive. Within the lower section of the core, between 270-50 cm the $\delta^{13}C$ values remain relatively constant at a value of about 0.5‰ with some

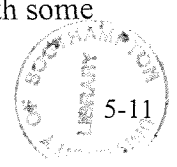

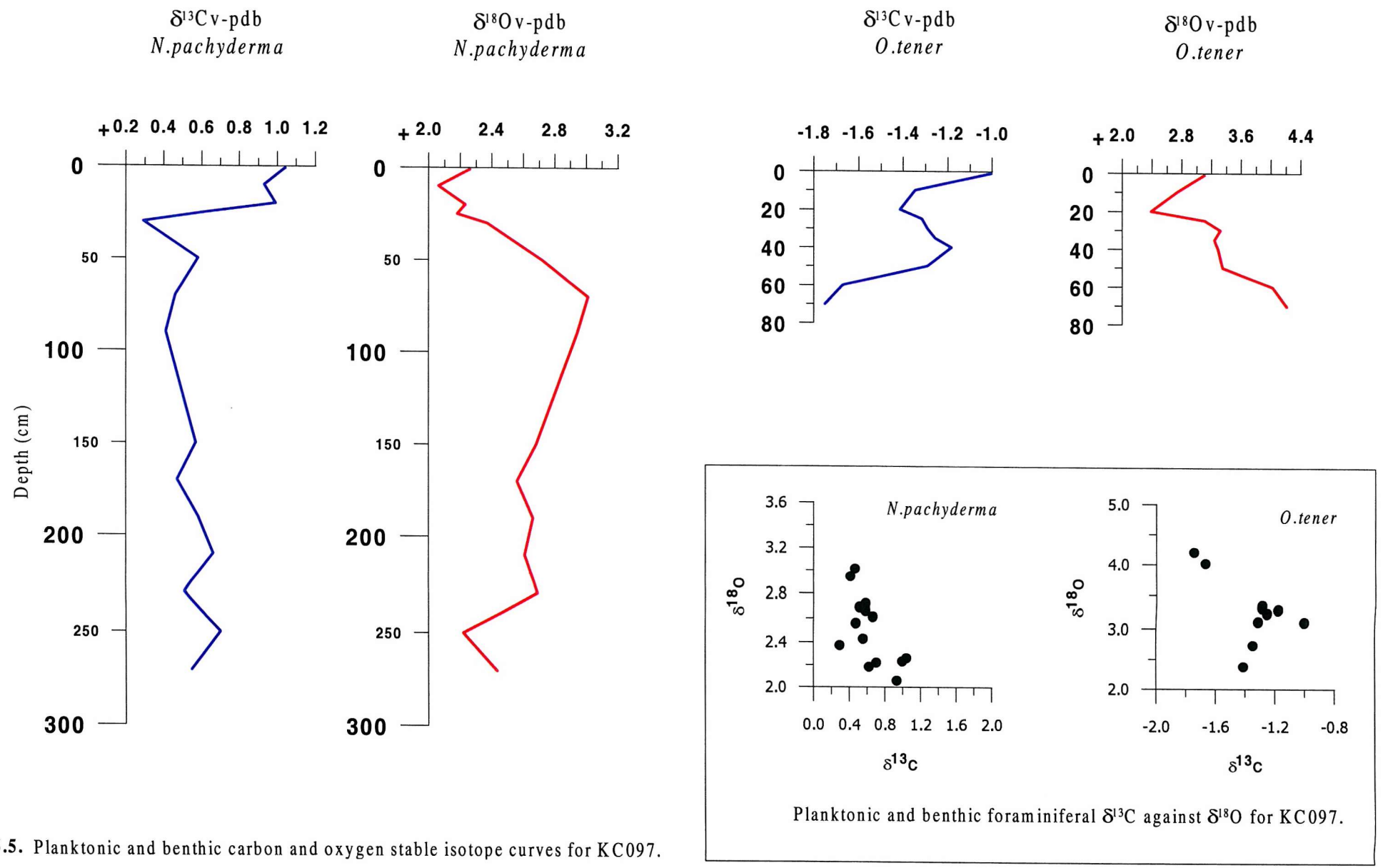

Figure 5.5. Planktonic and benthic carbon and oxygen stable isotope curves for KC097.

small-scale fluctuations. This is then followed by a subsequent decrease at 50cm to the minimum value at 30cm. There is then a more rapid and large increase within the top 30cm to the core top that records the maximum value for $\delta^{13}C$. This pattern is almost mirrored in the oxygen isotope curve, which shows a general decreasing trend up through the core and higher values on average in the lower part. After an initial increase to the maximum value at 70cm the $\delta^{18}O$ begins to decrease more rapidly to the minimum value near the top.

The benthic isotope values based on *O. tener* range from -1.01 to -1.67‰ for $\delta^{13}C$ and from 2.38 to 4.20‰ for $\delta^{18}O$. There is an overall increase in the benthic $\delta^{13}C$ record from the minimum value of the bottom sample at 70cm, up core becoming progressively more positive until the maximum value is reached in the surface sample. There is a small decrease to more negative values between 40-20cm. The $\delta^{18}O$ record shows the opposite general trend to the $\delta^{13}C$ with an overall decrease up core. There is an increase in $\delta^{18}O$ at 20cm that continues to the top sample at 1cm below the surface.

There is good agreement between the planktonic and benthic isotope records for both $\delta^{13}C$ and $\delta^{18}O$, with both records showing similar trends throughout the core. The changes in $\delta^{13}C$ are also accompanied by a change in $\delta^{18}O$ for both the planktonic and benthic isotope records. The plots of $\delta^{13}C$ against $\delta^{18}O$ for the benthic and planktonic foraminifera records are used to show if any fractionation of the isotopes has occurred during analysis. The results may show some fractionation in the benthic record (Fig.5.5) but the outlying samples show a deviation of only about 0.5‰ and this may be the result of environmental ambient conditions or vital effects.

5.1.6. Radiocarbon Dates

AMS radiocarbon analysis was carried out on four cores in this study, including the three cores from north of the PF. Results for KC097 are shown in Table 5.4.

Publication code	Sample	Conventional Radiocarbon Age (years BP ± 1σ)	Corrected Age (years BP)	Carbon content (% by wt.)	Material analysed
AA35128	KC097 1.5-3cm	3290 ± 45	1990	11.0	*N. pachyderma*
AA35129	KC097 20-21cm	5035 ± 50	3735	11.0	*N. pachyderma*
AA35130	KC097 25-26cm	5740 ± 55	4440	11.0	*N. pachyderma*
AA35131	KC097 30-31cm	6655 ± 55	5355	11.0	*N. pachyderma*
CAMS-60834	KC097 1.5-3cm	3540 ± 40	2240	0.70 #	Bulk organic carbon

Table 5.4. AMS radiocarbon dates for KC097 (# NB this is the % by wt. of the carbon in the treated, dried and homogenised sample).

The samples need to be corrected to take into account the reservoir age of the material and for Antarctic marine sediment this is commonly quoted as 1300 years (Goodwin, 1993; Berkman *et al.*, 1998; Ingolfsson *et al.*, 1998).

Radiocarbon data from Southern Ocean material must be interpreted with caution because of the possible effects of the Antarctic CO_2 reservoir from upwelling and meltwater CO_2, and reworking. The radiocarbon concentration of the Southern Ocean is dominated by the upwelling of deep water from the northern hemisphere at the Antarctic Divergence. Deep-water is depleted in ^{14}C, and although mixing with "younger" surface water south of the PF occurs, marine species which live in those waters have apparent radiocarbon ages that are 1000-1400 years older than the atmosphere (Broecker, 1963; Bjorck *et al.*, 1991; Gordon and Harkness, 1992; Bard *et al.*, 1993). Ages of several thousand years for core top sediment in KC097 indicates that some material was lost during coring (Howe and Pudsey, 1999). There are no *Cycladophora davisiana* or biogenic barium data available for KC097 so only the top section of this core can be dated using these radiocarbon ages.

5.1.7. Sedimentation Rate

A sedimentation rate plot for KC097 can be seen in Figure 5.6a. As radiocarbon dates have been obtained only for the top 30cm of the core, and there are no *C. davisiana* data available for this core, the sedimentation rate for this section only can be calculated. The average sedimentation rate for the top 30cm is approximately 9.9cm/1000 years. Therefore, assuming that the sedimentation rate remained constant the amount of material lost from the top of the core can be estimated as approximately 20cm.

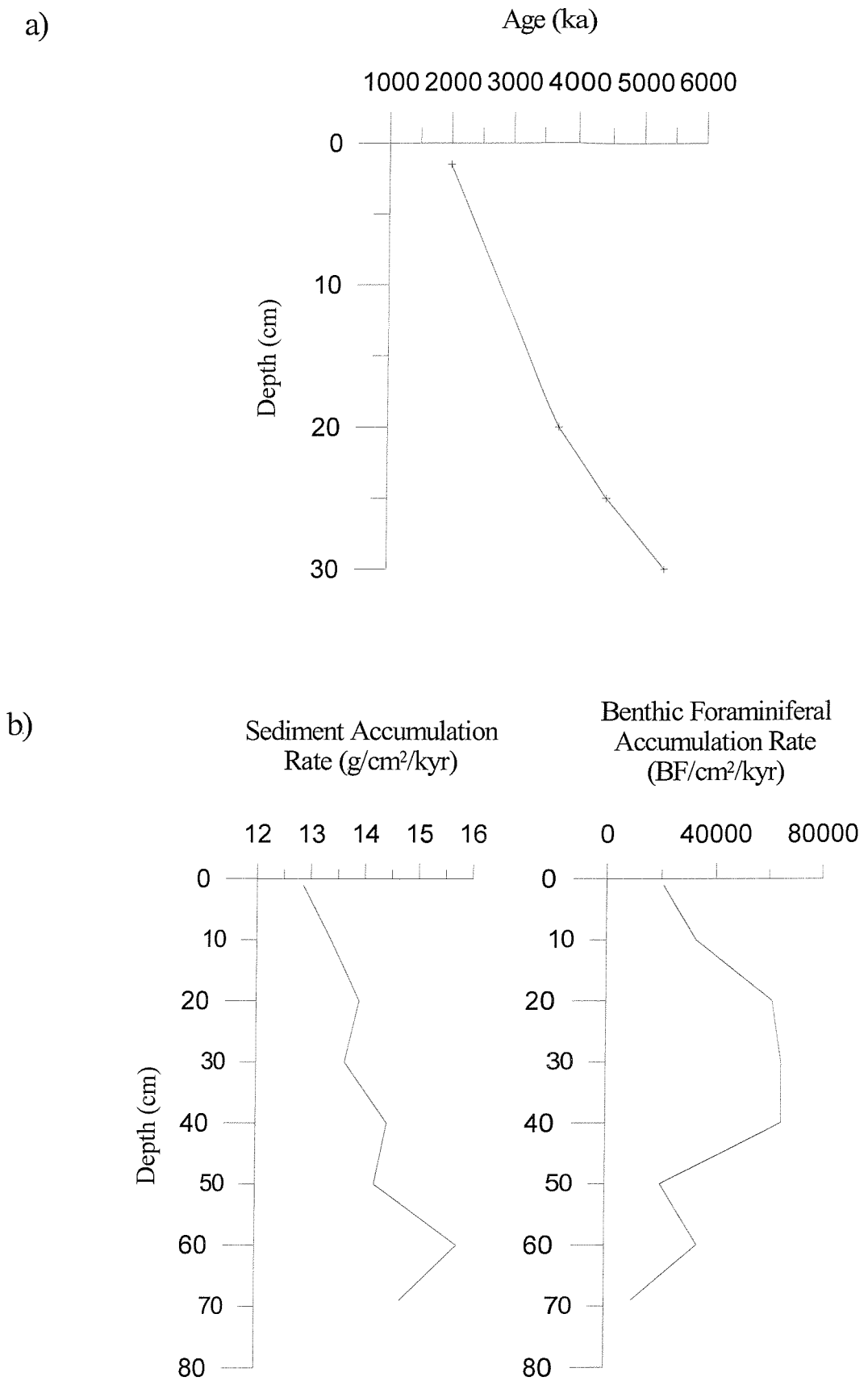

Figure 5.6. a) Sedimentation rate and b) SAR and BFAR plotted for KC097.

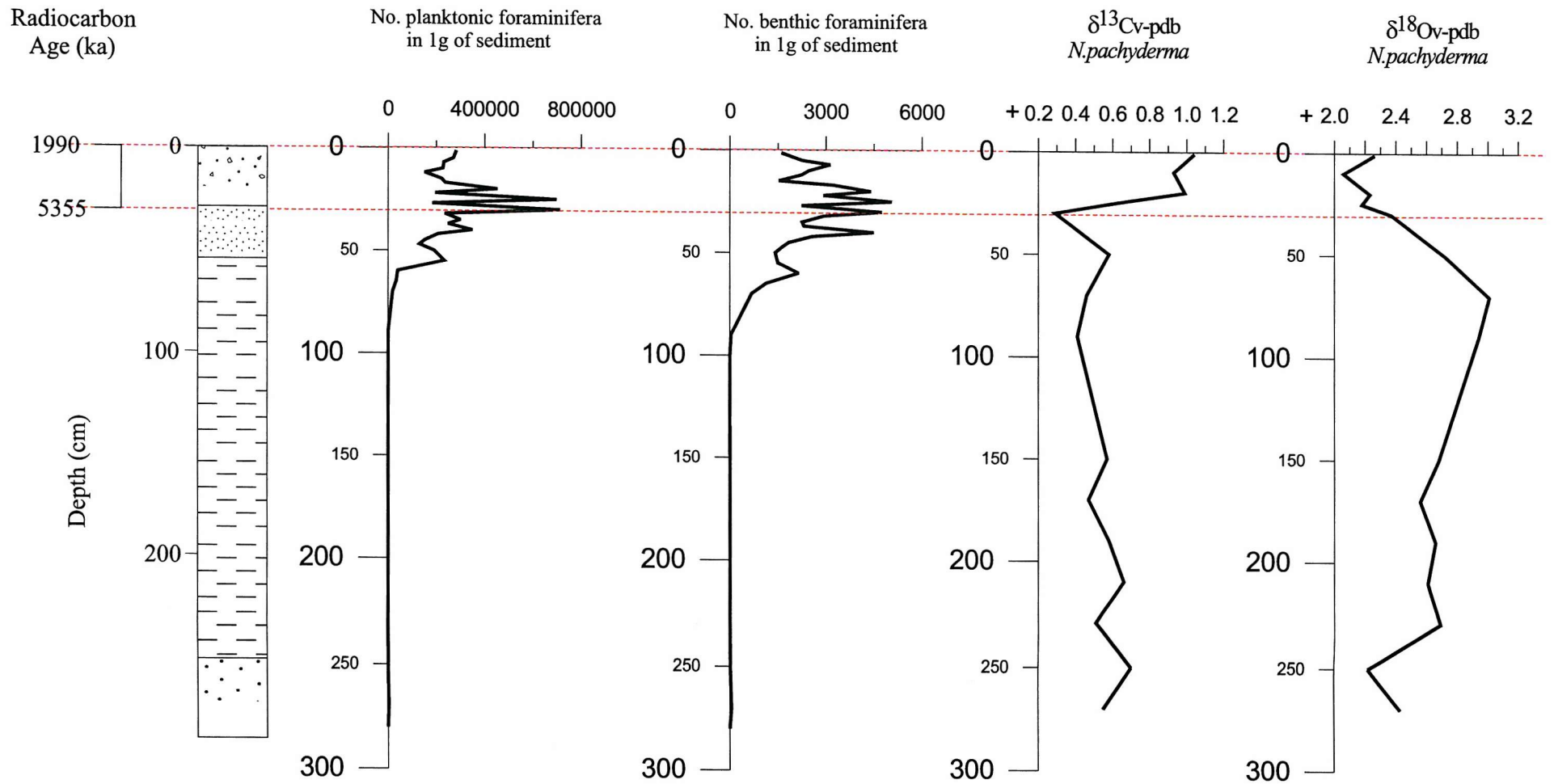

Figure 5.7. Summary diagram for KC097.

The SAR and BFAR were calculated down to almost 70cm below the sediment surface, and it was assumed that the sedimentation rate remained constant down through this section of the core. The results are shown in Appendix 7 and Figure 5.6b. The SAR shows a gradual decrease up through the section of almost 2 cm^2/kyr, from 14.69 cm^2/kyr at 69cm below the surface to 12.86 cm^2/kyr at the core top. The BFAR is generally quite high within this section of core with the greatest rates of accumulation occurring between 40-20cm below the surface. There is quite a large range between the lowest BFAR at 9945 BF/cm^2/kyr and the greatest at 64718 BF/cm^2/kyr, over a short section of core.

A summary diagram can be seen in Figure 5.7 showing the important results from KC097. There is a definite relationship between the planktonic and benthic records at this site as can be seen in both the foraminiferal abundance and planktonic isotope records. The peak in planktonic and benthic foraminiferal abundance appears to coincide with a marked decrease in $\delta^{13}C$ at about 5355 ka.

5.2. GC062

This core lies approximately 222 km to the north-west of the Polar Front in the western Falkland Trough and has been sampled down to a depth of 224cm below the surface. Using the radiocarbon dates obtained for this core (Fig.5.14a) it can be estimated that the sample interval is approximately 750 years and a total of 12 samples were picked from this core.
The lithology of this core shows an upward change from sandy muds at the base through diatom muds into a foraminiferal sand unit, which is overlain by a thin diatom ooze unit at the top. There is no carbonate present within most of the diatom mud unit but carbonate starts to appear in the sediment at about 60cm below the surface and is high within the foraminiferal sands and diatom ooze at the core top (Fig.4.1). The magnetic susceptibility corresponds to the lithological record, with higher susceptibility in the diatom muds (terrigenous) unit below about 40cm within the core (Fig.4.2).

5.2.1. Benthic Foraminiferal Abundance

The absolute abundance data are shown in Figure 5.8 and the raw data counts are included in Appendix 8.

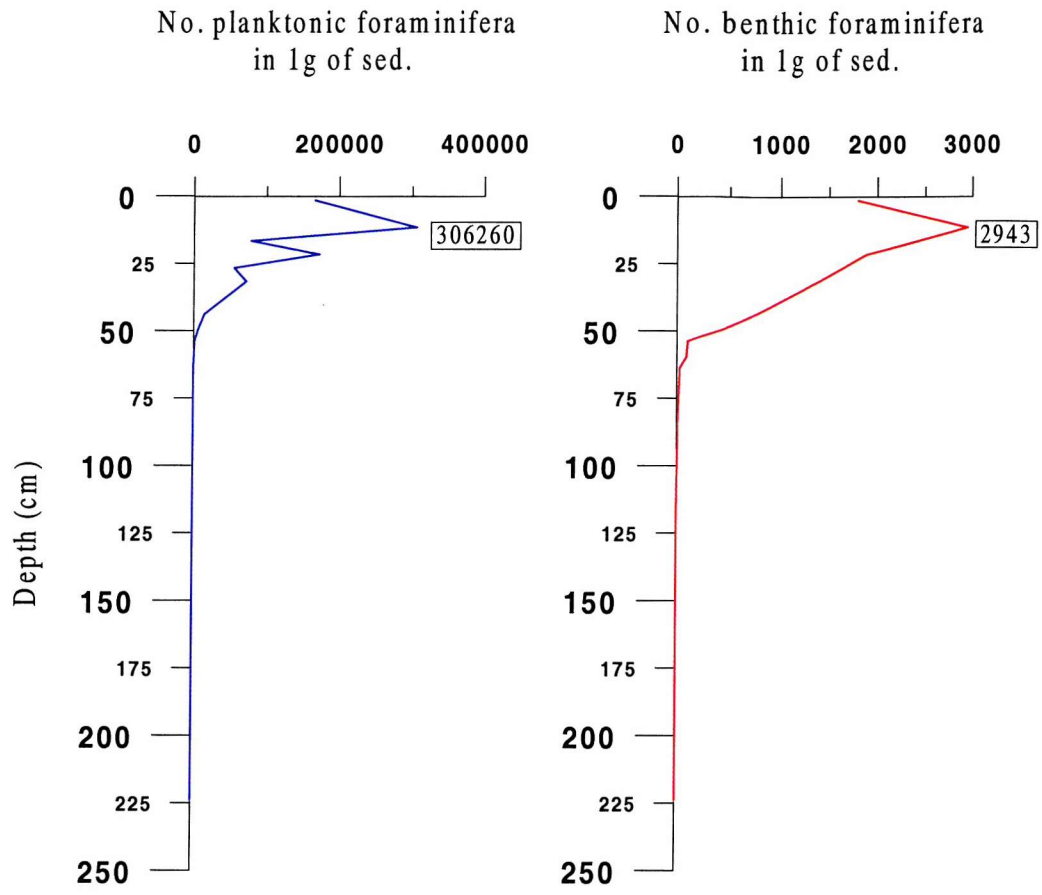

Figure 5.8. Planktonic and benthic foraminiferal absolute abundance for GC062.

Absolute abundance is generally quite high, up to 2943 foraminifera per gram with the abundance maximum occurring at 12cm below the sediment surface. Benthic foraminifera are absent from the sediment below 124cm within the core but there is a general increase in abundance above this level up through the core to the top. Abundance remains relatively low until about 50cm below the surface where there is a more rapid increase in numbers up through the top section of the core before showing a small decrease in abundance at the core top (Fig.5.8).

Plots of the relative abundance of individual species can be seen in Figure 5.9 and individual species counts are shown in Appendix 9.

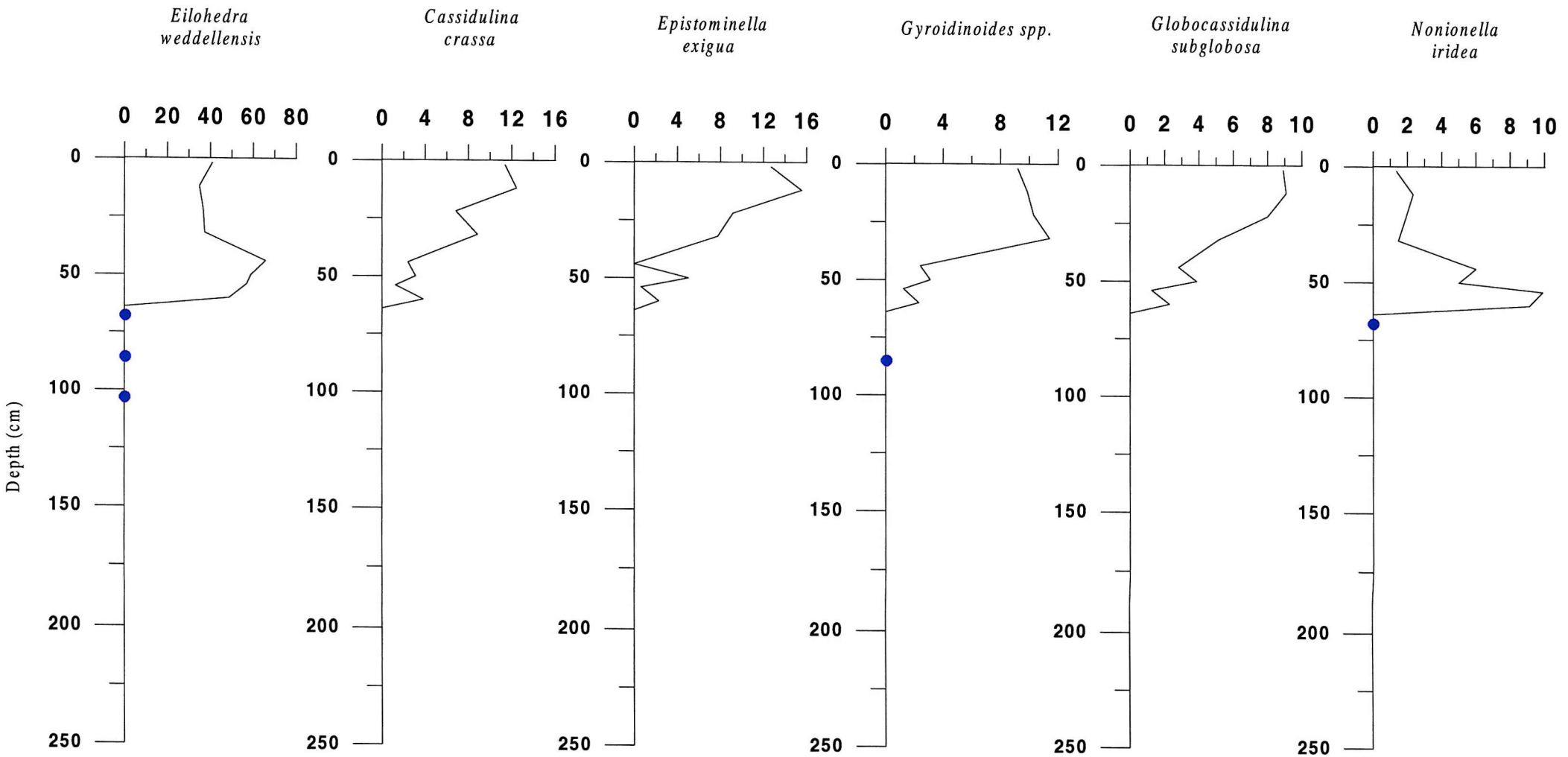

Figure 5.9. Relative abundance (%) of dominant benthic foraminifera for GC062.
● species present but foraminiferal abundance is statistically too low to calculate %.

There are 57 species from 39 different genera identified in this core with 3 unidentified taxa. The dominant taxa are shown below with the number of samples in which the species formed more than 5% of the assemblage and the benthic ranking with percentage means in brackets:

Eilohedra weddellensis	8	(43.25)
Epistominella exigua	5	(4.42)
Gyroidinoides spp.	4	(4.90)
Cassidulina crassa	4	(4.16)
Globocassidulina subglobosa	4	(3.44)
Nonionella iridea	4	

Other species that are common in most samples but are not abundant are *Fissurina* sp., *Lagena* spp., *Oridorsalis tener*, *Pullenia simplex* and *Bolivinellina translucens*. *Eilohedra weddellensis* is the dominant species occurring in much higher abundances in all samples and is the only species which is persistent throughout the samples which contain foraminifera.

The relative abundance of *C. crassa*, *E. exigua*, *Gyroidinoides* spp. and *G. subglobosa* all follow the absolute abundance record with a gradual initial increase from 64cm below the surface up through the core, followed by a more rapid increase to high abundance from about 40cm to the core top. *Eilohedra weddellensis* and *N. iridea* show the opposite trend with an initial rapid increase at about 60cm below the surface to the maximum abundance, followed by a subsequent decline in numbers up through the rest of the core to the core top. *Eilohedra weddellensis* remains relatively high and constant through the top section of the core (Fig.5.9).

Agglutinated taxa occur in low abundance and diversity with only 6 species being identified throughout the whole core. The most persistent species is *Eggerella bradyi* that occurs in most samples down to a depth of 60cm, but usually forms less than 2% of the total abundance.

5.2.2. Species Diversity

5.2.2.1. The Information Function H(S)

H(S) and H(S)max were computed for each sample where the population exceeded 60 individuals to avoid misleading results from small sample size (Appendix 5). The H(S) value ranges from 0.92 at 2cm to 1.88 at 60cm. Below 60cm there were not enough foraminifera

present for the samples to be included in the analysis (Appendix 8). There appears to be a general increase in H(S) down core with a section of higher diversity found between 15-35cm below the surface. The deepest sample records the highest H(S) value and therefore the highest diversity (Fig.5.10).

5.2.2.2. The Fisher Alpha Index (α)

The α value ranges from 6 to 10.5 (Appendix 5) and there are no values for α below 60cm due to low foraminiferal abundance. The record of alpha values within this section of the core shows a varied pattern with the greatest fluctuations occurring in the lower samples. Alpha values appear to be higher representing increased diversity between 25-40cm within the core and at 60cm(Fig.5.10).

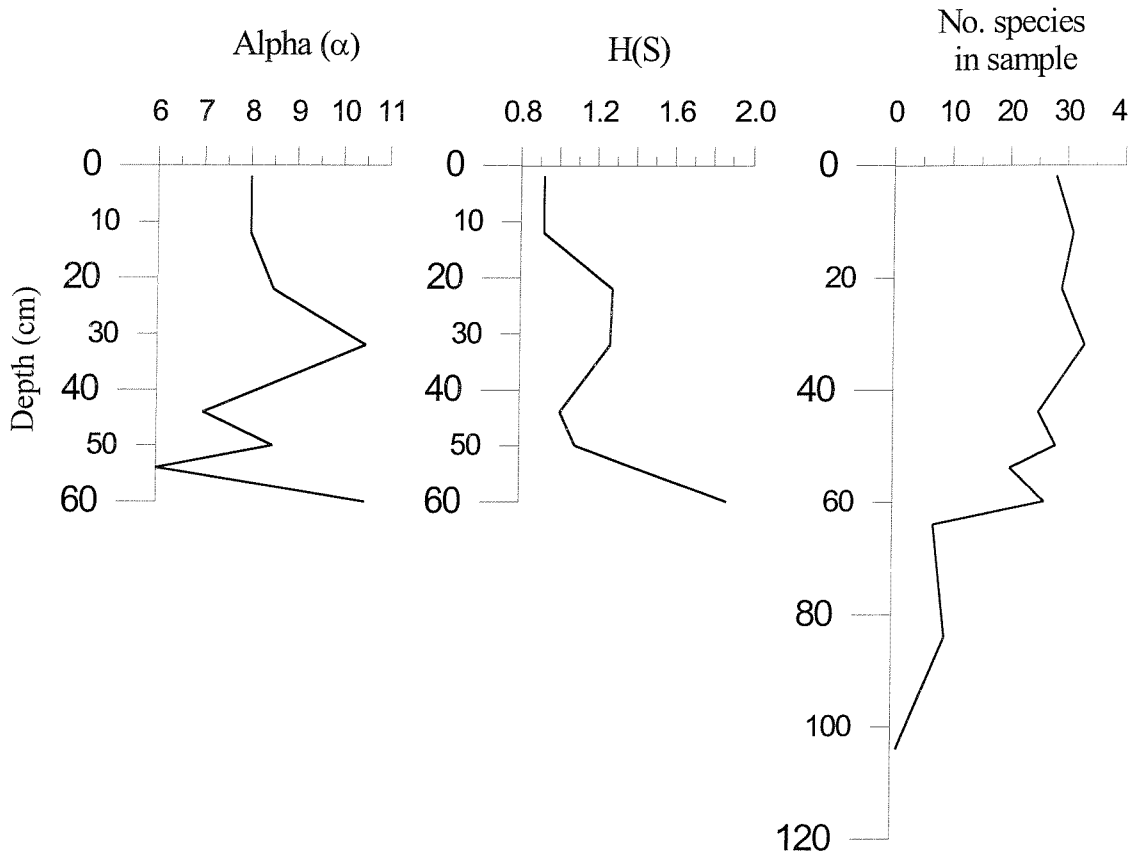

Figure 5.10. Species diversity functions for GC062.

The third graph in Figure 5.10 shows that the number of species in each sample increases up core which may indicate that species diversity also increases up core. This record is extended deeper in the core than the records for H(S) and Alpha as low abundance does not limit its use, and therefore it might be fair to say that H(S) and Alpha would both show a decrease in values below 60cm and down through the rest of the core.

5.2.3. Planktonic Foraminiferal Abundance

Absolute abundance data are shown in Figure 5.8 and raw data counts are included in Appendix 8.

The dominant foraminifer is the left-coiling (sinistral) *Neogloboquadrina pachyderma*. It occurs in almost every sample throughout the core and usually comprises over 95% of the total planktonic assemblage.

The absolute abundance is relatively high, up to 306260 foraminifera per gram with the abundance maximum occurring at 12cm below the sediment surface. Planktonic foraminifera are absent from the deepest 3 samples and there is a general trend of increasing abundance up-core. Abundance remains quite low until about 50cm below the surface where there is a rapid increase up through the rest of the core to maximum abundance values, before showing a decrease at the core top. This pattern complements the benthic foraminiferal absolute abundance record.

Seven other species of planktonic foraminifera also occur but in very low abundance and not in all samples, and therefore were not counted, but their presence was noted (Table 5.5). These are listed below with the number of samples in which they were found:

Globorotalia truncatulinoides	9
Globigerina bulloides	9
Globigerinita uvula	7
Globorotalia crassaformis	6
Globorotalia inflata	6
Turborotalita quinqueloba	2
Globigerinita glutinata	1

Assemblage	Planktonic species	2 - 4 cm	12 - 14 cm	17 - 18 cm	22 - 24 cm	27 - 28 cm	32 - 34 cm	44 - 46 cm	50 - 51 cm	54 - 56 cm	60 - 61 cm	64 - 66 cm	84 - 86 cm	104 - 106 cm	124 - 126 cm
Subtropical	*Globorotalia crassaformis*	*			*	*	*		*	*					
Subtropical / Transition	*Globorotalia truncatulinoides*	*	*	*	*	*	*	*	*		*				
Transition / cold-temperate	*Globorotalia inflata*	*	*				*	*	*		*				
Transition / cold-temperate	*Globigerinita glutinata*													*	
Subantarctic / upwelling	*Globigerina bulloides*	*	*		*	*	*	*		*		*	*		
Subantarctic	*Turborotalita quinqueloba*											*	*		
Subantarctic	*Globigerinita uvula*	*	*			*	*	*	*				*		
Antarctic	*Neogloboquadrina pachyderma*	*	*	*	*	*	*	*	*	*	*	*	*	*	*

Table 5.5. Planktonic foraminifera species found in GC062 (based on Blair, 1965; Be 1969, 1977).

The subtropical/transition species *G. truncatulinoides* and the subpolar species *G. bulloides* appears in many of the samples down to a depth of 60 and 84cm respectively within the core. These two species also occur in higher abundance within the samples than the other species named above.

5.2.4. Calcium Carbonate Dissolution

Where there is no value for the P:B ratio shown foraminifera were completely absent from the sample (Appendix 6). The P:B ratio remains high throughout the top 100cm of the core where foraminifera were found, and on average the percentage of planktonic foraminifera is greater than 90% (Fig.5.11). There is a general decrease in the percentage of planktonic foraminifera down through the top section of the core to a minimum value of about 70% at 64cm below the surface. The deepest two samples show percentages of planktonic foraminifera of over 90% but these samples may not be reliable indicators due to smaller sample size. Therefore it would appear that there is a an increase in the percentage of benthic foraminifera down through this section of the core. This general pattern can be seen more clearly in the carbonate record which shows a decreasing percentage of carbonate within the sediment down core from 63% in the top sample down to 6% at 60cm below the surface (Fig.5.11).

Foraminiferal test fragmentation is less pronounced than in the other cores but there is some increase down core and preservation of tests becomes worse within the lower section.

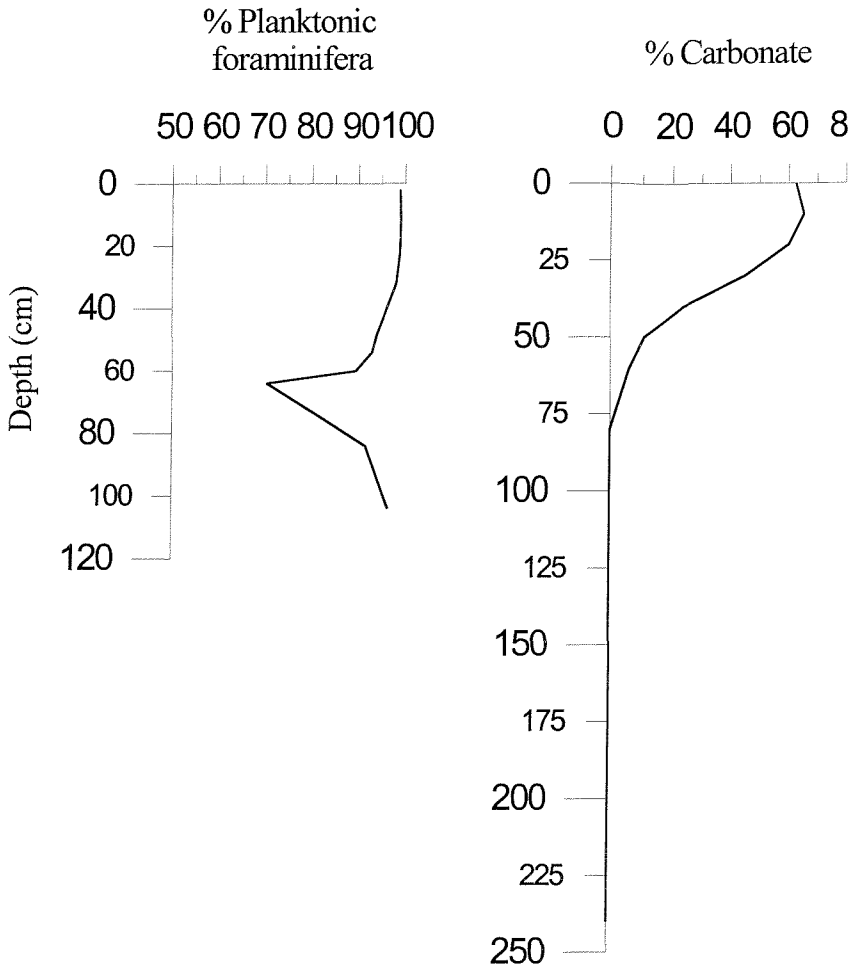

Figure 5.11. Dissolution indices for GC062.

5.2.5. Stable Isotopes

Carbon and oxygen stable isotope analysis was carried out for planktonic and benthic foraminifera in this core. The results are shown in Tables 5.6 and 5.7, and isotope curves can be seen in Figure 5.12. The results have not been adjusted to take into account vital effects.

Depth (cmbsf)	$\delta^{13}C$ (‰ PDB) *N. pachyderma*	$\delta^{18}O$ (‰ PDB) *N. pachyderma*
2-4	0.75	2.14
12-14	0.85	2.08
22-24	0.57	2.01
32-34	0.45	2.70
44-46	0.56	3.12
50-51	0.82	3.49
54-56	0.06	1.90
60-61	0.65	3.56
64-66	0.12	3.07
84-86	0.71	2.47
104-106	0.48	2.32

Table 5.6. Planktonic foraminiferal carbon and oxygen stable isotope data for GC062.

Depth (cmbsf)	$\delta^{13}C$ (‰ PDB) *O. tener*	$\delta^{18}O$ (‰ PDB) *O. tener*
2-4	-1.41	3.18
12-14	-1.18	3.35
22-24	-1.39	3.24
32-34	-1.50	2.84
44-46	-1.80	3.85
50-51	-1.77	4.09
54-56	-1.79	4.19
60-61	-1.82	4.48

Table 5.7. Benthic foraminiferal carbon and oxygen stable isotope data for GC062.

The planktonic isotope values based on *N. pachyderma* range from 0.06 to 0.85‰ for $\delta^{13}C$ and from 1.90 to 3.56‰ for $\delta^{18}O$. The $\delta^{13}C$ record shows an initial general decrease up through the core to just below 60cm where the $\delta^{13}C$ increases to a small peak before rapidly decreasing again to a minimum value for $\delta^{13}C$. There is then a general increase up through the rest of the core to the core top. Values for $\delta^{13}C$ are higher within the top 50cm of the core. The $\delta^{18}O$ record shows lower values at the bottom and top of this core section with increased $\delta^{18}O$ between 80-20cm within the core. There is a rapid decrease to a minimum value for $\delta^{18}O$ at about 60cm which returns to high $\delta^{18}O$ values immediately.

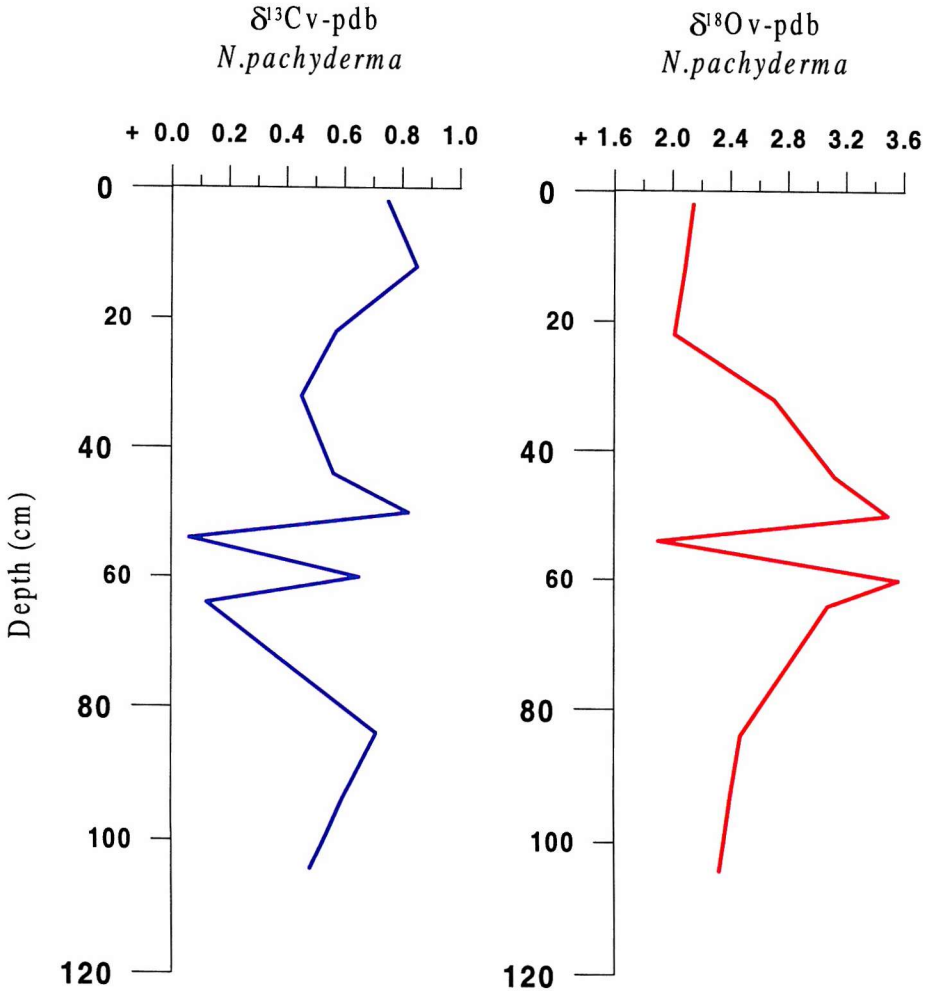

Figure 5.12. Planktonic and benthic stable isotope curves for GC062.

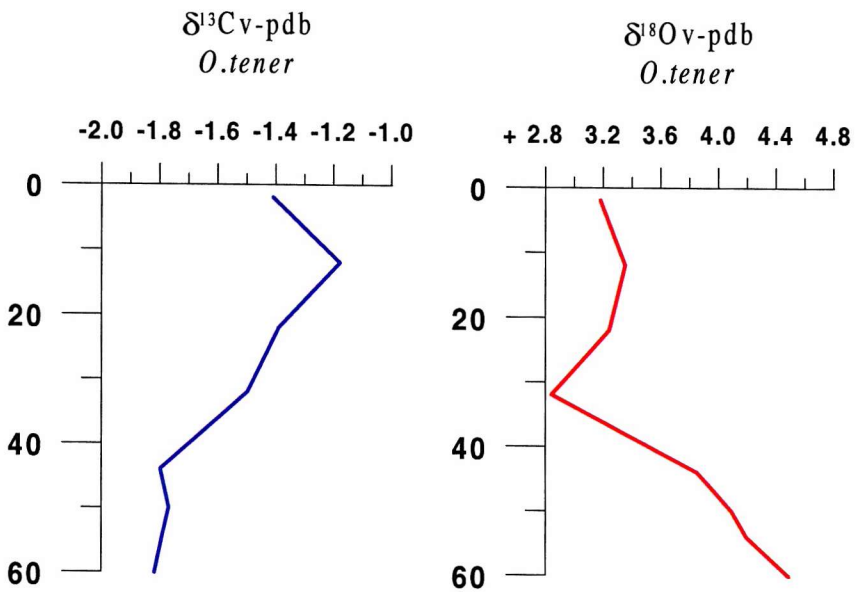

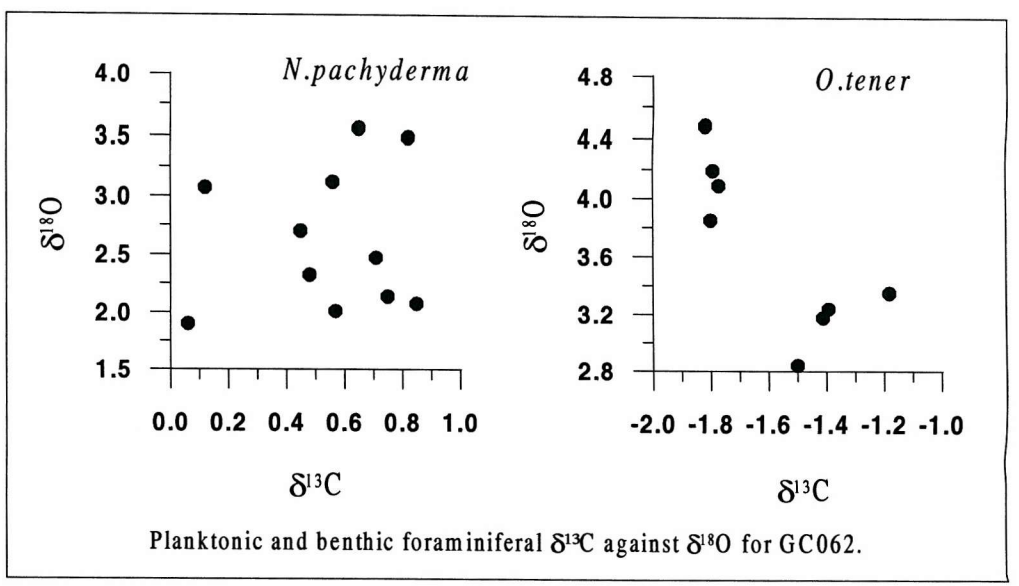

Planktonic and benthic foraminiferal $\delta^{13}C$ against $\delta^{18}O$ for GC062.

The benthic isotope values based on *O. tener* range from –1.18 to –1.82‰ for $\delta^{13}C$ and from 2.84 to 4.48‰ for $\delta^{18}O$. The $\delta^{13}C$ record shows an increase to less negative values up through the core before dropping off at the core top. This pattern is mirrored in the $\delta^{18}O$ record which shows a general decrease up core with a minimum value at about 30cm below the surface.

There is good agreement in the general trends between the planktonic and benthic isotope records for both $\delta^{13}C$ and $\delta^{18}O$, with similar patterns of lower $\delta^{13}C$ and higher $\delta^{18}O$ seen in the bottom section of the core, seen more clearly in the benthic record. Changes in the $\delta^{13}C$ record also seem to be accompanied by a similar change in $\delta^{18}O$ for both the planktonic and benthic records.

5.2.6. Radiocarbon Dates

Three AMS radiocarbon dates were obtained for this core (Table 5.8) but the age of the core top was not determined, and therefore there was no assessment of the reservoir effect.

Publication code	Sample	Conventional Radiocarbon Age (years BP ± 1σ)	Corrected Age (years BP)	Carbon content (% by wt.)	Material analysed
AA36269	GC062 17-18cm	5690 ± 55	4390	11.0	*N. pachyderma*
AA36270	GC062 22-23cm	7240 ± 65	5940	11.0	*N. pachyderma*
AA36271	GC062 27-28cm	8265 ± 60	6965	11.0	*N. pachyderma*

Table 5.8. AMS radiocarbon dates for GC062.

A correction of 1300 years has been applied to the conventional radiocarbon age to account for the Antarctic reservoir effect. Other dating methods can be applied which are the first down-core abundance peak of *Cycladophora davisiana* marking the position of the LGM at 100cm within this core (Fig.5.13). The lower relative abundance of *C. davisiana* at 1.6-2.0m lower down in this core may represent isotope stage 3 (Howe *et al.*, 1997). A downwards decrease in the amount of biogenic barium also marks the base of the Holocene (Stage 1) at about 80cm below the surface in this core.

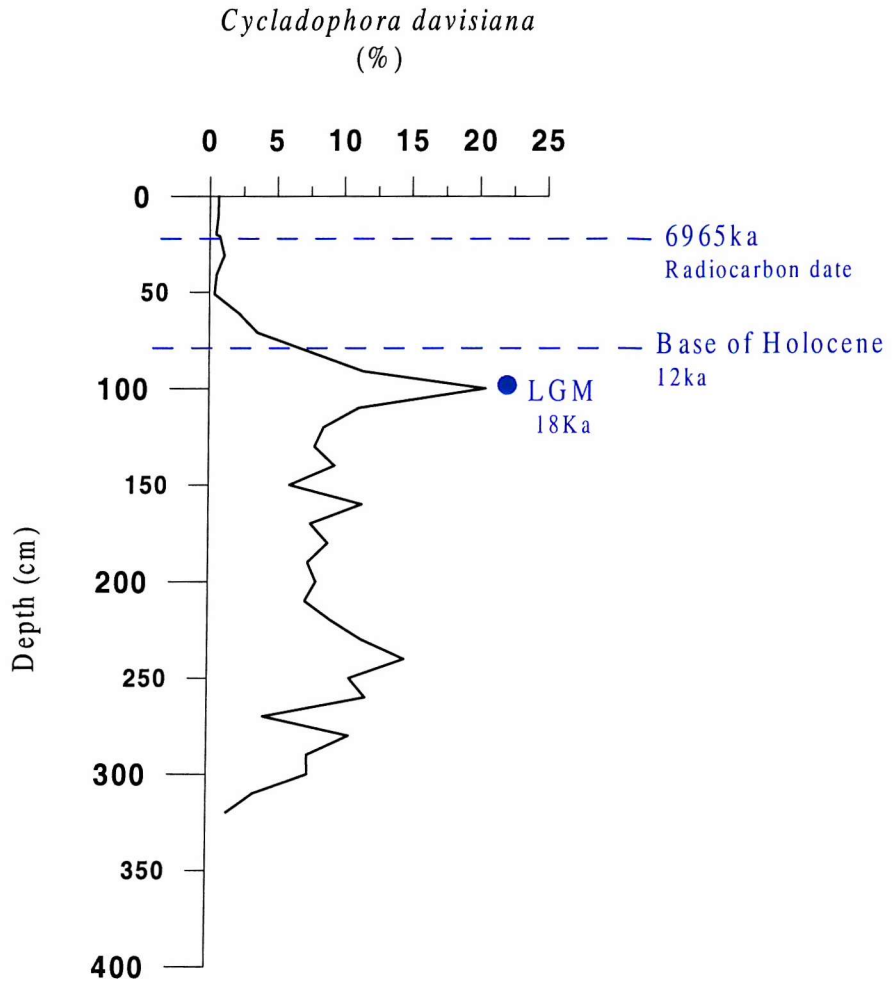

Figure 5.13. Dating of GC062 using *C.davisiana* abundance (LGM) and biogenic barium abundance (base of Holocene).
(*Cycladophora davisiana* data from T. Crawshaw, pers. comm., and biogenic barium data from Howe *et al.*, 1997).

5.2.7. Sedimentation Rate

The AMS radiocarbon dates and the estimated position of the LGM using *C. davisiana* abundance can be used to calculate the sedimentation rate down to a depth of 100cm below the surface in core GC062. The average sedimentation rate for this top 1m of the core is approximately 6.70cm/1000 years. The amount of sediment lost from the top of the core cannot be estimated as there are no available dates for the core top material and the sedimentation rate plot (Fig.5.14a) cannot be estimated upwards beyond the known available dates.

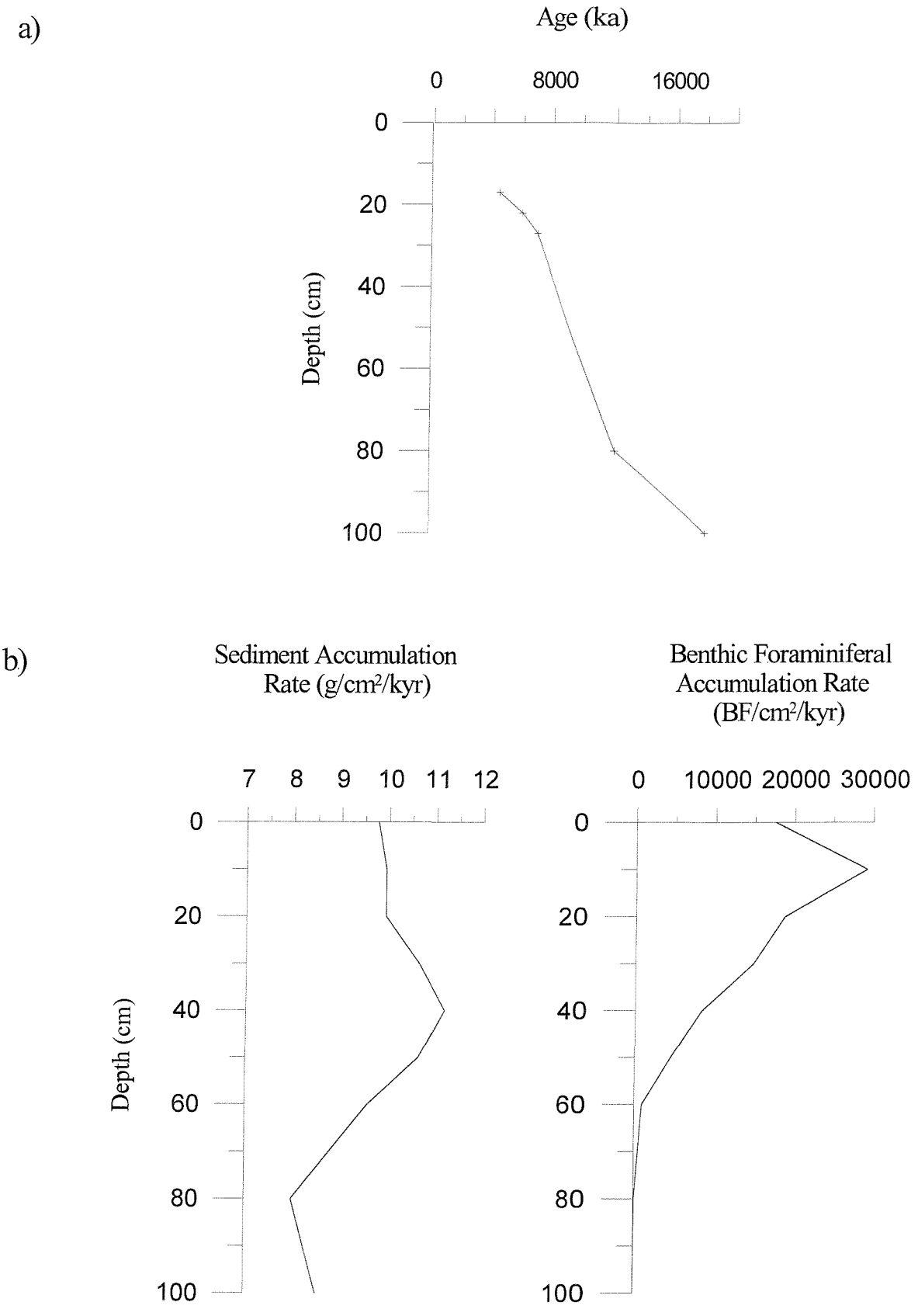

Figure 5.14. a) Sedimentation rate and b) SAR and BFAR plotted for GC062.

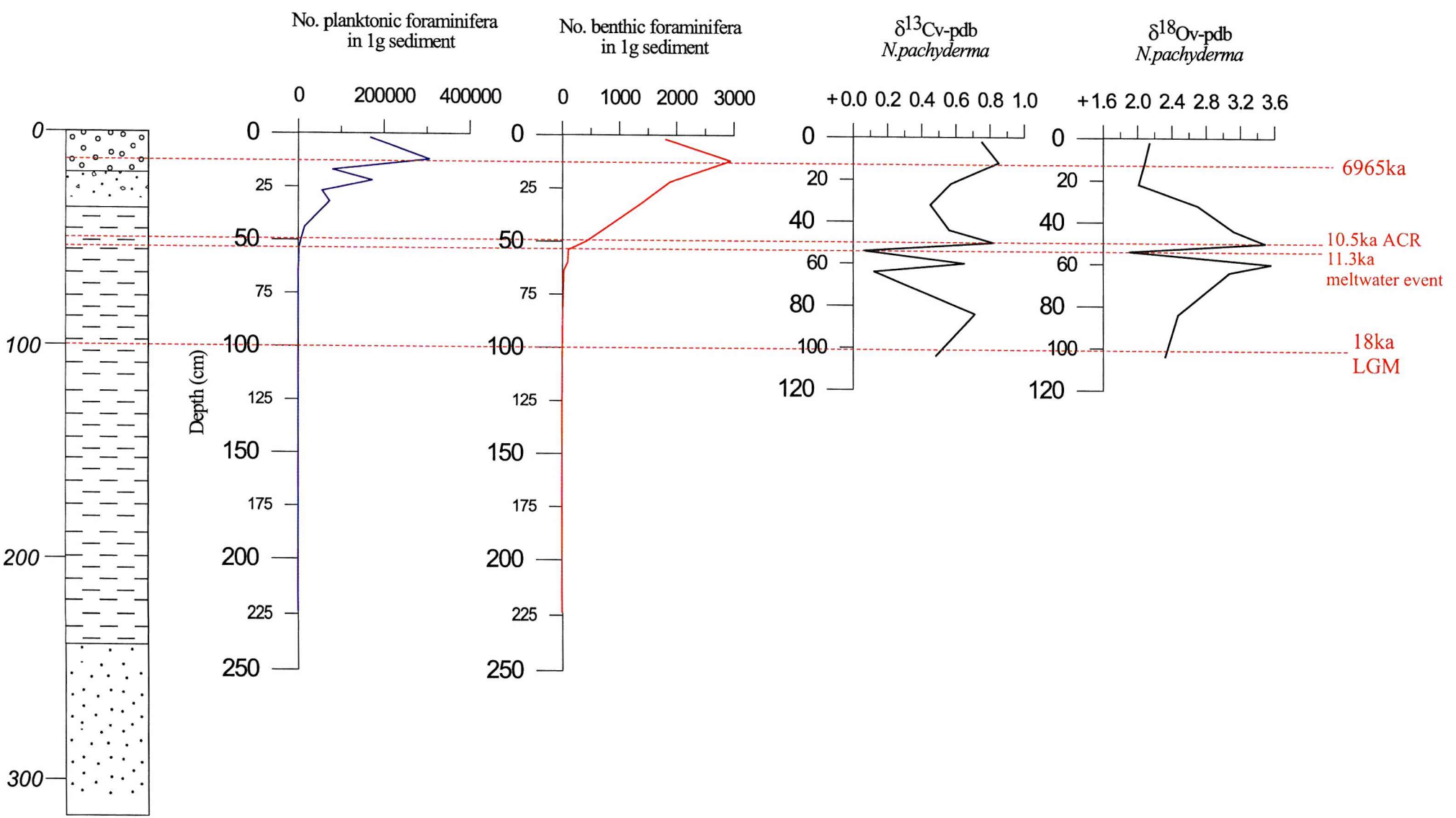

Figure 5.15. Summary diagram for GC062.

The SAR and BFAR were calculated down to 100cm below the sediment surface, and it was assumed that the sedimentation rate remained constant down through this section of the core. The results are shown in Appendix 7 and Figure 5.14b. The SAR shows a general increase up through the core from a minimum of 7.99 cm^2/kyr at 80cm below the surface to a maximum of 11.19 cm^2/kyr at 30cm, before decreasing towards the core top. The BFAR is generally quite high within this section of core with the greatest rates of accumulation occurring between 20-5cm below the surface. The record shows an increase up-core from 17 BF/cm^2/kyr at the base of this section of core to a maximum at 10cm below the surface of 29262 BF/cm^2/kyr, again with a decrease in accumulation rate at the core top.

A summary diagram can be seen in Figure 5.15 showing the important results from GC062. Both planktonic and benthic foraminiferal abundance start to increase significantly up core at about 50cm below the surface and a maximum in abundance seems to correspond to a maximum in the $\delta^{13}C$ record at about 15cm below the core top. The increase in foraminiferal abundance also seems to occur at the same level in the core as a sharp decline in $\delta^{18}O$ to less positive values at about 55cm. Assuming that the sedimentation rate remains constant throughout the core (see Fig.5.14a) the estimated age at this point in the core would be approximately 11.3ka.

5.3. KC099

This core lies approximately 444 km to the north-west of the Polar Front in the western Falkland Trough and has been sampled down to a depth of 60cm below the surface. Using the radiocarbon dates obtained during this study (Fig.5.22) it can be estimated that the sample interval is approximately 450 years and a total of 17 samples were picked from this core.
The lithology shows an upward change from diatom muds at the base of the core passing into a foraminiferal sand unit at about 35cm continuing to the top of the core (Fig.4.1). The only available carbonate data are for the top 20cm of sediment which records an average of 46.7% carbonate within the sediment. Magnetic susceptibility shows a corresponding record to the

lithology and is higher within the diatom mud (terrigenous) unit below about 35cm in the core (Fig.4.2).

5.3.1. Benthic Foraminiferal Abundance

The absolute abundance data are shown in Figure 5.16 and the raw data counts are included in Appendix 10.

Absolute abundance is generally quite high throughout this whole section of core and varies between 178 and 3526 foraminifera per gram, with the abundance maximum occurring at 30cm below the sediment surface. There is a general increase in abundance up core with highest abundance between 30-10cm and a decrease in abundance at the core top (Fig.5.16).

Plots of the relative abundance of individual species can be seen in Figure 5.17 and individual species counts are shown in Appendix 11.

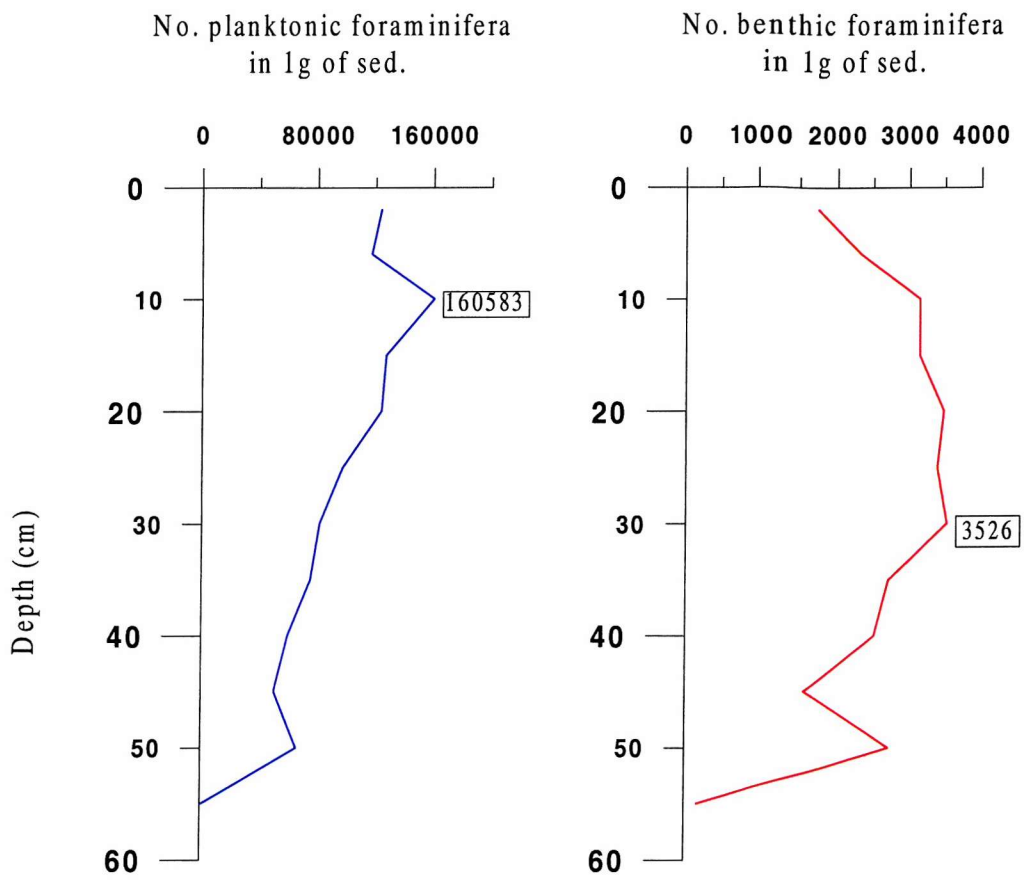

Figure 5.16. Planktonic and benthic foraminiferal absolute abundance for KC099.

There are 74 species from 42 different genera identified in this core with 5 unidentified taxa. The dominant taxa are shown below with the number of samples in which the species formed more than 5% of the assemblage and the benthic ranking with percentage means in brackets:

Eilohedra weddellensis	12	(21.32)
Cassidulina crassa	12	(7.96)
Epistominella exigua	11	(10.45)
Nonionella iridea	10	(6.74)
Gyroidinoides spp.	8	(3.95)
Globocassidulina subglobosa	8	

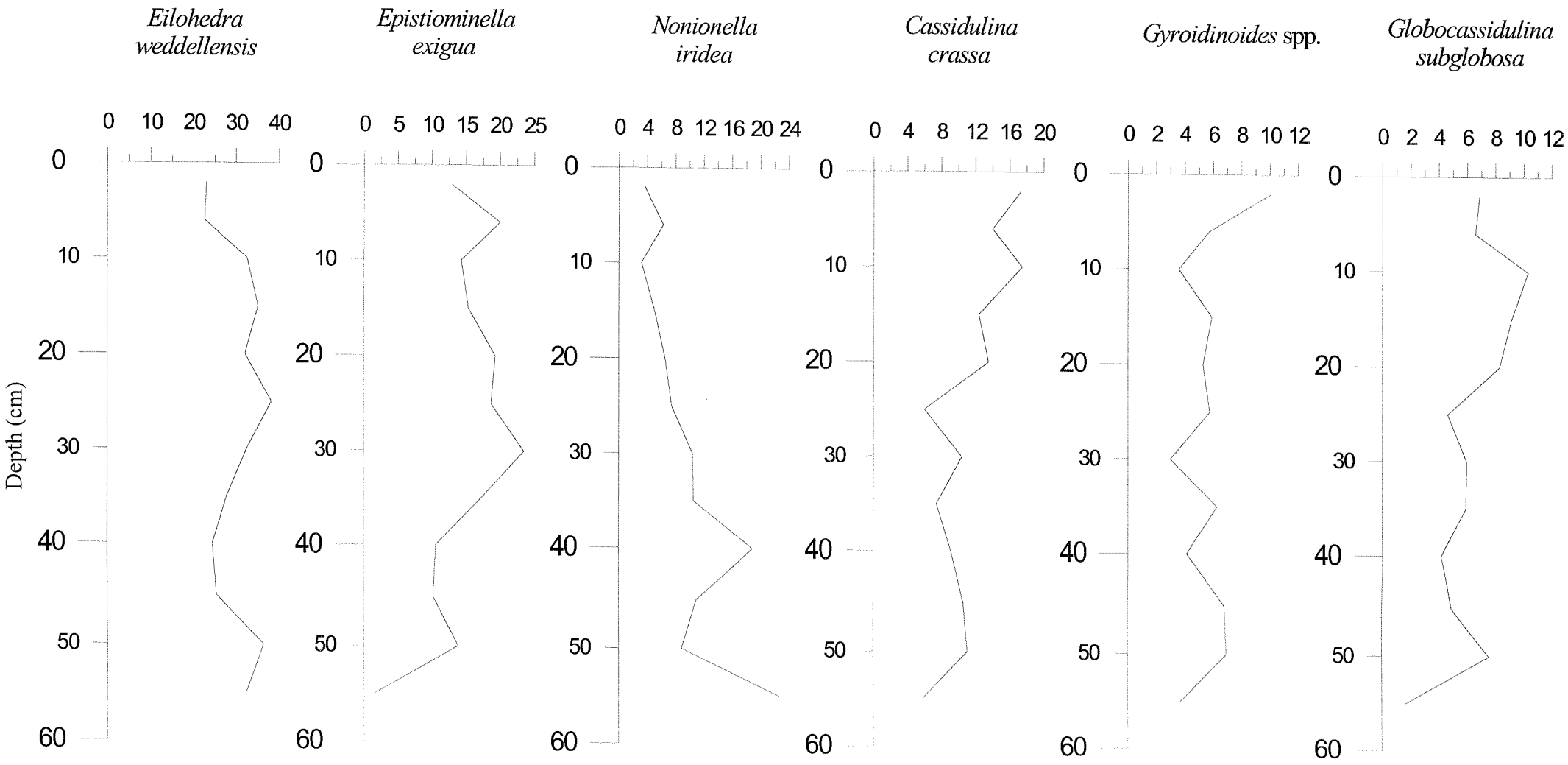

Figure 5.17. Relative abundance (%) of dominant benthic foraminifera for KC099.

Other species that are common in most samples but are not abundant are *Angulogerina angulosa*, *Bolivinita pseudothalmanni*, *Fissurina* spp. and *Lagena* spp. *Eilohedra weddellensis* is the dominant species occurring in much higher abundances in all the samples. The relative abundance of *E. weddellensis* and *E. exigua* remains almost constant throughout this section of core with a small increase between 30-10cm below the surface. The abundance of *N. iridea* shows a marked decrease of almost 20% up through the core over this section. This pattern is mirrored in the relative abundance of *C. crassa* and *G. subglobosa* which show an overall increase up core. There is little variation in the abundance of *Gyroidinoides* spp. apart from an increase at the very top of the core (Fig.5.17).

Agglutinated taxa occur in low abundance and diversity with only 5 species being identified throughout the whole core. The most persistent species is *Eggerella bradyi* that occurs in all but one of the samples studied but usually forms less than 1% of the total abundance.

5.3.2. Species Diversity

5.3.2.1. The Information Function H(S)

H(S) and H(S)max were computed for each sample where the population exceeded 60 individuals to avoid misleading results from small sample size (Appendix 5). The H(S) value ranges from 0.91 at 20cm to 1.42 at 2cm. There appears to be little variation in H(S) through this section of core with slightly higher values at 35cm below the surface and at the core top (Fig.5.18).

5.3.2.2. The Fisher Alpha Index (α)

The α value ranges from 6.5 to 11.5 (Appendix 5). The record of alpha values within this core is quite variable with higher values between 50-35cm and in the top 10cm of the core. There is a minimum value for alpha recorded at 30cm below the surface (Fig.5.18).

The third graph in Figure 5.18 shows that the number of species found in each sample is also quite variable within the core. There is again a maximum between 50-35cm and also at the core top and a minimum at 30cm below the surface, which is a similar pattern to that seen in the record of alpha values.

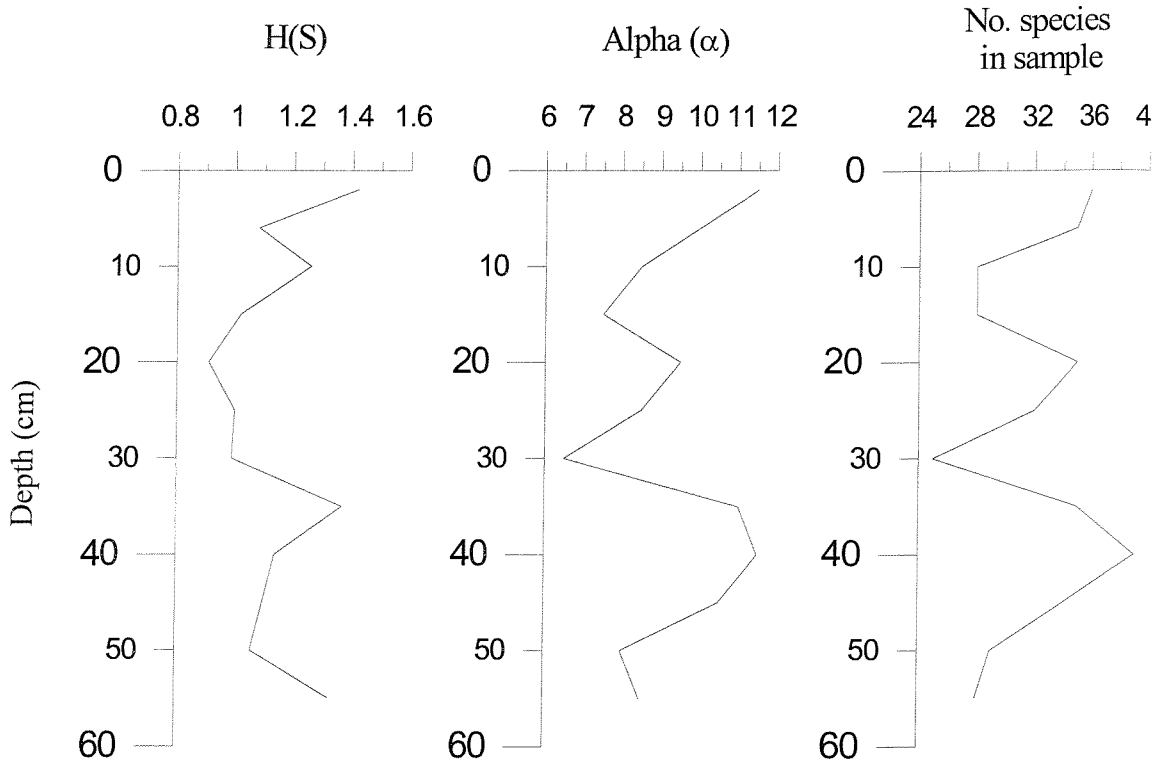

Figure 5.18. Species diversity functions for KC099.

5.3.3. Planktonic Foraminiferal Abundance

Absolute abundance data are shown in Figure 5.16 and raw data counts are included in Appendix 10.

The dominant foraminifer is the left-coiling (sinistral) *Neogloboquadrina pachyderma*. It occurs in every sample throughout the core and usually comprises over 95% of the total planktonic assemblage.

The absolute abundance is relatively high and varies between 972 and 160583 foraminifera per gram with the abundance maximum occurring at 10cm below the sediment surface. There is a general increase in planktonic foraminiferal abundance up through this section of core with no decline in numbers observed at the core top.

Seven other species of planktonic foraminifera also occur but in very low abundance and not in all samples, and therefore were not counted, but their presence was noted (Table 5.9). These are listed with the number of samples in which they were found:

Assemblage	Planktonic species	2 - 3 cm	6 - 7 cm	10 - 11 cm	15 - 16 cm	20 - 21 cm	25 - 26 cm	30 - 31 cm	35 - 36 cm	40 - 41 cm	45 - 46 cm	50 - 51 cm	55 - 56 cm
Subtropical	*Globorotalia crassaformis*	*	*	*	*	*	*	*	*	*	*	*	
Subtropical / Transition	*Globorotalia truncatulinoides*	*	*	*	*	*	*	*	*	*	*	*	*
Transition / cold-temperate	*Globorotalia inflata*	*	*	*	*	*	*	*	*	*	*	*	*
Transition / cold-temperate	*Globigerinita glutinata*									*			
Subantarctic / upwelling	*Globigerina bulloides*	*	*	*	*	*	*	*	*	*	*	*	*
Subantarctic	*Turborotalita quinqueloba*									*	*	*	*
Subantarctic	*Globigerinita uvula*	*	*	*	*	*	*	*	*	*	*	*	*
Antarctic	*Neogloboquadrina pachyderma*	*	*	*	*	*	*	*	*	*	*	*	*

Table 5.9. Planktonic foraminifera species found in KC099 (based on Blair, 1965; Be 1969, 1977).

Globorotalia truncatulinoides	12
Globigerina bulloides	12
Globigerinita uvula	12
Globorotalia inflata	12
Globorotalia crassaformis	11
Turborotalita quinqueloba	4
Globigerinita glutinata	1

The subtropical/transition species *G. truncatulinoides* and the subpolar species *G. bulloides* appear in all of the samples and are found in higher abundance than the other species listed above.

5.3.4. Calcium Carbonate Dissolution

The P:B ratio remains high throughout this section of the core of the core, and on average the percentage of planktonic foraminifera is greater than 95% (Appendix 6). There is a general decrease in the percentage of planktonic foraminifera down through the top section of the core to a minimum value of 85% at 55cm below the surface (Fig.5.19). Carbonate data are only available for the top 20cm of the core and so could not be used here to determine the extent of dissolution.

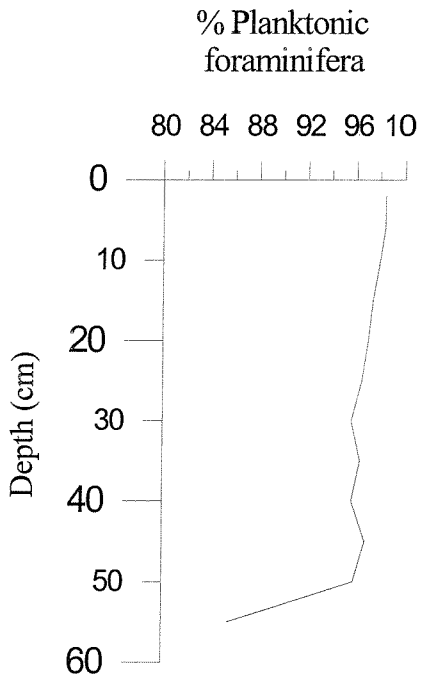

Figure 5.19. Dissolution index for KC099.

Foraminiferal test fragmentation is only observed in the deepest sample at 55cm below the surface and only to a small extent, so preservation is generally very good throughout this whole section of core.

5.3.5. Stable Isotopes

Carbon and oxygen stable isotope analysis was carried out for planktonic foraminifera only in this core. The results are shown in Table 5.10, and isotope curves can be seen in Figure 5.20. The results have not been adjusted to take into account vital effects.

Depth (cmbsf)	$\delta^{13}C$ ($^{0}/_{00}$ PDB) *N. pachyderma*	$\delta^{18}O$ ($^{0}/_{00}$ PDB) *N. pachyderma*
2-3	0.83	2.16
10-11	0.76	2.16
15-16	0.82	2.06
20-21	0.66	1.89
25-26	0.70	2.05
30-31	0.75	2.15
35-36	0.56	2.24
40-41	0.56	2.60
45-46	0.55	2.40
50-51	0.82	2.33
55-56	0.46	2.77
59-60	0.34	3.05

Table 5.10. Planktonic foraminiferal carbon and oxygen stable isotope data for KC099.

The planktonic isotope values based on range from 0.34 to 0.83‰ for $\delta^{13}C$ and from 1.89 to 3.05‰ for $\delta^{18}O$. The $\delta^{13}C$ record shows an overall increase up through this section of core to the highest $\delta^{13}C$ at the core top. There is also a small peak in $\delta^{13}C$ at about 50cm below the surface. The $\delta^{18}O$ record shows the opposite trend to $\delta^{13}C$ with a decrease up through this section of core to lowest vales within the top 20cm. There appears to be good agreement between the carbon and oxygen isotope records within this core.

5.3.6. Radiocarbon Dates

Three AMS radiocarbon dates were obtained for this core (Table 5.11) but the age of the core top was not determined, and therefore there was no assessment of the reservoir effect.

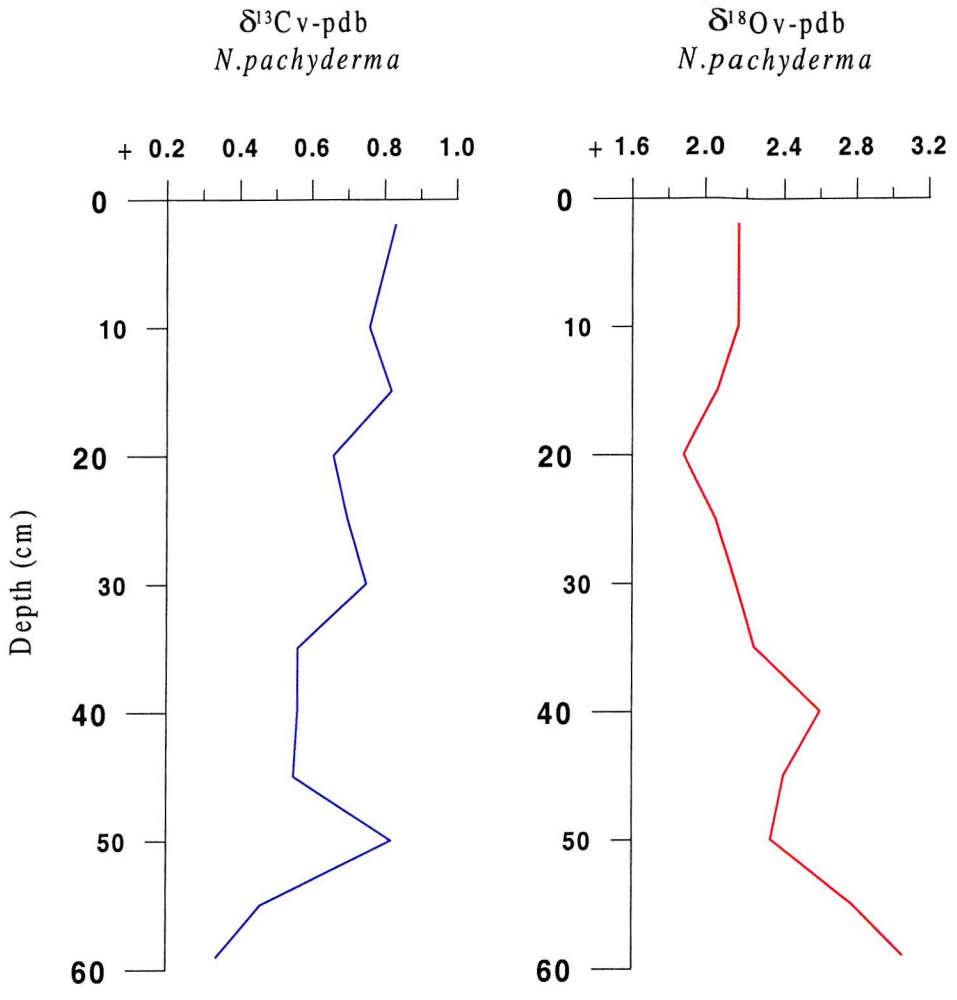

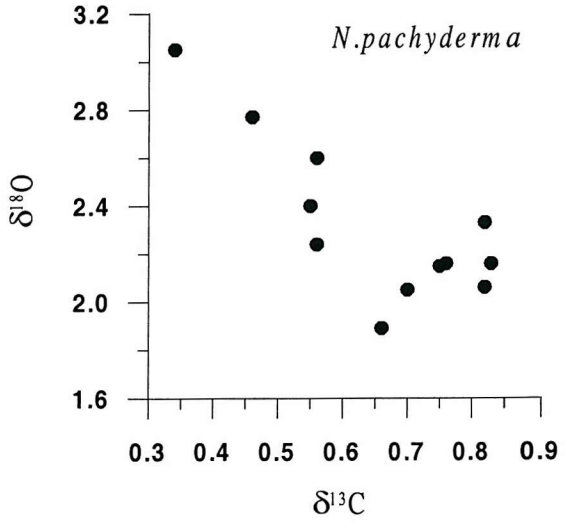

Planktonic foraminiferal $\delta^{13}C$ against $\delta^{18}O$ for KC099.

Figure 5.20. Planktonic stable isotopes curves for KC099.

Publication code	Sample	Conventional Radiocarbon Age (years BP ±1σ)	Corrected Age (years BP)	Carbon content (% by wt.)	Material analysed
AA36266	KC099 15-16cm	5215 ± 70	3915	11.0	*N. pachyderma*
AA36267	KC099 20-21cm	6140 ± 55	4840	10.0	*N. pachyderma*
AA36268	KC099 25-26cm	6660 ± 55	5360	10.0	*N. pachyderma*

Table 5.11. AMS radiocarbon dates for KC099.

A correction of 1300 years has been applied to the conventional radiocarbon age to account for the Antarctic reservoir effect. Another dating method can be applied which is the first down-core abundance peak of *Cycladophora davisiana* marking the position of the LGM at 180cm within this core (Fig.5.21). There were no biogenic barium data available to mark the base of the Holocene.

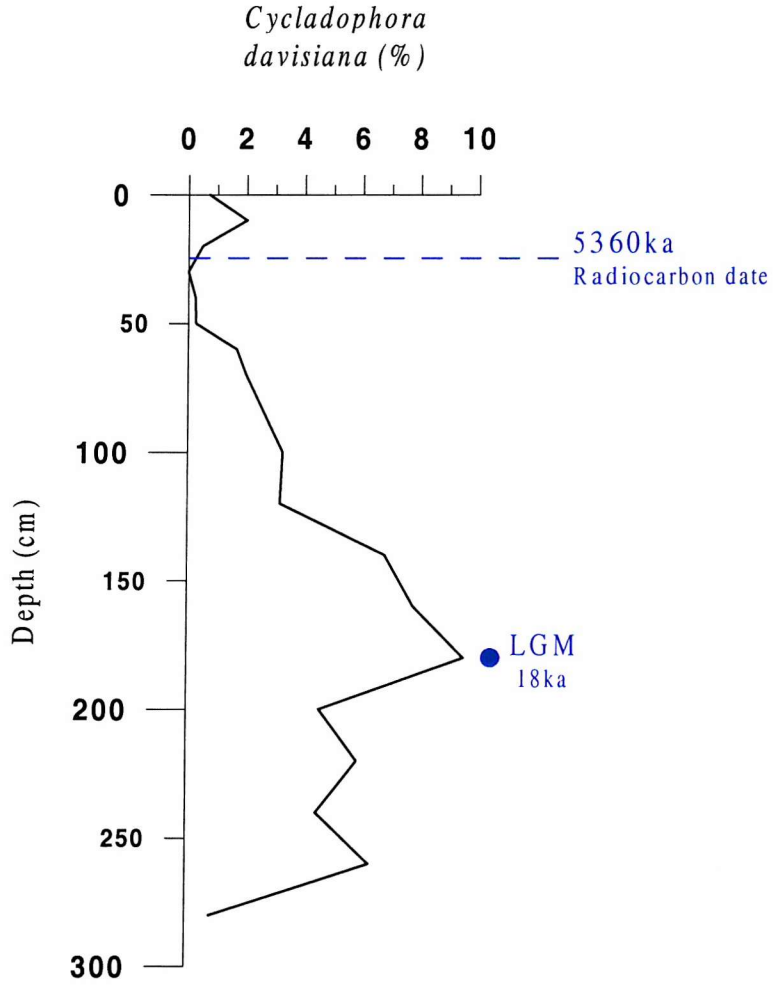

Figure 5.21. Dating of KC099 (*C.davisiana* data from T.Crawshaw, pers. comm.)

5.3.7. Sedimentation Rate

The AMS radiocarbon dates and the estimated position of the LGM using *C. davisiana* abundance can be used to calculate the sedimentation rate down to a depth of 180cm below the surface in core KC099. The average sedimentation rate for this section of the core is on average approximately 11.5 cm/1000 years. The amount of sediment lost from the top of the core cannot be estimated as there are no available dates for the core top material and the sedimentation rate plot (Fig.5.22) cannot be estimated upwards beyond the known available dates.

The SAR and BFAR were calculated using an average value for dry bulk density as water content values were available only for the top 20cm of the core. Therefore the sediment accumulation rate is assumed to remain constant throughout the core. The benthic foraminiferal accumulation rate has been calculated down to 55cm below the sediment surface, and it was assumed that the sedimentation rate also remained constant down through this section of the core (Fig.5.22). The results are shown in Appendix 7 and Figure 5.22. Therefore as the same SAR is used to calculate BFAR for each sample the record follows the general pattern seen in the benthic foraminiferal absolute abundance record (Fig.5.16). The values for the BFAR are generally quite high and range from 3147 BF/cm^2/kyr at the bottom of the core section and showing a general increase up through the core with a maximum rate of 6234 BF/cm^2/kyr at 30cm.

A summary diagram can be seen in Figure 5.23 which shows the main results from core KC099. There is good agreement between the planktonic and benthic environments at this core site as seen in the absolute abundance records. There is very little variation observed in the planktonic isotope records which show a general increase in $\delta^{13}C$ and a corresponding decrease in $\delta^{18}O$ up through this core section, representing a gradual recovery from glacial conditions.

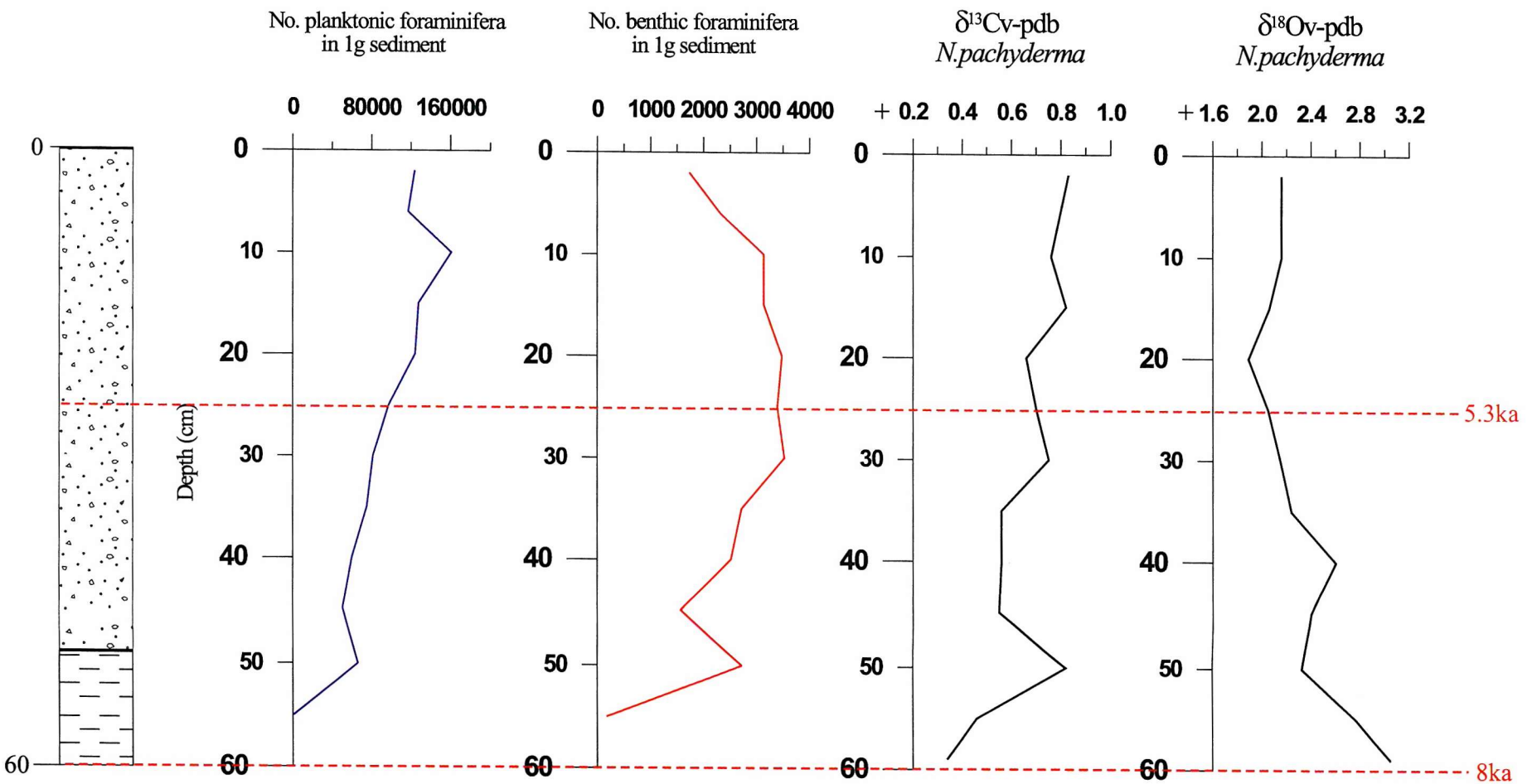

Figure 5.23. Summary diagram for KC099.

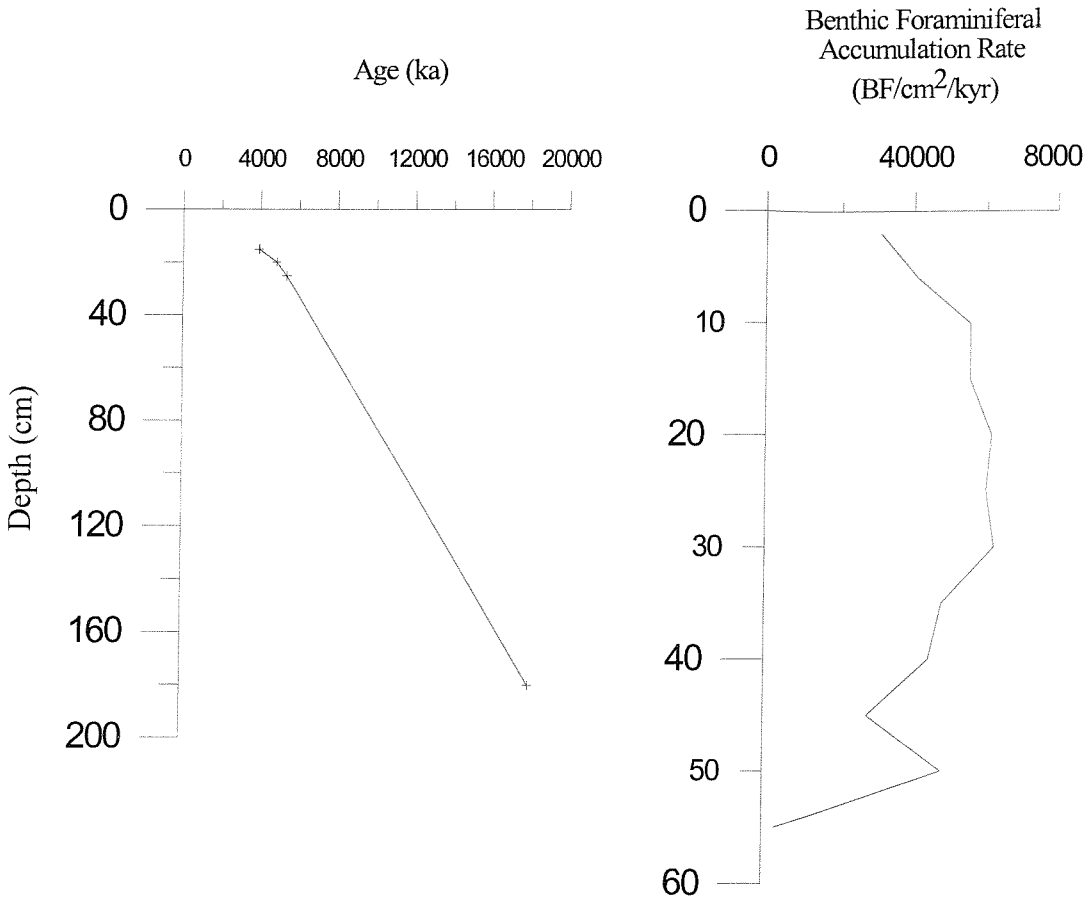

Figure 5.22. Sedimentation rate and BFAR plotted for KC099.

CORES FROM SOUTH OF THE POLAR FRONT

5.4. KC064

This core lies approximately 89 km to the south-east of the Polar Front in the northern Scotia Sea and has been sampled down to a depth of 300cm below the surface. Using the radiocarbon dates obtained during this study (Fig.5.30a) it can be estimated that the sample interval is approximately 350 years and a total of 42 samples were picked from this core.

The lithology shows an upward change from diatom muds at the base passing through muddy diatom ooze and diatom mud, to a foraminifera-bearing diatom mud unit at the top of the core. There is no carbonate present within the diatom ooze at the base of the core and $CaCO_3$ only appears as a significant percent within the foraminiferal sands towards the core top (Fig.4.1). Magnetic susceptibility shows a corresponding record to the lithology and is higher within the diatom ooze (terrigenous) unit below about 70cm in the core (Fig.4.3).

5.4.1. Benthic Foraminiferal Abundance

The absolute abundance data are shown in Figure 5.24 and the raw data counts are included in Appendix 12.

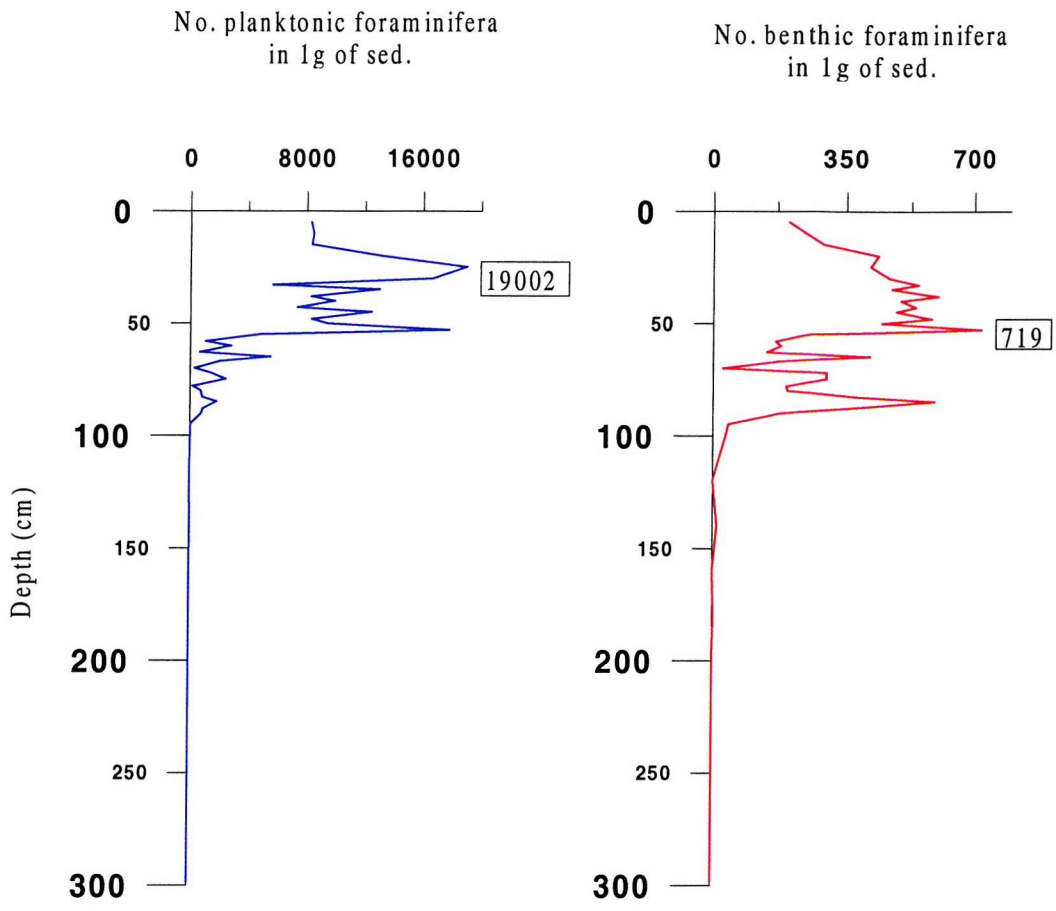

Figure 5.24. Planktonic and benthic foraminiferal absolute abundance for KC064.

Absolute abundance is much lower than in KC097, only up to 719 foraminifera per gram, with the abundance maximum occurring at 53cm below the sediment surface. Benthic

foraminifera are absent from the deepest six samples and occur only in low numbers in the lower section of the core. They appear in greater abundance at 100cm below the surface where there is a rapid initial increase in abundance up core followed by a decline in numbers to a very low abundance at 70cm. Abundance then continues to increase to the maximum value at 53cm followed by a more gradual decrease to the core top. The greatest variation in abundance occurs within the section between 50 and 100cm below the surface (Fig.5.24).

Plots of the relative abundance of individual species can be seen in Figure 5.25 and individual species counts are shown in Appendix 13.

There are 88 species from 54 different genera identified in this core with 8 unidentified taxa. The dominant taxa are shown below with the number of samples in which the species formed more than 5% of the assemblage and the benthic ranking with percentage means in brackets:

Eilohedra weddellensis	33	(41.82)
Gyroidinoides spp.	18	(4.7)
Lagena spp.	18	(4.56)
Globocassidulina subglobosa	13	(4.66)
Nuttallides umbonifera	6	(2.33)
Oridorsalis tener	5	
Melonis barleeanum	4	
Epistominella exigua	4	

Other species that are common in most samples but are not abundant are *Pullenia subcarinata, Eponides* sp. and *Fissurina* spp. *Eilohedra weddellensis* is the only species which is persistent throughout the top 100cm of the core, but is absent from samples below 180cm. The relative abundance of the individual species follows the general pattern of increased abundance up-core as seen in the benthic absolute abundance record described above.

The relative abundance of *Lagena* spp., *Gyroidinoides* spp., *G. subglobosa, N. umbonifera, E. exigua* and *M. barleeanum* all show a similar trend of a gradual increase up core with maximum abundance occurring in the top 50cm of the core, followed by a subsequent decrease towards the top of the core. The abundance records of *E. weddellensis* and *O. tener*

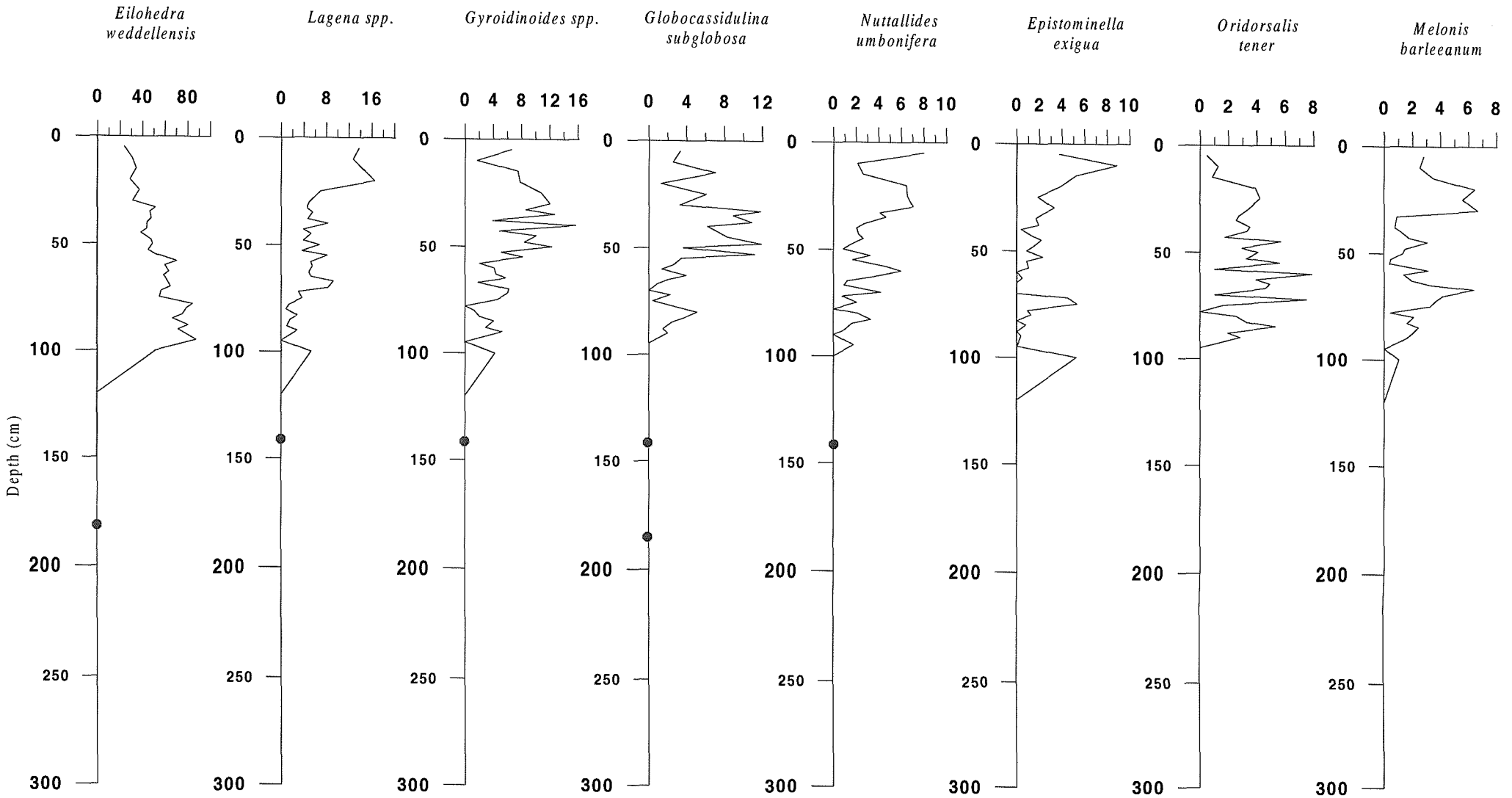

Figure 5.25. Relative abundance (%) of dominant benthic foraminifera for KC064.

● species present but foraminiferal abundance is statistically too low to calculate %.

however, show a different trend of a more rapid initial increase to maximum value within the 50-100cm section, followed by a more gradual decrease in abundance to the top of the core.

Agglutinated taxa occur in low abundance but with slightly higher diversity than KC097 diversity with 27 species from 20 different genera being identified throughout the whole core. There is no one dominant agglutinated foraminifer and the identified species appear quite consistently throughout the top 100cm of the core, but in low numbers.

5.4.2. Species Diversity

5.4.2.1. The Information Function H(S)

H(S) and H(S)max were computed for each sample where the population exceeded 60 individuals to avoid misleading results from small sample size (Appendix 5). The H(S) value ranges from 0.60 at 78cm to 1.70 within the top 10cm. Below 90cm there were not enough foraminifera present for the samples to be included in the analysis (Fig.5.26). There is a gradual increase in the H(S) value up through the core to the maximum within the top sample. The range of values is lower than for KC097 that may indicate lower diversity within this core.

5.4.2.2. The Fisher Alpha Index (α)

The α value ranges from 3.5 to 14 and tends to fluctuate mostly between values of 4 and 9 (Appendix 5). There are no values for α below 88cm due to low foraminiferal abundance. Alpha values show a steady increase up core to the maximum value at 10cm below the surface, which is similar to the H(S) value trend (Fig.5.26).

The third graph in Figure 5.26 shows that the number of species in each sample is increasing up through the core to the sample at 10cm which contains the maximum number of species, which may also indicate that diversity is lower towards the base of the core.

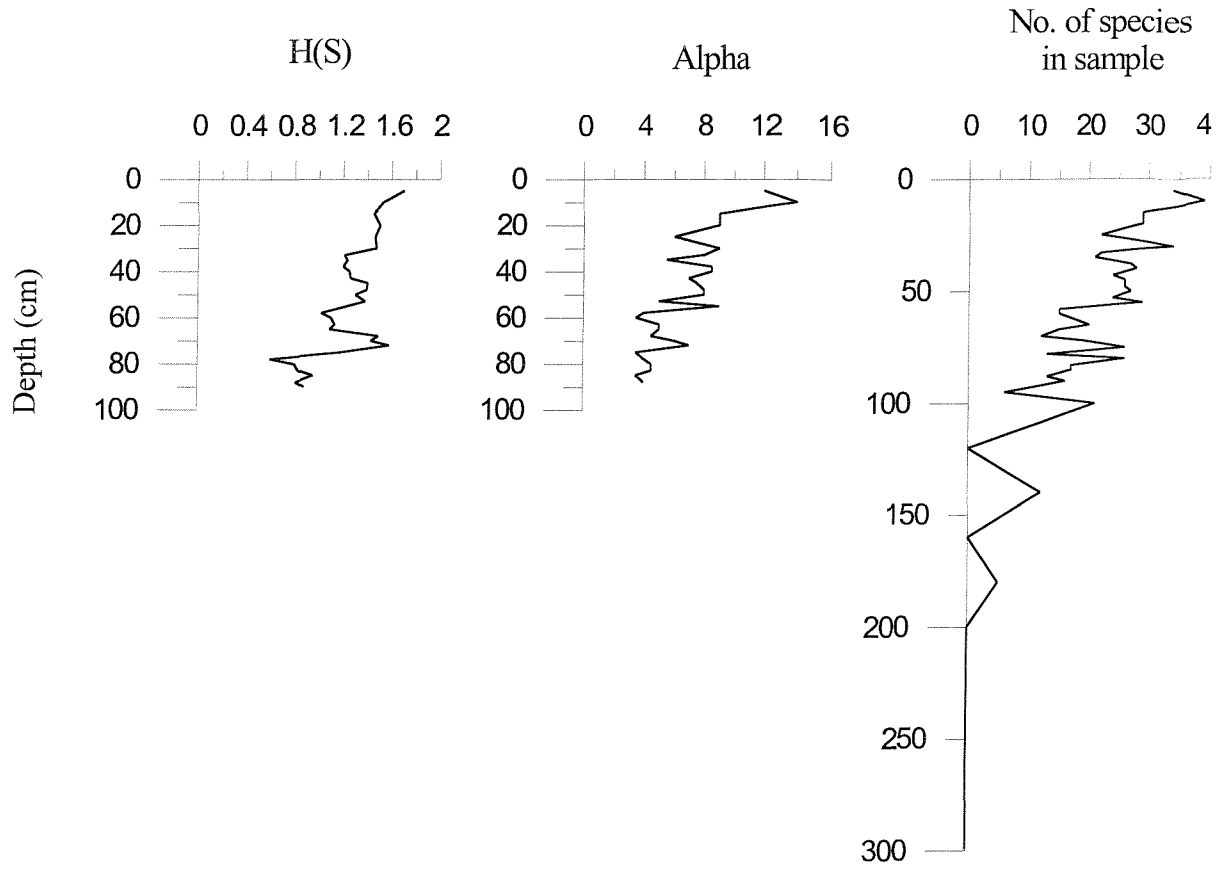

Figure 5.26. Species Diversity functions for KC064.

5.4.3. Planktonic Foraminiferal Abundance

Absolute abundance data are shown in Figure 5.24 and raw data counts are included in Appendix 12.

The absolute abundance is much lower than in KC097 but is still moderately high, up to 19002 foraminifera per gram with the abundance maximum occurring at 25cm below the sediment surface. Planktonic foraminifera are absent from the bottom samples and only start to appear in significant abundance at 100cm. Abundance remains quite constant before increasing rapidly at about 55cm to a peak value which is then followed by a decline in numbers. Another sharp increase in abundance to the maximum value at 25cm is then followed by a decrease in abundance to the core top.

Assemblage	Planktonic species	Top 10 cm	10 - 11 cm	15 - 16 cm	20 - 21 cm	25 - 26 cm	30 - 31 cm	33 34 cm	35 - 36 cm	38 - 39 cm	40 - 41 cm	43 - 44 cm	45 - 46 cm	48 - 49 cm	50 - 51 cm	53 - 54 cm	55 - 56 cm	58 - 59 cm	60 - 61 cm	63 - 64 cm	65 - 66 cm	67 - 68 cm	70 - 71 cm	72 - 73 cm	75 - 76 cm	78 - 79 cm	80 - 81 cm	83 - 84 cm	85 - 86 cm	88 - 89 cm	90 - 91 cm	95 - 96 cm	100 - 101 cm	140 - 141 cm	180 - 181 cm
Subtropical	*Globorotalia crassaformis*							*						*																				
Subtropical / Transition	*Globorotalia truncatulinoides*	*	*	*	*	*	*	*	*	*	*	*	*	*	*	*	*	*	*	*	*	*	*	*										
Transition / cold-temperate	*Globorotalia inflata*	*		*	*		*		*				*		*	*				*		*	*	*										
Subantarctic / upwelling	*Globigerina bulloides*	*		*	*	*	*		*				*		*	*				*	*	*	*	*	*	*								
Antarctic	*Neogloboquadrina pachyderma*	*	*	*	*	*	*	*	*	*	*	*	*	*	*	*	*	*	*	*	*	*	*	*	*	*	*	*	*	*	*	*	*	*

Table 5.12. Planktonic foraminifera species found in KC064 (based on Blair, 1965; Be 1969, 1977).

The dominant foraminifer is the left-coiling (sinistral) *Neogloboquadrina pachyderma*. It occurs in every sample throughout the core and usually comprises over 95% of the total planktonic assemblage.

Four other species of planktonic foraminifera also occur but in very low abundance and not in all samples, and therefore were not counted, but their presence was noted (Table 5.12). These are listed below with the number of samples in which they were found:

Globorotalia truncatulinoides	24
Globigerina bulloides	14
Globorotalia inflata	11
Globorotalia crassaformis	3

The subtropical/transition species *G. truncatulinoides* appears in many of the samples but in the top 75cm of the core. *Globigerina bulloides* occurs in fewer samples than *G. truncatulinoides* but is more abundant within those samples than the other species listed above.

5.4.4. Calcium Carbonate Dissolution

Where there is no value for the P:B ratio shown foraminifera were completely absent from the sample (Appendix 6). The P:B ratio remains high throughout the top 75cm of the core and on average the percentage of planktonic foraminifera is about 90% within this section (Fig.5.27). Below 75cm the P:B ratio decreases rapidly at first before fluctuating between a percentage of planktonic foraminifera of 0 and 78%. The percentage of planktonic foraminifera seems to be much lower in the bottom section of this core than in KC097. Therefore it would appear that as the P:B ratio decreases down core the effects of dissolution must be increasing as seen by the higher relative abundance of benthic foraminifera. This can also be seen in the carbonate record which shows a decreasing percentage of carbonate within the sediment down through the core from 6.3% in the top sample down to 0.3% at 100cm below the surface (Fig.5.27).

Foraminiferal test fragmentation increases down core and is accompanied by a decrease in test preservation. In the samples from the lower section of the core the planktonic

foraminifera often show evidence of holes within the walls of the individual chambers (see plate, section 12). Preservation of foraminiferal tests is much poorer than in KC097.

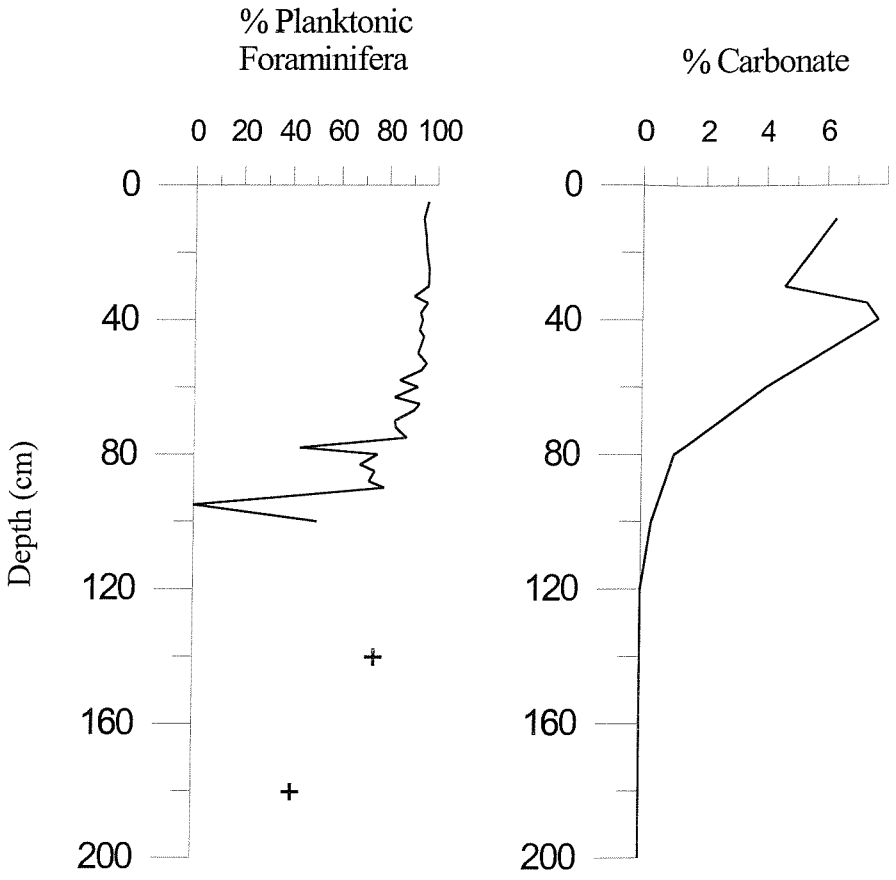

Figure 5.27. Dissolution indices for KC064.

5.4.5. Stable Isotopes

Carbon and oxygen stable isotope analysis was carried out for planktonic and benthic foraminifera in this core. The results are shown in Tables 5.13 and 5.14, and isotope curves can be seen in Figure 5.28. The results have not been adjusted to take into account vital effects.

Depth (cmbsf)	$\delta^{13}C$ (‰ PDB) *N. pachyderma*	$\delta^{18}O$ (‰ PDB) *N. pachyderma*
10	0.94	2.85
20	1.12	2.94
30	1.00	3.06
40	0.94	3.06
50	0.83	3.06
60	0.67	3.12
65	0.71	2.99
70	0.60	3.17
75	0.59	3.07
80	0.07	3.68
90	0.51	3.73
100	0.33	3.63
140	0.57	3.12

Table 5.13. Planktonic foraminiferal carbon and oxygen stable isotope data for KC064.

Depth (cmbsf)	$\delta^{13}C$ (‰ PDB) *O. tener*	$\delta^{18}O$ (‰ PDB) *O. tener*
20	-1.54	3.27
30	-1.74	2.69
40	-1.79	3.37
50	-2.39	3.47
65	-2.42	3.13
90	-2.11	4.24

Table 5.14. Benthic foraminiferal carbon and oxygen stable isotope data for KC064.

The planktonic isotope values based on *N. pachyderma* range from 0.07 to 1.12‰ for $\delta^{13}C$ and from 2.85 to 3.73‰ for $\delta^{18}O$. The $\delta^{13}C$ record shows an initial decrease to the lowest value at 80cm, followed by a subsequent increase up through the rest of the core to the core top. Values are generally higher within the top 80cm of the core. The $\delta^{18}O$ record shows an opposite trend of higher values within the lower section of the core with a sharp decrease at 80cm, followed by a gradual decreasing trend to the top sample. In both the $\delta^{13}C$ and $\delta^{18}O$ planktonic isotope record there is a sharp step in the curve at 80cm below the surface.

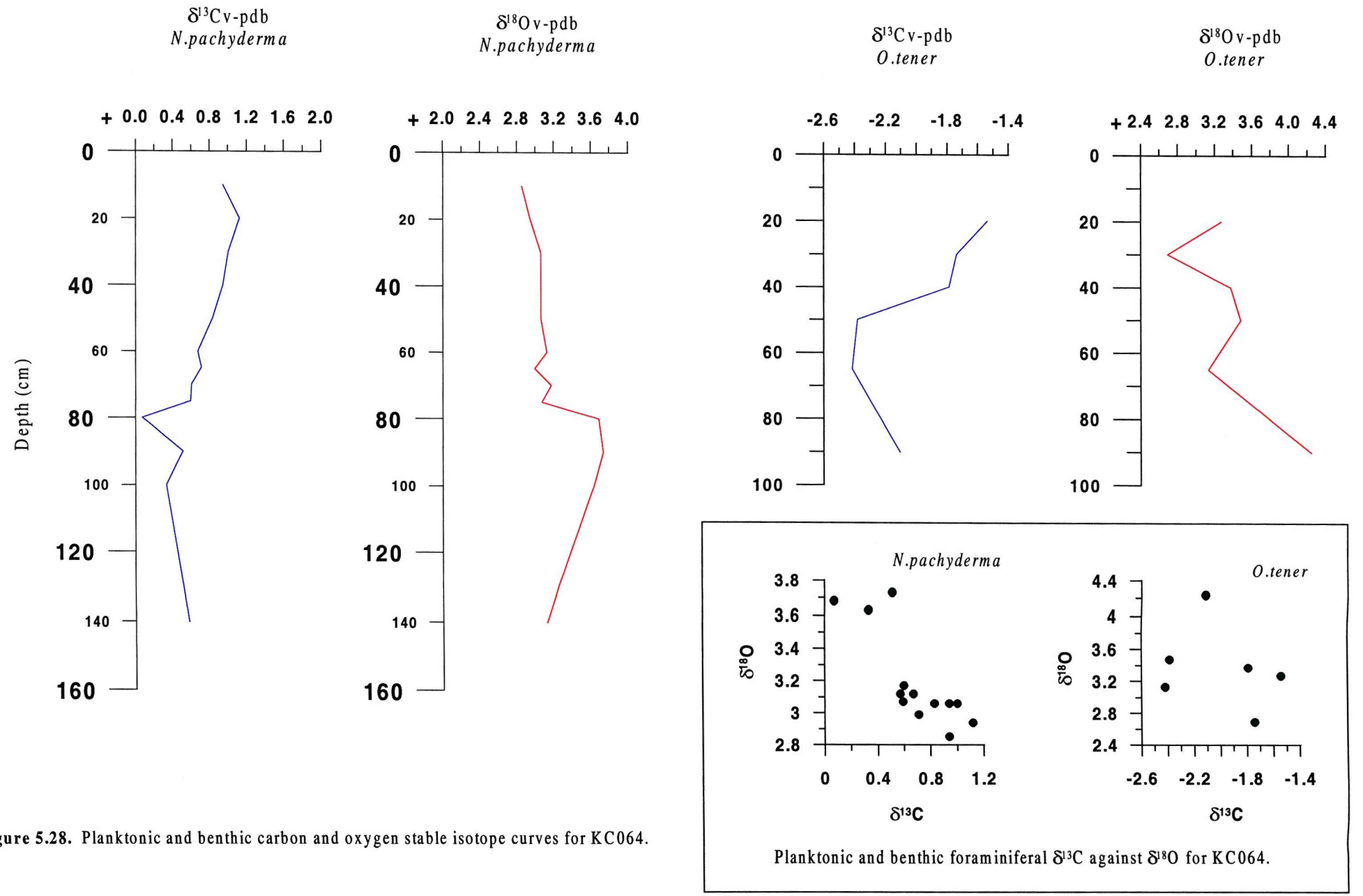

Figure 5.28. Planktonic and benthic carbon and oxygen stable isotope curves for KC064.

Planktonic and benthic foraminiferal $\delta^{13}C$ against $\delta^{18}O$ for KC064.

The benthic isotope values based on *O. tener* range from –1.54 to –2.42‰ for $\delta^{13}C$ and from 2.69 to 4.24‰ for $\delta^{18}O$. The $\delta^{13}C$ record shows an initial decrease to the most negative value at 65cm before subsequently increasing rapidly at 50cm up through the rest of the core. Benthic $\delta^{13}C$ is therefore generally higher towards the top of the core. This pattern is mirrored in the $\delta^{18}O$ curve, which shows the general trend of a decrease in $\delta^{18}O$ up through the core to the top sample.

There is good agreement between the planktonic and benthic isotope records for both $\delta^{13}C$ and $\delta^{18}O$, with similar patterns of lower $\delta^{13}C$ and higher $\delta^{18}O$ seen in the bottom section of the core. Changes in the $\delta^{13}C$ record also seem to be accompanied by a similar change in $\delta^{18}O$ for both the planktonic and benthic records.

5.4.6. Radiocarbon Dates

The AMS radiocarbon results are the only dates obtained for a core from south of the Polar Front in this study (Table 5.15).

Publication code	Sample	Conventional Radiocarbon Age (years BP ±1σ)	Corrected Age (years BP)	Carbon content (% by wt.)	Material analysed
CAMS-60836	KC064 Top 10cm	4310 ± 40	3010	10.40	*N. pachyderma*
CAMS-60837	KC064 75-76cm	11010 ± 80	9710	7.30	*N. pachyderma*
CAMS-60838	KC064 80-81cm	11900 ± 100	10600	8.40	*N. pachyderma*
AA35127	KC064 Top 10cm	12425 ± 80	11125	0.16 #	Bulk organic carbon

Table 5.15. AMS radiocarbon dates for KC064 (# NB this is the % by wt. of carbon in the treated, dried and homogenised sample).

A correction of 1300 years has been applied to the conventional radiocarbon age to account for the Antarctic reservoir effect, and again an age of several thousand years for core top material suggests that some sediment has been lost from the core top. An additional sample from 70-71cm was also submitted for dating but this failed to graphitise and so no date was recorded.

Other methods for dating core material are available for KC064 including the abundance of the radiolarian *Cycladophora davisiana* and the amount of biogenic barium (ppm) within the

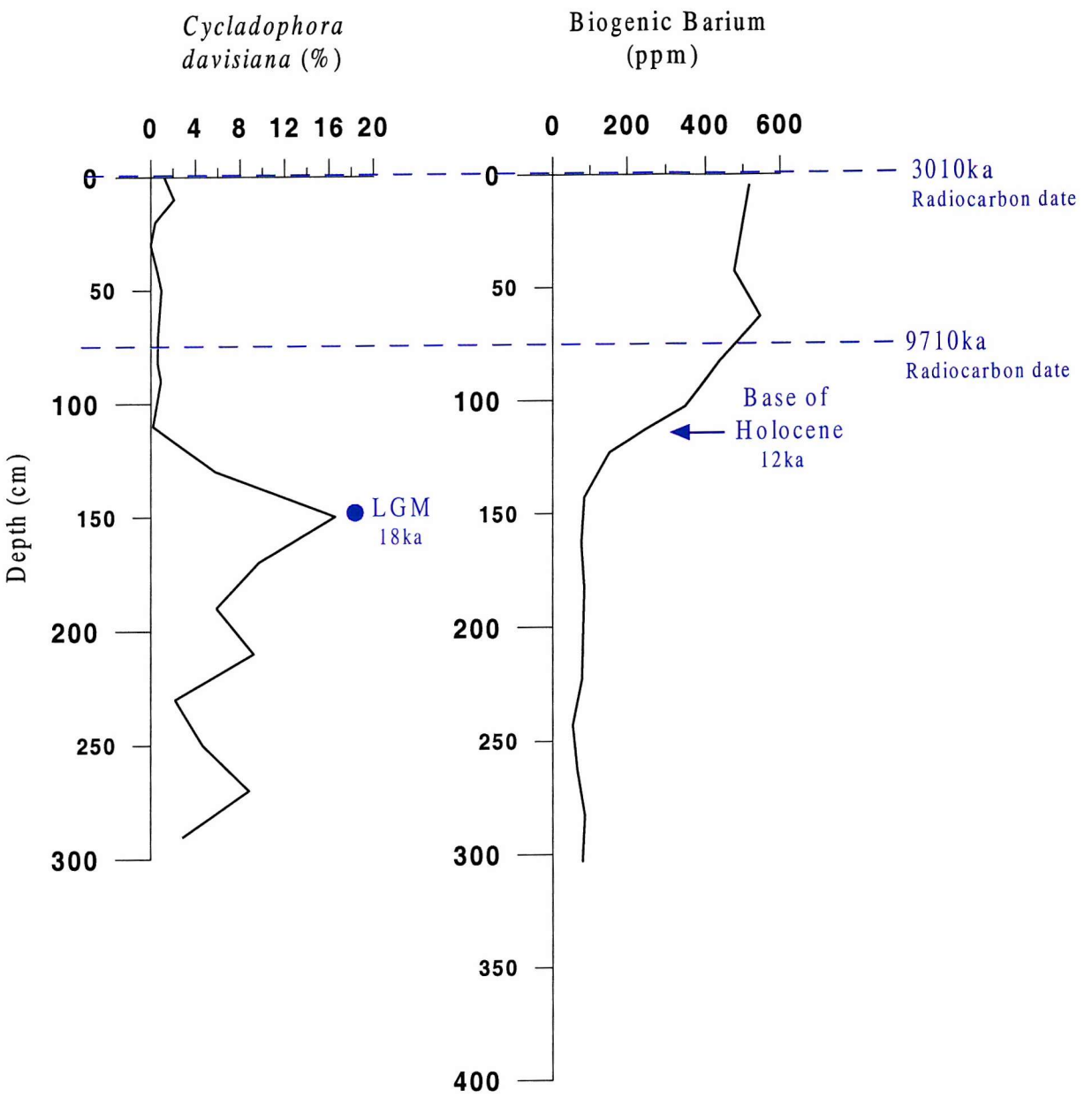

Figure 5.29. Dating of KC064 (*C.davisiana* data from T.Crawshaw, pers. comm., and biogenic barium data from Pudsey and Howe, 1998).

sediment (Fig.5.29). The first down-core abundance peak of *C. davisiana* can be used to mark the position of the LGM which occurs at 150cm, and a downward decrease in the amount of biogenic barium can be used to indicate the base of the Holocene (Stage 1) which occurs at about 120cm in KC064. These additional dates would seem to complement the AMS radiocarbon dates obtained in this study.

5.4.7. Sedimentation Rate

The AMS radiocarbon dates and the estimated position of the LGM using *C. davisiana* abundance can be used to calculate the sedimentation rate down to a depth of 150cm below the surface in this core (Fig.5.30a). The average sedimentation rate is approximately 10.7cm/1000 years from the core top to the base of Stage 1 and 9.9cm/1000 years from the core top to the LGM. Pudsey and Howe (1998) calculated the sedimentation rate for KC064 as 9.2cm/ka from the core top to the base of stage 1, and 8.9cm/ka from the core top to the LGM.

Therefore, assuming that the sedimentation rate remained constant the amount of material lost from the top of the core can be estimated as approximately 32cm.

The SAR and BFAR were calculated down to 300cm below the surface, assuming that the sedimentation rate remained constant down through the rest of the core. The results can be seen in Appendix 7 and Figure 5.30b.

There is a progressive decrease in the SAR up through the core of almost $3cm^2/kyr$, from the greatest rate of $19.28cm^2/kyr$ at 301cm to $16.45cm^2/kyr$ at the core top. The BFAR however, is greatest in the top 100cm of the core with the rate increasing up through the core to a peak rate of 8471 $BF/cm^2/kyr$ at about 40cm below the surface.

A summary diagram can be seen in Figure 5.31 showing some of the important results from KC064. There is again a clear relationship between the planktonic and benthic environments at this site, as seen in the abundance and planktonic isotope records. The shift in the isotope curve at 80cm (9.7ka) appears to coincide with a relatively low benthic foraminifera abundance at the base of the foraminiferal-bearing mud unit.

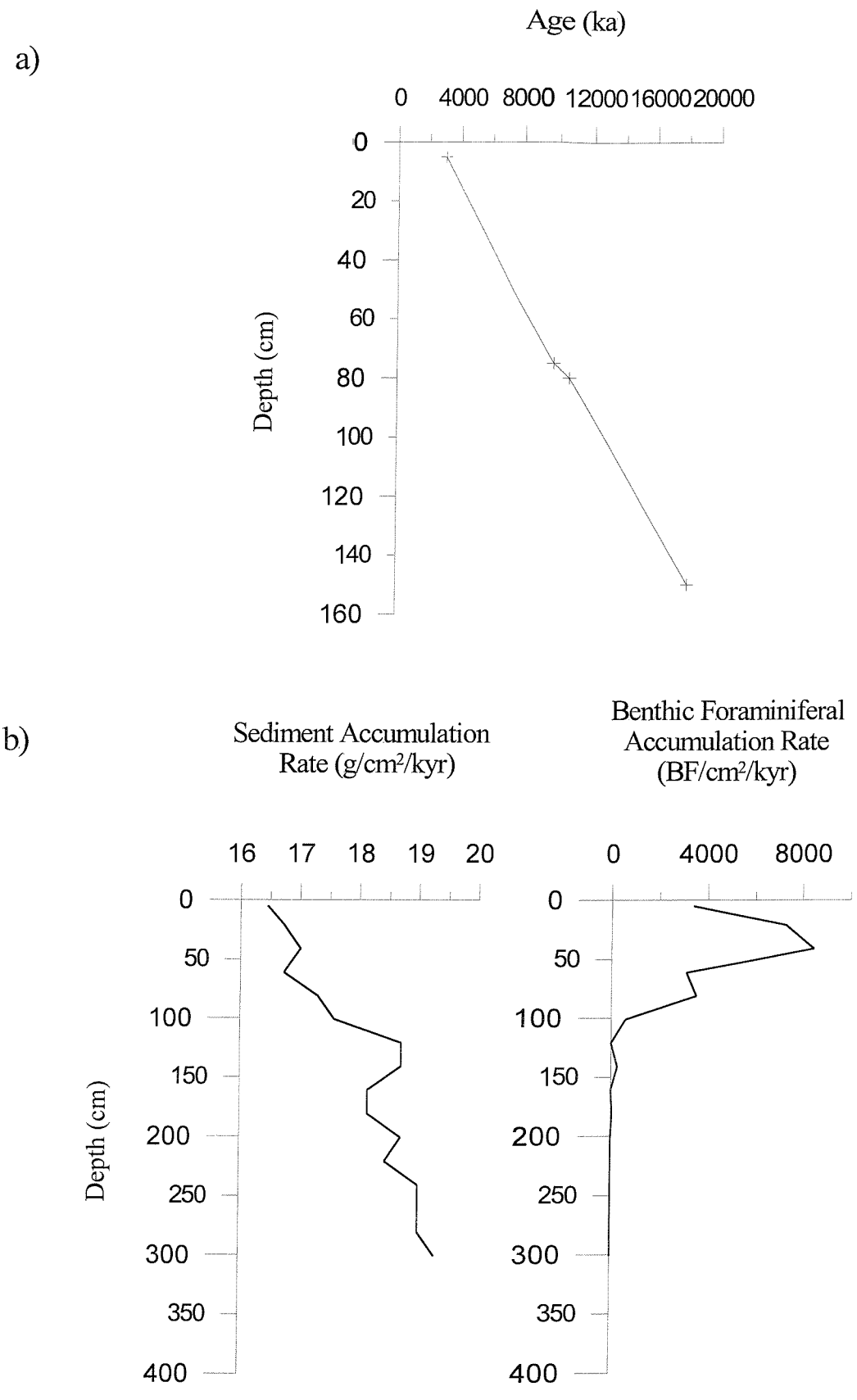

Figure 5.30. a) Sedimentation rate and b) SAR and BFAR plotted for KC064.

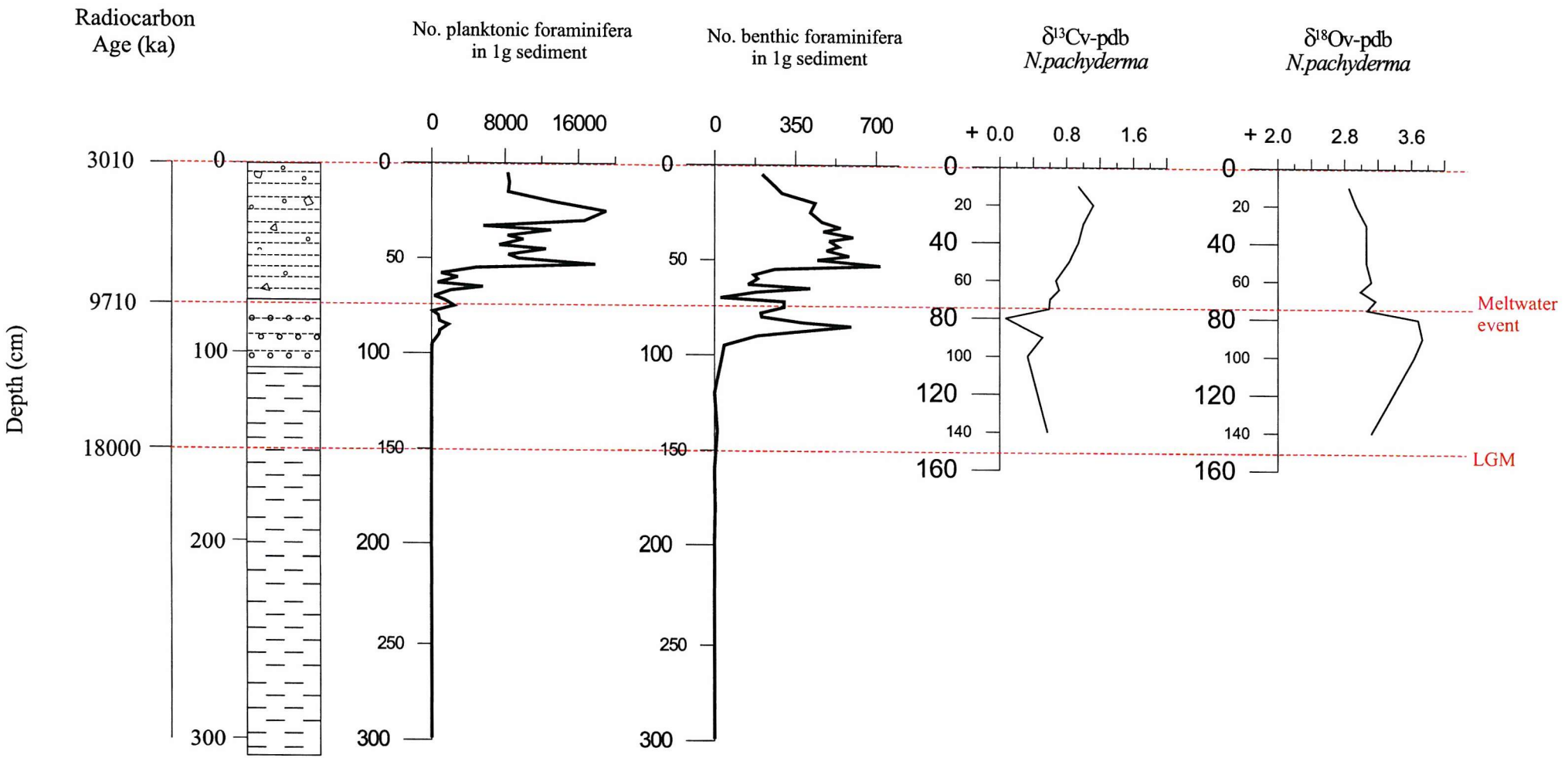

Figure 5.31. Summary of KC064 Results.

5.5. TC036

This core lies approximately 185 km to the south-east of the Polar Front in the eastern Falkland Trough and has been sampled down to a depth of 130cm below the surface. From BA/Al data the base of the Holocene (Stage 1) has been positioned at approximately 150cm below the surface (Fig.5.37) and therefore this section of the core represents the Holocene period only. It shows an up-core transition from foraminifera-bearing diatom muds at the base through to muddy diatom ooze and diatom mud towards the core top, with the change in lithology occurring at about 60cm below the surface. The carbonate content remains quite high throughout this section and only shows a decrease further down the core at about 160cm (Fig.4.1). The magnetic susceptibility record shows no real pattern or change with lithology and remains constant throughout this core section (Fig.4.3). A total of 25 samples were picked from this core.

5.5.1. Benthic Foraminiferal Abundance

The absolute abundance data are shown in Figure 5.32 and the raw data counts are included in Appendix 14.

Absolute abundance is higher than in KC064 and varies between 406 and 1580 foraminifera per gram, with the abundance maximum occurring at 30cm and the minimum at 110cm below the sediment surface. Benthic foraminifera are found in all samples studied from this core although there is a general increase in abundance up core. Abundance is highest, although quite variable within the top 80cm of the core (Fig.5.32). There is also no drop off in abundance at the core top as has been seen in the benthic foraminiferal absolute abundance in the cores previously discussed.

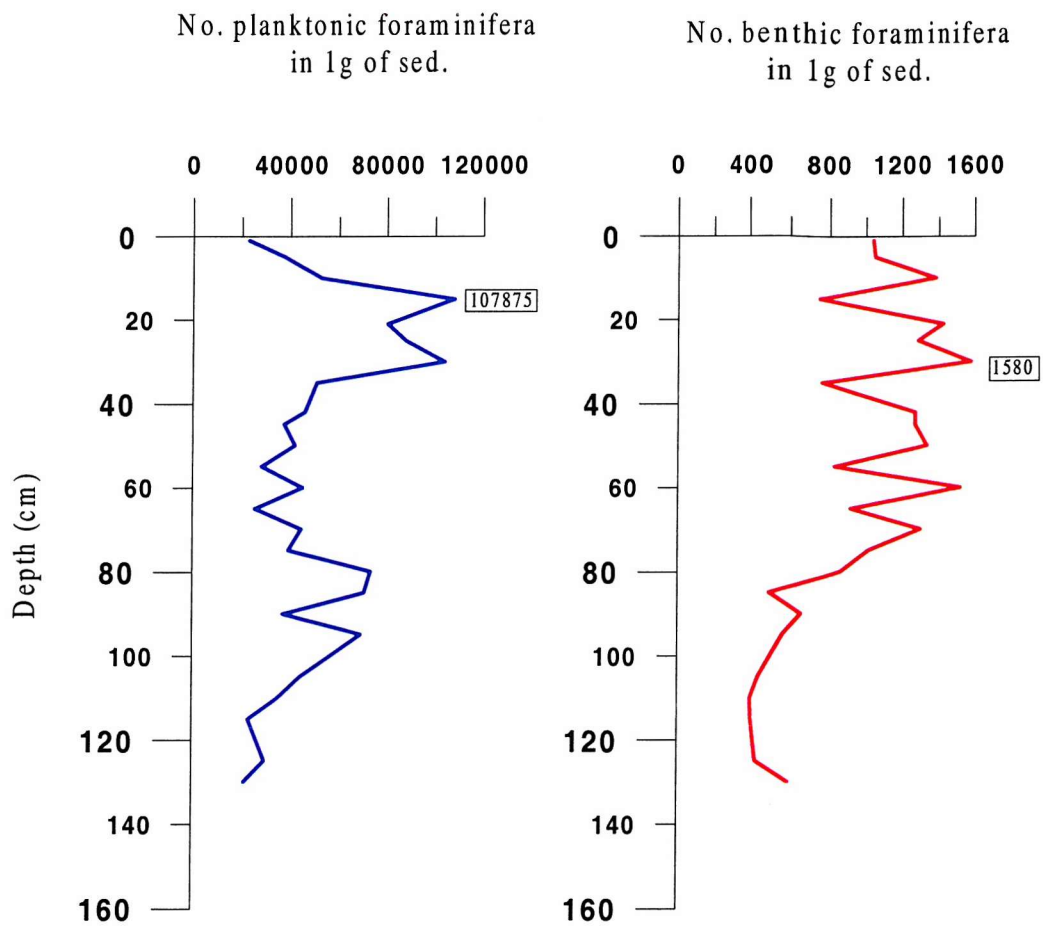

Figure 5.32. Planktonic and benthic foraminiferal absolute abundance for TC036.

Plots of the relative abundance of individual species can be seen in Figure 5.33 and individual species counts are shown in Appendix 15.

There are 74 species from 44 different genera identified in this core with 5 unidentified taxa. The dominant taxa are shown below with the number of samples in which the species formed more than 5% of the assemblage found and the benthic ranking with percentage means in brackets:

Eilohedra weddellensis	25	(34.34)
Globocassidulina subglobosa	25	(8.7)
Gyroidinoides spp.	25	(8.77)
Epistominella exigua	23	(7.39)
Nonionella iridea	23	(9.98)
Cassidulina crassa	14	
Oridorsalis tener	1	

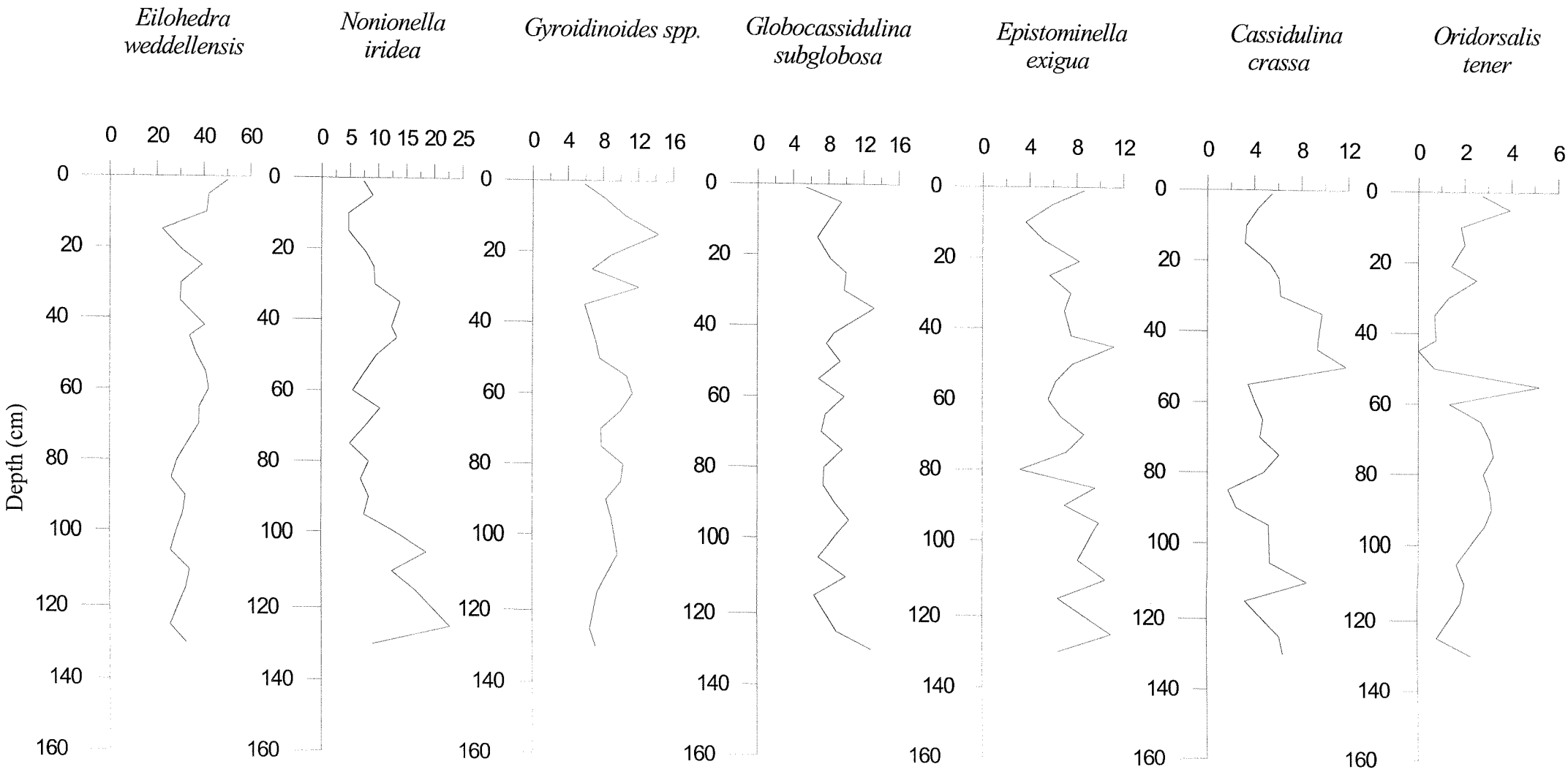

Figure 5.33. Relative abundance (%) of dominant benthic foraminifera for TC036.

Other species that are common in most samples but are not abundant are *Pullenia simplex*, *Fursenkoina complanta*, *Eponides* sp., *Fissurina* spp. and *Lagena* spp. The relative abundance records of the individual species do not reflect the pattern of absolute abundance within the core, as there appears to be no significant increase in relative abundance up core. The greatest variation is seen in the records of *C. crassa* and *O. tener* even though these two species occur in lower abundance than some of the other species named above. They both show a pronounced peak in abundance at about 50-55cm below the surface compared to relatively low abundance throughout the rest of the core. The relative abundance of *N. iridea* also shows some variation, and it occurs in higher abundance towards the base of this section of the core.

Agglutinated taxa occur in low abundance and diversity with only 8 species being identified throughout the whole core. The most persistent species is *Eggerella bradyi* which occurs in all but one sample, but rarely forms more than 2% of the absolute abundance.

5.5.2. Species Diversity

5.5.2.1. The Information Function H(S)

H(S) and H(S)max were computed for all samples and the H(S) value ranges from 0.84 at 60cm to 1.60 at 85cm (Appendix 5). There is little variation throughout the core except for a decrease to a minimum H(S) value at 60cm (Fig.5.34), however the range of H(S) is much lower in this core and this may be why there is less variation.

5.5.2.2. The Fisher Alpha Index (α)

The α value ranges from 5.5 to 13.5 (Appendix 5) and although there is some variation down through the core, there is no significant change in the pattern of diversity throughout this core (Fig.5.34).

The third graph in Figure 5.34 shows that the number of species identified in each sample remains quite consistent throughout the core and so again, there appears to be little change in diversity.

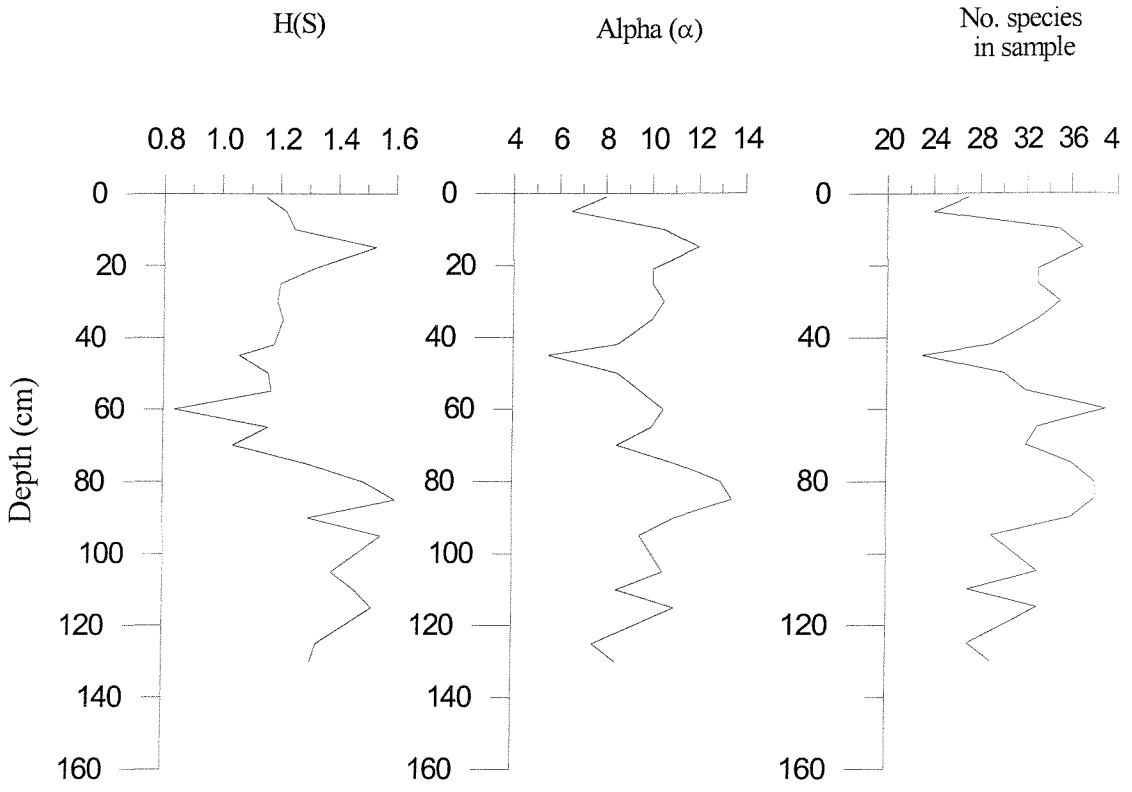

Figure 5.34. Species diversity functions for TC036.

5.5.3. Planktonic Foraminiferal Abundance

Absolute abundance data are shown in Figure 5.32 and raw data counts are included in Appendix 14.

The absolute abundance is quite high compared to KC064 and varies between 21504 and 107875 foraminifera per gram, with the abundance maximum occurring at 15cm below the sediment surface. Planktonic foraminifera are found in all samples throughout the core but there is a general trend to increased abundance towards the core top. The peak in abundance seems to correspond to the maxima in benthic foraminiferal absolute abundance which both occur in the same section of the core.

The dominant foraminifer is the left-coiling (sinistral) *Neogloboquadrina pachyderma*. It occurs in every sample throughout the core and usually comprises over 95% of the total planktonic assemblage.

Five other species of planktonic foraminifera also occur but in very low abundance and not in all samples, and therefore were not counted, but their presence was noted (Table 5.16). These are listed with the number of samples in which they were found:

Assemblage	Planktonic species	1 - 2 cm	5 - 6 cm	10 - 11 cm	15 - 16 cm	21 - 22 cm	25 - 26 cm	30 - 31 cm	35 - 36 cm	42 - 43 cm	45 - 46 cm	50 - 51 cm	55 - 56 cm	60 - 61 cm	65 - 66 cm	70 - 71 cm	75 - 76 cm	80 - 81 cm	85 - 86 cm	90 - 91 cm	95 - 96 cm	105 - 106 cm	110 - 111 cm	115 - 116 cm	125 - 126 cm	130 - 131 cm
Subtropical	*Globorotalia crassaformis*	*	*			*	*	*	*			*	*		*		*					*		*		
Subtropical / Transition	*Globorotalia truncatulinoides*	*	*	*	*	*	*	*	*	*	*	*	*	*	*	*	*	*	*			*	*	*	*	
Transition / cold-temperate	*Globorotalia inflata*	*		*			*	*				*					*							*		
Subantarctic	*Globigerinita uvula*		*	*				*	*	*				*			*		*		*	*	*			
Subantarctic / upwelling	*Globigerina bulloides*					*	*	*			*	*	*	*	*	*		*	*	*			*		*		
Antarctic	*Neogloboquadrina pachyderma*	*	*	*	*	*	*	*	*	*	*	*	*	*	*	*	*	*	*	*	*	*	*	*	*	*

Table 5.16. Planktonic foraminifera species found in TC036 (based on Blair, 1965; Be 1969, 1977).

Globorotalia truncatulinoides	17
Globigerina bulloides	14
Globorotalia crassaformis	10
Globigerinita uvula	8
Globorotalia inflata	6

The subtropical/transition species *G. truncatulinoides* and the subpolar/upwelling species *G. bulloides* are the second and third most abundant species. *Globigerina bulloides* is found almost down to the bottom sample within the core but *G. truncatulinoides* only appears at 85cm below the sediment surface.

5.5.4. Calcium Carbonate Dissolution

Foraminifera were present in every sample throughout the core and so a P:B ratio could be calculated for every sample (Appendix 6). The P:B ratio remains consistently high throughout this core section and the percent of planktonic foraminifera is never lower than 95% (Fig.5.35). There is little variation in the record and hence no clear signs of dissolution. This is also evident in the record of the amount of carbonate within the sediment which shows no increasing trend down core as seen in the previous cores, and again little variation throughout the core (Fig.5.35).

There were no clear signs of test fragmentation in any of the samples within the core and the foraminiferal tests generally showed good preservation.

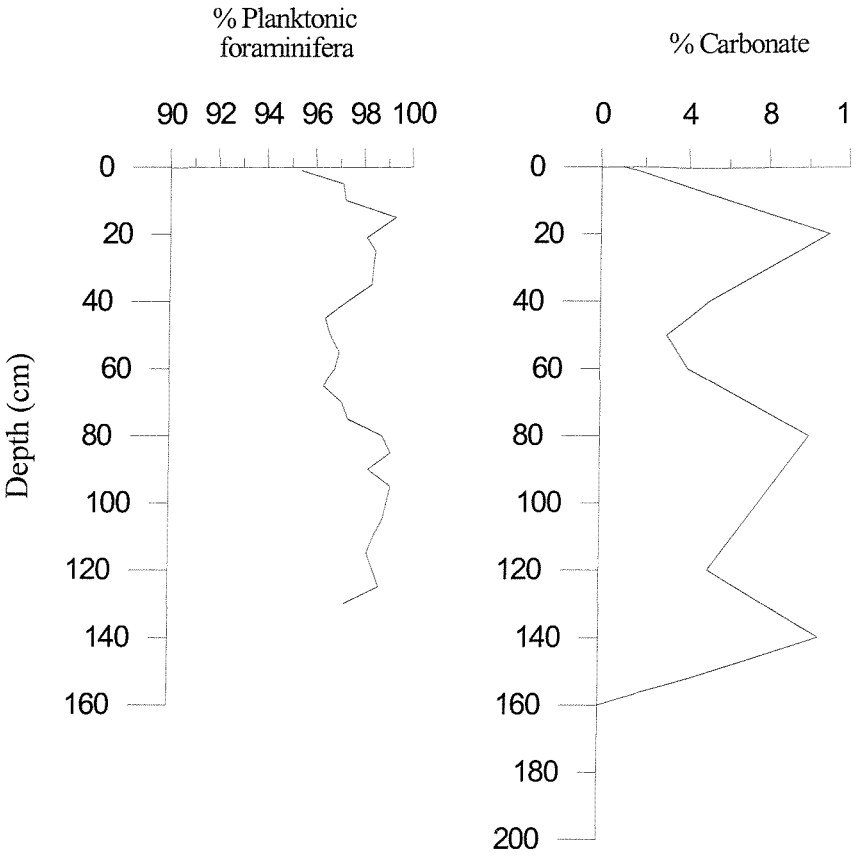

Figure 5.35. Dissolution indices for TC036.

5.5.5. Stable Isotopes

Carbon and oxygen stable isotope analysis was carried out on two species of planktonic foraminifera (*N. pachyderma* and *G. bulloides*) from this core, and were picked by Caroline Bertram at BAS (data from C. Pudsey, pers. comm.). The results for *N. pachyderma* only are shown (Table 5.17) so as to be able to compare the records to the other cores, and isotope curves can be seen in Figure 5.36. The results have not been adjusted to take into account vital effects.

Depth (cmbsf)	$\delta^{13}C$ (‰ PDB) *N. pachyderma*	$\delta^{18}O$ (‰ PDB) *N. pachyderma*
8	1.59	3.48
15	1.70	3.31
28	1.60	2.93
35	2.01	2.94
43	2.34	3.09
55	1.47	3.12
63	1.25	2.74
75	1.54	3.21
88	1.60	3.06
95	1.70	3.06
104	1.51	3.06
115	1.54	2.99
123	1.60	3.01
144	1.35	3.18

Table 5.17. Planktonic foraminiferal (*N. pachyderma*) carbon and oxygen stable isotope data for TC036, (144cm sample is from PC036).

The planktonic isotope values range from 1.35 to 2.34‰ for $\delta^{13}C$ and from 2.74 to 3.48‰ for $\delta^{18}O$. The planktonic $\delta^{13}C$ record shows a general increase up core with highest values in the top 60cm. There is a significant peak in $\delta^{13}C$ at about 40cm which occurs after an increase in $\delta^{13}C$ of about 1.20‰. The planktonic $\delta^{18}O$ record is quite consistent through the core with little variation but $\delta^{18}O$ may be slightly higher and more stable below about 80cm within the core. There is a decrease of about 0.5‰ to a minimum value at approximately 60cm below the surface and there also appears to be an increase in $\delta^{18}O$ towards the core top.

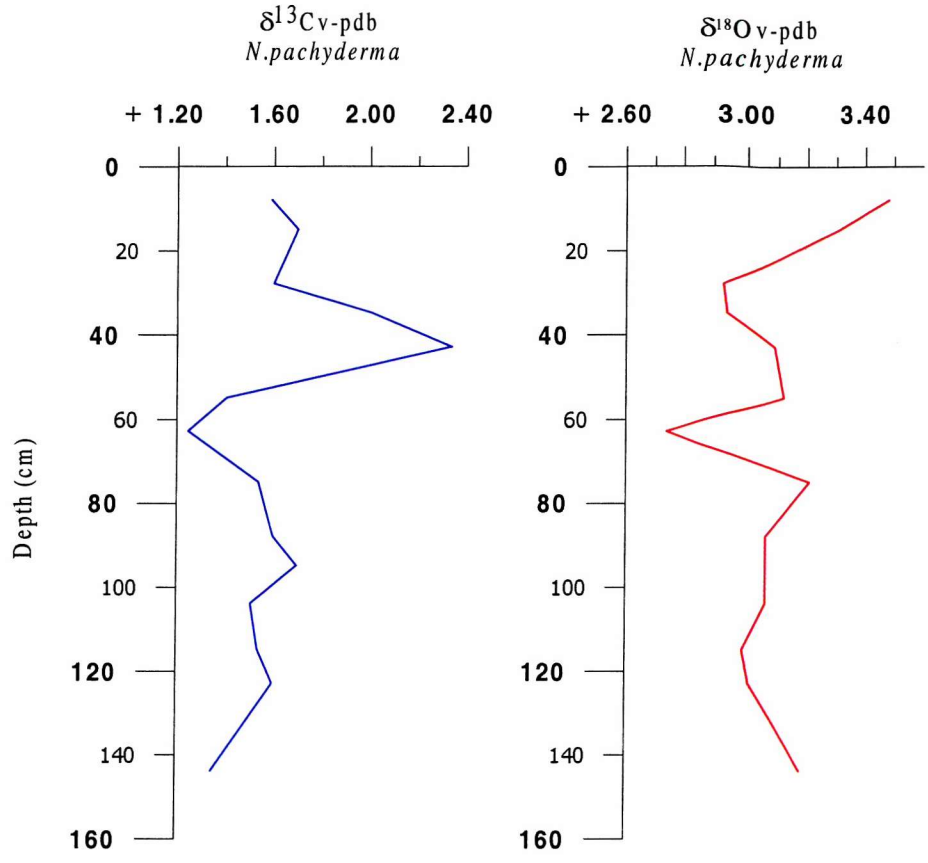

Figure 5.36. Planktonic carbon and oxygen stable isotopes for TC036 (data compiled by C.Bertram, BAS; C.Pudsey, pers. comm.).

5.5.6. Dating the core

AMS Radiocarbon analysis was not carried out on TC036 but other methods for estimating the position of stratigraphic markers are available. Figure 5.37 shows *C. davisiana* and Ba/Al data which mark the position of the LGM at about 240cm below the surface and the base of the Holocene (Stage 1) at about 150cm.

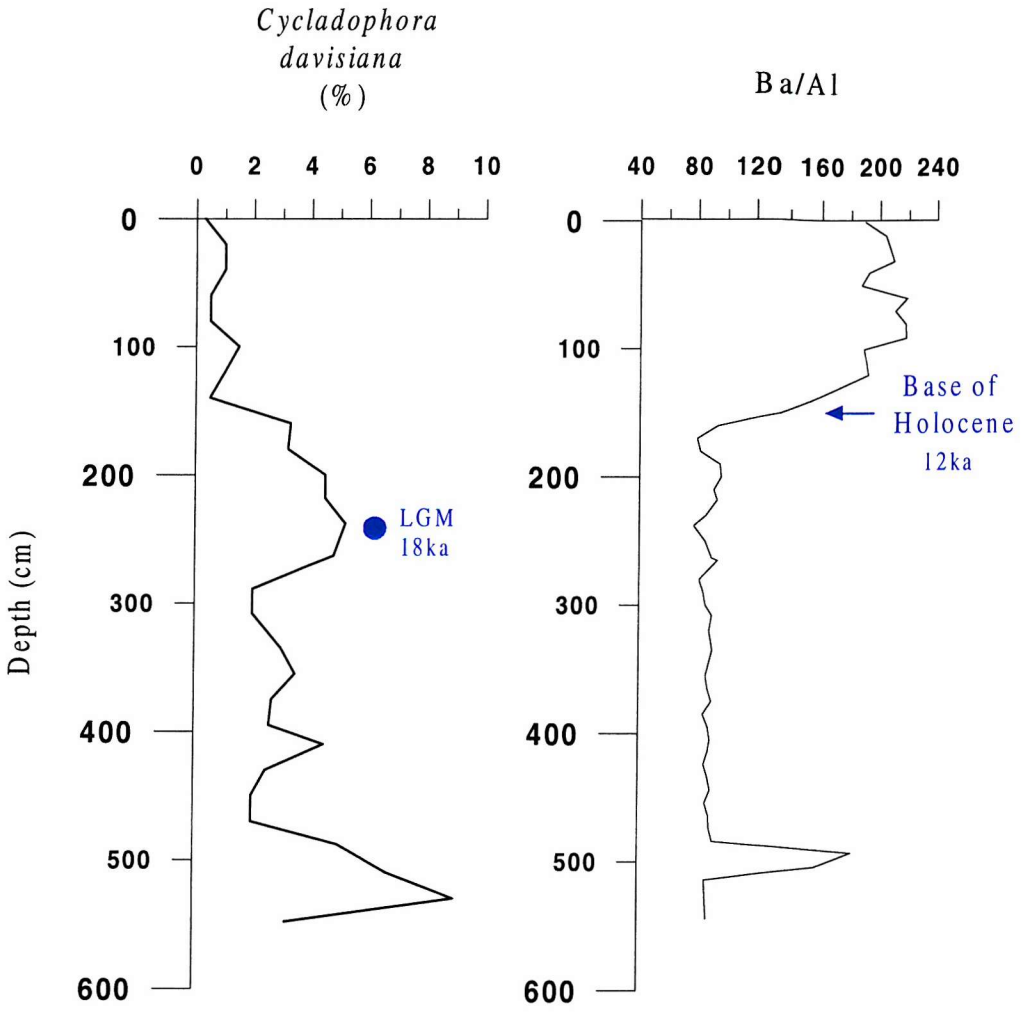

Figure 5.37. *Cycladophora davisiana* and Ba/Al data used to date TC036.

5.6. TC077

This core lies approximately 267 km to the south-east of the Polar Front in the northern Scotia Sea and has been sampled down to a depth of 20cm. Below this depth there is no carbonate present within the sediment and hence no foraminifera are likely to be found. However although a large section of core has not therefore been analysed, it is useful to know that calcareous foraminifera are still present this far south of the Polar Front. The lithology of the core shows an upward transition from diatom ooze at the base through to muddy diatom ooze and diatom mud into a foraminifera-bearing diatom mud unit at the core top (Fig.4.1).

The presence of carbonate within the sediment is recorded only within the top 10cm of the core but foraminifera are found down to about 20cm depth. The percent of carbonate within the sediment however is quite low at 17.2% at the core top and decreasing to 7.6% by 10cm depth. Magnetic susceptibility shows a corresponding record to the lithology and is higher within the diatom ooze (terrigenous) unit below about 40cm in the core (Fig.4.3).

The trigger core was sampled rather than the corresponding piston core for core 077 as PC077 had already been heavily sampled and also had 40cm missing from the core top, lost during the coring process. This top section was the most important part for this study as it was the only section containing carbonate, and so the trigger core was used as it had recovered a complete top section down to 70cm depth. The lithological records used for core 077 are therefore a combination of TC077 (down to 40cm depth) and PC077 (from 40-120cm). The trigger core data was spliced to the piston core using magnetic susceptibility (Pudsey and Howe, 1998). Only 4 samples were picked from this core.

5.6.1. Benthic Foraminiferal Abundance

The absolute abundance data are shown in Figure 5.38 and the raw data counts are included in Appendix 16.

Absolute abundance is much lower than in the other cores from south of the PF and varies between 1 and 138 foraminifera per gram with the abundance maximum occurring at 2cm below the sediment surface in the shallowest sample. Benthic foraminifera were absent below 20cm and the sample at 18cm contained only one large agglutinated foraminifer. There is an increase in abundance up through this short section of core with a more rapid increase above 10cm depth.

Plots of relative abundance have not been included as there was little variation in species composition over the 4 samples studied. There are 42 species from 33 different genera identified in this core, including 9 agglutinated species in very low abundance. Only 3 species were not identified. The dominant species are *Eilohedra weddellensis*, *Epistominella exigua*, *Gyroidinoides* spp., *Nuttallides umbonifera* and *Oridorsalis tener*. *Eilohedra weddellensis* was by far the most abundant species forming over 35% of the absolute abundance of each

sample. Other species which are common in the samples are *Lagena* spp., *Pullenia* spp., *Sphaeriodina bulloides* and *Uvigerina peregrina* (Appendix 17).

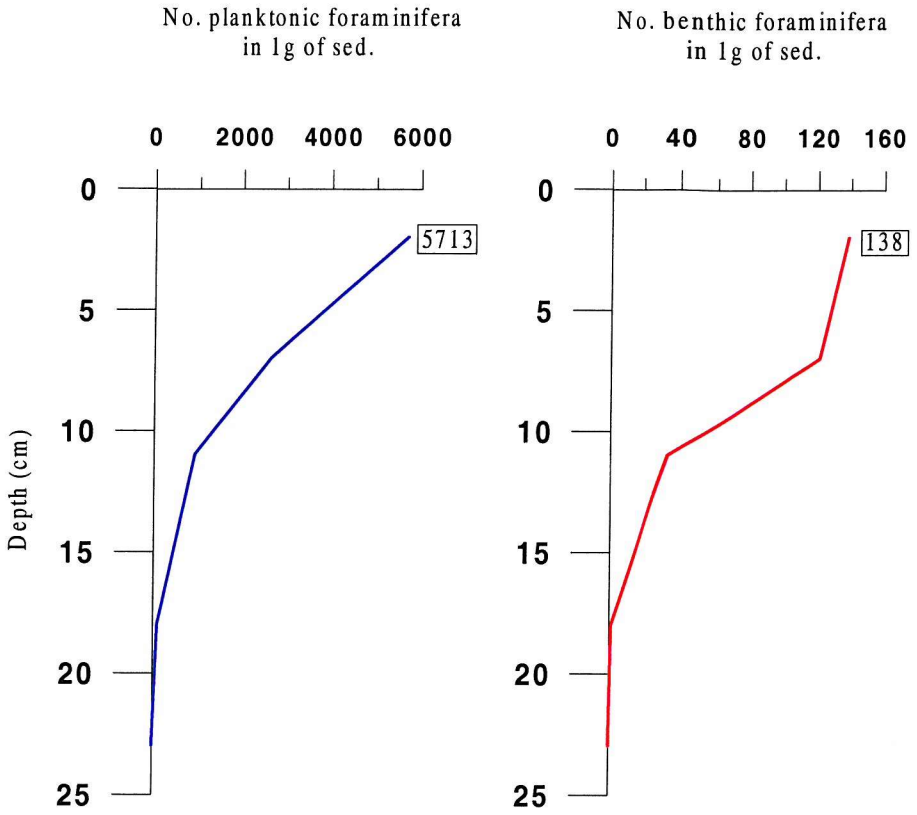

Figure 5.38. Planktonic and benthic foraminiferal absolute abundance for TC077.

5.6.2. Planktonic Foraminiferal Abundance

Absolute abundance data are shown in Figure 5.38 and raw data counts are included in Appendix 16.

The absolute abundance is again quite low and varies between 100 and 5713 foraminifera per gram with the abundance maximum occurring at 2cm within the top sample. Planktonic foraminifera were absent from the sediment below the sample at 18cm and show a gradual increase up core.

The dominant foraminifer is the left-coiling (sinistral) *Neogloboquadrina pachyderma* which occurs in all four samples from this core and comprises over 95% of the total planktonic assemblage. Three other planktonic species were recorded but occurring in much lower

abundance than *N. pachyderma*, these are *G. crassaformis*, *G. truncatulinoides* and *G. inflata*. Preservation of the foraminiferal tests is quite poor with a high percentage of fragmentation observed.

5.6.3. Dating the core

AMS Radiocarbon analysis was not carried out on TC077 but other methods for estimating the position of stratigraphic markers are available. Figure 5.39 shows *C. davisiana* and biogenic barium (ppm) data which mark the position of the LGM at about 120cm below the surface and the base of the Holocene (Stage 1) at about 50cm.

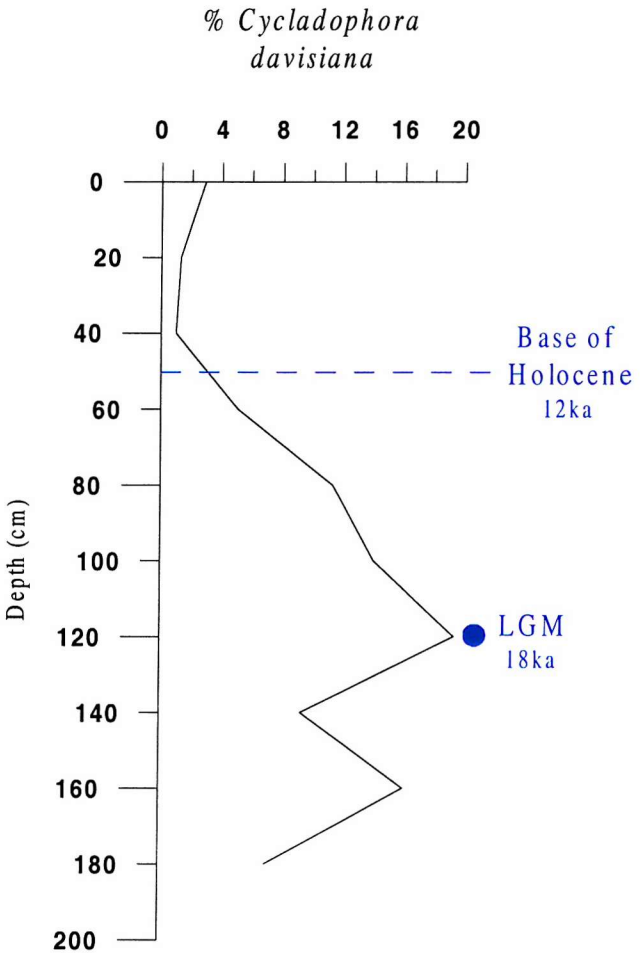

Figure 5.39. Dating of TC077 using *C.davisiana* abundance (LGM) and biogenic barium abundance (base of Holocene) (all data from TC,PC077; Pudsey and Howe, 1998).

Sedimentation rates have also been calculated for PC077 by Pudsey and Howe (1998) as 4.6 cm/ka from the core top to the base of stage 1, and 6.7 cm/ka from the core top to the LGM.

5.7. TC078

This core lies approximately 282km to the south-east of the Polar Front in the northern Scotia Sea and has been sampled down to a depth of 20cm, as below this point there are no foraminifera found. The average abundance of carbonate within the top 30cm of the core is quite low at only 4.9% and below this level there is no carbonate present within the sediment. The lithology of the core shows an upward transition from diatom ooze at the base through muddy diatom ooze and diatom muds, into another diatom ooze unit before passing into a muddy diatom ooze and diatom mud unit at the core top (Fig.4.1). The bottom section of the core shows repeated features below about 80cm depth indicating that repenetration during coring occurred. Magnetic susceptibility shows a corresponding record to the lithology and is higher within the lower diatom ooze unit below about 65cm depth (Fig.4.3). The trigger and piston core records of magnetic susceptibility can be correlated quite well as the peak at 0.8m in the trigger core (just above repenetration) corresponds to the peak at 0.9m in the piston core. Therefore the trigger core may not have a complete core top section at this site. Only 4 samples were picked from this core.

5.7.1. Benthic Foraminiferal Abundance

The absolute abundance data are shown in Figure 5.40 and the raw data counts are included in Appendix 16.

Absolute abundance is very low and varies between 1 and only 10 foraminifera per gram with the abundance maximum occurring at 14cm below the sediment surface. Benthic foraminifera were absent below 20cm and the sample at 19cm contained only one foraminifer which was calcareous. There is a decrease in abundance up core after the maximum at 14cm with a small increase at the core top.

Plots of relative abundance have not been included as so few benthic foraminifera were identified in each sample. Species diversity is very low with only 11 species identified and two of these are agglutinated species. Only two species were not identified. There were no dominant species identified within this section of core due to the low abundance.

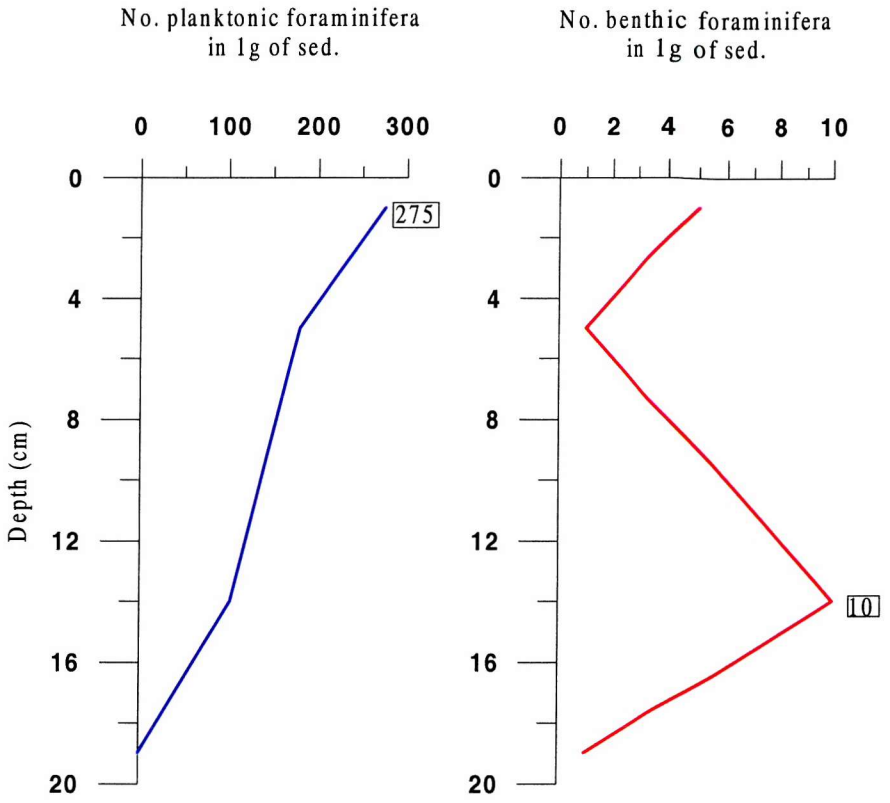

Figure 5.40. Planktonic and benthic foraminiferal absolute abundance for TC078.

5.7.2. Planktonic Foraminiferal Abundance

Absolute abundance data are shown in Figure 5.40 and raw data counts are included in Appendix 16.

The absolute abundance is again very low, up to 275 foraminifera per gram with the abundance maximum occurring at 1cm within the top sample. Planktonic foraminifera were absent from the sediment below the sample at 14cm and show a gradual increase in abundance up core.

The only planktonic foraminiferal species present within this core is the left-coiling (sinistral) *Neogloboquadrina pachyderma* and preservation of the tests is very poor, showing a high degree of test fragmentation.

5.7.3. Dating the core

AMS Radiocarbon analysis was carried out on TC078 and two dates were obtained (Table 5.18). These dates are not included in Figure 5.41 for reasons discussed below.

Publication code	Sample	Conventional Radiocarbon Age (years BP ±1σ)	Corrected Age (years BP)	Carbon content (% by wt.)	Material analysed
AA-28104	TC078-1/12-13	9570 ± 70	8270	0.3	Diatom ooze
AA-28105	TC078-1/20-21	14740 ± 100	13440	0.3	Diatom ooze

Table 5.18. AMS radiocarbon dates for TC078 (C. Pudsey and S. Moreton, BAS).

Other methods for estimating the position of stratigraphic markers are also available. Figure 5.41 shows *C. davisiana* abundance and biogenic barium (ppm) data, which mark the position of the LGM at about 105cm below the surface and the base of the Holocene (Stage 1) at about 95cm. Pudsey and Howe (1998) estimated the position of the LGM at 120cm using *C. davisiana* abundance data from TC,PC078.

There would seem to be conflicting evidence for dating sediment within this core, and the ^{14}C dates appear to indicate that the core top is thousands of years older than would be indicated by the *C. davisiana* and biogenic barium data. The barium profile shows very good data (Pudsey and Howe, 1998) and there is a fairly gradual increase in palaeoproductivity from 1.0 to 0.6m, so the estimate for the base of the Holocene at 0.95m seems to be accurate. There is also a strong *C. davisiana* peak at 1.05m which provides a reliable indicator of the position of the LGM (Fig.5.41). Therefore the presence of "old" reworked carbon may have had an influence on these ^{14}C dates making the core top look much older than it probably is. This appears to be a recurrent problem in the Scotia Sea, becoming worse farther south (C. Pudsey, pers. comm.). Therefore considering all the evidence for the dating of this core it can be assumed that the foraminiferal assemblage is probably Holocene in age, but accurate dating may not be feasible.

Sedimentation rates have also been calculated for PC078 by Pudsey and Howe (1998) as 7.5 cm/ka from the core top to the base of stage 1, and 6.7 cm/ka from the core top to the LGM.

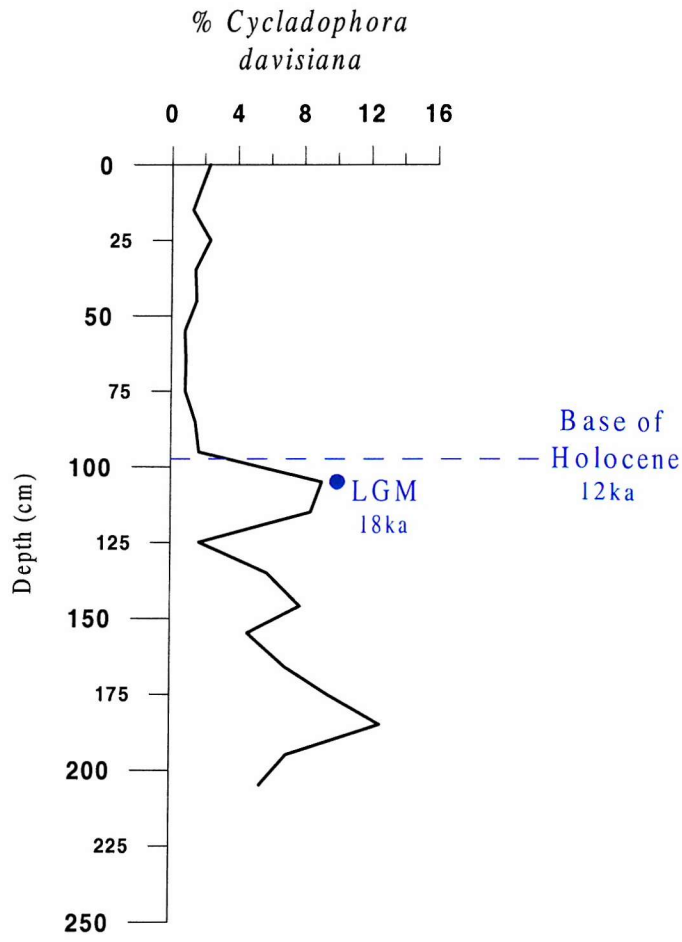

Figure 5.41. Dating of TC078 using *C.davisiana* abundance (LGM) and biogenic barium abundance (base of Holocene).
Data from TC,PC078; *C.davisiana* (T. Crawshaw, pers. comm.) and biogenic Barium (Pudsey and Howe, 1998). Alternative date for LGM at 120cm (Pudsey and Howe, 1998).

5.8. PRIMER Multivariate Analysis

5.8.1. KC097

5.8.1.1. Cluster Analysis and Multi-Dimensional Scaling

The results from the cluster analysis and corresponding MDS plot with no transformation of the data can be seen in figure 5.42. The cluster analysis was also performed with fourth root transformation of the data but the results are not presented here as they do not show any significantly different information.

The cluster analysis and MDS with no transformation of the data shows a number of groupings of samples at similarity levels of 60% and higher. One small group, which includes

samples at depths 60-61cm, 65-66cm and 70-71cm, shows a similarity between samples of about 78%. Within this group all three samples have very similar faunal compositions (Appendix 4), but show marked differences to all other samples within the core. The percentage of the nine dominant benthic foraminifera species identified in section 5.1.1. show some variations in abundance compared to the other samples within the core. The relative abundance of *Cassidulina crassa*, *Globocassidulina subglobosa*, *Gyroidinoides* spp., *Epistominella exigua*, *Oridorsalis tener* and *Fissurina* spp. are all low, with only *Eilohedra weddellensis* and *Nonionella iridea* showing an increase in abundance within these samples. However the increase in abundance in a number of other species is probably of more importance. There is a significant increase in the relative abundance of *Melonis barleeanum*, *Fursenkoina* spp., *Pullenia* spp., *Eponides* spp., *Quinqueloculina* spp. and *Bolivinellina translucens* within these samples. The sample at 90cm also shows some similar faunal characteristics to these three samples but this does not show up in the cluster analysis and instead shows a similarity value of only about 33%.

Samples from depths above this group in the core (55-1.5cm) can be grouped at a similarity level of about 62% and show little faunal variation between samples. All of these samples show higher species diversity and abundance of the dominant species.

Below the group at 60cm, the diversity and abundance are low and samples contain considerably fewer foraminifera. The majority of samples contain too few foraminifera to be included in the PRIMER analysis and even though the sample at 270cm below the surface has been included, the abundance is quite low and so it may not give totally reliable results. The only persistent species through these samples appear to be *E. weddellensis*, *Cibicides* sp. and *Angulogerina angulosa*.

The small group of three samples therefore appears to separate the samples of high abundance and diversity in the top part of the core, from those with low abundance and diversity in the lower section. The group also shows that a change in faunal composition occurs within that section of the core.

The results from the cluster analysis were then used to group samples on the MDS plot at certain levels of similarity. These can be seen as similarity "contour" lines on the MDS plots. The MDS analysis with no transformation of the data produced a plot with a stress value of

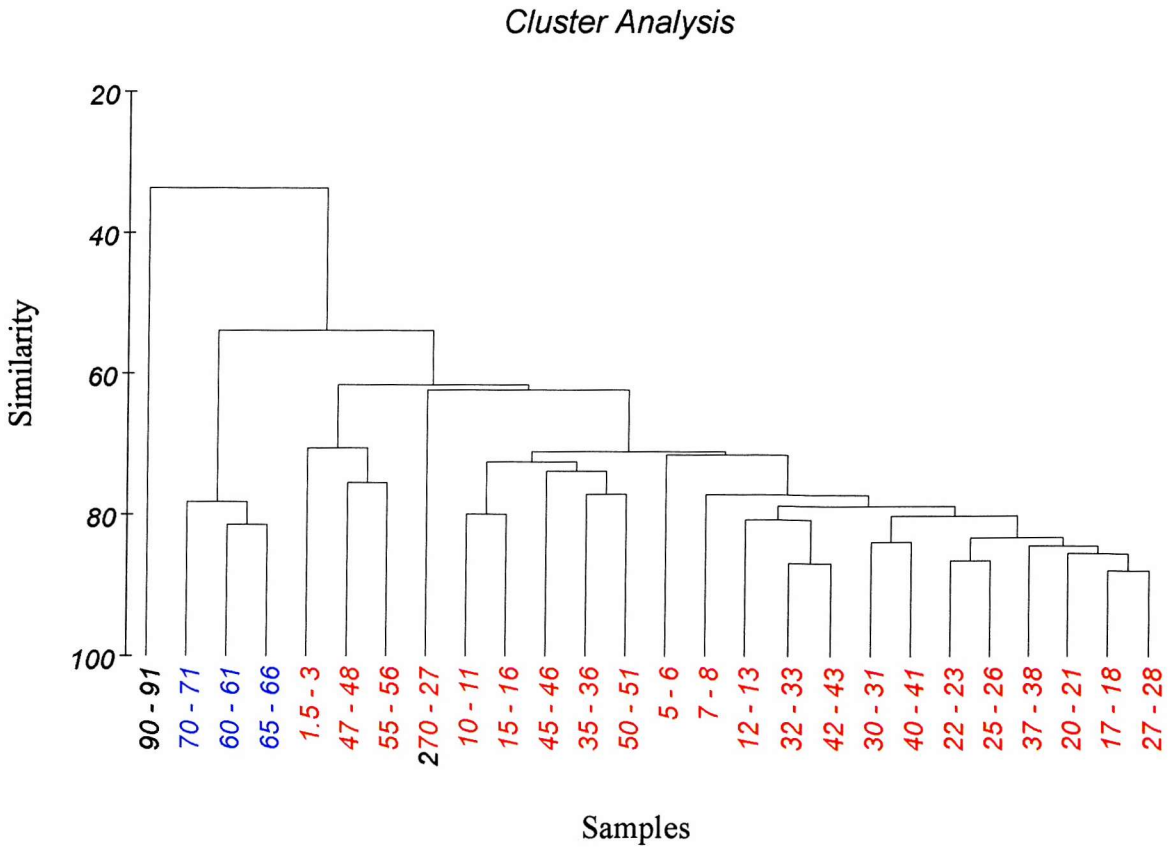

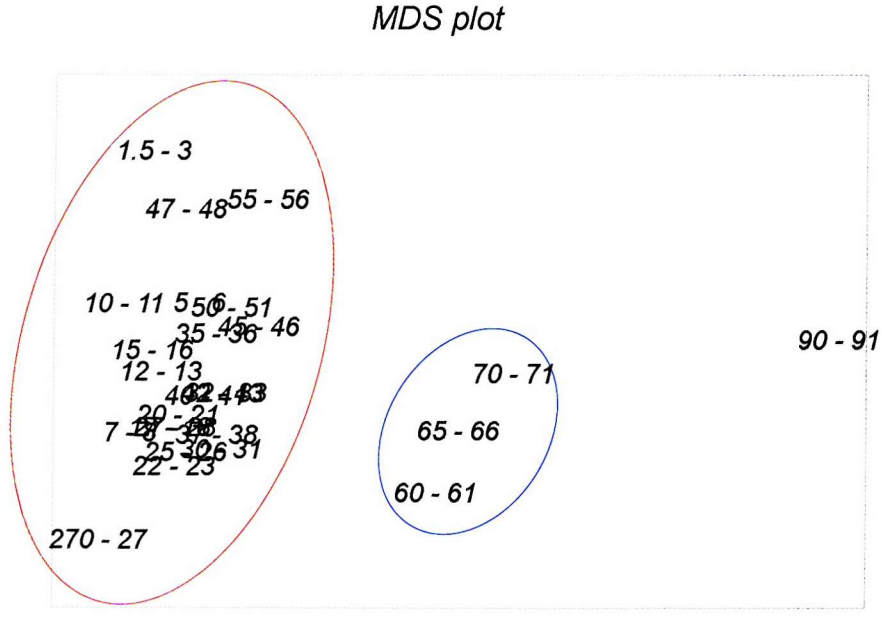

Figure 5.42. KC097 Cluster and MDS Analysis with no transformation of the data.

0.10 (Fig.5.42), which indicates a good ordination of the data. This was lower than the stress value of 0.13 for the MDS plot with fourth root transformation of the data.

5.8.1.2. Principal Components Analysis

A Q-mode PCA carried out on the data set yielded eigenvalues and associated percentages of the total variance each counts for, as shown in Table 5.19.

The data were reduced to include only the species which made up at least 3% of the total abundance in at least one sample, which reduced the number of benthic foraminiferal species to only 21 (Appendix 18). The most dominant species *Eilohedra weddellensis* was removed from the data set as it overwhelmed all the other species in the PCA and allowed no other abundance patterns to be seen within the data. The original data were then log transformed and not normalised which resulted in a covariance-based PCA.

The results showed that 3 principal components or assemblages accounted for 66.8% of the total variation, with 42.9% of the variation accounted for by the first principal component alone. The analysis was run to include 5 principal components originally but was reduced to 3 as the fourth and fifth groups combined accounted only for a further 3% of the total variance, and did not seem to contribute any more significant information. Table 5.20 shows the species composition of the benthic foraminiferal assemblages, including the dominant species and the important associated species. Down core fluctuations of the resulting faunal assemblages for core KC097 are presented in Figure 5.43a.

PC	Eigenvalues	% Variation	Cumulative % Variation
1	4.68	42.9	42.9
2	1.67	15.3	58.2
3	0.94	8.6	66.8

Table 5.19. Eigenvalues extracted using Q-mode PCA for KC097.

Q-mode assemblage	Dominant species	PCA score	Important Associated species	PCA score
PC1	*Epistominella exigua*	0.542	*Cassidulina crassa*	0.239
	Bolivina spp.	0.271	*Globocassidulina subglobosa*	0.217
			Gyroidinoides spp.	0.200
	Fursenkoina complanta	-0.374		
	Melonis barleeanum	-0.335		
	Eponides spp.	-0.251		
PC2	*Bolivina* spp.	0.019		
	Fissurina spp.	0.015		
	Nonionella iridea	-0.578		
	Quinqueloculina spp.	-0.322		
	Bolivinellina translucens	-0.299		
	Gyroidinoides spp.	-0.260		
	Globocassidulina subglobosa	-0.256		
PC3	*Nonionella iridea*	0.328	*Epistominella exigua*	0.222
	Cibicides spp.	-0.488		
	Angulogerina angulosa	-0.388		
	Oridorsalis tener	-0.292		
	Lagena sp.	-0.261		

Table 20. Species composition of Q-mode assemblages in KC097 showing Principal Component scores for faunas. A negative sign on the score indicates that the species decreases as the component increases (Parker and Arnold, 1999).

The positive end-member assemblage of PC1 is dominated by *E. exigua* which shows a positive relationship to well-oxygenated and highly saline NADW (Mackensen *et al.*, 1995). This assemblage is important throughout the top 50cm of KC097 and is replaced by the negative end-member group of PC1, dominated by *F. complanata* and *M. barleeanum*, between 70 cm and the base of the core. The negative end-member assemblage of PC1 may represent a high productivity fauna.

The positive end-member assemblage of PC2 is represented by *Bolivina* spp. and *Fissurina* spp. although they both show very low loadings in the group but are the only two positive species. This assemblage is important at the core top and below about 80 cm within the core. This is replaced by a negative end-member assemblage dominated by *N. iridea* between 80-20 cm below the surface.

The positive end-member of PC3 is dominated by *N. iridea* and this assemblage is important between the depth of 10-40 cm below the surface and then again below about 75 cm. The negative end-member assemblage dominated by the genus *Cibicides* spp. seems to be

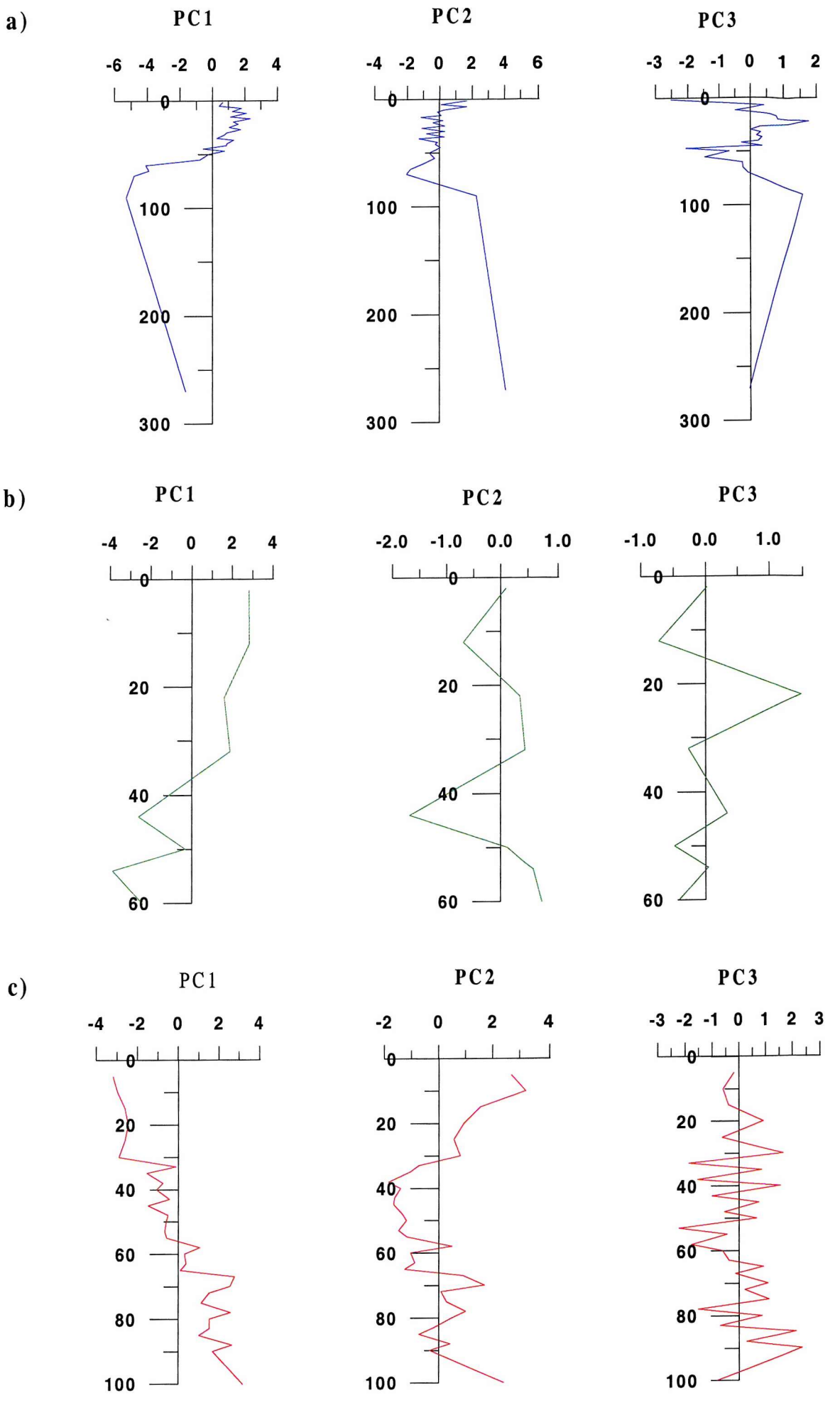

Figure 5.43. Distribution of Principal Components down-core in a) KC097, b) GC062 and c) KC064.

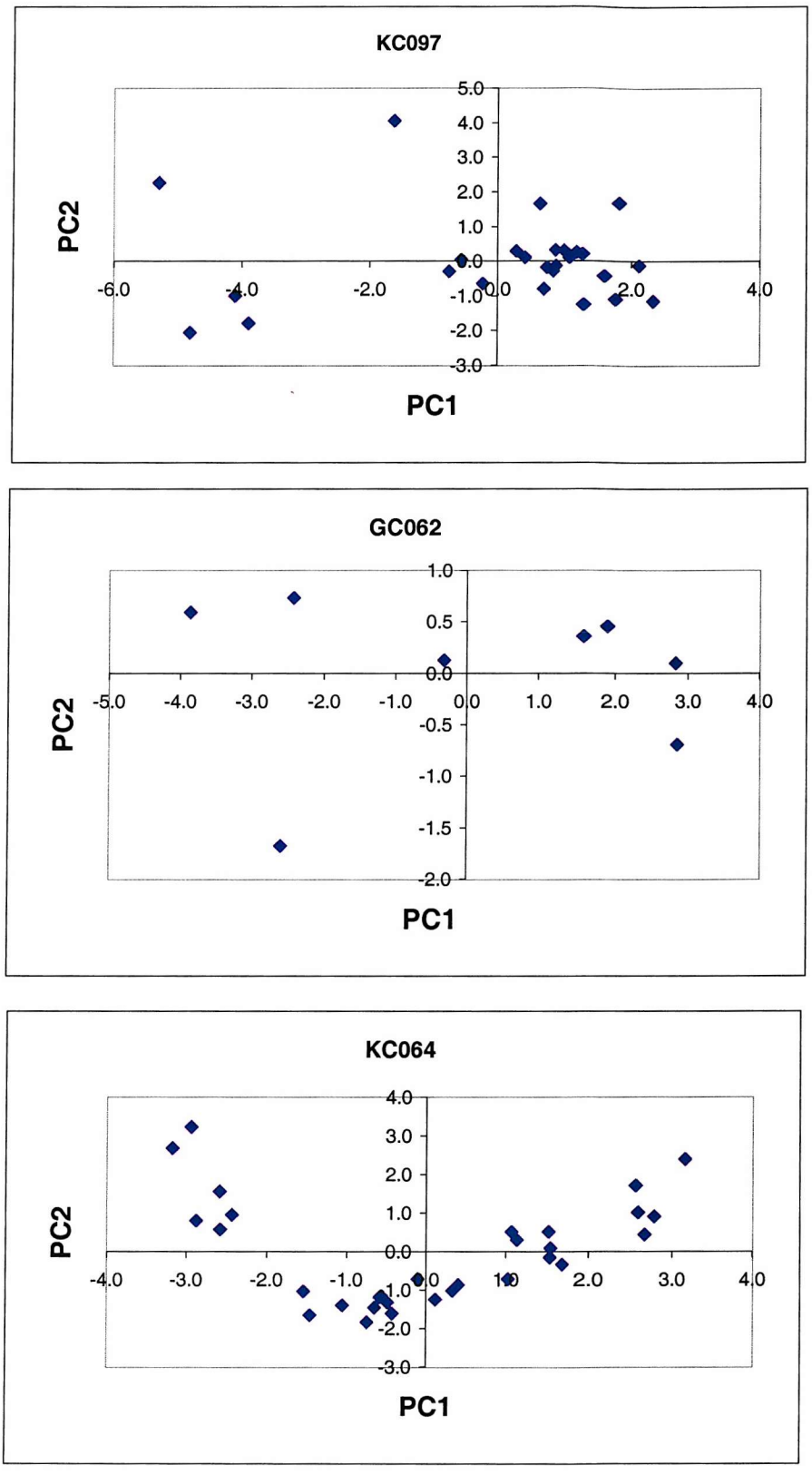

Figure 5.44. Sample scores for PC1 plotted against PC2.

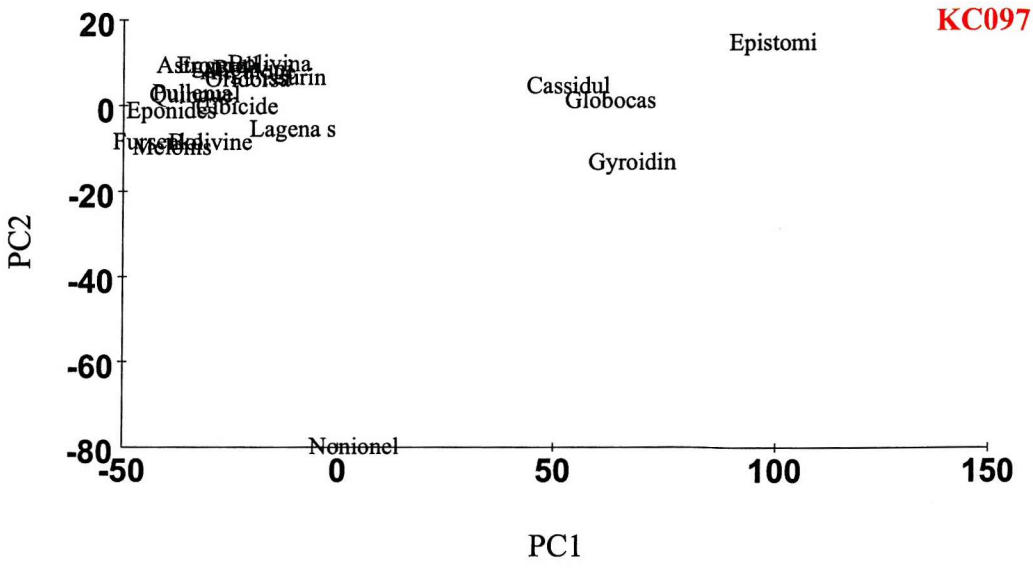

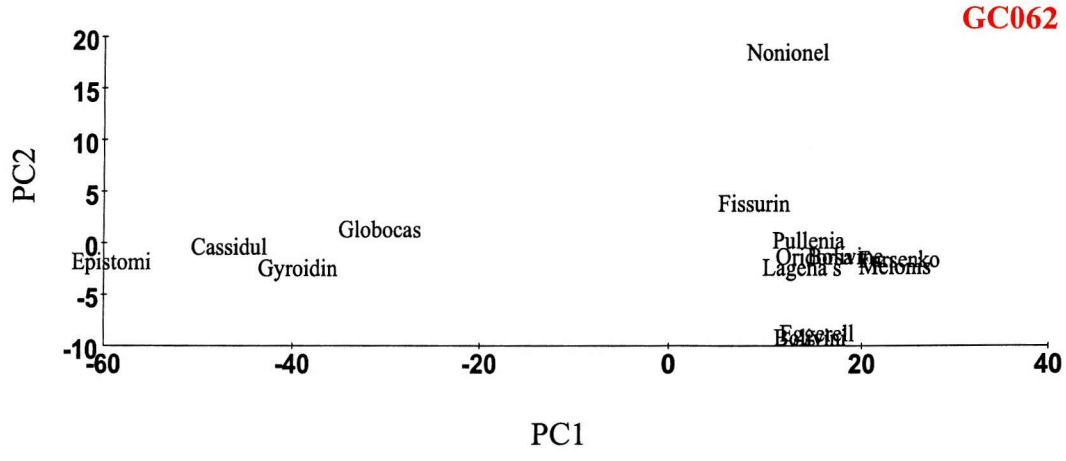

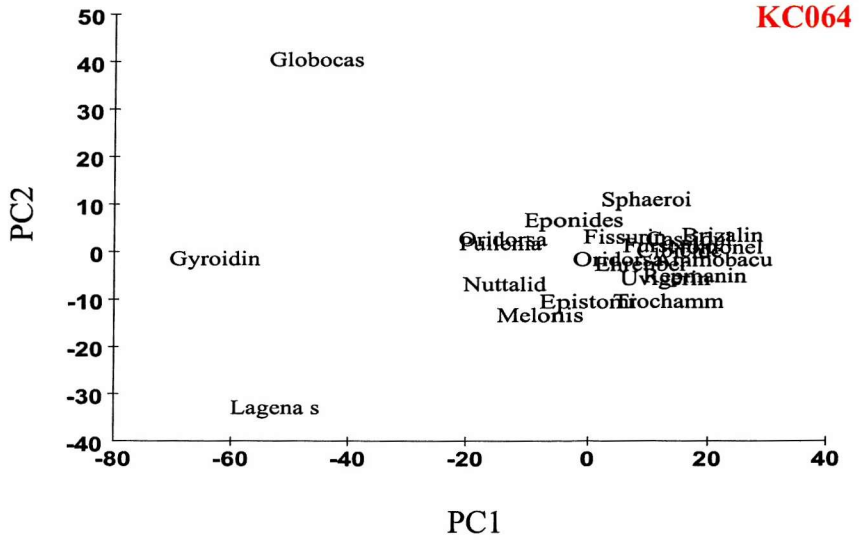

Figure 5.45. Species plotted on PC1 against PC2 for KC097, GC062 and KC064.

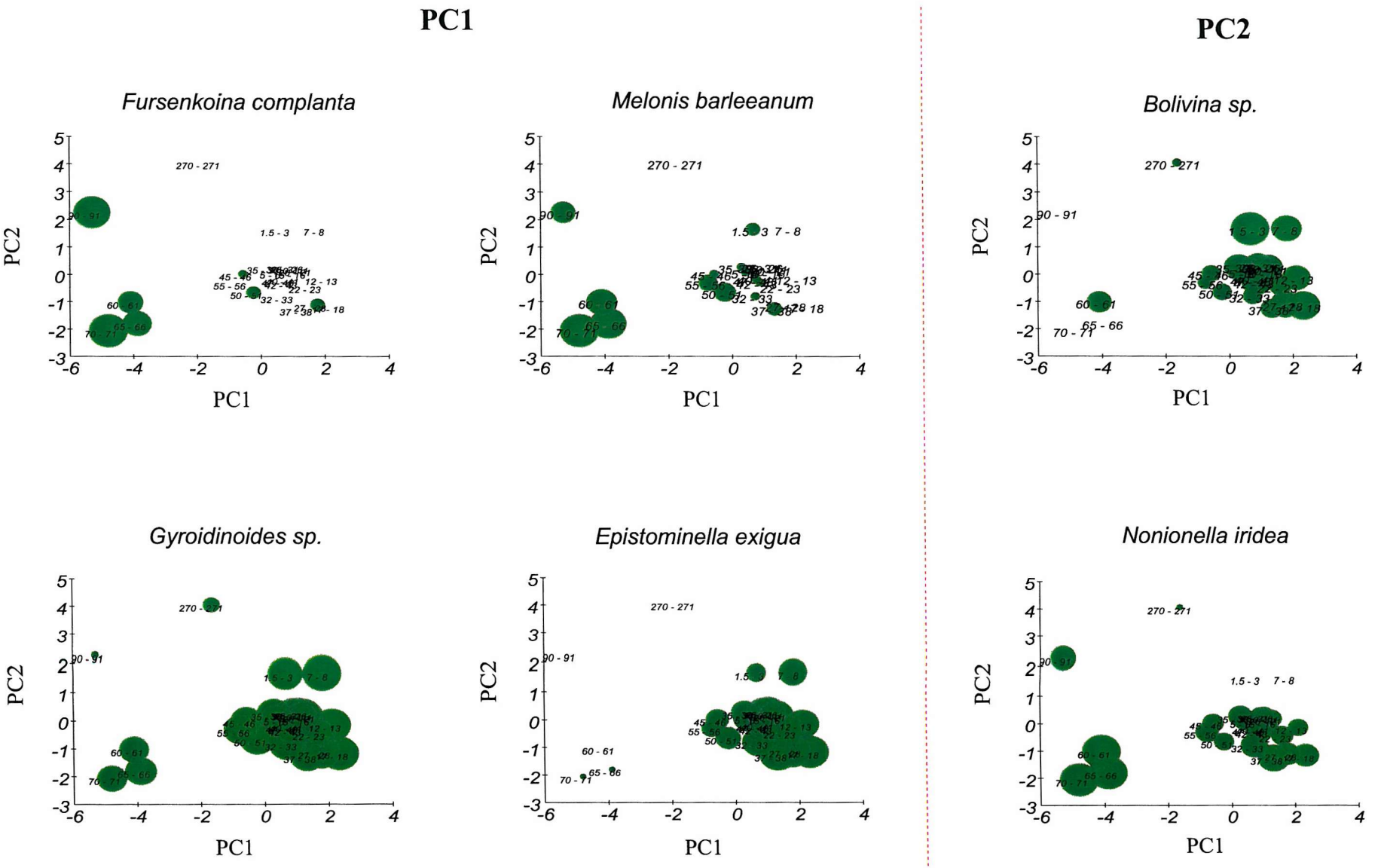

Figure 5.46. Bubble plots for dominant species in KC097. Size of bubble indicates relative importance of the species at that depth within the core. Bubble size is not comparable between species.

particularly important at the very top of the core and around 50 cm. *Cibicides* is found to live attached to the substrate (Nyholm, 1961; Loeblich and Tappan, 1964) and is also an indicator of well-oxygenated bottom water conditions. However this principal component accounts for a lower percentage of the total variance and so may not reveal any important palaeoecological information.

Figure 5.44 shows the sample scores for PC1 plotted against PC2. This plot reveals the same pattern shown for PC1 in Figure 5.43a as it shows two groups of samples within the core, separated into positive and negative loadings on PC1 at about 50 cm.

Figure 5.45 shows the position of the individual foraminifera species plotted on PC1 and PC2. This plot shows quite clearly the positive and negative end-member assemblages from the Q-mode PCA analysis and the group lying almost on 0 for both axes represents the species which are important in PC3. The foraminifera not included in any group on this diagram are not thought to contribute any significant ecological information to this analysis.

Figure 5.46 shows bubble diagram plots of the important species in the negative and positive end-member assemblages for PC1 and PC2. For each individual species the size of the bubbles indicates the relative importance of the species at different sample depths within the core. However bubble size is not comparable between species plots and should not be compared. Using this method the different faunal assemblages can be easily identified in the core.

5.8.2. GC062

5.8.2.1. Cluster Analysis and Multi-Dimensional Scaling

The results from the cluster analysis and corresponding MDS plot with no transformation of the data can be seen in Figure 5.47. The cluster analysis was also performed with fourth root transformation of the data.

The cluster analysis and MDS with no transformation of the data shows that all the samples are grouped at a similarity level of 60% and then subdivided into two smaller groups at a similarity of about 80%. The two groups are separated below 34cm, dividing the top four

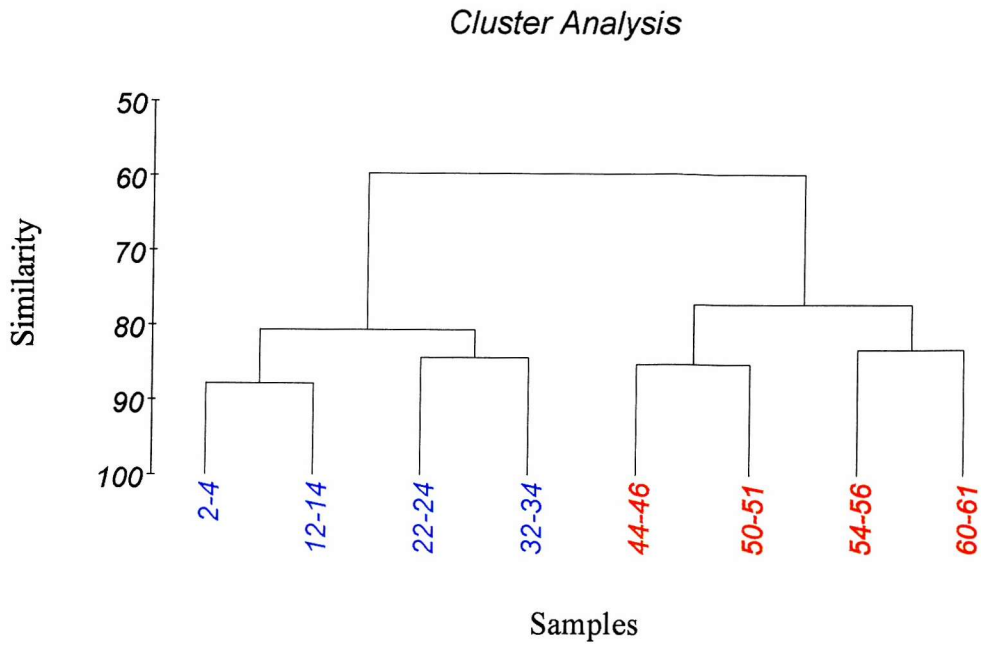

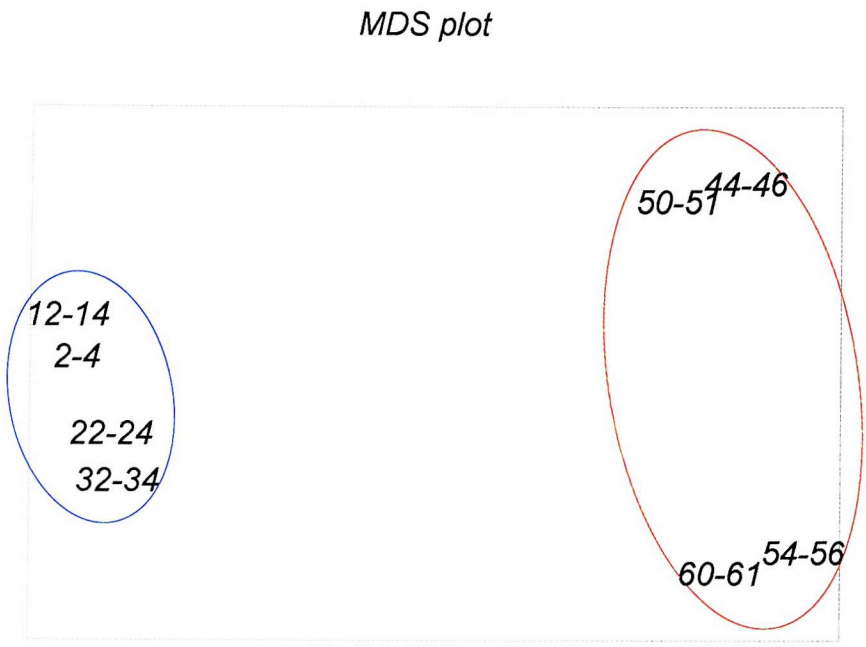

Figure 5.47. GC062 Cluster and MDS Analysis with no transformation of the data.

samples from the bottom four in this section of the core. Each group shows different a faunal composition with certain species being dominant in each group.

In the group at the top of the core from 2-34cm below the surface there are higher percentages of *C. crassa*, *E. exigua*, *G. subglobosa* and *Gyroidinoides* spp. These species become less important in the lower group but are still present. The second group includes samples from 44-60cm below the surface and shows an increase in *E. weddellensis* and *N. iridea*, although these species are also found higher up in the core. There is also a marked increase in *M. barleeanum* and *Fursenkoina* spp. which are very rare in the top section of the core.

The results from the cluster analysis were then used to group samples on the MDS plot at certain levels of similarity. These can be seen as similarity "contour" lines on the MDS plots. The MDS analysis with no transformation of the data produced a plot with a stress value of 0.01 (Fig.5.47), which indicates an excellent ordination of the data. This was lower than the stress value of 0.04 for the MDS plot with fourth root transformation of the data.

5.8.2.2. Principal Components Analysis

A Q-mode PCA carried out on the data set yielded eigenvalues and associated percentages of the total variance each counts for, as shown in Table 5.21.

The data were reduced to include only the species which made up at least 3% of the total abundance in at least one sample, which reduced the number of benthic foraminiferal species to only 15 (Appendix 18). The most dominant species *Eilohedra weddellensis* was removed from the data set as it overwhelmed all the other species in the PCA and allowed no other abundance patterns to be seen within the data set. The original data were then log transformed and not normalised which resulted in a covariance-based PCA.

The results showed that 3 principal components or assemblages accounted for 92.3% of the total variation, with 79.8% of the variation accounted for by the first principal component alone. The analysis was run to include 5 principal components originally but was reduced to 3 as the fourth and fifth groups combined accounted only for a further 3% of the total variance, and did not seem to contribute any more significant information. Table 5.22 shows the species composition of the benthic foraminiferal assemblages, including the dominant species

and the important associated species. Down core fluctuations of the resulting faunal assemblages for core GC062 are presented in Figure 5.43b.

PC	Eigenvalues	% Variation	Cumulative % Variation
1	7.15	79.8	79.8
2	0.65	7.2	87.1
3	0.47	5.3	92.3

Table 5.21. Eigenvalues extracted using Q-mode PCA for GC062.

Q-mode assemblage	Dominant Species	PCA score	Important Associated species	PCA score
PC1	*Epistominella exigua*	0.538		
	Gyroidinoides spp.	0.383		
	Cassidulina crassa	0.366		
	Globocassidulina subglobosa	0.331		
	Fursenkoina complanata	-0.278	*Melonis barleeanum*	-0.242
PC2	*Oridorsalis tener*	0.421		
	Epistominella exigua	0.412		
	Eggerella bradyi	0.397		
	Fissurina spp.	-0.292		
	Globocasidulina subglobosa	-0.285		
PC3	*Pullenia* spp.	0.376		
	Eggerella bradyi	0.342		
	Fissurina spp.	0.326		
	Bolivinita pseudothalmanni	-0.468		
	Melonis barleeanum	-0.392		

Table 5.22. Species composition of Q-mode assemblages in GC062 showing Principal Component scores for faunas. A negative sign on the score indicates that the species decreases as the component increases (Parker and Arnold, 1999).

The negative end-member assemblage of PC1 is dominated by *F. complanata* and *M. barleeanum*, and is important within the core below about 37 cm. Above this depth the sediment is dominated by the positive end-member of PC1 which is represented by the species *E. exigua* and *Gyroidinoides* spp. This change in assemblage is similar to that seen in

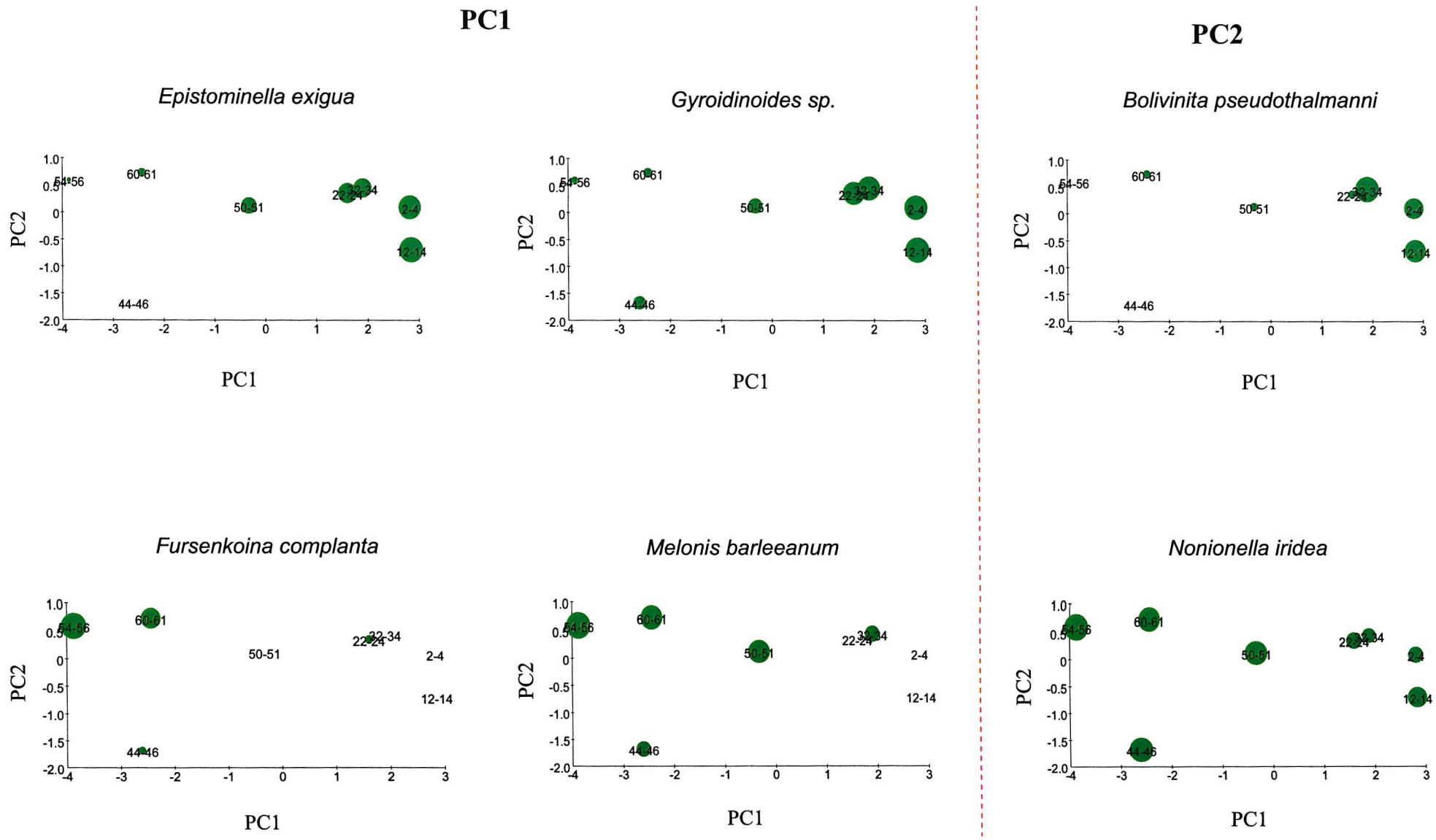

Figure 5.48. Bubble plots for dominant species in GC062.

KC097 with the top part of the core dominated by a NADW assemblage, and the lower part of the core dominated by high productivity indicator species.

The positive end-member of PC2 is dominated by *O. tener* and *E. exigua* and this assemblage is important below 50 cm and between 35-18 cm within the core. Between these depths the negative end-member assemblage dominated by *Fissurina* spp. and *G. subglobosa* is more important.

Principal Component 3 shows generally quite low values for species loadings with only a significant positive excursion centred at about 20 cm dominated by *Pullenia* spp., and most of the rest of the core is dominated by the negative end-member assemblage represented by *B. pseudothalmanni*. However this principal component only accounts for 5.3% of the total variance and so may not provide any significant ecological information.

Figure 5.44 shows the sample scores for PC1 plotted against PC2. This plot shows 2 very distinct groups of samples, from 0-32 cm and 44-base of the core.

Figure 5.45 shows the position of the individual foraminifera species plotted on PC1 and PC2. This plot shows quite clearly the positive and negative end-member assemblages from the Q-mode PCA analysis with a separate group lying near the 0 on both axes. This group contains the species which seem to stay fairly constant throughout the core section with little variation in relative abundance and so do not provide any information about environmental change.

Figure 5.48 shows bubble diagram plots of the important species in the negative and positive end-member assemblages for PC1 and PC2.

5.8.3. KC064

5.8.3.1. Cluster Analysis and Multi-Dimensional Scaling

The results from the cluster analysis and corresponding MDS plot with no transformation of the data can be seen in Figure 5.49. The cluster analysis was also performed with fourth root transformation of the data.

The cluster analysis and MDS with no transformation of the data identified three main groups of samples. The first group ranges from 90-58cm up through the core and these samples are grouped at a similarity level of about 73%. This group of samples is represented by low diversity and abundance of species but below this level in the core foraminifera have been almost absent from the samples. The foraminifer *E. weddellensis* is dominant within these samples and there may be a higher abundance of *O. tener*. Other calcareous forms (including all species identified in section 5.2.1.) occur but in low abundance and there is a lack of agglutinated species within this section of the core.

The second group ranges from 55-25cm (not including 30-31cm) up through the core and these samples are grouped at a similarity level of 75%. This group is represented by increased species diversity and abundance, and *E. weddellensis* is no longer the dominant foraminifer showing a decrease in relative abundance within this section. The calcareous species which were found in the first group continue to show increased abundance in this section, and other species such as *Uvigerina* spp., *A. angulosa, Fissurina* spp. and *Ehrenbergina* spp. now appear but in low abundance. There are still only very low numbers of agglutinated species within these samples.

The third group ranges from 30cm to the top 10cm (not including 25-26cm) up through the core and is grouped at a similarity level of 68%. These samples are represented by the highest diversity of species with all calcareous species persisting within this section and occurring in high abundance. Within these samples more agglutinated species appear in significant numbers, such as *Repmanina charoides, Trochammina* spp. and *Ammobaculites* spp. but still have quite a low abundance.

The two groups which form a combined range from 95-25cm can be grouped at a similarity level of 67% and so there is some overlap at the transition between these groups.

The results from the cluster analysis were then used to group samples on the MDS plot at certain levels of similarity. The MDS analysis with no transformation of the data produced a plot with a stress value of 0.10 (Fig.5.49), which indicates a good ordination of the data. This was lower than the stress value of 0.13 for the MDS plot with fourth root transformation of the data.

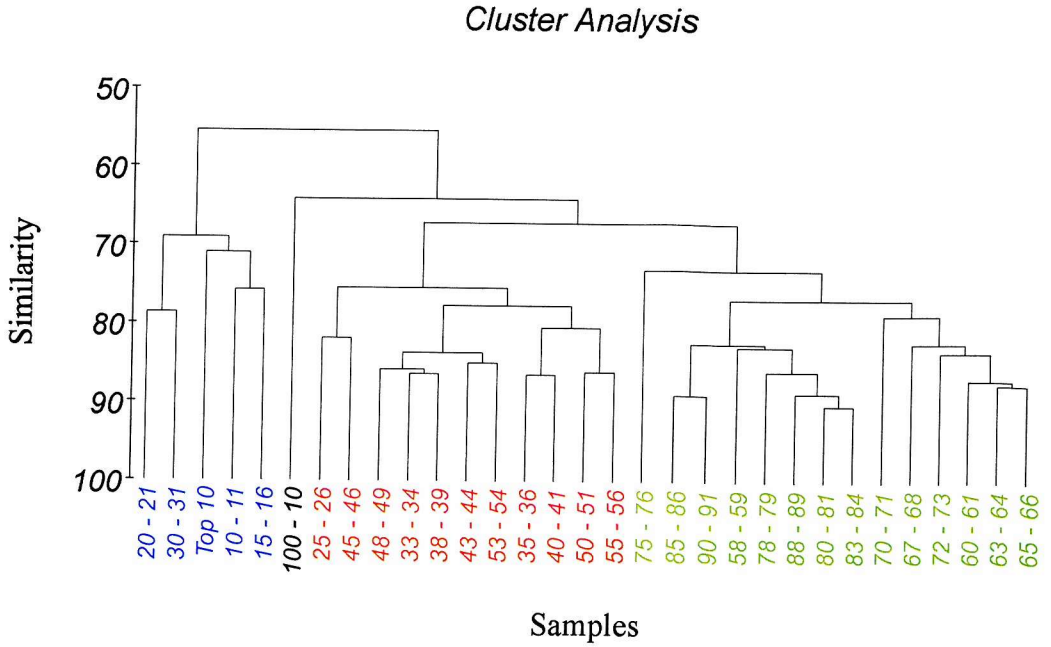

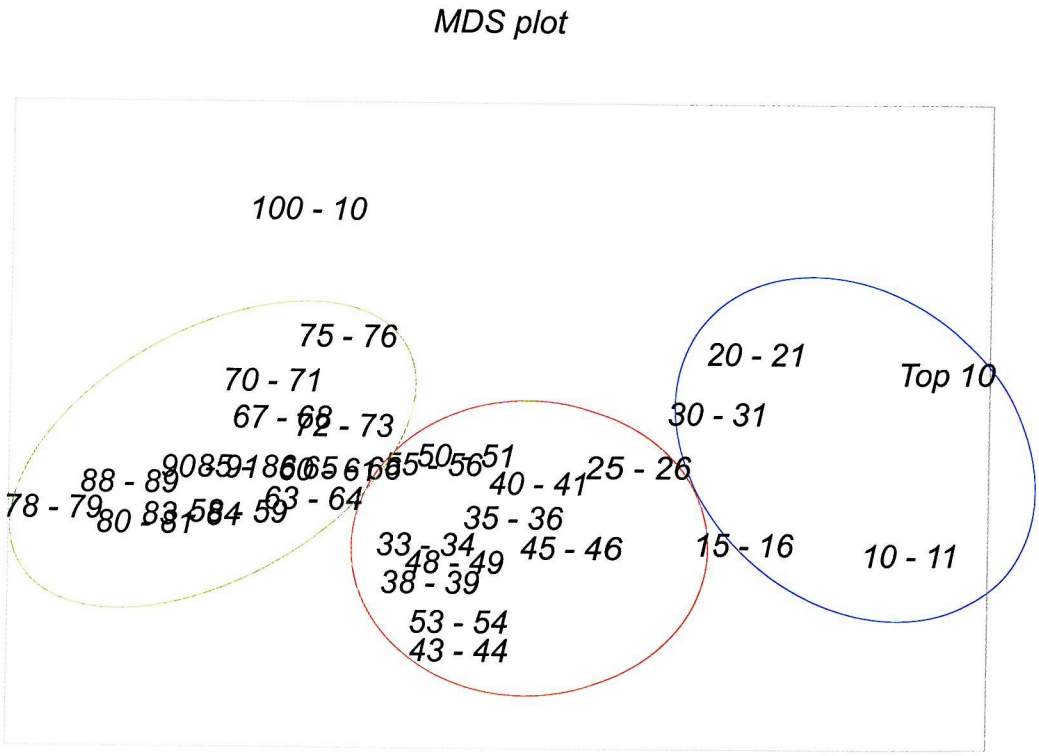

Figure 5.49. KC064 Cluster and MDS Analysis with no transformation of the data.

5.8.3.2. Principal Components Analysis

A Q-mode PCA carried out on the data set yielded eigenvalues and associated percentages of the total variance each accounts for, as shown in Table 5.23.

The data were reduced to include only the species which made up at least 3% of the total abundance in at least one sample, which reduced the number of benthic foraminiferal species to only 23 (Appendix 18). The most dominant species *Eilohedra weddellensis* was removed from the data set as it overwhelmed all the other species in the PCA and allowed no other abundance patterns to be seen within the data set. The original data were then log transformed and not normalised which resulted in a covariance-based PCA.

The results showed that 3 principal components or assemblages accounted for 61.1% of the total variation, with 31.7% of the variation accounted for by the first principal component alone. The analysis was run to include 5 principal components originally but was reduced to 3 as the fourth and fifth groups accounted only for a further 4% of the total variance, and did not seem to contribute any more significant information. Table 5.24 shows the species composition of the benthic foraminiferal assemblages, including the dominant species and the important associated species. Down core fluctuations of the resulting faunal assemblages for core KC064 are presented in Figure 5.43c.

PC	Eigenvalues	% Variation	Cumulative % Variation
1	3.52	31.7	31.7
2	1.87	16.8	48.5
3	1.40	12.6	61.1

Table 5.23. Eigenvalues extracted using Q-mode PCA for KC064.

Q-mode Assemblage	Dominant species	PCA score	Important Associated species	PCA score
PC1	*Sphaeroidina bulloides*	0.109		
	Nonionella iridea	0.024		
	Uvigerina spp.	-0.352		
	Ehrenbergina trigona	-0.342		
	Trochammina spp.	-0.333		
	Fissurina spp.	-0.313		
	Epistominella exigua	-0.278		
	Gyroidinoides spp.	-0.277		
	Lagena spp.	-0.274		
	Globocassidulina subglobosa	-0.272		
	Nuttallides umbonifera	-0.258		
PC2	*Trochammina* spp.	0.396		
	Repmanina charoides	0.309		
	Epistominella exigua	0.204		
	Globocassidulina subglobosa	-0.389		
	Oridorsalis tener	-0.372	*Pullenia* spp.	-0.206
	Eponides spp.	-0.370		
	Gyroidinoides spp.	-0.250		
PC3	*Oridorsalis* sp.	0.619		
	Shpaeroidina bulloides	-0.565		

Table 5.24. Species composition of Q-mode assemblages in KC064 showing Principal Component scores for faunas. A negative sign on the score indicates that the species decreases as the component increases (Parker and Arnold, 1999).

The negative end-member of PC1 is dominated by *E. exigua* and *Gyroidinoides* spp. and this assemblage shows high loadings throughout the top 55 cm of the core. This group contains species which are indicators of a number of water masses including NADW (*E exigua* and *Gyroidinoides* spp.), CDW (*G. subglobosa*) and AABW (*N. umbonifera*). The negative end-member assemblage is represented by *S. bulloides* and *N. iridea* but only as low loadings and is important in the core below 55 cm.

The negative end-member of PC2 is dominated by *G. subglobosa* and *O. tener* and is important within the core between 65-30 cm within the core. Below and above this depth the positive end-member assemblage dominates the core, and this is represented by *Trochammina* spp.

For PC3 the change in importance of assemblage is harder to recognise as the record is quite noisy. However in general the negative end-member assemblage is dominant in the middle

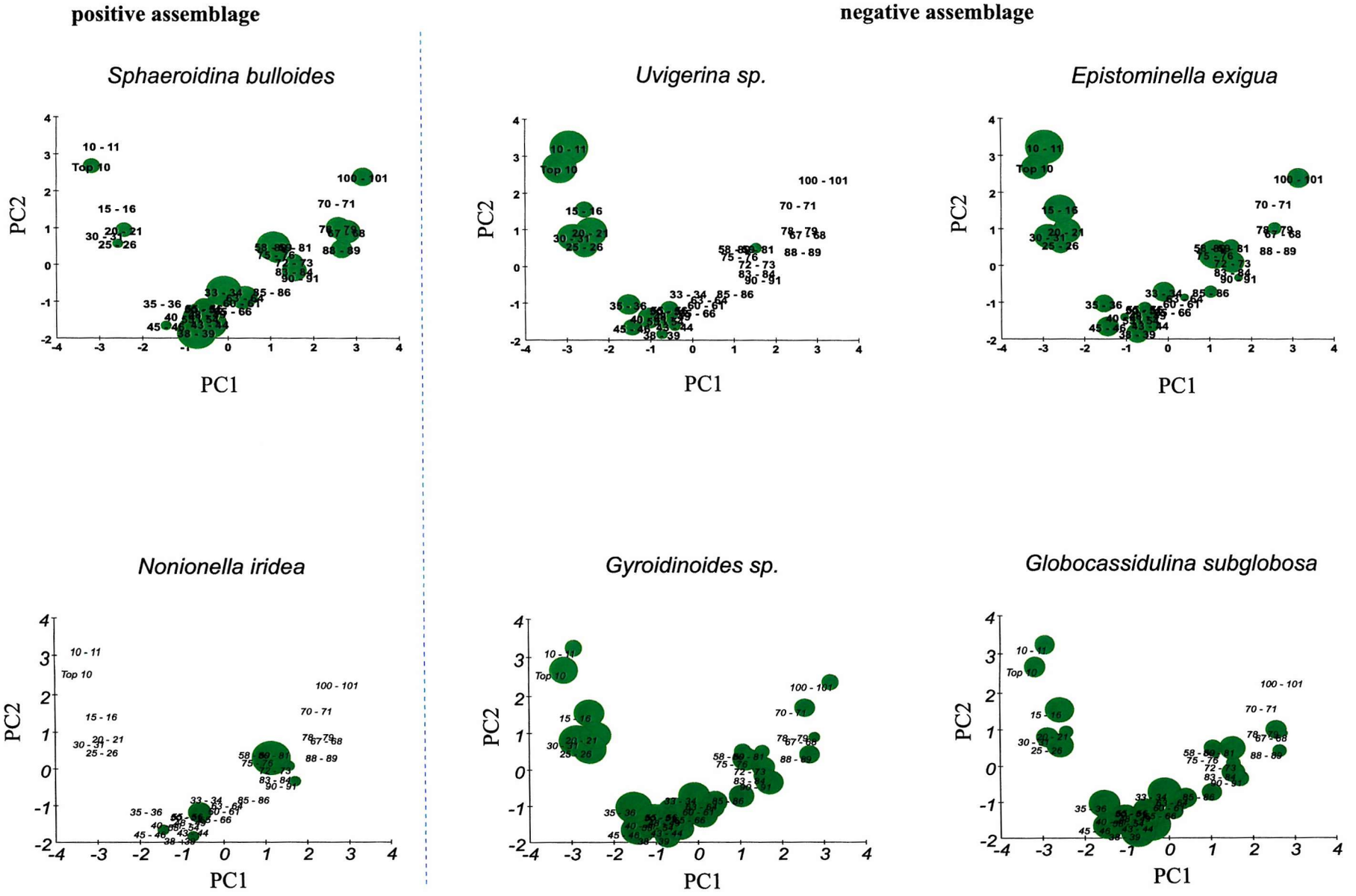

Figure 5.50. Bubble plots for dominant species in PC1 in KC064.

section of the core between 65-30cm and is represented by *S. bulloides*. The top and bottom sections of the core are represented by the positive end-member assemblage which is dominated by *Oridorsalis* sp.

Figure 5.44 shows the sample scores for PC1 plotted against PC2. This plot reveals a clear distinction between the samples which show positive and negative loadings on PC1.

Figure 5.45 shows the position of the individual foraminifera species plotted on PC1 and PC2. The foraminifera species seem to be more evenly distributed on both principal component axes in this analysis, and this may be due to the effect of PC1 showing only negative loadings throughout the core section. However the positive and negative end-member assemblages can still be seen and there are two smaller groups lying near the 0 on both axes which represent the PC3 assemblages and two species which show little variation in relative abundance throughout the core.

Figure 5.50 shows bubble diagram plots of the important species in the negative and positive end-member assemblages for PC1 and PC2.

5.9. Relationship between core site and position of the Polar Front

The number of benthic foraminiferal species in each core top and the number of benthic foraminifera per gram of sediment in the core top sample were plotted against distance from the PF (Figure 5.51).

The number of species (i.e. diversity) in the core top sample showed a general increase from south to north in the Scotia Sea, with the lowest number in core TC078 in the northern Scotia Sea and the highest in core KC097 in the western Falkland Trough (see Fig.1.1). The number of species is also relatively high however in KC064 which is located just south of the PF.

The number of foraminifera per gram of sediment in the core top sample also showed a general increase from south to north in the Scotia Sea, with very low numbers in TC078 and highest in GC062. There are also quite a high number of foraminifera recorded in TC036 to the south of the PF but not in KC064 as recorded by the number of species.

Figure 5.52 shows the difference in accumulation rate of the two phytodetritus exploiting species *E. weddellensis* and *E. exigua* as you move south across the PF, and shows that there is a definate decrease in bith species from north to south. The rate of accumulation is much slower in KC064 to the south of the PF.

Table 5.25 and Figure 5.53 show summaries of the results from the cluster and MDS analysis and the PCA. They show the characteristics by which the change in benthic foraminiferal assemblage can be identified through the glacial-interglacial transition, in cores from the north and south of the Polar Front.

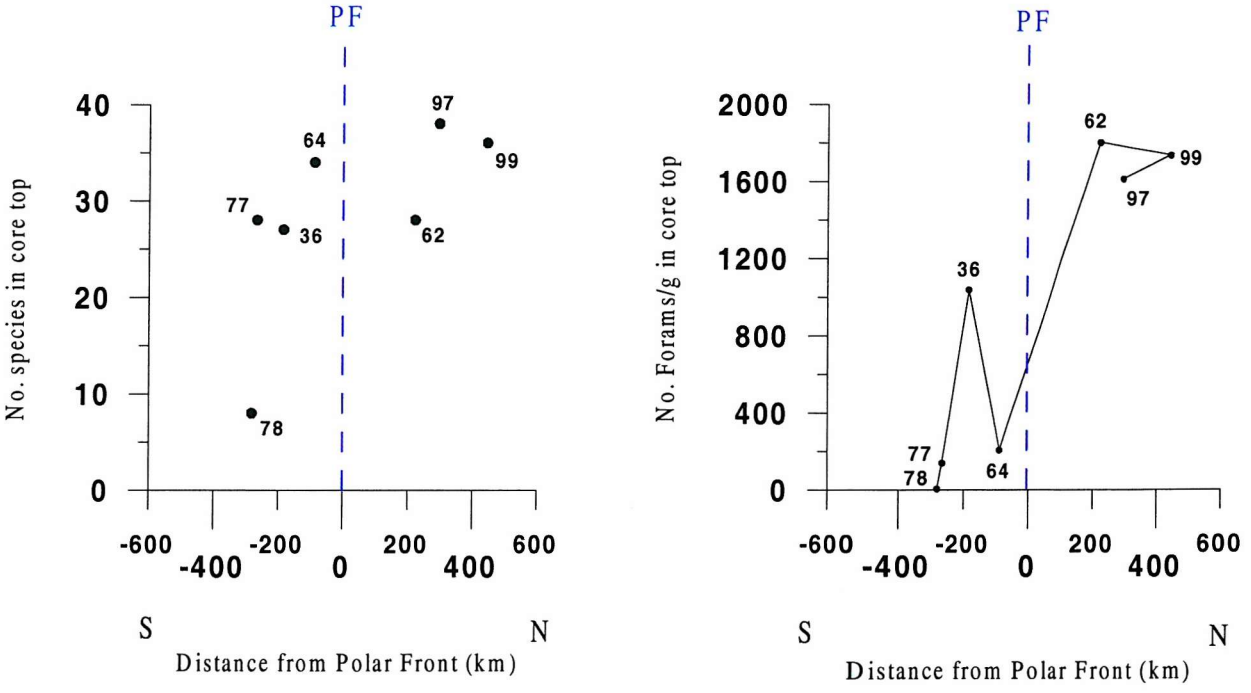

Figure 5.51. a) Number of benthic foraminifera species in core top sample and
b) Number of benthic foraminifera per gram of sediment in core top sample plotted against Distance from the Polar Front in km.

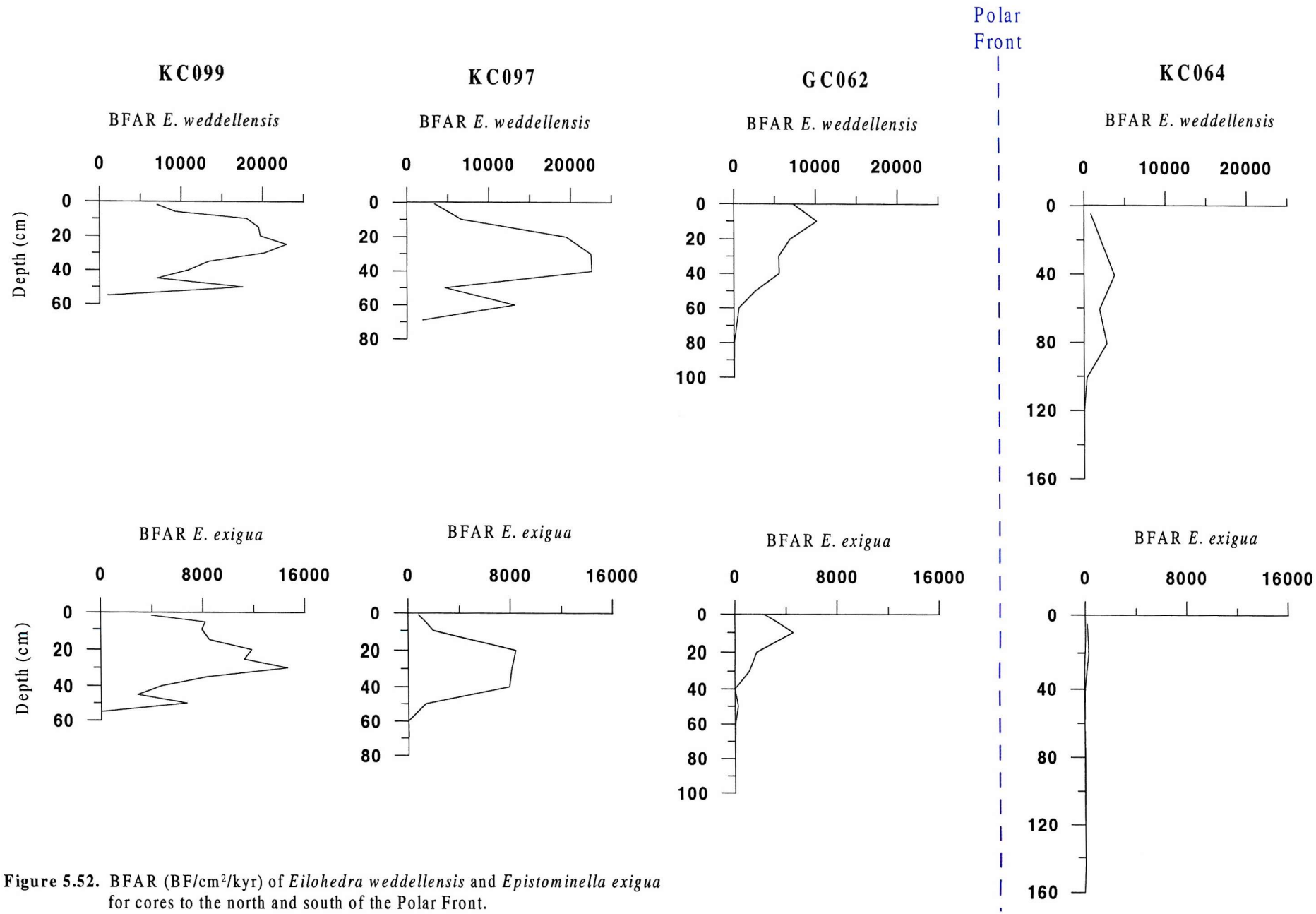

Figure 5.52. BFAR (BF/cm^2/kyr) of *Eilohedra weddellensis* and *Epistominella exigua* for cores to the north and south of the Polar Front.

	PF	
	NORTH	**SOUTH**
Cluster and MDS analysis	**Holocene:** High species diversity and high abundance of dominant benthic foraminifera species (e.g. see Fig.5.2). Dominance of phytodetritus species *E. weddellensis* and *E. exigua*. **Transition:** Dominant benthic foraminifera species abundant but also increase in high productivity indicator species *Melonis* spp., *Pullenia* spp. and *Fursenkoina* spp. **Glacial:** Low foraminiferal abundance and species diversity, absent towards base of core.	**Holocene:** High species diversity and high abundance of dominant benthic foraminifera species (e.g. see Fig.5.25). Lower abundance than cores to the N of the PF. Increased relative abundance of agglutinated species. **Transition:** Lower species diversity and foraminiferal abundance than Holocene section. **End of glacial:** Low species diversity and foraminiferal abundance. Only *E. weddellensis* and some *O. tener* found to persist.

Table 5.25. Summary table for results from Cluster and MDS analysis for cores to the north and south of the Polar Front.

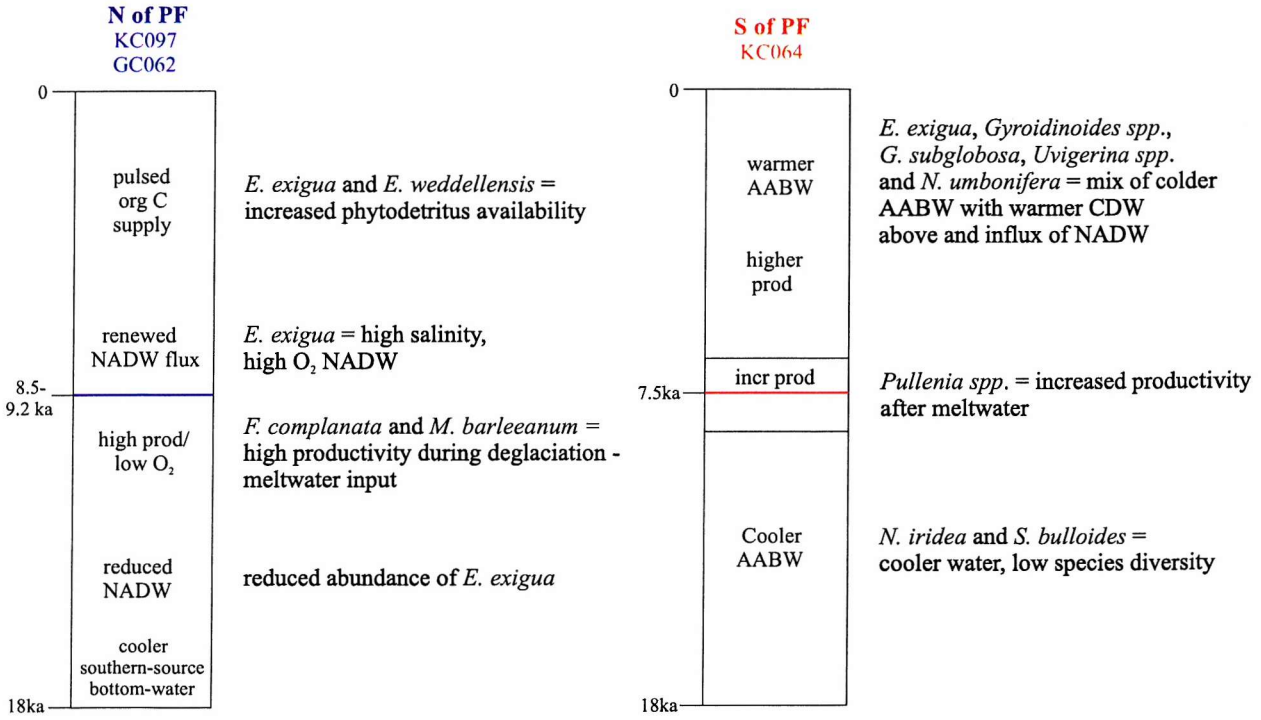

Figure 5.53. Summary diagram of results from PCA for cores to the north and south of the Polar Front. (Interpretation of the cores is based on the evidence listed at the side of each section).

Chapter Six

INTERPRETATION AND DISCUSSION

6.1. Benthic and Planktonic Foraminiferal Absolute Abundance

The benthic and planktonic absolute abundance data in all of the cores show a general trend of increasing abundance up-core, with higher foraminiferal content in the postglacial samples above the Last Glacial Maximum (LGM) at 18ka. Even in cores KC099, TC036, TC077 and TC078, which do not record a full glacial-interglacial transition, it can be seen that foraminiferal abundance decreases significantly with depth within the core section. This higher foraminiferal abundance during the transition from stage 2-1 and during the Holocene suggests that a climatic improvement to a warmer, more productive environment with ice-free conditions occurred, promoting increased benthic and planktonic foraminiferal productivity. This agrees with the conclusions from Pudsey *et al.* (1988), Pudsey (1992) and Gilbert *et al.* (1998) for studies from the Scotia Sea.

During the glacial stage the foraminiferal abundance was very low and some samples contain no carbonate at all. Sea surface temperature and the seasonally variable sea-ice edge both limit the production of diatoms and organic carbon which are the main food supply for planktonic and benthic foraminifera. This in turn limits the production of biogenic carbonate and silica (Pudsey and Howe, 1998), and hence due to continuous sea-ice coverage at most of

the core sites and at least winter sea-ice at the more northerly sites during the glacial stage, surface biogenic productivity would have been reduced (Fischer *et al.*, 1988). This can be seen from the diatom results (Appendix 19) which record a higher abundance of the ice-indicator species *Eucampia antarctica* (Jousé *et al.*, 1963) within the lower section of cores KC097 and KC064 to the north and south of the PF. Hays *et al.* (1976) concluded in their study of radiolaria in the South Atlantic Ocean, that the summer ice cover extended nearly to 55°S latitude at 18ka, whereas today it melts right back to the Antarctic continental margin. Pudsey and Howe (1998) suggested that the spring sea-ice edge was as far north as 55°S in the South Atlantic Ocean during the LGM based on diatom abundance. The winter ice-edge limit may have extended as far north as 47-50°S in the western and eastern parts of the Indian Ocean (Prell *et al.*, 1980). The effect of increased carbonate dissolution by a carbonate under-saturated water mass such as AABW may also inhibit the preservation of carbonate during glacials (Corliss, 1983). It is likely that an expansion of these polar waters accompanied the northward extension of sea-ice, which would have caused an increase in dissolution of foraminiferal tests. This northward expansion of polar waters has also been deduced from studies of radiolaria (Lozano, 1974; Hays *et al.*, 1976; Dow, 1978; Morley and Hays, 1979a; Crawshaw, 2000). Morley and Hays (1979a) also recorded a 5° northward shift in the zero calcium carbonate curve (CCD) south of 42°S in the South Atlantic at 18ka, which would have resulted in a northward expansion of the carbonate under-saturated water masses below the CCD. A rise in the CCD at the LGM was also observed by Hays *et al.* (1976) who noted that this would cause a southward increase in the thickness of the bottom water in the Southern Ocean at 18ka and hence lead to significantly greater carbonate corrosion. This expansion of polar waters into lower latitudes would reduce the area of $CaCO_3$ deposition at 18ka compared with today. During the Holocene, a high input of calcareous planktonic foraminiferal tests would depress the CCD by supplying $CaCO_3$ to the deep water, and thus preserving calcareous foraminifera at the seabed (Anderson, 1975b).

The reduced glacial foraminiferal abundance and preservation of the calcium carbonate tests could suggest that at the time of the LGM the PF had shifted north to at least the location of the cores within the Falkland Trough (52°S), and probably farther north, inferred from the complete absence of carbonate within the glacial sediments in all the cores. There are no cores from north of 52°S so the most northerly position of the PF at the LGM cannot be constrained in this area. A study by Pudsey and Howe (1998) based on sedimentological data noted a northward shift of the PF as far north as the south slope of the Falkland Plateau (see Fig.1.1). However it is difficult to obtain cores to restrain the position of the PF as only some

parts of the Scotia Sea and Falkland Trough contain suitable deep water sediments from within a continuous section. Mackensen *et al.* (1994) also recorded a northward shift of the PF by 7° in the South Atlantic to 43°S at 18ka, based on changes in the benthic foraminiferal fauna and $\delta^{13}C$ values. A number of studies based on various microfossil data have documented a northward migration of the PF at 18ka of between 1 and 10° latitude within the Southern Ocean (CLIMAP, 1976; Cline and Hays, 1976; Lozano and Hays, 1976; Williams, 1976; Hays *et al.*, 1976; Dow, 1978; Morley and Hays, 1979a; Morley, 1989; Prell *et al.*, 1980; Corliss, 1982; Burckle, 1984; Howard and Prell, 1992; Howe and Pudsey, 1999). There is also evidence from planktonic $\delta^{13}C$ in the Atlantic sector of the Southern Ocean, of a 5° northward shift of the zone of maximum CO_2 exchange between surface waters and the atmosphere, which represents the PF (Charles and Fairbanks, 1990). Howard and Prell (1992) also noticed the occurrence of IRD, another indicator of the PF, as far north as 45°S in the South Indian Ocean during glacials. This northward shift of the PF would explain the deposition of pure diatom ooze during the glacial stage when the southern part of the PFZ was north of all the core sites, and accumulation of calcareous ooze when the PFZ is well to the south of the core site and warmer, less productive SASW overlies it (Westall and Fenner, 1991). This is seen in the sediments of the present day Scotia Sea where calcareous sediment accumulation dominates to the north of the PF, and siliceous sedimentation to the south. The cores to the south do contain some calcareous sediment but the horizons are much thinner and contain fewer foraminifera, and are deposited as foraminifera-bearing diatom muds rather than as the foraminiferal sands found to the north of the PF (see Fig.4.1).

The deglaciation is marked by an initial gradual amelioration of the climate before a significant increase in planktonic and benthic foraminiferal abundance occurs at about 14.2ka in GC062 and 12ka in KC064 (the only cores with full glacial cycle dated, see summary diagrams). This relatively rapid improvement in climate may have been related to the poleward displacement of the PF and consequently the retreat of the winter sea-ice edge, which moved across the core sites in the Falkland Trough first before approaching the core sites in the northern Scotia Sea. At this time the cores would have been covered by warmer, more productive, ice-free waters which promoted enhanced primary productivity and hence foraminiferal abundance which has been recorded in a number of studies in the Southern Ocean (Morley, 1989; Prell *et al.*, 1980; Howard and Prell, 1992; Mackensen *et al.*, 1994). The diatom results also show an increased abundance during the Holocene period with greater relative abundance of the open-ocean indicator species *Nitzschia kerguelensis*

(Burckle *et al.*, 1987) and *Thalassiosira spp.* (Leventer and Dunbar, 1988) in cores KC097 and KC064. The influence of the sea-ice and ice-edge bloom indicator species *Nitzschia cylindrus* and *N. curta* (Smith and Nelson, 1985; Garrison and Buck, 1985) does not seem to be important during the glacial transition (Appendix 19). Howe and Pudsey (1999) used grain size analysis to provide a record of the strength of CDW flow over the last 18ka, and suggested that a northward shift of the PF (including stronger wind forcing) may explain the unsteadiness of CDW during glacials. They also proposed that a southward shift of the PF during the deglaciation and Holocene intervals may have resulted in the deposition of foraminifera-rich sandy contourites at core tops within the northern Scotia Sea (including core KC064 from this study).

A maximum in planktonic and benthic foraminiferal abundance is observed between about 7.5-4 ka during the Holocene within most of the cores (except TC077 and TC078). This may represent a period of enhanced primary productivity during peak interglacial conditions when the climate was warm and fully recovered from the last glacial. A similar productivity maximum was seen in a study by Rathburn *et al.* (1997) based on a number of microfossil groups in the Prydz Bay region of Antarctica at the later date of 4-2.7 ka. Evidence from Antarctic deep ice-core data recovered at Dome C, Vostok and Komsomolskaïa also record a Holocene climatic optimum between 10 and 7.5 ka (Ciais *et al.*, 1992). A short climatic optimum was also observed in the planktonic foraminiferal records from east of New Zealand by Weaver *et al.* (1998) which occurred between 8-6.4 ka. They also noted a subsequent decline of temperatures after the climatic optimum to present levels, which may be an explanation for the decrease in foraminiferal abundance at the top of the cores in this study (except TC077 and TC078). A return to cooler conditions after 5ka was observed in a study by Young and Schofield (1973) of pollen in Kerguelen subantarctic islands, which followed a warm temperature optimum around 8ka (see Fig. 6.1).

6.2. Benthic Foraminiferal Relative Abundance

There are some interesting species variations seen in cores KC097, GC062 and KC064 through the glacial-interglacial cycle, which may reveal information about changes in the palaeoceanography of the area over this time period. The individual benthic foraminiferal species all show a marked increase in abundance at the end of the transition from the glacial stage at approximately 12ka, which follows the same pattern as the absolute foraminiferal abundance data. In each core the same benthic species appear to be dominant and show

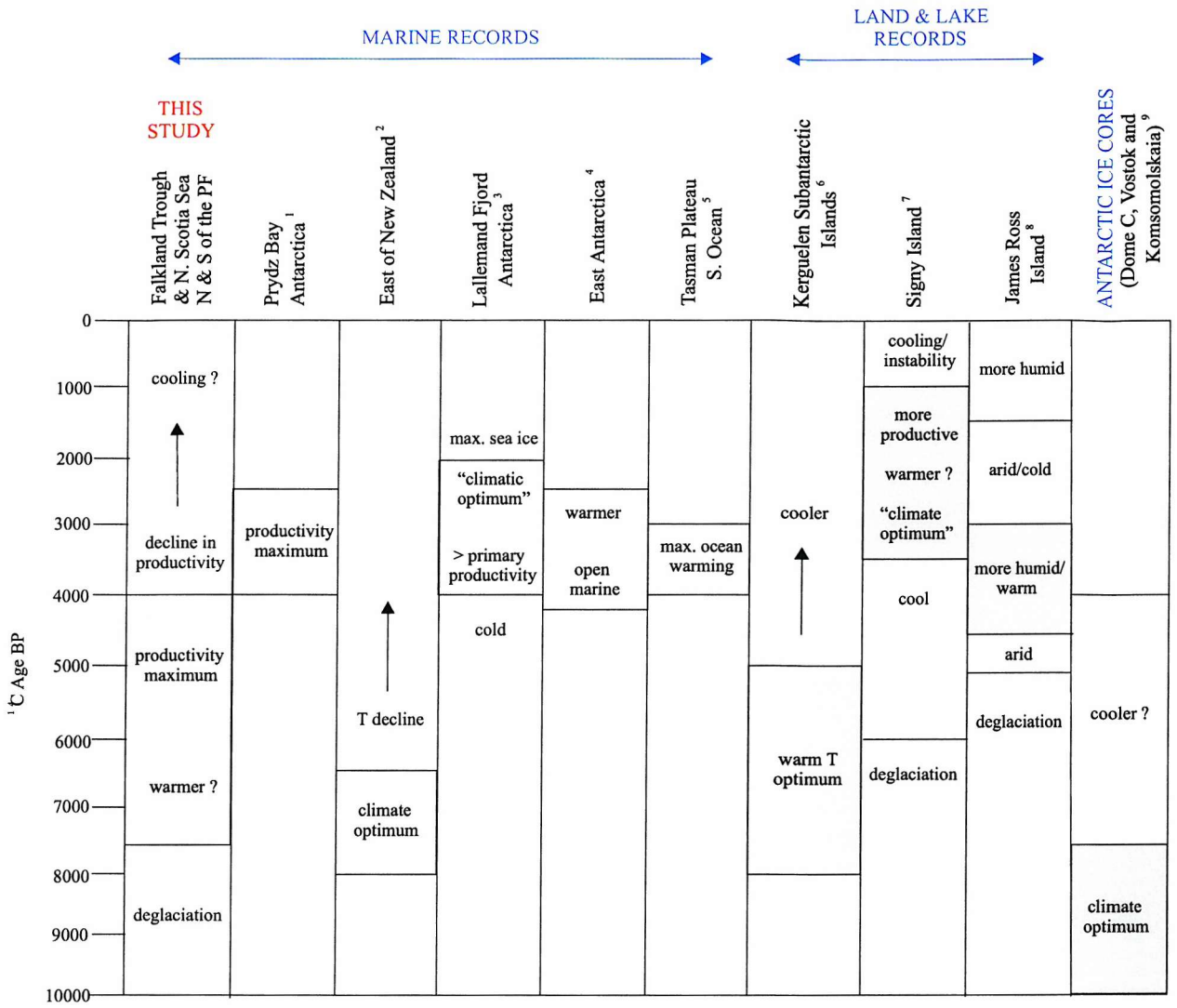

Figure 6.1. Summary of studies from Antarctica and the Southern Ocean recording a mid-Holocene climate event.

References: [1]Rathburn *et al.* (1997); [2]Weaver *et al.* (1998); [3]Domack and McClennen (1996); [4]Domack *et al.* (1991); [5]Ikehara *et al.* (1997); [6]Young and Schofield (1973); [7]Jones *et al.* (2000); [8]Bjork *et al.* (1996); [9]Ciais *et al.* (1992) and Lorius *et al.* (1979).

similar relative abundance records throughout the core. It should be noted that the microhabitat preferences of some benthic foraminifera are not fixed and can switch in response to food availability and oxygen gradients (Jorissen *et al.*, 1992; Linke and Lutze, 1993).

- ***Eilohedra weddellensis* and *Epistominella exigua***

Epistominella exigua is associated with *E. weddellensis* as an indicator of productivity and organic matter flux (Loubere, 1994; Mackensen *et al.*, 1995). These are both opportunistic species which can respond quickly to sudden changes in food supply with rapid growth and reproduction, and are associated with phytodetritus, especially in mid to high northern latitudes (Gooday and Lambshead, 1989; Gooday, 1988, 1993, 1996). The deposition of phytodetritus at high southern latitudes has not been reported in previous studies from the Southern Ocean. These species have the ability to adapt to a fluctuating food supply in a food-limited environment (Gooday, 1994). Phytodetritus originates in the euphotic zone (Riemann, 1989) and represents an important pathway for the supply of organic carbon to the seafloor. It settles to the seafloor after the spring bloom, constituting a seasonal pulse of food for the deep-sea benthic foraminifera (Rice *et al.*, 1986; Thiel *et al.*, 1989). The presence of these species in abundance in the sediment can therefore indicate periods of pulsed organic matter input (Smart *et al.*, 1994; Thomas *et al.*, 1995), and their abundance in the Southern Ocean may be related to the highly seasonal nature of phytoplankton production in this region (Fischer *et al.*, 1988). In a study by Loubere and Fariduddin (1999) of the organic carbon flux seasonality signal in benthic foraminiferal assemblages from deep-sea surface sediments in the Atlantic, Pacific and Indian Oceans, they found that both *E. weddellensis* and *E. exigua* were important taxa for estimating higher seasonality of the carbon flux to the deep-sea. Phytodetrital assemblages can be distinguished by their requirement for a strongly seasonal flux of organic carbon, as opposed to a higher and more sustained carbon supply needed to support the normal high productivity faunas (Corliss and Chen, 1988).

In cores KC097, GC062 and KC064 there seems to be an initial large increase in the abundance of *E. weddellensis* with a slight lag of *E. exigua* at the end of the deglaciation (~14-12 ka), indicating an increase in productivity and supply of organic material to the deep sea at the start of interglacial conditions. The increase in productivity may be due to a poleward migration of the PF across the core sites at the start of the interglacial and the introduction of glacial meltwater. The abundance remains high but variable through the Holocene with an abundance maximum at about 4.5ka in KC097 and at a similar time in

GC062 which may represent be a period of pulsed phytodetrital deposition in the Scotia Sea during the mid-Holocene. A similar rapid increase in abundance of *E. exigua* and *Alabaminella weddellensis* (similar to *Eilohedra weddellensis*) was recorded in the NE Atlantic following the most recent deglaciation and has been similarly linked to an increased production of phytodetritus following the northward retreat of the Arctic PF (Thomas *et al.*, 1992).

Epistominella exigua thrives between 1500m and the CCD but becomes outnumbered by the specialist species *Nuttallides umbonifera* below the carbonate lysocline. Therefore in the Southern Ocean the fossil deep-water fauna was found to be dominated by *N. umbonifera* or *E. exigua* depending on the depth of the lysocline (Mackensen *et al.*, 1993a).

- ***Epistominella exigua***

Mackensen *et al.* (1995) demonstrated that this species showed a positive correlation with salinity and therefore may correspond to the core of NADW which is the most saline water mass below AAIW. The distribution of *E. exigua* has been found to correspond to the spreading route of NADW through the whole Atlantic Ocean (Streeter, 1973; Schnitker, 1974, 1979, 1980; Lohmann, 1978a; Streeter and Shackleton, 1979; Weston and Murray, 1984; Murray, 1991; Mackensen *et al.*, 1993a). The initial increase in abundance at the end of the glacial period may represent the renewed influx of NADW into the Southern Ocean after being much reduced during the glacial stage. The influence of NADW continues to increase through the Holocene as reflected by the increased relative abundance of *E. exigua*. Mackensen *et al.* (1994) found that there was an increased flux of NADW during interglacials in the South Atlantic which is reflected by an increasing $\delta^{13}C$ record up-core.

- ***Globocassidulina subglobosa***

This species has been associated with strong bottom currents and well-sorted sandy sediments (Murray, 1991) in a number of studies, for example, during deglacial ice retreat (Brambati *et al.*, 2000), vigorous bottom currents in the PFZ (Sen Gupta and Machain-Castillo, 1993), and vigorous flow of AABW due to channelling in the South Atlantic (high energy benthic boundary layer group) (Mackensen *et al.*, 1995). In KC097, GC062 and KC064, this species appears most abundant within the top section of the core during the Holocene. At the time of the LGM the PF may have lain as far north as the Falkland Plateau and was not coincident with the axis of strongest deep ACC flow. The path of strongest deep

ACC flow must have remained in its present day position in the Scotia Sea during the LGM because of the topographic restriction of the North Scotia Ridge (Pudsey and Howe, 1998). If the PF began a poleward migration at the end of the glacial stage then during the Holocene the PF would have moved closer to the axis of strong ACC flow as indicated by an increase in the abundance of *G. subglobosa*. A study by Howe and Pudsey (1999) in the northern Scotia Sea has used grain-size analysis to provide an indication of the strength of CDW flow over the last 18ka. They found that increased winnowing at about 17ka was indicative of an unstable CDW, with stormier glacial benthic conditions producing random, high-energy currents. This may have been related to a northward migration of the PF (Pudsey and Howe, 1998) and higher glacial wind speeds driving the ACC (DeAngelis *et al.*, 1987). During the deglaciation and into the Holocene period (~10ka), CDW stabilised becoming less vigorous. The Falkland Trough (see Fig.1.1), however has been suggested as being a "backwater" during the LGM with reduced ACC flow across it. The reduction may be due to the decreased intensity of the Weddell Gyre and hence reduced CDW flow into the Falkland Trough, combined with lower sea levels (Howe *et al.*, 1997).

This species also shows a positive correlation to the carbonate content of the sediment and to sediment porosity (Mackensen *et al.*, 1995; Schmiedl *et al.*, 1997) and therefore shows an increase in abundance within the more productive Holocene period which is represented by the deposition of carbonate-rich foraminiferal sands (see Fig.4.1). *Globocassidulina subglobosa* has also been described as a widely distributed species that may be associated with phytodetritus deposits (Gooday, 1993) as possibly observed in the Holocene of the Scotia Sea.

- ***Nuttallides umbonifera***

This species has been associated with AABW in the South Atlantic (Anderson, 1975a; Lohmann, 1978; Mackensen *et al.*, 1995) and with the transition between LCDW and WSDW within the PF region of the southwest Atlantic (Mead, 1985). In a study by Bremer and Lohmann (1982) in the Atlantic Ocean, they concluded that it was the under-saturation and bottom-water corrosiveness of AABW which linked it to *N. umbonifera* as it is a relatively dissolution resistant species. *Nuttallides umbonifera* is only found in significant abundance in KC064 to the south of the present day PF, perhaps reflecting the increased influence of AABW farther south within the Scotia Sea. It is not found in cores TC077 and TC078 also to the south of the PF perhaps due to lower carbonate productivity farther south and hence a lower absolute foraminiferal abundance at these core sites. Within KC064 the

abundance increases towards the core top reflecting the necessary ice-free conditions for productivity to be enhanced. Even though there would have been an expansion of polar waters during the glacial period, the permanent ice cover would have prevented the proliferation of this species. It is also likely that there was reduced outflow of AABW from the weaker Weddell Gyre during the LGM (Jones, 1984; Fütterer *et al.*, 1988; Grobe and Mackensen, 1992; Pudsey, 1992; Shimmield *et al.*, 1994). However this species is also thought to be a non-opportunist (Gooday, 1993, 1994), able to survive on lower food supply than species such as *E. exigua* and it tends to flourish where food is scarce. It will be out-competed by *E. exigua* or *E. weddellensis* where phytodetritus is present. Therefore it can also be used an indicator of lower productivity (Loubere, 1991, 1994). This association can be seen clearly in KC064 where there is an inverse relationship between the relative abundance of *N. umbonifera* and *E. exigua*, suggesting that the end of the glacial period, and therefore perhaps earlier, were a time of lower productivity in the Scotia Sea.

- ***Gyroidinoides* spp.**

This genus has been associated with well oxygenated bottom water conditions (McKorkle *et al.*, 1990; King *et al.*, 1998) and with the youngest and best ventilated NADW by Mackensen *et al.* (1995), who included it in their lateral advection and bottom water ventilation group. In all of the cores there is an increase in this species at the start of the interglacial period in response to an increased flux of well-oxygenated NADW into the Southern Ocean. The outflow of NADW in the North Atlantic was greatly reduced during the LGM and the area was instead occupied by an "aged" water mass containing less oxygen than the present day water mass (Streeter, 1973; Schnitker, 1974, 1979, 1980). The abundance record of this species quite closely follows that of *E. exigua* which has also been associated with NADW flux.

- ***Nonionella iridea***

In a study by Mackensen *et al.* (1990) of live foraminifera in the Weddell Sea, this species was associated with the highest organic carbon content in the sediment. It lives within the upper 3cm of the sediment (Gooday, 1986; Mackensen, 1988) and Mackensen *et al.* (1990) suggested that it may depend on high organic carbon fluxes to survive within the sediment. However they did not find it preserved in the dead assemblage probably due to calcite dissolution in the upper sediment, enhanced by the relatively high organic carbon content. It

has also been documented in a live benthic foraminiferal assemblage from the Bransfield Strait (Mackensen, 1988). However in this study it may have a significant association with water masses. Domack *et al.* (1995) have associated *N. iridea* with the presence of a cooler water mass, which supports only a low diversity fauna with reduced abundance of other calcareous benthic foraminiferal species. Sen Gupta and Machain-Castillo (1993) also recorded this species as an indicator of low diversity able to live in low-oxygen environments of the World Ocean. The appearance of this species in abundance in core KC097 during the deglaciation and the start of the interglacial period may suggest that it is associated with cold AABW which was overlying the site at this time, just as the PF was starting to migrate south. The presence of well-oxygenated NADW may still be less influential than the polar water mass at this time. As the Holocene progresses and the climate continues to warm, the relative abundance of this cooler water species decreases to lower abundances.

- ***Minor species***

There is little information on the microhabitat preferences of *Lagena* and *Fissurina* species from any of the world's oceans other than they are both infaunal and cosmopolitan in nature. Therefore their significance in the benthic foraminiferal assemblage of cores KC097 and KC064 is unknown. Another species which does not seem to be described in any great detail in studies of the Southern Ocean is the infaunal, cold water species *Cassidulina crassa*. It has been described by Fariduddin and Loubere (1997) in a study from the low latitude Atlantic, as an indicator of low productivity associated with *G. subglobosa*. However in an earlier study by Sen Gupta and Machain-Castillo (1993), they describe *C. crassa* as indicating lower diversity, able to survive in low oxygen conditions and showing a positive correlation to TOC content within the sediment. Therefore these two studies disagree on the influence that productivity has on the distribution of this species.

The other two species which have not been discussed here are *Oridorsalis tener* and *Melonis barleeanum*, which represent a lower proportion of the total abundance than the other dominant species. However as part of the Principal Component Analysis (PCA) assemblages their distribution appears to be more important as indicators of AABW circulation and high productivity respectively. This can be seen in core KC064 which records a maximum in the abundance of *M. barleeanum* at approximately 5.2ka which may indicate a period of high productivity as observed in the absolute abundance records (see section 6.1.). These species will be discussed in more detail in the PCA analysis (section 6.3.).

The relative abundance records for KC099 and TC036 do not record the glacial-interglacial transition and there appears to be little faunal variation within the Holocene section of the cores. However the species *N. iridea* does show a marked decrease up through the Holocene section possibly representing the retreating influence of a cooler water mass as the climate continues to warm.

6.3. Benthic Foraminiferal Species Diversity

The species diversity (α) and evenness of the distribution of the species H(S) were only measured for samples representing the deglaciation and Holocene period, as foraminiferal abundance was too low during the glacial to be included in the analysis. Cores TC077 and TC078 were not included, due to a very low foraminiferal abundance throughout the whole glacial-interglacial cycle.

In KC097 there is little change in H(S) which remains relatively low throughout the top 50cm of the core. However α shows some variation with increased species diversity corresponding to the productivity maxima identified in the absolute abundance records (Fig.5.1). The start of the period of increased diversity is hard to constrain due to a lack of core dates below 30cm, but diversity only starts to decrease after approximately 5.5ka.

The species diversity in GC062 shows some subtle changes superimposed on the general trend of increasing diversity up through the Holocene. At approximately 55cm (11.3ka) diversity starts to increase, possibly after the initiation of a meltwater event (see isotope results) at the end of the glacial period. This is followed by a small decrease in diversity at 50cm (10.5ka) which may represent a return to colder conditions for a short period of time. These changes are also observed in the planktonic $\delta^{18}O$ record at the same level in the core (Fig.5.12) and will be discussed in section 6.6. There is some evidence in the relative abundance record for a meltwater event and the Antarctic Cold Reversal (ACR) as indicated by an increase in the cooler-water species *N. iridea*, accompanied by a decrease in the abundance of the other species. However the changes in abundance are so small that these variations in the general recovery trend might be just "noise" in the record.

At around this time many parts of the World Ocean experienced an interruption in the climatic warming after the glacial period had ended. In the northern hemisphere this reversal to cooler conditions between 11,000 and 10,000 years is called the Younger Dryas (YD) (Dansgaard *et al.*, 1989; Alley *et al.*, 1993) and there is evidence for a similar event in the

southern hemisphere. Labracherie *et al.* (1989) studied the deglacial records of three cores from the Indian sector of the Southern Ocean and showed that a major cool "oscillation" interrupted the warming phase between 12,000 and 11,000 years, which may have preceded the northern hemisphere YD by as much as 1,000 years. However it has been noted that the glacial-interglacial warming in Antarctica occurred in two steps interrupted by a slightly colder period, and does not show such a strong signal as the YD (Jouzel *et al.*, 1987a, 1992, 1995; Jansen and Veum, 1990; Blunier *et al.*, 1997, 1998). This ACR was noted at approximately 11ka in a study by Weaver *et al.* (1998) of planktonic foraminifera in cores from the SW Pacific. Shimmield *et al.* (1994) also documented a synchronous cooling event in the Atlantic sector of the Southern Ocean and the Weddell Sea as indicated by a decrease in excess barium, lower $CaCO_3$ and higher planktonic $\delta^{18}O$, and suggested that it represented a period of expanding sea-ice extent and lower palaeoproductivity. However it should be noted that the sampling and dating resolution in this study might not be high enough to adequately identify such a short-lived event and there is no significant evidence of such an event in the absolute abundance records of benthic foraminifera. The H(S) record for GC062 does not seem to show any significant variation and remains relatively low throughout the Holocene.

In KC064 a general trend of increasing species diversity and evenness of the distribution of species can be seen up through the Holocene. This implies that the benthic foraminiferal assemblage is becoming more variable as the climate improves following the transition from the last glacial period, as has been previously proposed from the abundance records. This is also seen in the record of the number of species in each sample which increases significantly in the post-glacial samples in all five cores.

Core TC036 shows a marked decrease in H(S) at 60cm which represents a change to an assemblage dominated by only a few species, and a general decrease in species diversity. This corresponds to a decrease in the planktonic $\delta^{18}O$ at this level in the core (Fig.5.36) but the reason for these mid-Holocene changes is not known.

There are no significant changes in species diversity or evenness in core KC099.

The literature contains no comparable studies of species diversity from the Scotia Sea or other parts of the Southern Ocean, so foraminiferal species diversity can only be compared to results from other oceans. Murray (1991) has summarised diversity data for living assemblages from a number of microhabitat settings within the World Ocean. Considering that the cores from this study are located in a slope (bathyal) setting, it would appear that the

values for H(S) and α measured from the Scotia Sea and Falkland Trough fall at the lower end of the range for this marine setting. Murray (1991) suggests that α values lower than 5 may indicate a normal marine environment but with a high dominance of a single species, and this is probably the reason for low species diversity in this area with a dominance of *E. weddellensis*.

The effects of calcium carbonate dissolution and diagenesis within the sediment, leading to a lack of foraminiferal test preservation during the glacial period and through the deglaciation, should also be considered as an explanation for the diversity record observed (see section 6.5).

6.4. Planktonic Foraminifera

Planktonic foraminifera are one of the major groups of calcareous zooplankton in the Scotia Sea and can be related to different water masses within the region (Chen, 1966). In this study the dominant foraminifer to the south of the PF in the Antarctic Zone is *Neogloboquadrina pachyderma* (sinistral). This polar species is found in all samples through the glacial-interglacial cycle indicating the influence of a cold water mass at all times in this area. Within the glacial samples and through the deglaciation *N. pachyderma* (s) is the sole persistent species with only sporadic appearances of some additional subpolar species but in low abundance. The more temperate species do not appear until later around 12ka (GC062) and 9.7ka (KC064), and also in KC097 and then remain persistent throughout the Holocene. It can be seen that this occurs earlier in the core from north of the PF. Cores KC099 and TC036 show a mixed temperate and polar assemblage throughout the Holocene section.

In a study by Blair (1965) of core top samples from the Drake Passage and the South Pacific sector of the Southern Ocean, he identified three faunal groups which can be used to separate the species in this study into Antarctic, cold temperate and temperate groups:

1) Antarctic – *N. pachyderma* (s)

2) Cold temperate – *G. quinqueloba*, *G. glutinata* and *G. uvula* (randomly distributed in sediments on both sides of the PF)

3) Temperate – *G. bulloides*, *G. inflata*, *G. truncatulinoides* and *G. crassaformis* (increase in abundance northward from the PF).

These groups could also correspond to the Antarctic, Transition and Subantarctic Zones recognised by Chen and Bé (1965) in the Drake Passage. However there are some differences

to the foraminiferal zones described by Bé (1968, 1977) from waters south of 35°S and from the World Ocean respectively, which are summarised below:

1) Subtropical – *G. crassaformis*
2) Subtropical/Transition – *G. truncatulinoides* and *G. glutinata*
3) Transition – *G. inflata*
4) Subantarctic – *G. quinqueloba*, *G. uvula* and *G. bulloides*
5) Antarctic – *N. pachyderma*

Chen (1966) also associated some of these species with certain water mass characteristics including *N. pachyderma* (s) (max. T layer south of PF), *G. quinqueloba* (AASW), *G. uvula* (northward movement of bottom water, south of the PF abundance increases with depth), *G. bulloides* and *G. inflata* (SASW) and *G. truncatulinoides* (AAIW). More recent studies which show evidence of similar faunal associations include Williams (1976), Williams *et al.* (1985), Pujol and Bourrouilh (1991), Howard and Prell (1992), Niebler and Gersonde (1998) and Weaver *et al.* (1998). Blair (1965) also noted that cores raised from north of the PF show an alternation of warmer intervals containing an abundance of temperate water species and colder intervals dominated by the Antarctic fauna which could be related to glacial and interglacial periods . The warmer intervals appeared to be shorter with a high $CaCO_3$ content, and the colder intervals are longer with only small amounts of $CaCO_3$.

The presence of a dominantly Antarctic planktonic foraminiferal assemblage with low abundance of only cold temperate species during the glacial interval and during the deglaciation in the Scotia Sea may be explained by the northward movement of the PF during this time and the expansion of cold polar waters and sea-ice cover. Howard and Prell (1992) noted that faunas dominated by polar species have been found equatorward of 46°S in the Southern Indian Ocean during glacial intervals. The southward movement of the PF at the start of the Holocene then coincides with the appearance of the temperate and warmer water species. Therefore it would appear that the distribution of planktonic foraminifera is largely controlled by the mean position of the PF in the Scotia Sea. The cores to the north of the PF seem to contain a more diverse planktonic assemblage, possibly supported by the increased influence of warmer, more productive waters.

One important point to note about planktonic foraminiferal faunal studies is the choice of sieve mesh size used to retain the foraminifera during processing. A number of studies only sieve at 125 μm or greater which does not retain some of the smaller species such as *G. uvula* and *G. quinqueloba*. These have been found to be important constituents of the planktonic

foraminiferal assemblage of the Scotia Sea in this study, but have not always been recorded in other studies from the region.

6.5. Calcium Carbonate Dissolution

Calcium carbonate dissolution selectively alters the planktonic foraminiferal assemblage and causes test fragmentation and increased number of benthic foraminifera. Intense periods of $CaCO_3$ dissolution are associated with glacial intervals (Williams and Keany, 1978), and may reflect an increase in AABW activity as well as changes in surface-water mass positions. However, in contrast to the equatorial Pacific, Olausson (1965) showed that interglacials can be assigned to high-carbonate stages and glacials to low-carbonate stages in the Atlantic Ocean.

The results from this study show a high percent of $CaCO_3$ within the sediment accompanied by a high percent of planktonic foraminifera during the Holocene period. There is a sharp decrease in both parameters during the transition and into the glacial interval with increasing percent of benthic foraminifera in stage 2. According to Berger (1973b), calcareous benthic foraminifera are approximately three times more resistant to dissolution than planktonic foraminifera. This would suggest that $CaCO_3$ dissolution was much more pronounced during the glacial interval in the Scotia Sea than during the Holocene. This is also supported by evidence from increased test fragmentation and coarser grain size (Pudsey and Howe, 1998) during the glacial stage. Increased fragmentation of planktonic foraminiferal tests produces more fine size fraction material which is more easily removed by winnowing. Therefore an increase in the percent of coarse grains may indicate a period of increased dissolution. An increased abundance of calcareous nannofossils in KC097 to the north of the PF and during the Holocene interval within this core would also indicate an increase in dissolution to the south of the PF and during the glacial stage within the Scotia Sea.

In a study by Hays *et al.* (1976) of the Atlantic and Western Indian Ocean sectors of the Southern Ocean at 18ka, they found that $CaCO_3$ was lower than today and that the degree of change of $CaCO_3$ content from 18ka to today was not related to water depth at the core site. They suggested that the pattern observed may instead be related to changes in surface-water characteristics between today and 18ka. They also noted that the cores which showed the maximum change in $CaCO_3$ content between today and 18ka were raised from under subantarctic waters, and this could be explained by a glacial northward shift of the PF (by

approximately 7° latitude). This can be seen in the cores from north of the PF in this study which show much higher $CaCO_3$ content and also show the greatest difference between the glacial and today. In the present day Scotia Sea there is a concentration of calcareous benthic and planktonic foraminifera to the north where the CCD is deeper and the water is saturated with respect to $CaCO_3$. However to the south the CCD shallows and dissolution of calcareous foraminifera is greater in a $CaCO_3$ under-saturated water mass (Echols, 1971). Therefore in this study the increased $CaCO_3$ dissolution may also be explained by a similar northward migration of the PF and expansion of carbonate aggressive bottom water during the glacial interval. Hays *et al.* (1976) also suggested that the CCD may have been steeper over a latitudinal range of 35° to 55°S in the eastern South Atlantic at the LGM compared with today. This would imply a southward increase in the thickness of the bottom water at 18 ka which may have caused significantly greater erosion of calcareous foraminifera and reduced the area of $CaCO_3$ deposition in the Antarctic. Herguera (1994) pointed out however, that although increased dissolution of planktonic foraminifera below the CCD would result in increased abundance of benthic foraminifera, this enrichment might be compensated by the lower sediment accumulation rates at depths below the CCD. This may lead to a possible trend of conservative behaviour of benthic foraminifera accumulation at depths below the CCD.

However due to the location of the cores in this study close to the PF and the control that the PF exerts on the underlying sediments (Goodell, 1973), it is difficult to separate the dissolution effects from productivity changes induced by migrations of the PF (Williams and Keany, 1978; Williams *et al.*, 1985; Howard and Prell, 1994). To the south of the PF the sediments are dominated by siliceous material with very few benthic or planktonic foraminifera. The fluctuations of the PF may affect all of the dissolution indices used in this study by decreasing the input of foraminifera from surface waters during the glacial stage.

6.6 Stable Isotopes

- **Benthic foraminiferal $\delta^{13}C$**

In most of the World Ocean a correlation is found between $\delta^{13}C_{\Sigma CO2}$ values and nutrient contents of the deep and bottom water masses. These parameters are controlled by the interaction of biological uptake at the sea surface and decomposition in the deeper water with the general ocean circulation (Kroopnick, 1980, 1985), and are therefore used as a proxy for

the reconstruction of deep ocean palaeocirculation (Duplessy *et al.*, 1984; Curry *et al.*, 1988; Oppo *et al.*, 1990; Raymo *et al.*, 1990; Boyle, 1992; Sarnthein *et al.*, 1994; Mackensen and Bickert, 1999). The deep South Atlantic is an ideal location to observe changes in the depth distribution of deep water properties, because it contains the mixing zone between NADW and a southern-component deep-water mass (Reid, 1996, Mackensen and Bickert, 1999). Although it may not seem to be the most direct approach, the advantage of studying the record of North Atlantic thermohaline instability in the Southern Ocean is that it reveals the clearest indication of global scale thermohaline effects (Ninnemann *et al.*, 1999). However the amplitude of $\delta^{13}C$ fluctuations is larger than would be expected from water mass mixing only, and other influences on benthic foraminiferal $\delta^{13}C$ such as global changes in the $\delta^{13}C$ of $\sum CO_2$ of seawater due to changes in the oceanic carbon reservoir (Curry *et al.*, 1988; Duplessy *et al.*, 1988), and changing intensity of surface productivity (Mackensen *et al.*, 1993b) have been suggested.

The $\delta^{13}C$ record of *O. tener* in KC097, GC062 and KC064 (Fig.6.2) shows an increase up through the core of between -0.7 and -0.8 ‰, but there are no data from the glacial period. Isotope results have only been obtained from the end of the deglaciation and into the interglacial stage. However based on other studies from the Southern Ocean the mean glacial-interglacial $\delta^{13}C$ amplitude from this area was calculated as -0.81 ‰ (Curry *et al.*, 1988) or 0.99 ‰ (Mackensen *et al.*, 1995). The largest glacial-interglacial $\delta^{13}C$ amplitude observed to date is about 1.1 ‰ from the $\delta^{13}C$ record of *Cibicidoides* spp. in the South Atlantic sector of the Southern Ocean (Mackensen *et al.*, 1994). The global mean increase in the $\delta^{13}C$ of the ocean at the end of the deglaciation is inferred as being between -0.32 ‰ (Duplessy *et al.*, 1988) and a maximum of -0.46 ‰ (Curry *et al.*, 1988). The Southern Ocean amplitude is therefore greater than from any other ocean and represents the lowest $\delta^{13}C$ in the glacial ocean (Curry *et al.*, 1988). However this large glacial-interglacial amplitude may have been influenced by a northward migration of the PF and the associated high productivity belt, with the possible effect of changing foraminiferal assemblage and primary productivity on the $\delta^{13}C$ record (Hays *et al.*, 1976; Defelice and Wise, 1981).

The results from this study would seem to fall into the accepted range for the Southern Ocean and hence $\delta^{13}C$ values were probably only slightly lighter during the glacial period than the lowest value recorded in these core sections. The increasing $\delta^{13}C$ after the deglaciation and through the Holocene is likely to represent the reinitiation of a strong NADW production and flux into the Southern Ocean resulting in better ventilation of the deep water (Curry and

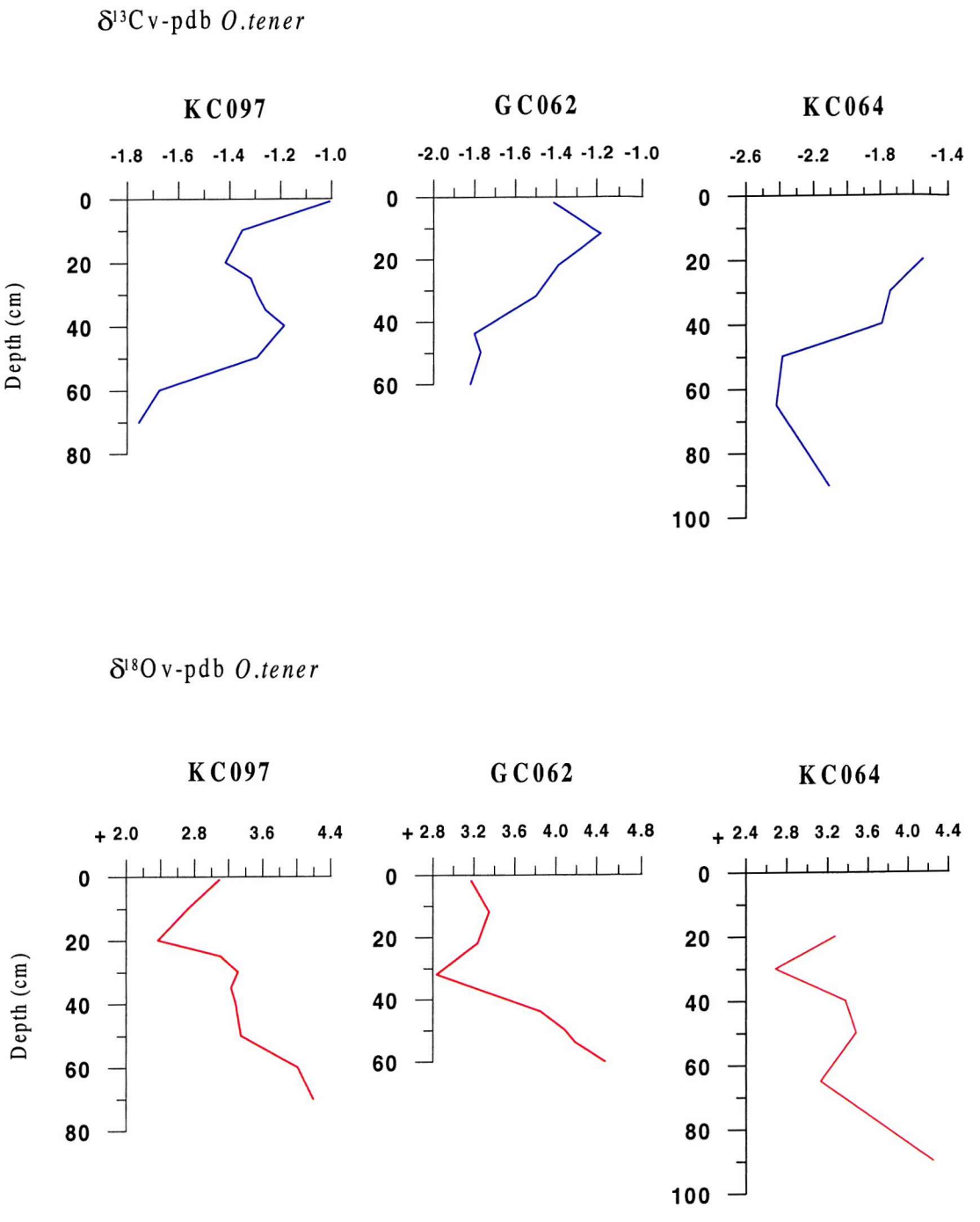

Figure 6.2. Summary diagram of benthic $\delta^{13}C$ and $\delta^{18}O$ compared between cores.

Lohmann, 1982; Labeyrie *et al.*, 1987; Oppo *et al.*, 1990; Schmiedl and Mackensen, 1997). North Atlantic Deep Water has a high $\delta^{13}C$ because it contains a large amount of upper ocean water which has been enriched in $\delta^{13}C$ as a result of isotopic fractionation by marine plants prior to deep-water formation (Oppo and Fairbanks, 1987). This is supported by the micropalaeontological evidence from this study which shows an increase in benthic foraminiferal NADW indicator species at this time. This "turn on" of NADW at the start of the interglacial is thought to have occurred abruptly with the transition from low to high $\delta^{13}C$ values lasting only about 400 years (Charles and Fairbanks, 1992). If little or no NADW entered the Southern Ocean during the LGM, indicated by low benthic $\delta^{13}C$ values, the relative contribution of a southern-source deep-water mass in the deep Atlantic Ocean would have been much greater than today (Oppo and Fairbanks, 1987; Curry *et al.*, 1988; Duplessy *et al.*, 1988; Raymo *et al.*, 1990; Sarnthein *et al.*, 1994; Curry, 1996; Raymo *et al.*, 1997). This is in agreement with results from Cd data (Boyle and Keigwin, 1982, 1985), the distribution of benthic foraminifera (Streeter and Shackleton, 1979; Caralp, 1987) and the changes in the CCD (Gardner and Hays, 1976). Curry and Lohmann (1982) suggest a lower benthic $\delta^{13}C$ difference between the Pacific and Atlantic Ocean basins during the LGM, indicating that the North Atlantic was not the primary source of deep-water formation at this time. However other studies based on different proxies do not agree with the suggestion that Southern Ocean benthic $\delta^{13}C$ provides an accurate reflection of global scale changes in thermohaline circulation through the glacial-interglacial cycle (e.g. Boyle, 1992; Yu *et al.*, 1996). Yu *et al.* (1996) used radiochemical tracers in the Atlantic Ocean to suggest that Glacial North Atlantic Intermediate Water (GNAIW) export during the LGM was at least as great as NADW export today.

However it is unlikely that the whole glacial-interglacial amplitude is accounted for by a glacial reduction of NADW. This amplitude can be partly explained by global changes in the isotopic composition of the ΣCO_2 in the ocean, which is dependent on the amount of ^{13}C-depleted organic carbon stored in the terrestrial biomass (Shackleton, 1977). An increased $\delta^{13}C$ value in the Holocene samples of the cores from this study may also be a function of an increase in global primary productivity and changes in nutrient distributions during this time. This productivity signal is also found to overprint the planktonic foraminiferal $\delta^{13}C$ records.

In core KC097 there is a pronounced decrease in $\delta^{13}C$ to lighter values at approximately 5ka which corresponds to an increase in benthic foraminiferal absolute abundance. This period of $\delta^{13}C$ depletion may be related to an episode of strong seasonal surface ocean productivity

with rapidly deposited organic matter resulting in the development of a phytodetritus layer at the seafloor. High amounts of isotopically light CO_2 would be released into the phytodetritus layer during respiration and would alter the composition of the $\delta^{13}C_{\Sigma CO2}$ and ultimately the $\delta^{13}C$ of *O. tener* as it calcifies within this low $\delta^{13}C$ epifaunal habitat (Mackensen *et al.*, 1994). This low $\delta^{13}C$ is supported by the faunal data which shows an increase in the phytodetritus exploiting species at this time (see PRIMER results, section 6.9).

- **Planktonic foraminiferal $\delta^{13}C$**

The most widely used indicator of surface ocean productivity is the carbon isotope ratio of planktonic foraminifera. Within the oceans this ratio provides clues to carbon cycle variability as the $\delta^{13}C$ content of surface water ΣCO_2 is a function of mean ocean nutrient levels, surface productivity and air-sea CO_2 exchange (Broecker and Peng, 1982).

The increased supply of nutrients and remineralised organic material from upwelling has the effect of lowering surface $\delta^{13}C$. The glacial-Holocene difference in planktonic $\delta^{13}C$ has been calculated as 1.2 ‰ in the South Atlantic and would appear to be much greater than in any other ocean (Ninnemann and Charles, 1997). In this study however, the amplitude only varies between 0.5-0.75 ‰ and LGM values were not obtained. A number of authors interpret the low glacial planktonic $\delta^{13}C$ values in the Southern Ocean as a nutrient enrichment in surface waters (Charles and Fairbanks, 1990; Charles *et al.*, 1996; Ninnemann and Charles, 1997). A reduction in nutrient-depleted NADW flux into the Southern Ocean during glacials (supported by benthic foraminiferal $\delta^{13}C$ data) and increased influence of nutrient-rich southern-source bottom water may explain the surface water nutrient enrichment (Charles and Fairbanks, 1990). Higher glacial nutrient concentrations subsequently fell as productivity increased at the end of the glacial period (Mortlock *et al.*, 1991). During interglacials NADW, high in $\delta^{13}C$ and nutrient-depleted, influences CDW as it enters the Southern Ocean (Weyl, 1968; Jacobs *et al.*, 1985; Broecker and Peng, 1989) and is then transmitted to the surface via upwelling at the Antarctic Divergence (Hodell *et al.*, 2000). Some conflicting evidence has been observed from Cd/Ca and Ba/Ca ratios of benthic foraminifera which suggests that nutrient concentrations of CDW remained close to the modern level during the LGM (Lea, 1995; Boyle and Rosenthal, 1996). However as Mackensen *et al.* (1993b) have suggested, other influences such as surface productivity can lower the $\delta^{13}C$ without necessarily indicating a mean Southern Ocean increase in nutrient content (see Mulitza *et al.*, 1999 for review of other possible explanations).

During times of increased productivity as is observed in the Holocene, photosynthesis occurs in the surface water and preferentially uses ^{12}C leaving the waters enriched in ^{13}C, and planktonic foraminifera calcify their tests under these conditions. During glacial times the sea-ice extent inhibits primary productivity due to lack of light resulting in a reduced consumption of nutrients and hence lower ^{13}C values (Mix and Fairbanks, 1985; Grobe *et al.*, 1990). This can be seen in core KC097 which shows a low $\delta^{13}C$ value for most of the bottom section of the core representing low productivity during the glacial period. Core GC062 shows some variation in the general increasing trend of $\delta^{13}C$ up through the Holocene which may be related to global or local climate events within the Southern Ocean. Heavy $\delta^{13}C$ values occur at approximately 10.5ka in response to a meltwater event identified in the planktonic $\delta^{18}O$ record. Lighter $\delta^{13}C$ values occur after about 10.5ka directly following a peak in $\delta^{18}O$ which may correspond to an Antarctic Cooling event (see discussion on oxygen isotopes). It seems unclear why the planktonic isotope records for KC097 and GC062 are so different when they are located very close to each other in the Falkland Trough. KC097 does not seem to have recorded any of the detail identified in the deglacial section of GC062 (Fig.6.3). One possible explanation for this may be due to a high occurrence of bioturbation in KC097 which would disturb the sediment record.

In the Southern Ocean however, $^{13}C_{\Sigma CO2}$ is not only influenced by nutrient concentration and productivity, and if there is sufficient time for isotopic equilibration to occur, air-sea exchange of CO_2 leaves surface waters enriched in ^{13}C (Charles and Fairbanks, 1990). There is a latitudinal gradient in ^{13}C north of the PF because subtropical waters have residence times long enough to allow isotopic equilibrium with the atmosphere. In subantarctic waters, even with lower residence times, persistently high exchange rates near the PF (Liss and Merlivat, 1986) allow partial equilibration with the atmosphere. South of the PF there is a decrease influence of air-sea exchange probably because the residence time of the water is too short and possibly because seasonal ice cover prevents significant gas exchange, particularly during glacial periods (Charles and Fairbanks, 1990). If this is the case then the suggestion of increased Southern Ocean productivity and a subsequent sink for CO_2 during times of extended polar ice is not supported. Reduced glacial productivity and less efficient utilisation of nutrients during the last ice age would indicate that the biological pump did not operate as efficiently and so did not allow increased CO_2 drawdown in the Southern Ocean (Grobe, 1986; Mackensen *et al.*, 1989; Mortlock *et al.*, 1991; Kumar *et al.*, 1993; Shemesh *et al.*, 1993; Singer and Shemesh, 1995).

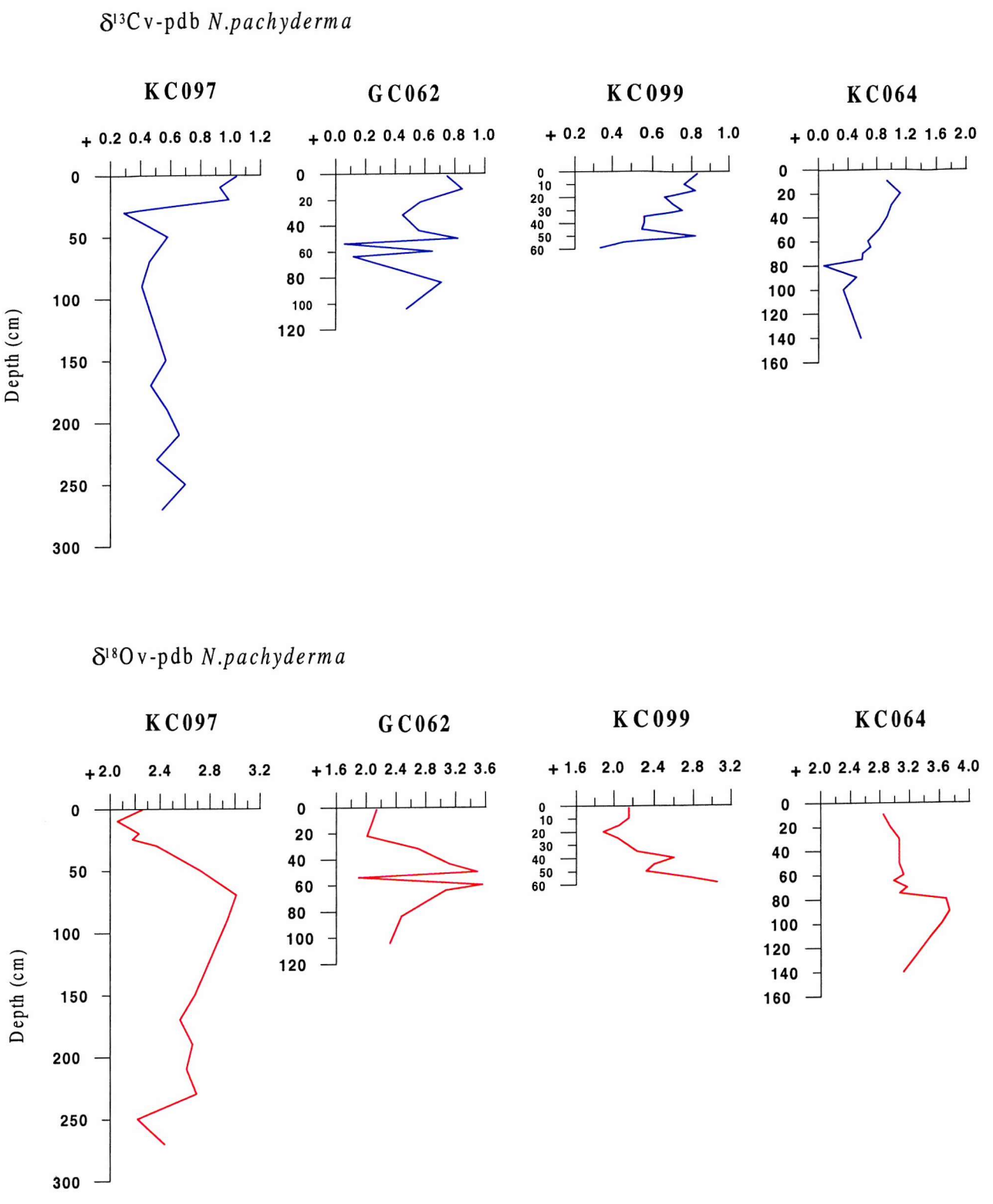

Figure 6.3. Summary diagram of planktonic $\delta^{13}C$ and $\delta^{18}O$ compared between cores.

The degree of similarity between the $\delta^{13}C$ records of planktonic and benthic foraminifera at high latitudes can be used as an indicator of the presence of deep-water sources through the glacial-interglacial cycle (Duplessy *et al.*, 1988). Only in regions of deep-water formation are surface and deep waters closely linked. Convection is so strong in these areas during times of surface water sinking that the water column is homogenous from the surface to the seabed (Lazier, 1973). The cores from this study show a general correspondence between the planktonic and benthic $\delta^{13}C$ records with lower $\delta^{13}C$ values towards the bottom of the core and increasing within the Holocene. Although there are no benthic $\delta^{13}C$ data from the glacial period, the glacial-interglacial amplitude calculated is within the accepted value for the Southern Ocean and hence it can be assumed that the glacial $\delta^{13}C$ would be only slightly lighter than the lowest value observed, which is recorded in the planktonic foraminifera. Therefore it can be suggested that convection between surface and deep water has occurred throughout the glacial-interglacial cycle and that formation of AABW has been a permanent feature through this climatic cycle as deduced by Duplessy *et al.* (1988) and Grobe *et al.* (1990) in the South Atlantic and at the Antarctic continental margin. Production of AABW during glacial and interglacial intervals therefore contrasts with NADW production, which suggests that there is no direct link between the circulation of these two deep water masses and changes in oceanographic conditions in the Southern Ocean had little effect on AABW formation. However the contribution of different source locations for deep-water production may have changed during the glacial period (Corliss *et al.*, 1986). It can also be concluded that the covariance of the magnitude and timing of the $\delta^{13}C$ shift over the last deglaciation indicates that the core sites were influenced by the same water mass, and any random deviations in the record are probably as a result of microhabitat changes or localised organic flux to the seafloor (Mackensen *et al.*, 1993b; Ninnemann *et al.*, 1997).

- **Benthic foraminiferal $\delta^{18}O$**

The $\delta^{18}O$ variations measured in foraminiferal tests are a function of two major influences, the global variations in the isotopic composition of the oceans due to changes in the whole ocean ice volume, and the fractionation between calcium carbonate and water during the shell crystallisation which strongly depends on the sea water temperature (Bard *et al.*, 1990). Oxygen isotopic data of deep-sea benthic foraminifera have been used mostly to infer bottom-water temperature fluctuations.

The Southern Ocean $\delta^{18}O$ glacial-interglacial amplitude has been calculated as 1.52 ‰ with increased values during interglacials, compared to a mean ocean (Pacific, Atlantic, Indian and Southern Oceans) value of 1.47 ‰ (Curry *et al.*, 1988). In other studies from the Southern Ocean the glacial-interglacial difference is estimated to be as high as 1.5 – 2.0 ‰ in the Atlantic sector (Schmiedl and Mackensen, 1997) and 1.6 – 1.7 ‰ in the Indian sector (Labracherie *et al.*, 1989). Mackensen *et al.* (1989) recorded a glacial-interglacial $\delta^{18}O$ range of 1.2 ‰ from the Weddell Sea during the Brunhes and late Matuyama chrons, which is well within the values of 1.1 – 1.6 ‰ proposed for the global "ice volume effect" (Duplessy *et al.*, 1981; Labeyrie *et al.*, 1987). In this study the value ranges from 1.3 – 1.8 ‰ but again there is no value for the LGM only the deglaciation and up through the Holocene. However the values do seem to compare well with previous studies from the same area, and it is unlikely that the glacial $\delta^{18}O$ would be much heavier than the lowest value recorded. The heavy glacial $\delta^{18}O$ values reflect the lower temperature of CDW, which was a more important influence relative to NADW in the Southern Ocean at the LGM. Therefore an increase in benthic $\delta^{18}O$ up through the core may be explained by a warming of the deep-water at the core sites during deglaciation with the reinitiation of warm NADW (Labeyrie *et al.*, 1987), but this may only account for a small amount of the amplitude. More importantly the results reflect the effect of global changes in the mean ocean ice volume on the benthic foraminiferal $\delta^{18}O$ signal.

The benthic $\delta^{18}O$ and $\delta^{13}C$ records can therefore be used as an indicator of the influence of NADW on Southern Ocean climate through the glacial-interglacial cycle.

- **Planktonic foraminiferal $\delta^{18}O$**

The present day Southern Ocean shows a 0.4 ‰ negative gradient in the surface water isotopic ratio from north to south through the PF. Subtropical water is enriched in ^{18}O by evaporation (+ 0.2 ‰ relative to standard mean ocean water, SMOW), and AASW is depleted by excess precipitation (- 0.2‰) (Duplessy, 1970; Labeyrie *et al.*, 1986). This is observed on a more extensive scale as a 3 ‰ increase in the $\delta^{18}O$ of *N. pachyderma* from 41 to 60°S, which represents nearly half of the predicted pole-to-equator gradient in $\delta^{18}O_{calcite}$. Highest values are recorded in core tops from the PF where gas exchange rates are highest (Charles and Fairbanks, 1990). Planktonic foraminiferal $\delta^{18}O$ is used primarily to define the rapid changes in surface ocean sea surface temperature (SST) (Labeyrie *et al.*, 1996), but also

reflects changes in the global ice volume. It has been estimated that a 1 ‰ change in $\delta^{18}O$ corresponds to an apparent change in temperature of 5°C (taking into account salinity-related effects) (Wefer *et al.*, 1999).

Charles and Fairbanks (1990) observed that glacial $\delta^{18}O$ values were increased by 1.3 ‰ relative to core top samples from the Atlantic sector of the Southern Ocean, and noted that this amplitude was of the same magnitude as estimates of the glacial-interglacial ice volume effect (Mix, 1987; Duplessy *et al.*, 1981; Labeyrie *et al.*, 1987). They concluded that there was little change in the thermal gradient of surface waters from 41 to 53°S. The glacial-interglacial amplitude in this study ranges from 0.6 to 1.5 ‰ with the largest change occurring in GC062 between about 12ka at the end of the glacial period and the Holocene. The difference in $\delta^{18}O$ between the LGM and the Holocene is only 0.35 ‰ in GC062.

In cores KC064 and GC062 a shift to lighter $\delta^{18}O$ values indicating a warming of the surface waters does not appear to start until after 12ka at the end of the glacial period, and the core to the north of the PF (GC062) was first to warm. In GC062 this was immediately followed by a $\delta^{18}O$ isotopically light peak at about 11.3ka with an amplitude change of 1.6 ‰. This light $\delta^{18}O$ at the start of the interglacial period may represent a meltwater event as identified in other studies from the Southern Ocean (Labeyrie *et al.*, 1986; Bard *et al.*, 1990; Grobe *et al.*, 1990). A similar event has also possibly been identified in KC064 but at the later time of about 9.7ka. The formation and melting of glacial ice has an important influence on the variations of planktonic foraminiferal $\delta^{18}O$ (Shackleton and Opdyke, 1973). During the destruction of large parts of the Antarctic ice shelves during post-glacial sea-level rise, there was a significant contribution of isotopically light water from the melting ice (Weiss *et al.*, 1979) and this may have influenced the composition of the surface water. In GC062 this meltwater event is followed by a rapid change to heavy $\delta^{18}O$ values beginning any time after 11.3ka and centred at about 10.5ka, indicating a period of cooling of the surface ocean. This may be explained by the onset of an event termed the Antarctic Cold Reversal which was thought to have been a localised cooling event in the Southern Ocean starting between 12 and 11.5 ka and lasting to about 10.5ka (Labracherie *et al.*, 1989). This event has also been identified in Antarctic ice core records (Dome C and Vostok) at the same time interval (Jouzel *et al.*, 1995; Charles *et al.*, 1996). This cooling event is then followed by a decrease to lower $\delta^{18}O$ values associated with Holocene SST. Although the cooling event has not been identified in KC064 and KC097 (or the meltwater event in KC097) the same climatic optimum with high SST as indicated by lighter $\delta^{18}O$ values, is identified during the mid-

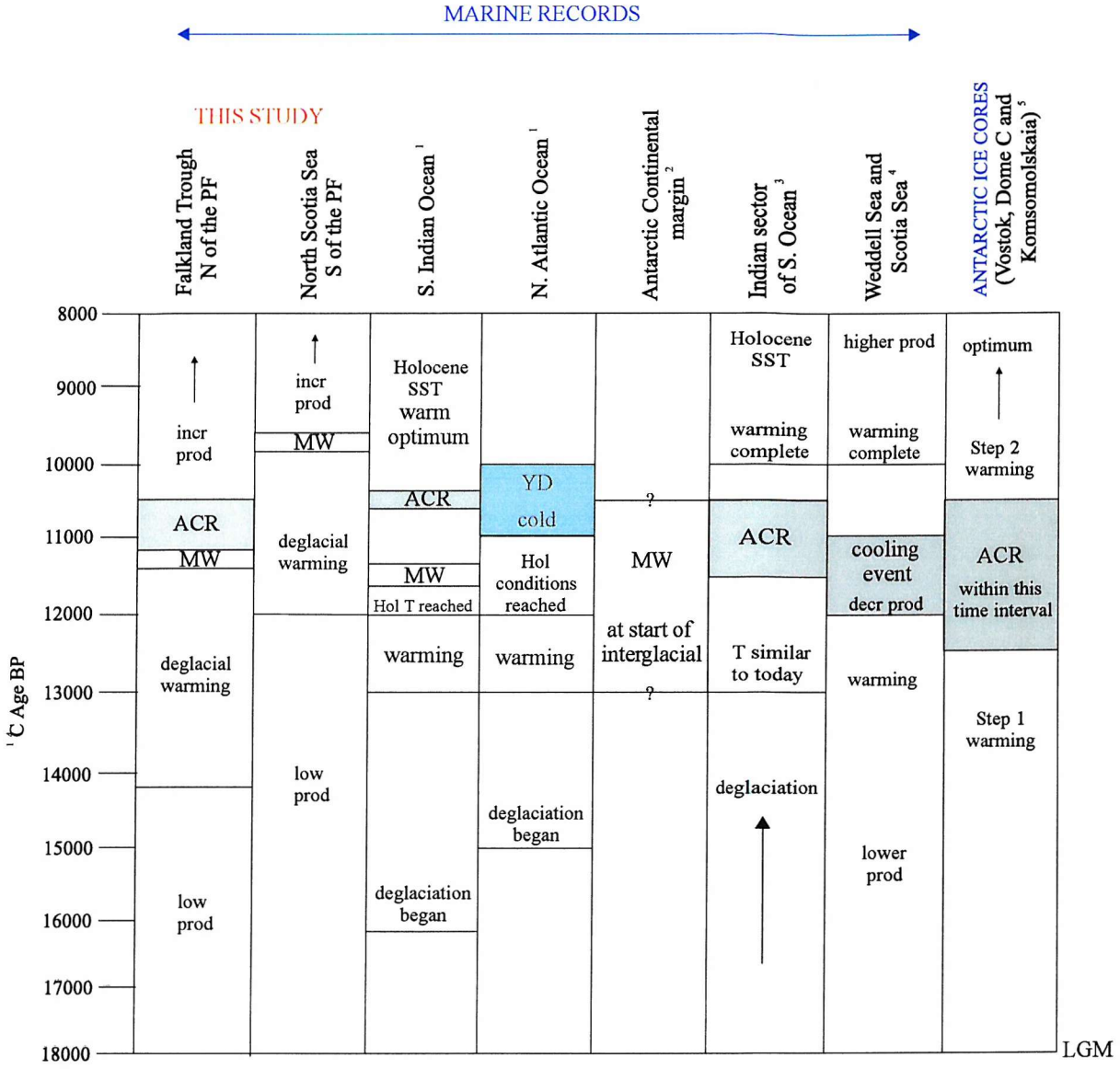

Figure 6.4. Summary of studies from Antarctica and the Southern Ocean recording the glacial-interglacial transition

MW Meltwater event ACR Antarctic Cold Reversal YD Younger Dryas cold event

References: [1]Bard *et al.* (1990); [2]Grobe *et al.* (1990); [3]Labracherie *et al.* (1989); [4]Shimmeild *et al.* (1994); [5]Blunier *et al.* (1997, 1998); Lorius *et al.* (1979); Jouzel *et al.* (1987b, 1992, 1995); Charles *et al.* (1996) and Ciais *et al.* (1992).

Holocene. A similar series of events through the deglaciation at almost identical time intervals to core GC062 is described by Bard *et al.* (1990) from a core at 55°S in the Indian sector of the Southern Ocean. Therefore these events may not be localised to the Atlantic sector but may have occurred over the whole Southern Ocean (see Fig.6.4).

The SST changes during the deglaciation calculated by Labracherie *et al.* (1989) for three cores from the Indian sector of the Southern Ocean exceeded 5-7°C due to the southward migration of the PF. Therefore the isotopic shift at the end of the glacial period may be partly attributed to a simple temperature effect as the PF starts to move south across the core sites.

However it should be considered that none of the events described above were found in all of the cores and the sampling resolution may be too low to be able to identify events of such short duration. However the low sedimentation rates in the Holocene of the Scotia Sea should also be considered.

6.7. Radiocarbon dates

Two AMS ^{14}C dates were obtained for core top material from cores KC097 and KC064, a foraminiferal carbonate and an organic carbon sample. The results from KC064 showed a large offset of some 8115 years which is most probably an indication that the bulk organic carbon date is not accurate as it is unexpectedly old. However the results from KC097 show very similar ages with the bulk organic carbon sample being determined as only 250 years older than the foraminiferal carbonate sample.

This analysis follows on from a study by Howe and Pudsey (1999) who reported an offset of 2430 years between core top samples for core TC063 in the North Scotia Sea. This was more than a thousand years greater than the offset observed between foraminiferal carbonate and organic carbon samples taken from a sediment trap at the same location, and the sediment trap organic carbon age (1480 yr) was only slightly greater than the commonly quoted Antarctic reservoir age of 1300 yr by Ingolfsson *et al.* (1998). The deployment of the sediment trap within the nepheloid layer may explain the age discrepancy of the samples as it would collect foraminifera settling from the surface, and bulk organic carbon particles resuspended and transported in the ACC, and therefore likely to be older. They concluded that there must therefore be more reworking of "old" fine-grained organic carbon than foraminifera tests during the 1000 years or more that surface sediment may spend within the bioturbated layer in this high-energy area. However the results from this study show only a

small increase in age between the foraminiferal carbonate and bulk organic carbon samples in KC097, and although this may support the evidence that there is more reworking of organic carbon than foraminiferal tests at the sediment surface, the age difference is probably too small to be conclusive.

6.8. Sedimentation and Sediment Accumulation Rates

In general the cores from the Falkland Trough and northern Scotia Sea show high sedimentation rates, probably due to a significant input of terrigenous material as suspended sediment from the Antarctic Peninsula (Pudsey and Howe, 1998). Rathburn *et al.* (1998) suggested that there was a decrease in sedimentation rate from values of 7-10 cm/kyrs in the northern Scotia Sea and Falkland Trough to 3-4 cm/kyrs near 60°S (Grunig, 1991) to as low as 0.4 cm/kyrs in the Weddell Sea.

Sedimentation rates for cores KC097, GC062, KC099 and KC064 range from 6.7 – 11.5 cm/kyrs with the highest rate being recorded in KC099 to the north of the PF. There appears to be little change in sedimentation rate through the glacial-interglacial cycle except for a small increase in the postglacial stage in KC064. Pudsey and Howe (1998) also recorded higher Holocene sedimentation rates compared to glacial values for KC064 and TC078, as well as in other cores farther south in the Scotia Sea. The higher Holocene sedimentation rates are probably a result of the increase in biological productivity in the Scotia Sea as indicated by increased foraminiferal and diatom abundance. However as Bard *et al.* (1989) reported from cores in the Indian sector of the Southern Ocean, the lower glacial sedimentation rates may also be due to increased dissolution.

The accumulation rate of benthic foraminifera tests appears to provide a good quantitative estimate of surface palaeoproductivity (Herguera and Berger, 1991; Berger and Herguera, 1992; Herguera, 1992; King *et al.*, 1998). The Benthic Foraminiferal Accumulation Rate for KC097, GC062, KC099 and KC064 therefore reflects increased productivity during the Holocene, with a productivity maximum observed in all four cores at approximately 6-7.5 ka. This supports the evidence of increased productivity at this time as observed in the planktonic and benthic absolute abundance data.

6.9. Multivariate Analysis

The results of the Principal Components Analysis (PCA) for KC097 reveal two significant faunal assemblages which can be related to different palaeoenvironmental parameters. PC1 appears to be controlled primarily by water mass influence and a productivity signal at different levels in the core. The positive end-member assemblage is dominated by *E. exigua* and is important within the top 50cm of the core (~ last 9.2ka of the Holocene, assuming constant sedimentation rate). This species show a positive correlation to well-oxygenated and highly saline NADW (Mackensen *et al.*, 1995), which would have resumed a stronger influx to the Southern Ocean during the interglacial period when the PF was south of the core site. The presence of *E. exigua* and *G. subglobosa* may also indicate that the Holocene was a period of greater availability of phytodetritus which provided a pulsed food supply for these opportunist species. In a number of studies however it has been shown that there is no consistent relationship between *E. exigua* and deep-water hydrography (Braatz and Corliss, 1987; Gooday, 1993) and a study by Smart *et al.* (1994) in the northeast Atlantic suggested that the abundance of *E. exigua* over time reflected variability of the production of phytodetritus instead. A relatively high loading of *C. crassa* in this assemblage associated with *G. subglobosa* may also suggest lower productivity in general (Fariduddin and Loubere, 1997), but perhaps instead with a pulsed supply of food to the benthos. It is uncertain what the significance is of *Bolivina* spp. in this assemblage.

The negative end-member assemblage is dominated by *F. complanata* and *M. barleeanum* and is important below 50cm down to the base of the core (glacial through to about ~9.2ka). These infaunal species are both high productivity indicators and show a positive relationship to organic-rich sediments (Mackensen *et al.*, 1985, 1993a; Berger, 1989; Asioli, 1995). *Fursenkoina* spp. has been described by Mackensen *et al.* (1993a) from the PF region of the South Atlantic as being specially adapted to a high productivity/low-oxygen environment, and by Bernhard and Sen Gupta (1999) as indicative of severely oxygen-depleted conditions. *Melonis barleeanum* has also been linked to depressed oxygen levels (Corliss, 1985) and to cooler intervals associated with *Pullenia* spp. (Corliss, 1983). Nees *et al.* (1997) also suggested that the presence of *Melonis* spp. within the sediment was an indicator of an increased organic matter flux possibly induced by a meltwater event. These species associations suggest that during the deglacial period the PF was still north of the core site and hence a high productivity assemblage developed in the area of highest bio-siliceous primary productivity, south of the PF but north of the winter sea-ice limit (similar to that described by

Mackensen *et al.*, 1993a), stimulated by the input of deglacial meltwater. The presence of species associated with a cooler water mass and lower oxygen levels may also indicate a reduced influence of NADW during the glacial stage and into the deglaciation, in favour of a colder southern-component bottom water.

Therefore it would appear that although the presence of a northern or southern component bottom water mass exerts an overall influence on the faunal assemblage, the supply of organic matter to the benthos clearly overprints this record. The open-ocean phytodetrital assemblage (positive PC1) can be distinguished from the high productivity fauna (negative PC1) as the former requires only a strong seasonal flux of organic matter rather than a higher and possibly more sustained flux necessary to support high productivity species (Gooday, 1993, 1994, 1996; Fariduddin and Loubere, 1997).

The cluster analysis results also identify a group of samples between 70-60 cm within the core which show an increase in the high productivity species identified in the PCA. These samples are grouped at a high similarity value and represent a period of increased productivity before full interglacial conditions are reached. The samples below this level are from the glacial period and are represented by low foraminiferal abundance.

The negative end-member assemblage of PC2 is dominated by *N. iridea* which is important within the sediment between 80-20 cm. This species is thought to indicate colder water and so may represent a period of influence of cooler bottom water, associated with the reduced abundance of other calcareous benthic species (Domack *et al.*, 1995). It has also been described from the Weddell Sea by Mackensen *et al.* (1990) as coinciding with the highest organic carbon levels in its live form. However in this extreme environment it may depend on high organic carbon fluxes to thrive at the seabed. It was not documented in the dead assemblage due to severe calcite dissolution in this area. Mackensen *et al.* (1988) have also described it from the Bransfield Strait and so these studies may help to substantiate a preference for colder water masses.

The positive end-member assemblage is represented by *Bolivina* spp. which is important within the top 20 cm of the core and below about 80cm. This small, thin-shelled infaunal species has been described from many oceans as an indicator of low-oxygen levels and high-TOC content (Phleger and Soutar, 1973; Lohmann, 1978; Bernhard, 1986) often from the Oxygen Minimum Zone (OMZ) (Sen Gupta, 1999). It is often grouped with other infaunal species such as *Bulimina* spp. (Sen Gupta and Machain-Castillo (1993), and Mead (1985)

described *Bulimina* spp. from the South Atlantic associated with highly productive, warm CDW. It is hard to define only one important environmental variable in this case, and it is probable that a tolerance to oxygen depletion and a preference for organic-rich sediments may be inter-changeable attributes of some hypoxia-tolerant species (Van der Zwann and Jorissen, 1991). Sen Gupta and Machain-Castillo (1993) also suggested that there is no one modern species whose mere presence in the sediment can be taken to reflect a low-oxygen bottom water or pore water. In this case PC2 may just be a reflection of the temperature of the deep water at the core site through the glacial-interglacial transition, with the influence of warmer CDW not dominating over that of AABW until well into the Holocene period. The presence of the *Bolivina* spp. assemblage below 80cm and therefore in the glacial interval is not fully understood and the species is represented only as very low loadings in the assemblage. The change in assemblage down-core may also be influenced by lower foraminiferal abundance in the lower part of the core which may affect the reliability of the PCA analysis in this section of the core.

The faunal assemblage explained by PC3 accounts for only a smaller percent of the total variance and hence it is likely that it does not reveal any significant palaeoenvironmental information. However the positive end-member assemblage is represented by *N. iridea* and *E. exigua* and the occurrence of *E. exigua* from between about 8.2-2.8 ka may indicate an increased supply of organic matter in the form of phytodetritus to the seafloor at this time.
The negative end-member assemblage is dominated by *Cibicides* spp. which is important throughout the rest of the core and particularly at the core top. *Cibicides* sp. is found to live attached to the substrate (Nyholm, 1961; Loeblich and Tappan, 1964) and is also an indicator of well-oxygenated bottom water conditions (McCorkle *et al.*, 1990). Therefore it has been suggested that this species may be an indicator of palaeocurrents (bottom-water activity) in some locations (Osterman and Kellogg, 1979). The shape of some epifaunal species such as *Cibicides* spp. and *Oridorsalis* sp. may be beneficial for attachment to the sediment during times of turbulence, or for travelling on or near the surface (Corliss, 1991). Lutze and Thiel (1987) suggested that *Cibicides wuellerstorfi* was adapted to a niche where there was a fairly steady supply of food particles obtained from bottom currents. The species *Oridorsalis umbonatus* has been described by Mackensen *et al.* (1995) from an area where lateral advection continuously "cleans" the sediment surface to maintain interstitial ventilation. Therefore this PC may represent the strength of the bottom water currents during the glacial-interglacial cycle, and indicate that phytodetritus was unable to remain on the seafloor during

times of increased current activity. The increase in current activity at the top of the core may represent the present situation in the Scotia Sea when the PF is coincident with the axis of strongest deep-water flow of the ACC (Pudsey and Howe, 1998).

In core GC062 PC1 shows a very similar faunal assemblage to PC1 in KC097. The positive end-member assemblage is dominated by *E. exigua* and *Gyroidinoides* spp. which is important from 8.5 ka to the present. Below this level the negative end-member assemblage dominated by *F. complanata* and *M. barleeanum*, is important. This shows the general change in conditions from the deglacial period dominated by a high productivity fauna with a high and sustained supply or organic carbon, through to the Holocene period influenced by increased influx of NADW into the Southern Ocean, and possible increased availability of phytodetritus at the seabed.
The cluster analysis seems to show the same record as PC1 with the core being split in half, and dominated by the colder water, high productivity species during the deglaciation, and the lower-productivity, phytodetritus exploiting, warmer water species being dominant during the Holocene.

Principal Component 2 is dominated by *O. tener* and *E. exigua* below ~10.2 ka and between 8.5-5 ka, and by *G. subglobosa* between these dates and from 5ka to the present. The distribution of these species within the core does not seem to follow any clear pattern but as this principal component represents only a low percentage of the total variance it may not reveal any significant ecological information.

There appears to be no clear relationship shown between PC3 and any environmental variable and only a small percent of the total variation is explained by this assemblage. It would appear that the influence of PC1 is completely dominant within this core.

In KC064 the negative end-member assemblage of PC1 is important throughout the top 55cm (~ last 7.5 ka). This assemblage is dominated by a number of species which are indicators of different water masses including NADW (*E. exigua* and *Gyroidinoides* spp.), CDW (*G. subglobosa* and *Uvigerina* spp.) and AABW (*N. umbonifera*) (Lohmann, 1978; Schnitker, 1980; Mackensen *et al.*, 1995). In a study by Corliss (1979b) from the southeast Indian

Ocean, he recognised an AABW benthic foraminiferal assemblage but suggested that it might be split into two groups. One of the groups represented a warmer type of AABW, where the assemblage contained the characteristic AABW indicator species (*N. umbonifera*) but also the presence of species such as *G. subglobosa*, *P. bulloides* and *O.tener*. He suggested that the presence of this warmer AABW was due to mixing of the cold bottom water mass with CDW above. The negative end-member assemblage for PC1 in this study contains the same species as identified by Corliss (1979), including NADW indicator species, and hence may suggest a period of influence of a warmer type of ABBW which has resulted from mixing with CDW and NADW in the South Atlantic. *Uvigerina* spp. is associated with CDW in the western South Atlantic (Schnitker, 1980; Lohmann, 1981), and with high-TOC in a number of oceanic settings (Mackensen *et al.*, 1995; Fariduddin and Loubere, 1997; Sen Gupta, 1999). However Streeter and Shackleton (1979) traced the occurrence of *Uvigerina* spp. throughout the whole of the Atlantic Ocean and found that although they crossed many different productivity gradients, the species followed the distribution of lowered oxygen levels instead. This species has also been described by Corliss (1979b, 1982, 1983) from the southeast Indian Ocean as indicating the presence of a glacial water mass present in the Southern Ocean that has not been described before. However this assemblage is important within the core after about 7.5 ka which would mean that it was probably not showing an association with a glacial water mass. The association of *Uvigerina* spp. with CDW and *E. exigua* with NADW would instead suggest the presence of a warmer water mass during this time perhaps supporting higher productivity.

The positive end-member assemblage is represented by *S. bulloides* and *N. iridea* and may indicate the presence of a cooler water mass, possibly with carbonate corrosive properties resulting in lower species diversity before 7.5 ka. This may represent the colder AABW as it originates in the Weddell Sea. The consistent influence of AABW at this site as the dominant bottom water mass may reflect the more southerly position of this core in the Scotia Sea. *Sphaeroidina bulloides* has been described from an OMZ in the Gulf of Mexico by Sen Gupta and Machain-Castillo (1993). There do not seem to be many descriptions of this species from deep-sea environments.

The negative end-member assemblage of PC2 is dominated by *G. subglobosa*, *O. tener* and with *Pullenia* spp. as an important associated species and is found within the core between about 9-6 ka during the Holocene. This assemblage may represent a period of increased foraminiferal diversity after the end of the glacial period due to the influence of warmer,

more productive waters over the core site. *Pullenia* spp. has been described from the eastern South Atlantic as a high productivty indicator associated with organic-rich sediments (Mackensen *et al.*, 1993a).

The positive end-member assemblage of PC2 is dominated by *Trochammina* spp. and *R. charoides* which are both agglutinated species. This assemblage is important at the end of the glacial and during the deglacial period when the core site is still being influenced by a more carbonate aggressive water mass. The presence of this assemblage at the core top and therefore in the more recent Scotia Sea may represent the present day location of the core site below the PF with possibly increased dissolution at the sediment surface. In a study by Pudsey *et al.* (1987) on the South Orkney Shelf, they identified a benthic foraminifera assemblage dominated by the agglutinated foraminifer *Miliammina arenacea* at the core tops. They inferred that the increase in relative abundance of agglutinated benthic foraminifera indicated increased dissolution at the sediment surface caused by corrosive bottom waters.

The cluster analysis also identified the assemblage between about 9-6 ka which showed an increase in species diversity over this period. This was then replaced by an increase in the number of agglutinated species towards the core top.

The record for PC3 in this core is quite "noisy" and does not seem to show any clear variation with time.

6.10. Differences to the North and South of the Polar Front

The location of the PF in the Scotia Sea at the present day and during the glacial-interglacial cycle has exerted a controlling influence on the distribution and abundance of both planktonic and benthic foraminifera.

All of the cores studied show a similar pattern of foraminiferal distribution through the glacial cycle which suggests that the deglaciation was experienced almost simultaneously over the Scotia Sea and Falkland Trough, and was not a localised effect. From studies in other sectors of the Southern Ocean it would also appear that this effect was not just basin-wide in extent but was a circumpolar event. However the main difference between core sites within the Scotia Sea is the magnitude of the change in foraminiferal abundance from the glacial to the interglacial period in relation to the position of the PF. The cores to the north of

the PF show a much greater increase in abundance at the end of the glacial period with much higher absolute abundance values (see Table 6.1).

Core	No. benthic foraminifera / g	No. planktonic foraminifera / g
KC099	3526	160583
KC097	5048	710085
GC062	2943	306260
KC064	719	19002
TC036	1580	107875
TC077	138	5713
TC078	10	275

Table 6.1. Summary of benthic and planktonic foraminiferal absolute abundance (double line = present position of the Polar Front).

The lowest abundance is found in the core farthest to the south (TC078) where there is very little carbonate within the sediment even during peak interglacials due to a dominance of bio-siliceous deposition and lower surface productivity. This suggests that carbonate production is related to the position of the PF and that foraminiferal productivity generally increases from south to north in the Scotia Sea. There is also a band of increased productivity located just south of the PF which is represented by higher benthic and planktonic foraminiferal abundance in core TC036 which is just south of the PF in the eastern Falkland Trough (see Fig.1.1). There is no significant increase in foraminiferal abundance recorded in KC064 however, which is also located just south of the PF but is over a degree of latitude further south than TC036. Core TC036 is in fact the most northerly core in this study but due to the N-S path of the PF through the North Scotia Ridge, it is still south of the PF.

The benthic foraminiferal faunal assemblage seems to be very similar in cores from north and south of the PF with a dominance of the phytodetritus exploiting species *E. weddellensis* and *E exigua* in all cores but with generally higher species diversity in the cores to the north of the PF. *Eilohedra weddellensis* does seem to occur as a higher percentage of the assemblage on average as you move south across the PF and species diversity decreases. However there is a greater relative abundance of both *N. umbonifera* and some agglutinated species in the cores to the south of the PF where the CCD is slightly shallower and the influence of the

carbonate aggressive AABW is greater. These species are more resistant to carbonate dissolution than the other calcareous foraminifera identified in this study. There is no increase seen in these species during the glacial period as may be expected during a time of expansion of polar waters, due to the restriction of surface productivity by increased ice cover. Evidence for increased dissolution of foraminiferal tests can be seen during the glacial interval and especially in the cores to the south of the PF in the form of test fragmentation and an increase in the number of benthic foraminifera compared to planktonic foraminifera.

The planktonic foraminiferal relative abundance data shows the appearance of a similar cold/temperate faunal assemblage at all core sites to the north and south of the PF but warmer/subtropical species are only observed at the core sites from north of the PF during the Holocene. Therefore it would appear that the distribution of planktonic foraminifera is largely controlled by the mean position of the PF in the Scotia Sea. The cores to the north of the PF seem to contain a more diverse planktonic assemblage, possibly supported by the increased influence of warmer, more productive waters.

The carbon and oxygen stable isotope results show a similar trend through the glacial-interglacial cycle with higher planktonic and benthic $\delta^{18}O$ in the glacial stage becoming lighter in the Holocene, and lower planktonic and benthic $\delta^{13}C$ in the glacial becoming heavier within the interglacial samples. The $\delta^{18}O$ values in the cores from north of the PF are however lower than in the cores to the south of the PF, and this increase from low to high latitudes reflects the influence of temperature on the isotopic ratio in foraminiferal carbonate. Therefore as the cores from north of the PF are influenced by warmer water masses the $\delta^{18}O$ in foraminiferal carbonate would be expected to be lower.

Productivity indicators such as the BFAR and foraminiferal absolute abundance seem to show higher levels of productivity in the cores to the north of the PF during the glacial-interglacial cycle, perhaps influenced by warmer, more productive water masses. However the band of high productivity just to the south of the PF may also have influenced this record with highest productivity values recorded in the cores between approximately 7.5-4 ka during the Holocene when the PF may have been moving southwards over the core sites (Fig.5.52). In the present day Scotia Sea there does not appear to be significantly higher productivity recorded in the two cores just to the south of the PF (some increase at the site of TC036) but they may not actually lie directly beneath this enhanced productivity zone.

Chapter Seven

SYNTHESIS

7.0. Summary of Palaeoceanography

This section will summarise the important results from this study and highlight how this has contributed new information to the subject and also how it can confirm previous studies. The use of benthic foraminifera to provide information about certain environmental parameters will also be discussed.

7.1. Surface Water Palaeoceanography

During the last glacial cycle in the Southern Ocean there was a major change in surface water conditions and this is largely due to the increased sea-ice cover during the glacial stage. At the LGM the spring sea-ice edge may have extended as far north as 55° (Pudsey and Howe, 1998) and so the winter sea-ice edge may have lain even farther north. This had the effect of limiting biogenic productivity at all the core sites in this study which all record low foraminiferal abundance during the glacial interval. During this time the PF had moved northwards at least as far as 52°S which is the most northerly core site in this study, and a subsequent expansion of polar waters occurred which then covered the study area. The PF

probably moved north in response to the influence of increased sea-ice or increased wind stress which may have expanded the polar gyre (Hays *et al.*, 1976). Towards the end of stage 2 the PF began to move polewards and the climate began to warm, with productivity starting to increase north of the PF first at approximately 14ka and then spreading south. The abundance of warmer water planktonic foraminifera began to increase at the start of the Holocene indicating that the influence of subantarctic water masses in the Scotia Sea had resumed at this time. This is also seen in the planktonic oxygen isotope record as a shift to lighter $\delta^{18}O$ values to the north of the PF at about 12ka by as much as 1.5 ‰ which may indicate a temperature increase of approximately 7.5°C. This seems to be a higher temperature change than that experienced to the south of the PF. At about the same time in the Scotia Sea there is a shift to heavier planktonic $\delta^{13}C$ values indicating an increase in productivity and subsequent decrease in nutrient levels in the surface water which continues to an optimum at about 7.5ka.

The Holocene period is represented by the deposition of foraminiferal sands in the Scotia Sea and may be a time of unusual surface water conditions when compared to other interglacial intervals. During the last interglacial stage 5e there is no record of the deposition of such sediments or at least if there was they have been removed by bottom currents (Howe and Pudsey, 1999). Therefore the Holocene in the Scotia Sea would seem to be a period of open marine, warm water conditions with uniform ACC flow (Howe *et al.*, 1997). During the last glacial stage surface waters would have been much cooler with the PF lying farther to the north and increased sea-ice cover, but surface water flow would have been unaffected as it is mainly wind-driven (Howe *et al.*, 1997). The change in surface water conditions during the deglaciation may have been quite rapid as the change from diatom-poor (low productivity) to diatom-rich (high productivity) sediments in the Scotia Sea took less than 1000 years (Pudsey and Howe, 1998), and foraminiferal abundance increased significantly within 2000 years.

7.2. Deep Water Palaeoceanography

The main change in the deep water palaeoceanography of the Scotia Sea occurred at the glacial-interglacial transition and involved the change in influence between northern and southern component deep water masses. During the glacial stage southward flux of NADW was greatly reduced due to a decrease of bottom water formation in the North Atlantic. Therefore a southern-component bottom water mass was dominant in the area during this

time and penetrated farther north than it does at present (Oppo and Fairbanks, 1987; Curry *et al.*, 1988; Duplessy *et al.*, 1988; Charles and Fairbanks, 1992). The benthic $\delta^{18}O$ record shows higher values during the glacial stage indicating a cooling of the bottom waters due to a lack of the warming influence of NADW. The bottom waters become warmer up through the glacial cycle into the Holocene as the reinitiation of NADW flux occurs. The correlation between the benthic and planktonic $\delta^{13}C$ records indicates that the formation of AABW did not cease during the glacial period but it was probably reduced. The removal of NADW flux and reduced AABW formation during the LGM may have resulted in CDW being driven only by wind (Howe and Pudsey, 1999).

The glacial transition is also marked in the palaeoflow record of bottom waters in the Scotia Sea with high energy intermittent CDW flow and increased benthic storm activity during the glacial stage being replaced by moderated bottom current activity during the Holocene (Howe and Pudsey, 1999). However during the glacial stage the PF was located farther north in the Scotia Sea and was not coincident with the axis of strongest deep ACC flow (Pudsey and Howe, 1998). Therefore the benthic foraminifera record an increase in flow at the start of the interglacial stage when productivity is enhanced below the PF at the site of strong deep ACC flow. Pudsey and Howe (1998) inferred a period of strong bottom-current flow at the end of the glacial stage from an interval of moderately well sorted silts in certain cores from the Scotia Sea, and during this time flow may have been more vigorous than before or since. This event probably pre-dated the meltwater event identified in the cores from this study. The increased flux of NADW at the start of the Holocene also promoted better ventilation of the deep water as indicated by increased benthic $\delta^{13}C$ values.

Although there should be some changes in oxygen content of the water bottom masses during the glacial transition it is difficult to use any particular benthic foraminifera to infer this property. Benthic foraminifera seem to be much more effective proxies for very low oxygen content (< 1 ml l^{-1}) but once it becomes abundant (> 1-2 ml l^{-1}) they become less useful, and even at very low oxygen levels it may not be the only limiting factor. At present there is no one species which is confined to low oxygen environments (Murray, 2001) and therefore it is difficult to confidently infer any changes in oxygen levels of the water masses through the glacial cycle. However due to a reduction of NADW flux during the glacial stage CDW would have had a lower supply of well-oxygenated water from the north.

7.3. Productivity and Phytodetritus Availability

Productivity was found to be enhanced in all cores from this study during the Holocene interval and greatly reduced during the glacial stage. The effects of continuous sea-ice cover and dissolution are probably responsible for reduced productivity south of the PF during the glacial stage when the PF occupied a more northerly position. However superimposed on this general trend are some smaller scale variations in productivity which highlight some interesting features of the glacial transition and climate recovery in the Scotia Sea.

The deglaciation is marked by the increase in some high productivity benthic foraminiferal species such as *Melonis* spp., *Fusenkoina* spp. and *Pullenia* spp. which is a response to a meltwater event at the start of the interglacial period. These species require a high and constant supply of organic carbon to the sea floor and are only dominant for a short period of time. They are replaced by an assemblage dominated by phytodetritus exploiting benthic foraminifera such as *E. weddellensis* and *E. exigua* which are dominant during the Holocene. The maximum relative abundance of these species would seem to correspond to a general productivity maximum between 7.4 and 4 ka during the mid-Holocene which may indicate a period of increased phytodetritus deposition. This would represent a period of pulsed organic carbon supply to the sea floor as opposed to the sustained supply during the deglaciation. However although these species can be used as an indicator of phytodetritus in the fossil record (Smart *et al.*, 1994) it is still not possible to quantify the amount, duration or frequency of the input (Murray, 2001). Previously similar increases in phytodetritus have only been described from northern high latitudes (Gooday, 1988, 1996; Gooday and Lambshead, 1989).

This mid-Holocene productivity maximum can be correlated to similar "climatic optimum" events in other studies from the Southern Ocean and Antarctica (Fig.6.1). The studies from east of New Zealand based on planktonic foraminifera (Weaver *et al.*, 1998) and the Kerguelen Subantarctic Islands based on pollen counts (Young and Schofield, 1973) seem to correspond very well to the results from this study, particularly as they indicate a period of subsequent cooling which has also been proposed from this study, due to decreasing foraminiferal productivity in the latest Holocene. The other studies indicate that the climatic optimum occurred later between 4 and 1 ka but this may just be a slower response to the same event, which is likely to have been a localised warming rather than a global-scale feature. Evidence from Antarctic ice core studies indicates that this mid-Holocene warming may only have resulted in a temperature increase of 1°C over the Antarctic continent (Ciais *et*

al., 1992), whereas the atmospheric temperature change measured from $\delta^{18}O$ in ice may have been as high as 6-10°C in polar regions during the whole of the last glacial cycle (Bard *et al.*, 1997).

7.4. Glacial to Holocene Transition

18-12 ka: Low planktonic and benthic foraminiferal productivity indicates the persistence of glacial ice after the LGM. Productivity begins a slow recovery at first and then becomes more rapid towards the end of this period, increasing first in the cores to the north of the PF as the PF begins a southward transition and the climate begins to warm. Many studies from the Southern Ocean and Antarctica report that temperatures reached Holocene levels by approximately 12ka (Fig. 6.4).

12-10 ka: The start of the interglacial is marked by a meltwater event in GC062 at 11.3ka and in KC064 at 9.7ka as identified in the planktonic $\delta^{18}O$ record. This meltwater event may have stimulated productivity at this time as indicated by increased foraminiferal abundance. In core GC062 to the north of the PF the meltwater event is followed closely by a cooling event (the ACR) which peaks at approximately 10.5ka and has also been recorded in other studies from the Southern Ocean (Fig. 6.4). The introduction of warmer water planktonic foraminifera indicates the increasing influence of subantarctic water masses in the Scotia Sea and the presence of certain benthic foraminifera indicate the reinitiation of NADW flux into the Southern Ocean.

10ka – present day: Following the ACR there appears to be a return to higher productivity which continues to increase to a maximum between 7.5 and 4 ka to the north and south of the PF. The PF may now have passed over the core sites and lie to the south within the Scotia Sea. Productivity then starts to decline as indicated by decreasing foraminiferal abundance to the present day, perhaps indicating a period of cooling.

A summary of the palaeoceanographic changes in the Scotia Sea through the last glacial – interglacial transition can be seen in Figure 7.1.

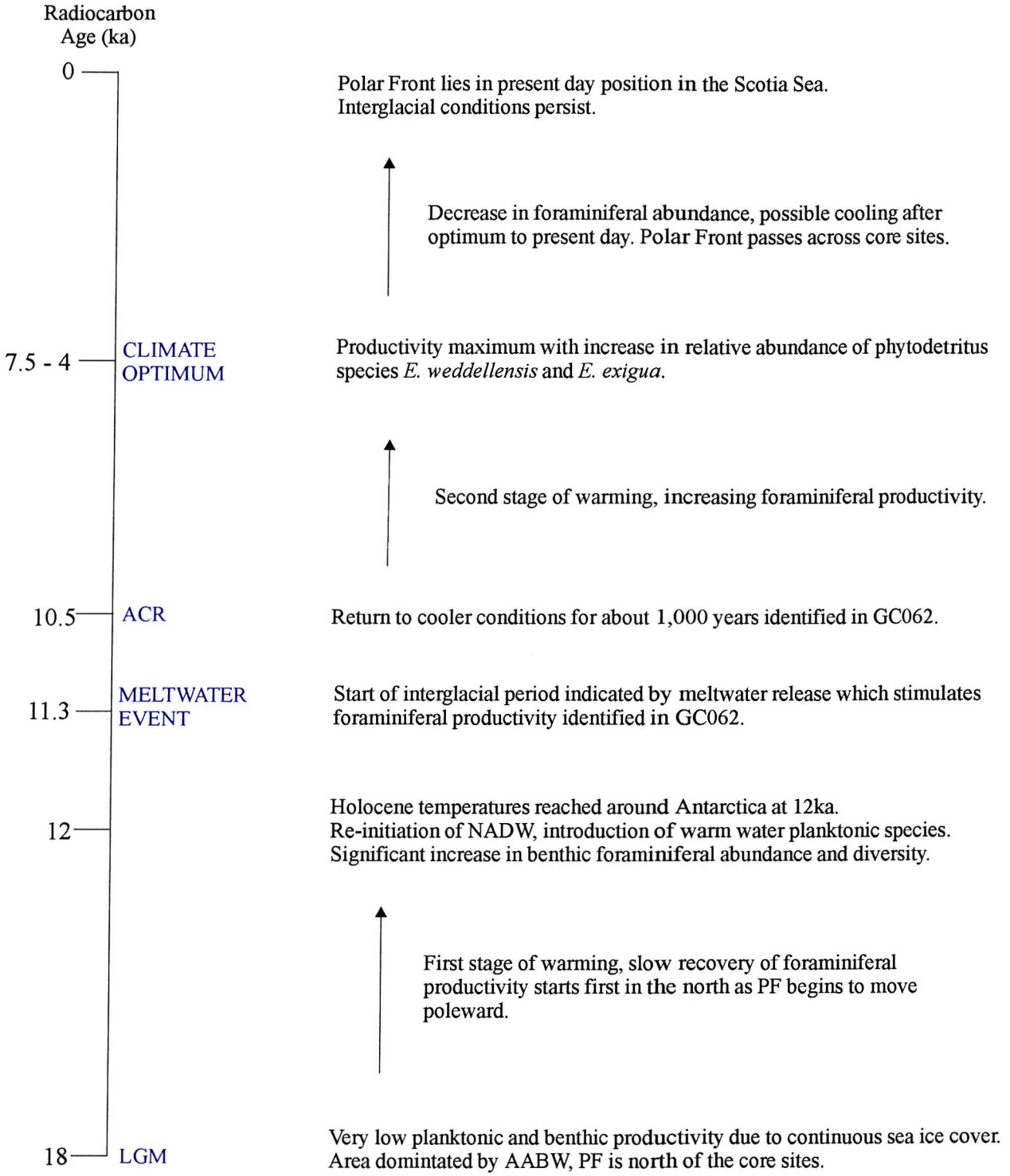

Figure 7.1. Summary of palaeoceanography of the Scotia Sea through the last glacial cycle.

An important aspect of understanding the last deglaciation is the synchroneity of the event between the northern and southern hemispheres. The start of the last deglaciation in the Southern Ocean has been dated between 16.5 and 13 ka (Bard *et al.*, 1990) or even as early as between 22-15 ka (Broecker, 1998) and was well established by 13ka (Labracherie *et al.*, 1989; this study), while it may not have begun for another thousand years in the North Atlantic (Bard *et al.*, 1990; Jansen and Veum, 1990). This initial warming phase continues to the start of the interglacial where a meltwater event is identified at a number of locations in the Southern Ocean (Fig. 6.4) including the Scotia Sea (slightly later to the south of the PF). This is then closely followed by an interruption in the warming trend and a return to cooler conditions in the Southern Ocean called the ACR. This event appears to occur widely throughout Antarctica and the Southern Ocean and although it may correspond to the northern hemisphere YD cooling event, the ACR seems to start slightly earlier in the Scotia Sea (this study). Other studies which have recorded this event from the southern hemisphere including those by Labracherie *et al.* (1989) from the Indian sector of the Southern Ocean and Shimmield *et al.* (1994) from the Weddell Sea (see Fig.6.4), also suggest that it starts slightly earlier, and it has been proposed that the ACR may lead the YD by about a thousand years. Results from ice core studies from Anatrctica (Blunier *et al.*, 1997, 1998; Lorius *et al.*, 1979; Jouzel *et al.*, 1987b, 1992, 1995; Charles *et al.*, 1996; Ciais *et al.*, 1992) also show a possible lead of about 1500 years.

From studies of the $\delta^{18}O$ in ice cores from Greenland and Antarctica Broecker (1998) concluded that although on a 100,000 year timescale Antarctic climate changed in phase with the northern hemisphere during the deglaciation, millennial duration modulations were in antiphase. Therefore during the pronounced Bolling-Allerød warm interval in the North Atlantic, the deglacial warming in Antarctica stalled, and during the Younger Dryas cold event in the North Atlantic, strong warming in Antarctica occurred. The results from this study in the Scotia Sea would seem to show that the second stage of warming which begins after the ACR in the Southern Ocean starts before the end of the YD in the northern hemisphere. The timing of these events on a global scale is still not well constrained and the mechanism for causing these changes in climate is not fully understood. Switching on and off the global thermohaline circulation has been suggested to explain warming and cooling events in the North Atlantic, and model studies suggest that northern and southern hemisphere temperatures should have changed in opposite directions if this is the main control (Stocker and Wright, 1996; Mikolajewicz, 1998). However some evidence from

glacier readvance and oceanic palaeotemperatures indicate interhemispheric synchrony during the deglaciation and this casts doubt on the proposal that thermohaline circulation is the only cause of climate connection (Bard *et al.*, 1997). Recently however, Broecker (1996) proposed that ocean circulation may have an indirect effect on the southern hemisphere and that the reason Antarctica may not react in phase with the rest of the globe during the last deglaciation may lie in the pattern of heat release from the ocean. Therefore the lead of the second phase of warming after the ACR in Antarctica which may have occurred in phase with the YD in the northern hemisphere and might have been caused by heat release to the atmosphere in response to an increase in deep-sea ventilation in the Southern Ocean (Broecker, 1998). Even if these cold events may be correlated the amplitude of the temperature decrease during the ACR in the Southern Ocean is as much as three times weaker than the YD measured in Greenland (Jouzel *et al.*, 1995).

However neither the meltwater event nor the ACR have been recorded in all the cores from this study and therefore to be able to correlate these events with northern hemisphere records and determine whether they are global or regional in character, more cores from the Scotia Sea would need to be studied. A problem with obtaining more isotope records from the Scotia Sea is the paucity of biogenic carbonate to the south of the PF and therefore there is a lack of previous studies from this area. However there is also the possibility that the cores from this study were not sampled for isotope analysis at a close enough interval and that short lived climate events such as the meltwater event and the ACR were missed in cores KC097 and KC099.

Chapter Eight

SEDIMENT TRAP ANALYSIS

Two sediment trap samples from Moorings IX and XI (Table 8.1) in the Scotia Sea were studied for the presence of planktonic and benthic foraminifera. These could then be compared to core top samples in order to evaluate the faithfulness of the core top assemblages.

Mooring	Deployed	Position	Water Depth (m)	Height Above Seabed (m)
IX	1993 - 95 edge of ACC	53°56′S 48°03′W	3956	21
XI	1993 - 95 central Scotia Sea	56°45′S 42°58′W	3657	21

Table 8.1. Sediment trap details.

The moorings generally incorporate two sediment traps, the upper trap collects only material sinking from the upper ocean water layers, the lower trap (21m above the sea floor) collects material transported in the nepheloid layer.

The traps are square-section fibreglass funnels (height - 0.7m, x-sectional area - up to 0.26m^2) with the top of each funnel containing slabs of "aeroweb" honeycomb, 64mm high with hexagonal cells 13mm in diameter.

The samples were wet sieved at 63μm mesh size and dried in an oven over night. As the samples contained quite a lot of organic material they had to be brushed through a smaller sieve to separate the foraminifera from this material. The planktonic foraminiferal species found in the sediment traps are noted in Table 8.2.

Mooring 9 53°56′S	**Mooring 11** 56°45′S
N. pachyderma *G. bulloides* *G. inflata* *G. quinqueloba* *G. uvula* *G. crassaformis* *G. glutinata* *G. truncatulinoides*	*N. pachyderma* *G. bulloides* *G. quinqueloba*

Table 8.2. Planktonic foraminiferal species found in sediment traps.

The planktonic foraminiferal species identified in mooring 9 are exactly the same as those noted in the core top samples to the north of the PF. The assemblage shows quite high species diversity with the full range of distributional zones from subtropical to Antarctic represented. The relative abundance of each of the species does not vary between the sediment trap and core top sample, with a clear dominance of the polar species *N. pachyderma* (s). There is a smaller range of planktonic species identified in mooring 11 as is the case in the core tops to the south of the PF, and these seem to represent only the Antarctic and cold-temperate zones. *Neogloboquadrina pachyderma* (s) is completely dominant in this sediment trap sample with the two other species only present in very low abundance. This is slightly different to the core top samples to the south of the Polar Front which show higher relative abundance of the minor species. The location of mooring 11 farther south in the Scotia Sea may explain the reduced species diversity and the dominance of the polar species *N. pachyderma*. Therefore it would appear that the core top samples are representative of the conditions within the present day Scotia Sea and there has been little change in this area during the latest Holocene.

There were a number of benthic foraminifera identified in both moorings and although only found in very low abundance, their presence in the sediment traps suspended 20m above the sea floor indicates that bottom turbulence must be strong enough to suspend the foraminifera into the water column demonstrating the high energy nature of bottom water flow in this area. Present day occurrences of benthic storm activity have been recorded in the northern Scotia Sea, and during the LGM this activity is believed to have been stronger (Howe and Pudsey, 1999).

In contrast to the planktonic foraminiferal results, a study of the radiolaria in the same sediment trap samples (Crawshaw, 2000) showed an increase in species diversity in the sediment trap samples compared to the core top samples. This may indicate that benthic processes such as bioturbation and dissolution at the seabed are more destructive to radiolaria than foraminifera in the Scotia Sea.

Chapter Nine

CONCLUSIONS

1. Planktonic and benthic foraminiferal abundance was very low in the Scotia Sea and Falkland Trough during the last glacial stage due to increased sea-ice cover and increased dissolution to the south of the PF. The PF lay farther north at the LGM at 52°S at the least and probably farther north. This may have been in response to the northward expansion of the sea-ice edge during glaciation.
2. At the end of the glacial stage, foraminiferal abundance increased significantly over a short period of time in response to a southward movement of the PF across the northern Scotia Sea as the climate began to warm and productivity was enhanced. This warming occurred to the north of the PF first starting at approximately 14ka.
3. The end of the glacial is marked by an increase in the high productivity benthic foraminiferal indicator species *Melonis barleeanum* and *Fursenkona* spp. which require a sustained high supply of organic carbon to the sea floor.
4. The first phase of deglacial warming is characterised by evidence from the planktonic $\delta^{18}O$ record for a meltwater event in the Scotia Sea at approximately 11.3ka in GC062 and 1500 years later to the south in KC064. This event introduced a large amount of isotopically light water to the surface ocean as the ice shelves began to melt. A similar event has been reported from other areas of the Southern Ocean.
5. The meltwater event was followed by a return to colder conditions which lasted about 1000 years and was centred at approximately 10.5ka in GC062. This shift to colder temperatures has been called the Antarctic Cold Reversal (ACR) and may be connected to the Younger Dryas cold event in the northern hemisphere, but cooling appears to start

slightly earlier in the south. Evidence for the ACR has been recorded from other areas of Antarctica and the Southern Ocean between 12-10.5 ka, and is followed by a second phase of deglacial warming in the Holocene.

6. During the mid-Holocene period between 7.5 and 4 ka there was a maximum in foraminiferal abundance in the Scotia Sea which corresponded to a climate and productivity optimum experienced at a number of locations in Antarctica and the Southern Ocean. This may have been a response to a localised event in Antarctica rather than a global phenomenon. This warm optimum was followed by a decrease in foraminiferal productivity and temperature to the present day.
7. The time of the productivity maximum during the mid-Holocene in the Scotia Sea is represented by an increase in the relative abundance of the benthic foraminiferal species *Eilohedra weddellensis* and *Epistominella exigua* indicating that it may have been a period of increased phytodetritus availability. There is also a decrease in $\delta^{13}C$ in KC097 at this time perhaps in response to increased respiration within the phytodetritus layer at the sediment surface.
8. Changes in biogenic productivity are accompanied by water mass changes in the Scotia Sea during the deglaciation. During the glacial period there was reduced flux of warm NADW into the Southern Ocean and the Scotia Sea was instead dominated by a southern source bottom water. Previous studies show that there was no cessation of AABW formation during the glacial stage although it was reduced. The reinitiation of NADW at the start of the interglacial period is marked by an increase in species such as *Epistominella exigua* and *Gyroidinoides* spp.
9. The planktonic foraminifera show reduced species diversity during the glacial stage with the introduction of warmer water species at the start of the Holocene representing the increased influence of subantarctic waters in the Scotia Sea. There is increased dissolution of foraminifera during the glacial stage due to the expansion of carbonate-undersaturated polar water masses.
10. The cores from this study all seem to have responded similarly at surface and deep water levels to the same environmental changes and therefore it can be concluded that over the last glacial cycle the core sites were influenced by the same water mass and any small-scale variations may be due to localised organic carbon flux to the sea floor. However the cores to the north of the PF do seem to respond earlier to climatic warming. The results

from this study also seem to support other studies from the Southern Ocean and therefore these changes appear to be circumpolar in extent.

11. Cores to the north of the PF show a greater amplitude of change during the deglaciation but this may be because productivity is much greater at all times. Increasing foraminiferal abundance and species diversity towards the north and increasing dissolution towards the south indicates that the PF exerts a major controlling influence on carbonate production and deposition in the Scotia Sea.
12. The connection between the northern and southern hemispheres during the deglaciation is still uncertain and more correlation between marine sediment records and ice core data is needed to be able to accurately predict the timing and synchroneity of these events throughout the globe. This subject would also benefit from extended study to the south of the PF where there is less previous work due to lack of carbonate within the sediment.
13. The last glacial transition was a time of significant change in the surface and deep waters of the Scotia Sea with major changes in foraminiferal distributions observed. However the Holocene period also seems to be a time of fluctuation of the climate but perhaps on a more localised scale in the Southern Ocean.

10.0 FUTURE WORK

- There is scope for further study of the benthic foraminiferal assemblage changes through the last glacial cycle and into the Holocene in the Scotia Sea as there are still a number of cores which have not been analysed to the north and south of the Polar Front. However due to the lack of carbonate preserved in the sediment towards the south in the Scotia Sea, this study may be limited. Therefore it may be more beneficial to expand the existing study to provide a higher resolution record.
- It would be useful to carry out further planktonic and benthic stable isotope analysis at a higher resolution in the cores from this study and also on other cores especially to the south of the Polar Front. This would provide a more accurate and correlatable isotope record and increase the existing knowledge to the south of the Polar Front where carbonate levels are very low.
- The planktonic foraminifera have not been studied in great detail here and it might be interesting to expand this study to include absolute and relative abundance of the planktonic species present.
- Comparison with other microfossil group studies (radiolaria, dinoflagellates, coccoliths and diatoms) from the Scotia Sea would provide a more complete record of the palaeoceanography of the region.
- It may be useful to compare this study to other interglacial stages such as stage 5 to see if the oceanographic conditions identified here are unique to the Holocene period. Samples are available from the Bellingshausen Sea margin.

11.0. FAUNAL REFERENCE LIST

The species names used in this study are given together with the original name if it is different.

Adercotryma glomerata (Brady) = *Lituola glomerata* Brady, 1878.
Ammobaculites agglutinans (d'Orbigny) = *Spirolina agglutinans* d'Orbigny, 1846.
Ammodsicus anguillae Høglund, 1947.
Ammodiscus tenuis (Brady) = *Trochammina (Ammodiscus) tenuis* Brady, 1881.
Angulogerina angulosa (Williamson) = *Uvigerina angulosa* Willaimson, 1858.
Astrononion antarcticus Parr, 1950.
Astrononion echolsi Kennett, 1967.
BOLIVINA d'Orbigny, 1839.
Bolivina decussata Brady, 1884.
Bolivina earlandi Parr, 1950.
Bolivina malovensis Heron-Allen and Earland, 1932.
Bolivina pseudoplicata Heron-Allen and Earland, 1930.
Bolivina pseudopunctata Höglund, 1947.
Bolivina subspinescens Cushman, 1922.
Bolivinella folia (Parker and Jones) = *Textularia agglutinans* var. *folium* Parker and Jones, 1865.
Bolivinellina translucens (Phleger and Parker) = *Bolivina translucens* Phleger and Parker, 1951.
Bolivinita pseudothalmanni Boltovskoy and Giussani de Kahn, 1981.
Brizalina pygmaea (Brady) = *Bulimina (Bolivina) pygmaea* Brady, 1881.
Brizalina semicostata (Cushman) = *Bolivina semicostata* Cushman, 1911.
Brizalina spathulata (Williamson) = *Textularia variabilis* Williamson var. *spathulata* Williamson, 1858.
Bulimina aculeata d'Orbigny, 1826.
Bulimina elongata d'Orbigny, 1826.
Bulimina marginata d'Orbigny, 1826.
Bulimina rostrata Brady, 1884.
Cassidulina crassa d'orbigny, 1839.
Cassidulina laevigata d'Orbigny, 1826.
Cassidulina laevigata d'Orbigny var. *carinata* Cushman 1922.
CIBICIDES de Montfort, 1808.
Cibicides grossepunctatus Earland, 1934.
Cibicides lobatulus (Walker and Jacob) = *Nautilus lobatulus* Walker and Jacob, 1798.
Cibicides refulgens Montfort, 1808.
Cibicides wuellerstorfi (Schwager) = *Anomalina wuellerstorfi* Schwager, 1866.
Cribrostomoides subglobosus (Cushman) = *Haplophragmoides subglobosum* Cushman, 1910.
Dentalina advena (Cushman) = *Nodosaria advena* Cushman, 1923.
Discorbinella bertheloti (d'Orbigny) = *Rosalina bertheloti* d'Orbigny, 1839.
Eggerella bradyi (Cushman) = *Verneuilina bradyi* Cushman, 1911.
Ehrenbergina glabra Heron-Allen and earland = *Ehrenbergina hystrix* var. *glabra* Heron-Allen and Earland, 1922.
Ehrenbergina pupa (d'Orbigny) = *Cassidulina pupa* d'Orbigny, 1839.
Ehrenbergina trigona Goës, 1896.
Eilohedra weddellensis (Earland) = *Eponides weddellensis* Earland, 1936.

Epistominella exigua (Brady) = *Pulvinalina exigua* Brady, 1844.
EPONIDES de Montfort, 1808.
Eponides tumidulus (Brady) = *Truncatulina tumidula* Brady, 1884.
FISSURINA Reuss, 1856.
Fursenkoina complanata (Egger) = *Virgulina shreibersiana* Czjzek var. *complanata* |Egger, 1893.
Fursenkoina earlandi (Parr) = *Bolivina earlandi* Parr, 1950.
Fursenkoina fusiformis (Williamson) = *Bulimina pupoides* d'Orbigny var. *fusiformis* Williamson, 1858.
Fursenkoina rotunda (Parr) = *Virgulina rotunda* Parr, 1950.
Fursenkoina texturata (Brady) = *Virgulina texturata* Brady, 1884.
Globocassidulina subglobosa (Brady) = *Cassidulina subglobosa* Brady, 1881.
GLOBOTROCHAMMINOPSIS Brönnimann and Zaninetti, 1984.
Glomospira gordialis (Jones and Parker) = *Trochammina squamata* var. *gordialis* Jones and Parker, 1860.
GYROIDINOIDES Brotzen, 1942.
HAPLOPHRAGMOIDES Cushman, 1910.
Haplophragmoides canariensis (d'Orbigny) = *Nonionina canariensis* d'Orbigny, 1839.
Haplophragmoides quadratus Earland, 1934.
HERONALLENIA Chapman and Parr, 1931.
Hoeglundina elegans (d'Orbigny) = *Rotalina elegans* d'Orbigny, 1826.
Karrerulina conversa (Grzybowski) = *Gaudryina conversa* Grzybowski, 1901.
LAGENA Walker and Jacob, 1798.
Lagenammina difflugiformis (Brady) = *Reophax difflugiformis* Brady, 1879.
Laticarinina pauperata (Parker and Jones) = *Pulvinulina repanda* var. *pauperata* Parker and Jones, 1865.
LENTICULINA Lamarck, 1804.
Loeblichopsis sabulosa (Brady) = *Reophax sabulosa* Brady, 1881.
Marginulina obesa (Cushman) = *Marginulina glabra* var. *obesa* Cushman, 1923.
Melonis barleeanum (Williamson) = *Nonionina barleeana* Williamson, 1858.
Melonis pompilioides (Fichtel and Moll) = *Nautilus pompilioides* Fichtel and Moll, 1798.
Melonis zaandamae (Van Voorthuysen) = *Anomalinoides barleeanum* (Williamson) *zaandamae* Van Voorthuysen, 1952.
Neolenticulina variabilis (Reuss) = *Cristellaria variabilis* Reuss, 1850.
NODOSARIA Lamarck, 1812.
Nonionella bradii (Chapman) = *Nonionina scapha* var. *bradii* Chapman, 1916.
Nonionella iridea Heron-Allen and Earland, 1932.
Nuttallides umbonifera (Cushman) = *Pulvinulina umbonifera* Cushman, 1933.
OOLINA d'Orbigny, 1839.
ORIDORSALIS Anderson, 1961.
Oridorsalis tener (Brady) = *Truncatulina tenera* Brady, 1884.
Patellina antarctica Parr, 1950.
Planulina wuellerstorfi (Schwager) = *Anomalina wuellerstorfi* Schwager, 1866.
PORTATROCHAMMINA Echols, 1971.
Portatrochammina antarctica (Parr) = *Trochammina antarctica* Parr, 1950.
Portatrochammina wiesneri (Parr) = *Trochammina wiesneri* Parr, 1950.
Pullenia bulloides (d'Orbigny) = *Nonionina bulloides* d'Orbigny, 1846.
Pullenia osloensis Feyling-Hanssen, 1954.
Pullenia simplex Rhumbler, 1931.
Pullenia subcarinata (d'Orbigny) = *Nonionina subcarinata* d'Orbigny, 1839.

PYRGO Defrance, 1824.
Pyrgo laevis Defrance, 1824.
Pyrgo murrhina (Schwager) = *Biloculina murrhina* Schwager, 1866.
Pyrgo serrata (Bailey) = *Biloculina serrata* Bailey, 1861.
Pyrulina angusta (Egger) = *Polymorphina angusta* Egger, 1857.
QUNIQUELOCULINA d'Orbigny, 1826.
Quinqueloculina seminulum (Linné) = *Serpula seminlum* Linné, 1758.
Quinqueloculina venusta Karrer, 1868.
Reophax fusiformis (Williamson) = *Proteonina fusiformis* Williamson, 1858.
Repmanina charoides (Jones and Parker) = *Trochammina squamata* Jones and Parker var. *charoides* Jones and Parker, 1860.
Siphotextularia catenata (Cushman) = *Textularia catenata* Cushman, 1911.
Siphouvigerina asperula (Brady) = *Uvigerina asperula* Brady, 1884.
Sphaeroidina bulloides d'Orbigny, 1826.
Spirolocammina tenuis Earland, 1934.
Spiroplectammina biformis (Parker and Jones) = *Textularia agglutinans* var. *biformis* Parker and Jones, 1865.
Spirosigmoilina pusilla (Earland) = *Spiroloculina pusilla* Earland, 1934.
Spirosigmoilina tenuis (Czjzek) = *Quinqueloculina tenuis* Czjzek, 1848.
Tosaia hanzawai Takayanagi, 1953.
TRILOCULINA d'Orbigny, 1826.
Triloculina tricarinata Parker, Jones and Brady, 1865.
TROCHAMMINA Parker and Jones, 1859.
Trochammina discorbis Earland, 1934.
Trochammina glabra Heron-Allen and Earland, 1932.
Trochammina heronallenia (Mikhalevich) = *Tritaxis heronallenia* Mikhalevich, 1972.
UVIGERINA d'Orbigny, 1826.
Uvigerina auberiana d'Orbigny, 1839.
Uvigerina brunnensis Karrer, 1877.
Uvigerina canariensis d'Orbigny, 1839.
Uvigerina peregrina Cushman, 1923.
Veleroninoides wiesneri (Parr) = *Labrospira wiesneri* Parr, 1950.

12.0. PLATE

1 *Eilohedra weddellensis* (Earland)
Apertural view; 125μm.

2 *Eilohedra weddellensis* (Earland)
Spiral view; 125μm.

3 *Epistominella exigua* (Brady)
Spiral view; 150μm.

4 *Globocassidulina subglobosa* (Brady)
125μm.

5 *Lagena* sp.
200μm.

6 *Gyroidinoides* sp.
Apertural view; 175μm.

7 *Gyroidinoides* sp.
Spiral view; 175μm.

8 *Melonis barleeanum* (Williamson)
210μm.

9 *Nonionella iridea* Heron-Allen and Earland
110μm.

10 *Nuttallides umbonifera* (Cushman)
Spiral view; 300μm.

11 *Oridorsalis tener* (Brady)
Spiral view; 200μm.

12 *Oridorsalis tener* (Brady)
Apertural view; 200μm.

13 *Bolivina* sp.
125μm.

14 *Neogloboquadrina pachyderma* (Ehrenberg)
Apertural view; 300μm. Sediment trap (mooring 3 – N. Weddell Sea)
No calcification or overgrowth.

15 *Neogloboquadrina pachyderma* (Earland)
Apertural view. KC064 / 20cm.

16 *Neogloboquadrina pachyderma* (Earland)
Spiral view. KC064 / 70cm.

17 *Neogloboquadrina pachyderma* (Earland)
Apertural view. KC064 / 140cm.

18 *Neogloboquadrina pachyderma* (Earland)
Apertural view. KC097 / 1.5cm.

19 *Neogloboquadrina pachyderma* (Earland)
Side view. KC097 / 90cm.

20 *Neogloboquadrina pachyderma* (Earland)
Apertural view. KC097 / 270cm.

15-20: All foraminifera have a diameter between 125-300 μm.
Effects of increasing dissolution observed down core, seen as fragmentation of the test and loss of preservation.

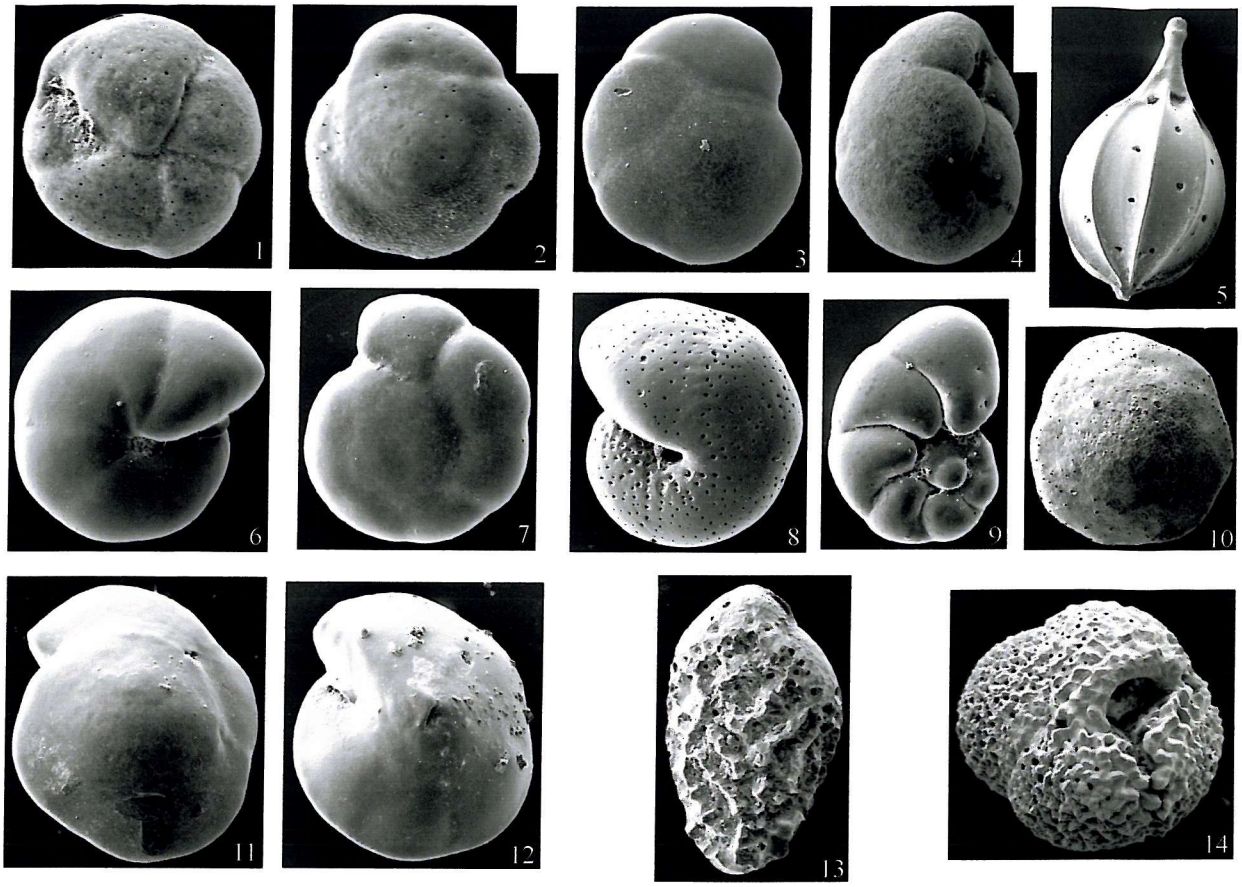
1
2
3
4
5
6
7
8
9
10
11
12
13
14

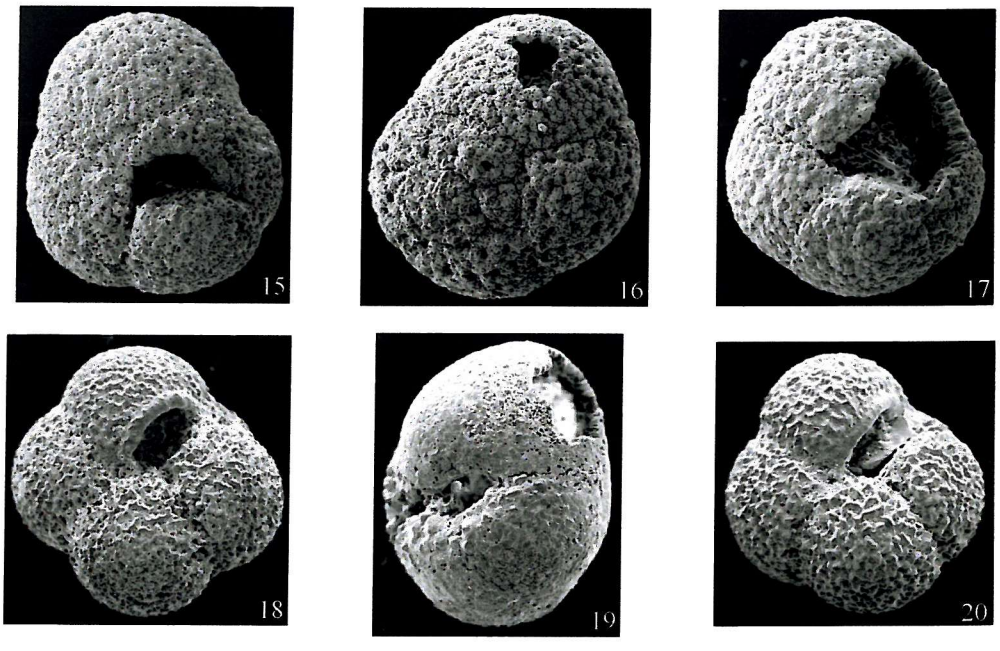
15
16
17
18
19
20

13.0. REFERENCES

Abbott, M. R., Richman, J. G., Letelier, R. M. and Bartlett, J. S., 2000. The spring bloom in the Antarctic Polar Frontal Zone as observed from a mesoscale array of bio-optical sensors. *Deep-Sea Res. II*, **47**: 3285-3314.

Ainley, D. and Jacobs, S. S., 1981. Sea-bird affinities for ocean and ice boundaries in the Antarctic. *Deep-Sea Res.*, **28**: 1173-1185.

Alley, R., Bond, G., Chappellaz, J., Clapperton, C., Del Genio, A., Keigwin, L. and Peteet, D., 1993a. Global Younger Dryas? *EOS*, **74**: 587-589.

Altenbach, A. V., 1992. Short term processes and patterns in the foraminiferal response to organic fluxes. *Mar. Micropal.*, **19**: 119-129.

Altenbach, A. V., 1988. Deep sea benthic foraminifera and flux rates of organic carbon. *Rev. Paléobiol.* (vol. spéc), **2**:719-720.

Altenbach, A. V. and Sarnthein, M., 1988. Paleoproductivity records in benthic foraminifera. In: W. H. Berger, V. S. Smetacek and G. Wefer (Eds.), *Productivity of the Ocean: Present and Past*. John Wiley and Sons Ltd, U.K., pp. 255-269.

Altenbach, A. V. and Sarnthein, M., 1989. Productivity record in Benthic Foraminifera. In: W. H. Berger, V. S. Smatacek and G. Wefer (Eds.), *Productivity of the Ocean: Past and Present*. John Wiley and Sons Limited, pp. 255-269.

Altenbach, A. V., Pflaumann, U., Schiebel, R., Thies, A., Timm, S. and Trauth, M., 1999. Scaling percentages and distributional patterns of benthic foraminifera with flux rates of organic carbon. *J. Foram. Res.*, **29**: 173-185.

Anderson, J. B., 1975a. Ecology and distribution of foraminifera in the Weddell Sea of Antarctica. *Micropaleontology*, **21**: 69-96.

Anderson, J. B., 1975b. Factors controlling $CaCO_3$ distribution in the Weddell Sea from foraminiferal distribution patterns. *Mar. Geol.*, **19**: 315-332.

Anderson, J. B., Kurtz, D. D., Domack, E. W. and Balshaw, K. M., 1980. Glacial and glacial marine sediments of the Antarctic continental shelf. *J. Geol.*, **88**: 399-414.

Anderson, R. F., 1998a. Southern Ocean Sediments Yield Evidence of Past Abrupt Climate Changes. *U.S. JGOFS Newsletter, V9, No.3.*

Anderson, R. F., Kumar, N., Mortlock, R. A., Froelich, P. N., Kubik, P., Dittrich- Hannen, B., Suter, M., 1998b. Late Quaternary changes in productivity of the Southern Ocean. *J. Mar. Syst.*, **17**: 497-514.

Anderson, J. B., 1999. *Antarctic Marine Geology*. Cambridge University Press, 289 pp.

Arrigo, K. R., Robinson, D. H., Worthen, D. L., Dundar, R. B., DiTullio, G. R., van Woert, M. and Lizotte, M. P., 1999. Phytoplankton community structure and the drawdown of nutrients and CO_2 in the Southern Ocean. *Science*, **283**: 265- 267.

Asioli, A., 1995. Living (stained) benthic Foraminifera distribution in the western Ross Sea (Antarctica). *Palaeopelagos*, **5**: 201-214.

Bandy, O. L. and Echols, R. J., 1964. Antarctic foraminiferal zonation. In: M. O. Lee (Ed.), Biology of the Antarctic Seas. *Ant. Res. Ser.*, **1**: 73-91.

Banse, K., 1996. Low seasonality of low concentrations of surface chlorophyll in the Subantarctic water ring: underwater irradiance, iron or grazing? *Prog. Oceanogr.*, **37**: 241-291.

Bard, E., Labeyrie, L., arnold, M., Labracherie, M., Pichon, J.-J., Duprat, J. and Duplessy, J.-C., 1989. AMS-^{14}C Ages Measured in Deep Sea Cores from the Southern Ocean: Implications for Sedimentation Rates during Isotope Stage 2. *Quat. Res.*, **31**: 309-317.

Bard, E., Labeyrie, L. D., Pichon, J.-J., Labracherie, M., Arnold, M., Duprat, J., Moyes, J. and Duplessy, J.-C., 1990. The last deglaciation in the Southern and Northern hemispheres: A comparison based on oxygen isotope, sea surface temperature estimates, and accelerator ^{14}C dating from deep-sea sediments. In: U. Bleil and J. Thiede (Eds.), *Geological History of the Polar Oceans: Arctic versus Antarctic.* Kluwer Academic Publishers, Netherlands, pp. 405-415.

Bard, E., Arnold, M., Fairbanks, R. G. and Hamelin, B., 1993. ^{230}Th – ^{234}U and ^{14}C ages obtained by mass spectrometry on corals. *Radiocarbon*, **35**: 191-199.

Bard, E., Rostek, F. and Sonzogni, C., 1997. Interhemispheric synchrony of the last deglaciation inferred from alkenone palaeothermometry. *Nature*, **385**: 707-710.

Barker, P. F. and Burrell, J., 1977. The opening of Drake Passage. *Mar. Geol.*, **25**: 15-34.

Barker, P. F. and Burrell, J., 1982. The Influence upon Southern Ocean Circulation, Sedimentation, and Climate of the Opening of Drake Passage. In: C. Craddock (Ed.), *Antarctic Geoscience.* The University of Wisconsin Press, Wisconsin, pp. 377-385.

Barker, P. F. and Hill, I. A., 1981. Back-arc extension in the Scotia Sea. *Philos. Trans. R. Soc. London,* A300, 249-262.

Barker, P. F., Dalziel, I. W. D. and Storey, B. C., 1991. Tectonic development of the Scotia arc region. In: R. J. Tingey (Ed.), *The Geology of Antarctica.* Oxford Monographs on Geology and Geophysics, Vol. 17, Oxford University Press, New York, pp. 215-248.

Barth, J. A., Cowles, T. J. and Pierce, S. D. Mesoscale physical and bio-optical structure of the Antarctic Polar Front near 170°W during spring. *J. Geophys. Res.*, submitted.

Bathmann, U. V., Scharek, R., Klaas, C., Dubischar, C. D. and Smetacek, V., 1997. Spring development of phytoplankton biomass and composition in major water masses of the Atlantic sector of the Southern Ocean. *Deep-Sea Res. II*, **44**: 51-67.

Bé, A. W. H., 1969. Distribution of Selected Groups of Marine Invertebrates in Waters South of 35°S Latitude. *Ant. Map Folio Ser.*, **11**: 9-12. Am. Geog. Soc.

Bé, A. W. H., 1977. An Ecological, Zoogeographic and Taxonomic Review of Recent Planktonic Foraminifera. In: A. T. S. Ramsay (Ed.), *Oceanic Micropaleontology, Volume 1.* Academic Press, London, Chapter 1, pp. 1-100.

Belanger, P. E., Curry, W. B. and Matthews, R. K., 1981. Core-top evaluation of benthic foraminiferal isotopic ratios for paleoceanographic interpretations. *Palaeogeogr., Palaeoclimatol., Palaeoecol.*, **33**: 205-220.

Berger, W. H., 1973. Deep sea carbonates: Pleistocene dissolution cycles. *J. Foram. Res.*, **3**: 187-195.

Berger, W. H., 1989. Appendix - global maps of ocean productivity. In: W. H. Berger, V. S. Smetacek and G. Wefer (Eds.), *Productivity of the Ocean: Present and Past. Life Sci. Res. Rep.*, **44**.

Berger, W. H., Fischer, K., Lai, C. and Wu, G, 1988. Ocean carbon flux: global maps of primary production and export production. In: C. R. Agegian (Ed.), *Biogeochemical cycling and fluxes between the deep euphotic zone and other oceanic realms.* NOAA National Undersea Research Program, Research Reports, 88: 131-176.

Berger, W. H. and Herguera, J. C., 1992. Reading the sedimentary record of the oceans productivity. In: P. G. Falkowski and A. D. Woodhead (Eds.), *Primary Productivity and Biogeochemical Cycles in the sea*. Plenum Press, New York, pp. 455-486.

Berkman, P. A., Andrews, J. T., Björk, S., Colhoun, E. A., Emslie, S. D., *et al.*, 1998. Circum-Antarctic coastal environmental shifts during the Late Quaternary reflected by emerged marine deposits. *Ant. Sci.*, **10**: 345-362.

Bernard, J. M., 1986. Characteristic assemblages and morphologies of benthic foraminifera from anoxic, organic-rich deposits: Jurassic through Holocene. *J. Foram. Res.*, **16**: 297-215.

Bernhard, J. M. and Sen Gupta, B. K., 1999. Foraminifera of oxygen-depleted environments. In: B. K. Sen Gupta (Ed.), *Modern Foraminifera*. Kluwer, Dordrecht, pp. 201-216.

Betts, M., 1991. Southern Ocean's role in world climate examined in major oceanographic study. *ANARE News, December*, pp. 21-22.

Betzer, P. R., Showers, W. J., Laws, E. A., Winn, C. D., Ditullio, G. R. and Kroopnick, P. M., 1984. Primary ptroductivity and particle fluxes on a transect of the equator at 153°W in the Pacific Ocean. *Deep-Sea Res.*, **31**: 1-11.

Björk, S., Hakansson, H., Zale, R., Karlen, W. and Jönsson, B. L., 1991. A Late Holocene lake sediment sequence from Livingston Island, South Shetland Islands, with paleoclimatic implications. *Antarct. Sci.*, **3**: 61-72.

Blair, D. G., 1965. The distribution of planktonic foraminifera in deep-sea cores form the Southern Ocean, Antarctica. *Florida State University, Department of Geology, Sedimentological Research Laboratory Contribution*, **10**, 141pp.

Blanc, F., Blanc-Vernet, L. and Le Campion, J., 1972. Application paléoécologique de la méthode d'analyse factorielle en comosantes principales: interprétation des microfaunes de Foraminifères planctonique quateraires en Méditerranée. 1 - étude des espèces de Méditerranée occidentale. *Tethys*, **4**: 761-778.

Blunier, T., Schwander, J., Stauffer, B., Stocker, T., Dällenbach, A., Indermühle, A., Tschumi, J., *et al.*, 1997. Timing of the Antarctic Cold Reversal and the atmospheric CO_2 increase with respect to the Younger Dryas event. *Geophys. Res. Letts.*, **24**: 2683-2686.

Blunier, T., Chappellaz, J., Schwander, J., Dällenbach, A., Stauffer, B., *et al.*, 1998. Asynchrony of Antarctic and Greenland climate change during the last glacial period. *Nature*, **391**: 739-743.

Bonn, W. J., 1995. Biogenopal und biogenes Barium als Indikatoren für spätquartäre Produktivitäs-änderungen am antarktischen Kontinentalhang, atlantischer Sektor. *Ber Polarforsch Bremerhaven*, **180**: 1-186.

Botnikov, V. N., 1963. Geographical position of the Antarctic Convergence Zone in the Antarctic Ocean. *Soviet Antarctic Exped. Inf. Bull. 41 (English ed.)*, **4**: 324-327.

Boyle, E. A., 1988. The role of chemical fractionation in controlling late Quaternary atmospheric carbon dioxide. *J. Geophys. Res.*, **93**: 15701-15714.

Boyle, E. A., 1992. Cadmium and the δ13C paleochemical ocean distributions during stage 2 glacial maximum. *Ann. Rev. Earth Planet Sci.*, **20**: 245-287.

Boyle, E. A. and Keigwin, L. D., 1982 Deep circulation of the North Atlantic over the last 200,000 years: Geochemical evidence. *Science*, **218**: 784-787.

Boyle, E. A. and Keigwin, L. D., 1985. Comparison of Atlantic and Pacific paleo- chemical records for the last 215,000 years: Changes in deep ocean circulation and chemical inventories. *Earth Planet. Sci. Letts.*, **76**: 135-150.

Boyle, E. A. and Keigwin, L. D., 1987. North Atlantic thermohaline circulation during the past 20,000 years linked to high-latitude surface temperature. *Nature*, **330**: 35-40.

Boyle, E. A. and Rosenthal, Y., 1996. Chemical hydrography of the South Atlantic during the Last Glacial Maximum: Cd vs. $\delta^{13}C$. In: G. Wefer, W. H. Berger, Siedler, G. and Webb, D (Eds.), *The South Atlantic: Present and Past Circulation*. Springer, Berlin, pp. 423-443.

Braatz, B. V. and Corliss, B. H., 1987. Calcium carbonate undersaturation of bottom waters in the South Australian Basin during the last 3.2 million years. *J. Foram. Res.*, **17**: 257-271.

Brady, H. B., 1884. Report on the foraminifera dredged by the HMS *Challenger* during the years 1873-1876. *Rept. Sci. Results Voyage HMS Challenger*, **9**, 814 pp.

Bray, J. R. and Curtis, J. T., 1957. An ordination of the upland forest communities of Southern Wisconsin. *Ecol. Monogr.*, **27**: 325-349.

Bremer, M. L. and Lohmann, G. P., 1982. Evidence for primary control of the distribution of certain Atlantic Ocean benthonic foraminifera by degree of carbonate saturation. *Deep-Sea Res.*, **29**: 987-998.

Brennecke, W., 1921. Die ozeanographischen Arbeiten Den deutschen antarktischen Expedition 1911-1912. *Ans dem Arkivdem Deuchen Seewarte*, **39**: 1-214.

Broecker, W. S., 1963. Radiocarbon ages of Antarctic materials. *Polar Record*, **11**: 472-473.

Broecker, W. S., 1982. Glacial to interglacial changes in ocean chemistry. *Progress in Oceanography.*, **11**: 151-197.

Broecker, W. S., 1996. Paleoclimatology. *Geotimes*, **41**: 40-41.

Broecker, W. S., 1998. Paleocean circulation during the last deglaciation: A bipolar seesaw? *Paleoceanography*, **13**: 119-121.

Broecker, W. S. and Peng, T. H., 1982. *Tracers in the Sea*. Eldigio Press, Palisades, 690 pp.

Broecker, W. S., Peteet, D. M., Rind, D., 1985. Does the ocean-atmosphere system have more than one stable mode of operation? *Nature*, **315**: 21-26.

Broecker, W. S., Bond, G., Klas, M., 1990. A salt oscillator in the glacial Atlantic? 1. The concept. *Paleoceanography*, **5**: 469-477.

Bryden, H. L., 1983. The Southern Ocean. In: A. L. Robinson (Ed.), *Eddies in marine science*. Springer-Verlag, Berlin, 609 pp.

Bryden, H. L. and Pillsbury, R. D., 1977. Variability of deep flow in the Drake Passage from year-long current measurements. *J. Phys. Oceanogr.*, **7**: 803-810.

Burckle, L. H., 1984. Diatom distribution and paleoceanographic reconstruction in the Southern Ocean – present and last glacial maximum. *Mar. Micropal.*, **9**: 241-261.

Burckle, L. H. and Cirilli, J., 1987. Origin of diatom ooze belt in the Southern Ocean: Implications for Late Quaternary paleoceanography. *Micropaleontology*, **33**: 82-86.

Burckle, L. H., Jacobs, S. S. and McLaughlin, R., 1987. Late Spring diatom distributions between New Zealand and the Ross Sea: Correlation with hydrography and bottom sediments. *Micropaleontology*, **33**: 74-81.

Caralp, M.-H., 1984. Impact de la matière organique dans des zones de forte productivité sur certains foraminiferes benthiques. *Oceanol. Acta.*, **7**: 509-515.

Caralp, M., 1987. Deep-sea circulation in the northeastern Atlantic over the past 30,000 years: The benthic foraminiferal record. *Oceanol. Acta.*, **10**: 27-40.

Carmack, E. C., 1973. Silicate and potential temperature in the deep and bottom waters of the western Weddell Sea. *Deep-Sea Res.*, **20**: 927-932.

Carmack, E. C., 1977. Water characteristics of the southern ocean south of the Polar Front. In: M. Angel (Ed.), *A Voyage of Discovery*. Pergammon Press, Oxford, pp. 15-37.

Carmack, E. C. and Foster, T. D., 1975. On the flow of water out of the Weddell Sea. *Deep-Sea Res.*, **22**: 711-724.

Carmack, E. C. and Killworth, P. D., 1978. Formation and interleaving of abyssal water masses off Wilkes Land, Antarctica. *Deep-Sea Res.*, **25**: 357-369.

Chapman, F. 1916a. Report on the Foraminifera and Ostracoda out of marine muds from sounding in the Ross Sea. *Rept. Sci. Invest. Brit. Antarctic Exped., 1907-1909. Geology,* **2**: 53-80.

Chapman, F. 1916b. Report on the Foraminifera and Ostracoda from elevated deposits on the shores of the Ross Sea. *Rept. Sci. Invest. Brit. Antarctic Exped., 1907-1909. Geology,* **2**: 25-52.

Chapman, F. and Parr, W. J., 1937. Foraminifera. *Australasian Antarctic Exped., 1911-1914, Ser. C,* **1**: 1-190.

Charles, C. D. and Fairbanks, R. G., 1990. Glacial to Interglacial Changes in the Isotopic Gradients of Southern Ocean Surface Water. In: U. Bleil and J. Thiede (Eds.), *Geological History of the Polar Oceans: Arctic Versus Antarctic.* Kluwer Academic Publishers, Netherlands, pp. 519-538.

Charles, C. D. and Fairbanks, R. G., 1992.Evidence from Southern Ocean sediments for the effect of North Atlantic deep-water flux on climate. *Nature*, **355**: 416-419.

Charles, C. D., Froelich, P. N., Zibello, M. A., Mortlock, R. A., Morley, J. J., 1991. Biogenic opal in Southern Ocean sediments over the last 450,000 years: implications for surface water chemistry and circulation. *Paleoceanography*, **6**: 697-728.

Charles, C. D., Lynch-Stieglitz, J., Ninnemann, U. S. and Fairbanks, R. G., 1996. Climate connections between the hemispheres revealed by deep sea sediment core/ice core correlations. *Earth Planet. Sci. Letts.*, **142**: 19-27.

Chen, C., 1966. Calcareous zooplankton in the Scotia Sea and Drake Passage. *Nature*, **212**: 678-681.

Chen, C. and Bé, A. W. H., 1965. Zonation of calcareous zooplankton in the Scotia Sea and Drake Passage (abstract). *Program. Geol. Soc. Am. Ann. Meeting*, p.31.

Ciais, P., Petit, J. R., Lorius, C., Barkov, N. I., Lipenkov, V. and Nicolaïv, V., 1992. Evidence for an early Holocene climatic optimum in the Antarctic deep ice-core record. *Clim. Dynam.*, **6**: 169-177.

Clarke, K. R. and Warwick, R. M., 1994. *Change in Marine Communities: An Approach to Statistical Analysis and Interpretation.* Bourne Press Ltd, Bournemouth, 144 pp.

Clifford, M. A., 193. *A descriptive study of the zonation of the Antarctic Circumpolar Current and its relation to wind stress and ice cover.* M.S. Thesis, Tex. A&M University, College Station, 93 pp.

CLIMAP Project Members, 1976. The surface of the ice-age earth. *Science*, **191**: 1131-1137.

Cline, R. M. and Hays, J. D., 1976. *Investigations of Late Quaternary paleoceanography and paleoclimatology.* Geol. Soc. Am. Mem., 145, 464 pp.

Cooke, D. W. and Hays, J. D., 1982. Estimates of Antarctic Ocean seasonal ice cover during glacial intervals. In: C. Craddock (Ed.), *Antarctic Geoscience.* Univ. of Wisconsin Press, Madison, pp. 1017-1025.

Corliss, B. H., 1979a. Taxonomy of recent deep-sea benthonic foraminifera from the Southeast Indian Ocean. *Micropaleontology*, **25**: 1-19.

Corliss, B. H., 1979b. Quaternary Antarctic Bottom Water history: deep-sea benthonic foraminiferal evidence from the south-east Indian Ocean. *Quat. Res.*, **12**: 271-289.

Corliss, B. H., 1982. Linkage of North Atlantic and Southern Ocean deep-water circulation during glacial intervals. *Nature*, **298**: 458-460.

Corliss, B. H., 1983. Quaternary circulation of the Antarctic Circumpolar Current. *Deep-Sea Res.*, **30**: 47-61.

Corliss, B. H., 1985. Microhabitats of benthic foraminifera within deep-sea sediments. *Nature*, **314**: 435-438.

Corliss, B. H., 1991. Morphology and microhabitat preferences of benthic foraminifera from the northwest Atlantic Ocean. *Mar. Micropal.*, **17**: 195-236.

Corliss, B. H. and Chen, C., 1988. Morphotype patterns of Norwegian Sea deep-sea benthic foraminifera and ecological implications. *Geology*, **16**: 716-719.

Corliss, B. H., Martinson, D. G. and Keffer, T., 1986. Late Quaternary deep-ocean circulation. *Geol. Soc. Am. Bull.*, **97**: 1106-1121.

Cosimo, J. C., McClain, C. R., Sullivan, C. W., Ryan, J. P. and Leonard, C. L., 1993. Coastal zone color scanner pigment concentrations in the Southern Ocean and relationships to geophysical surface features. *J. Geophys. Res.*, **98**: 2419-2451.

Crawshaw, T. J., 2000. *The Antarctic Circumpolar Current: Oceanographic and Climatic Significance in the Late Quaternary*. Unpublished PhD thesis, UCL, 405pp.

Cronin, T. M., 1999. *Principles of Paleoclimatology*. Columbia University Press, New York, 560 pp.

Curry, W. B., 1996. Late Quaternary deep circulation in the western equatorial Atlantic. In: G. Wefer, W. H. Berger, G. Siedler and D. J. Webb (Eds.), *The South Atlantic: Present and Past Circulation*. Springer, Berlin, pp. 577-598.

Curry, W. B. and Lohmann, G. P., 1982. Carbon isotopic changes in benthic foraminifera from the western south Atlantic: Reconstruction of glacial abyssal circulation patterns. *Quat. Res.*, **18**: 218-235.

Curry, W. B., Duplessy, J.-C., Labeyrie, L. D., Shackleton, N. J., 1988. Changes in the distribution of $\delta^{13}C$ of deep water ΣCO_2 between the last glaciation and the Holocene. *Paleoceanography*, **3**: 317-341.

Daly, K. L., Smith, W, O., Johnson, G. C., Ditullio, G. R., Jones, D. R., Mordy, C. W., Feely, R. A., Hansell, D. A. and Zhiang, J-Z., 2001. Hydrography, nutrients, and carbon pools in the Pacific sector of the Southern Ocean: implications for carbon flux. *J. Geophys. Res.*, **106**: 7107-7124.

Dansgaard, W., White, J. W. and Johnsen, S. J., 1989. The abrupt termination of the Younger Dryas climate event. *Nature*, **339**: 532-534.

Deacon, G. E. R., 1933. A general account of the hydrology of South Atlantic Ocean. *Discovery Reports*, **7**: 171-238.

Deacon, G. E. R., 1937. The hydrology of the Southern Ocean. *Discovery Reports*, **15**: 1-124.

Deacon, G. E. R. and Moorey, J. A., 1975. The boundary region between currents from the Weddell Sea and Drake Passage. *Deep-Sea Res.*, **28A**: 265-268.

Deacon, G. E. R., 1977. Antarctic water masses and circulation. In: M. J. Dunbar (Editor), *Polar Oceans*. Procceedings of the Polar Oceans Conference, McGill University, Montreal, May 1974.

Deacon, G. E. R., 1979. The Weddell Gyre. *Deep-Sea Res.*, **26**: 981-998.

Deacon, G. E. R., 1982. Physical and biological zonation in the Southern Ocean. *Deep-Sea Res.*, **29**: 1-15.

DeAngelis, M., Barkov, N. I. And Petrov, V. N., 1987. Aerosol concentrations over the last climatic cycle (160 kyr) from an Antarctic ice core. *Nature*, **325**: 318-321.

De Baar, H. J. W., De Jong, J. M. M., Bakker, D. C. E., Loscher, B. M., Veth, C., Bathmann, U. and Smetacek, V., 1995. Importance of iron for plankton blooms and carbon dioxide drawdown in the Southern Ocean. *Nature*, **373**: 412-415.

Defant, A., 1961. *Physical Oceanography, Vol. 1.* Pergammon Press, 729 pp.

Defelice, D. R. and Wise, S. W. Jr., 1981. Surface lithofacies, biofacies, and diatom diversity patterns as models for delineation of climatic change in the south-east Atlantic Ocean. *Mar. Micropal.*, **6**: 29-70.

Demaster, D. J., 1981. The supply and accumulation of silica in the marine environment. *Geochim. Cosmochim. Acta.*, **45**: 1715-1732.

Domack, E. W., Jull, A. J. and Nakao, S., 1991. Advance of east Antarctic outlet glaciers during the Hypisthermal: implications for the volume state of the Antarctic ice sheet under global warming. *Geology*, **19**: 1059-1062.

Domack, E. W., Ishman, S. E., Stein, A. B., McClennen, C. E. and Jull, A. J., 1995. Late Holocene advance of the Müller Ice Shelf, Antarctic Peninsula: sedimentological, geochemical and palaeontological evidence. *Ant. Sci.*, **7**: 159-170.

Domack, E. W. and McClennen, C. E., 1996. Accumulation of glacial marine sediments in fjords of the Antarctic Peninsula and their use as late Holocene paleoenvironmental indicators. *Am. Geophys. Un., Ant. Res. Ser.*, **70**: 1356.

Douglas, R. G. and Woodruff, F., 1981. Deep-sea benthic foraminifera. In: C. Emiliani (Ed.), *The Oceanic Lithosphere, The Sea, Vol. 7.* Wiley, New York, pp. 1233-1327. Dow, R. L., 1978. Radiolarian distribution and the late Pleistocene history of the South-eastern Indian Ocean. *Mar. Micropal.*, **3**: 203-227.

Drewry, D. J., Barker, P. F., Curry, F. C., Gardiner, B. G., Heywood, R. B., Jarvis, M. J., Paren, J. G., Priddle, J., Smith, G. J., Thomson, M. R. A. and Walton, D. W. H., 1993. Antarctic Science: a British perspective. Interdisciplinary Science Reviews, 18 (1).

Duplessy, J.-C., Shackleton, N. J., Matthews, R. K., Prell, W., Ruddiman, W. F., Caralp, M. and Hendy, C. H., 1984. ^{13}C record of benthic foraminifera in the last interglacial ocean: Inmplications for the carbon cycle and the global deep water circulation. *Quat. Res.*, **21**: 225-243.

Duplessy, J.-C., 1970. Note préliminaire sur les variations de la composition isotopique des eaux superficielles de l'Océan Indien: La relation O18-salinité. *C. R. Acad. Sci. Paris*, **271**: 1075-1078.

Duplessy, J.-C., Delibrias, G., Turon, J.-L., Pujol, C. and Duprat, J., 1981. Deglacial warming of the northeastern Atlantic Ocean: Correlation with the paleoclimatic evolution of the European continent. *Palaeogeogr., Palaeoclimatol., Palaeoecol.*, **35**: 121-144.

Duplessy, J.-C., Shackleton, N. J., Fairbanks, R. G., Labeyrie, L. D., Oppo, D. W. and Kallel, N., 1988. Deep water source variations during the last climatic variations and their impact on the global deep water circulation. *Paleoceanography*, **3**: 343-360.

Dymond, J., Suess, E. and Lyle, M., 1992. Barium in deep-sea sediment: a geochemical proxy for paleoproductivity. *Paleoceanography*, **7**: 163-181.

Earland, A., 1933. Foraminifera, 2, South Georgia. *Discovery Rept.*, **7**: 27-138.

Earland, A., 1934. Foraminifera, 3, The Falklands sector of the Antarctic (excluding South Georgia). *Discovery Rept.*, **10**: 1-208.

Earland, A., 1936. Foraminifera, 4, Additional records from the Weddell Sea sector from material obtained by the S. Y. *Scotia. Discovery Rept.*, **13**: 1-76.

Echols, R. J., 1971. Distribution of foraminifera in sediments of the Scotia Sea area, Antarctic waters. In: J. L. Reid (Ed.), Antarctic Oceanology 1. *Ant. Res. Ser.*, **15**: 93-168.

Edmond, J. M., Jacobs, S. S., Gordon, A. L., Mantyla, A. W. and Weiss, R. F., 1979. Water column anomalies in dissolved silica over opaline pelagic sediments and the origin of the deep silica maximum. *J. Geophys. Res.*, **84**: 7809-7826.

El-Sayed, S. Z., 1978. Primary productivity and estimates of potential yields on the Southern Ocean. In: M. A. McWhinnie (Ed.), *Polar Research. To the Present and the Future.* AAAS Selected Symposia 7, pp. 141-160.

Emiliani, C., 1955. Pleistocene temperatures. *J. Geol.*, **63**: 538-578.

Emiliani, C., 1966. Paleotemperature analysis of Caribbean cores P6304-8 and P6304-9 and a generalised temperature curve for the past 425,000 years. *J. Geol.*, **74**: 109-125.

Epstein, S., Buchsbaum, R., Lowenstam, H. A. and Urey, H. C., 1953. Revised carbonate-water isotopic temperature scale. *Bull. Geol. Soc. Amer.*, **64**: 1315- 1325.

Fandry, C. and Pillsbury, R. D., 1979. On the estimation of absolute geostrophic volume transport applied to the Antarctic Circumpolar Current. *J. Phys. Oceanogr.*, **9**: 49-455.

Fariduddin, M. and Loubere, P., 1997. The surface ocean productivity response of deep water benthic foraminifera in the Atlantic Ocean. *Mar. Micropal.*, **32**: 289-310.

Fillon, R. H., 1974. Late Cenozoic foraminiferal paleoecology of the Ross Sea, Antarctica. *Micropaleontology,* **20**: 129-151.

Fischer, G., Futterer, D., Gersonde, R., Honjo, S., Ostermann, D., Wefer, G., 1988. Seasonal variability of particle flux in the Weddell Sea and its relation to ice cover. *Nature*, **335**: 426-428.

Fisher, R. A., Corbet, A. S., Williams, C. B., 1943. The relationship between the number of species and the number of individuals in a random sample of an animal population. *J. Animal. Res.*, **12**: 42-58.

Foldvik, A. and Kvinge, T., 1974. *Bottom currents in the Weddell Sea.* Report No. 37, Geophysical Institute, Div. A. University of Bergen, 43 pp.

Foldvik, A., Gammelsrod, T. and Torresen, T., 1985a. Hydrographic observations from the Weddell Sea during the Norwegian Antarctic Research Expedition 1976/77. *Polar Res.*, **3**: 177-193.

Foldvik, A., Gammelsrod, T. and Torresen, T., 1985b. Physical oceanography studies in the Weddell Sea during the Norwegian Antarctic Expedition 1978/79. *Polar Res.*, **3**: 195-207.

Foldvik, A. and Gammelsrod, T., 1988. Notes on Southern Ocean hydrography, sea-ice and bottom water formation. *Palaeogeogr., Palaeoclimatol., Palaeoecol.*, **67**: 3-17.

Foster, T. D. and Carmack, E. C., 1976. Frontal zone mixing and Antarctic Bottom Water formation in the Southern Weddell Sea. *Deep-Sea Res.*, **23**: 301-317.

Foster, T. D. and Middleton, J. H., 1984. The oceanographic structure of the eastern Scotia Sea – 1. Physical Oceanography. *Deep-Sea Res.*, **31**: 529-550.

Francois, R., Altabet, M. A. and Burckle, L. H., 1992. Glacial to interglacial changes in surface nitrate utilisation in the Indian sector of the Southern Ocean as recorded by sediment $\delta^{15}N$. *Paleoceanography*, **7**: 589-606.

Frank, M., 1995. *Reconstruction of late Quaternary environmental conditions applying the natural.radionuclides ^{230}Th, ^{10}Be, ^{231}Pa and ^{238}U: a study of deep-sea sediments from the eastern sector of the Antarctic circumpolar current system.* PhD dissertation, University of Heidelberg.

Fütterer, D. K., Grobe, H. and Grünig, S., 1988. Quaternary sediment patterns in the Weddell Sea: Relations and environmental conditions. *Paleoceanography*, **3**: 551-561.

Ganachaud, A. and Wunsch, C., 2000. Improved estimates of global ocean circulation, heat transport and mixing from hydrographic data. *Nature*, **408**: 453-456.

Gardner, J. V., 1975. Late Pleistocene carbonate dissolution cycles in the eastern equatorial Atlantic. In: *Dissolution of Deep-Sea Carbonates*. Cush. Found. Foram. Res. Spec. Publ., 13: 129-141.

Gardner, J. V. and Hays, J. D., 1976. Responses of sea-surface temperature and circulation to global climatic change during the past 200,000 years in the Eastern Equatorial Atlantic Ocean. *Mem. Geol. Soc. Am.*, **145**: 221-246.

Garrison, D. L. and Buck, K. R., 1985. Sea-ice algal communities in the Weddell Sea: species composition in ice and plankton assemblages. In: J. S. Gray and M. E. Christiansen (Eds.), *Marine Biology of Polar Regions and Effects of Stress on Marine Organisms*. Wiley, New York, pp. 103-122.

Georgi, D. T., 1978. Fine structure in the Antarctic Polar Front Zone: its characteristics and possible relationship to internal waves. *J. Geophys. Res.*, **83**: 4579-4588.

Gibson, T. G., 1989. Planktonic:Benthonic foraminiferal ratios: modern patterns and Tertiary applicability. *Mar. Micropal.*, **15**: 29-52.

Gilbert, I. M., Pudsey, C. J. and Murray, J. W., 1998. A sediment record of cyclic bottom-current variability from the northwest Weddell Sea. *Sed. Geol.*, **115**: 185-214.

Gill, A. E., 1973. Circulation and bottom water production in the Weddell Sea. *Deep-Sea Res.*, **20**: 111-140.

Gille, S. T., 1994. Mean sea surface height of the Antarctic Circumpolar Current from Geosat data: Method and application. *J. Geophys. Res.*, **99**: 18255- 18273.

Gloerson, P., Campbell, W. J., Cavalieri, D. J., Comiso, J. C., Parkinson, C. L. and Zwally, H. J., 1992.Arctic and Antarctic sea-ice, 1978-1987: satellite passive microwave obsevations and analysis. *NASA Spec. Rep.*, **511**, 290 pp.

Goeyens, L., Sorensson, F., Tregner, P., Morvan, J., Panouse, M. and Dehairs, F., 1991. Spatiotemporal variability of inorganic nitrogen stocks and uptake fluxes in the Scotia-Weddell Confluence area during November and December 1988. *Mar. Ecol. Prog. Ser.*, **77**: 7-19.

Goeyens, L., Semeneh, M., Baumann, M. E. M., Elskens, M., Shopova, D. and Dehairs, F., 1998. Phytoplankton nutrient utilisation and nutrient signature in the Southern Ocean. *J. Mar. Syst.*, **17**: 143-157.

Gooday, A. J., 1988. A benthic foraminiferal response to the deposition of phytodetritus in the deep sea. *Nature*, **322**: 70-73.

Gooday, A. J., 1993. Deep-sea benthic foraminiferal species which exploit phytodetritus: Characteristic features and controls on distribution. *Mar. Micropal.*, **22**: 187-205.

Gooday, A. J., 1994. The biology of deep-sea foraminifera: a review of some advances and their applications in palaeoceanography. *Palaios*, **9**: 14-31.

Gooday, A. J., 1996. Epifaunal and shallow infaunal foraminiferal communities at three abyssal NE Atlantic sites subject to differing phytodetritus input regimes. *Deep-Sea Res.*, **43**: 1395-1421.

Gooday, A. J. and Lambshead, P. J. D., 1989. Influence of seasonally deposited phytodetritus on benthic foraminiferal populations in the bathyal Atlantic: the species response. *Mar. Ecol. Prog. Ser.*, **58**: 53-67.

Gooday, A. J., Shiros, R. and Jones, A., 1997. Large deep-sea agglutinated foraminifera: two differing kinds of organisation and their possible ecological significance. *J. Foram. Res.*, **27**: 278-291.

Goodell, H. G., 1973. The sediments. In: H. G. Goodell *et al.* (Eds.), Marine Sediments of the Southern Oceans. *Antarctic Map Folio Ser.*, **17**, Am. Geogr. Soc. N.Y., pp. 1-9.

Goodwin, I. D., 1993. Holocene deglaciation, sea-level change, and the emergence of the Windmill Islands, Budd Coast, Antarctica. *Quat. Res.*, **40**: 70-80.

Gordon, A. L., 1966. Potential temperature, oxygen and circulation of bottom water in the Southern Ocean. *Deep-Sea Res.*, **13**: 1125-1138.

Gordon, A. L., 1967. Structure of Antarctic waters between 20°W and 170°W. In: V. C. Bushnell (Ed.), *Antarctic Map Folio Ser.*, **6**: 1-10.

Gordon, A. L., 1971. Antarctic Polar Front Zone. In: J. L.Reid (Editor), Antarctic Oceanology 1. *Antarct. Res. Ser.*, **15**: 205-221.

Gordon, A. L., 1971. Recent physical oceanographic studies of Antarctic Waters. In: L. O. Quam (Ed.), *Research in the Antarctic*. American Association for the Advancement of Science, Washington D. C., pp. 609-630.

Gordon, A. L., Georgi, D. T. and Taylor, H. W., 1977. Antarctic Polar Front Zone in the Western Scotia Sea – Summer 1975. *J. Phys. Oceanogr.*, **7**: 309-328.

Gordon, A. L., 1988. Spatial and temporal variability within the Southern Ocean. In: D. Sahrage (Ed.), *Antarctic Ocean and Resources Variablity*. Springer-Verlag, New York, pp. 41-56.

Gordon, A. L. and Goldberg, R. D., 1970. Circumpolar characteristics of Antarctic waters. In: V. C. Bushnell (Ed.), *Antarctic Map Folio Ser.*, **13**: 1-5.

Gordon, A. L. and Tchernia, P. T., 1972. Waters of the continental margin off Adelie Coast, Antarctica. In: D. E. Hayes (Ed.), Antarctic Oceanography II: The Australian - New Zealand sector. *Ant. Res. Ser.*, **9**. American Geophysical Union, pp. 59-69.

Gordon, A. L. and Taylor, H. W., 1975. Heat and salt balance within the cold waters of the world ocean. In: ? (Eds.), *Numerical Models of Ocean Circulation*. National Academy of Sciences, Washington, pp. 54-56.

Gordon, A. L., Georgi, D. T. and Taylor, H. W., 1977. Antarctic Polar Front Zone in the Western Scotia Sea - Summer 1975. *J. Phys. Oceanogr.*, **7**: 309-328.

Gordon, A. L., Molinelli, E. and Baker, T., 1978. Large-scale dynamic topography of the Southern Ocean. *J. Geophys. Res.*, **87**: 3023-3032.

Gordon, A. L. and Molinelli, E. M., 1982. *The Southern Ocean Atlas: Thermohaline and Chemical Distributions and the Atlas Data Set*. Columbia University Press, New York.

Gordon, A. L., Weiss, R. F., Smethie, W. M. and Warner, M. J., 1992. Thermocline and intermediate water communication between the South Atlantic and Indian Oceans. *J. Geophys. Res.*, **97**: 7223-7240.

Gordon, J. E. and Harkness, D. D., 1992. Magnitude and geographic variation of the radio-carbon content in Antarctic marine life: implications for the reservoir corrections in radio-carbon dating. *Quat. Sci. Revs.*, **11**: 697-708.

Graham, D. W., Corliss, B. H., Bender, M. L. and Keigwin, L. D., 1981. Carbon and oxygen isotope disequilibria of Recent deep-sea benthic foraminifera. *Mar. Micropal.*, **6**: 483-497.

Grobe, H., 1986. Sedimentation processes on the Antarctic continental margin at Kapp Norvegia during the late Pleistocene. *Geol. Runssch.*, **75**: 97-104.

Grobe, H., Mackensen, A., Hubberten, H.-W., Spiess, V., Futterer, D. K., 1990. Stable isotope record and late Quaternary sedimentation rates at the Antarctic continental margin. In: U. Bleil and J. Thiede (Eds.), *Geological History of the Polar Oceans: Arctic versus Antarctic*. Kluwer Academic Publishers, pp. 539-572.

Grobe, H. and Mackensen, A., 1992. Late Quaternary climatic cycles as recorded in sediments from the Antarctic continental margin. In: J. P. Kennett and D. A. Warnke

(Eds.), *The Antarctic Paleoenvironment: A Perspective on Global Change*. Ant. Res. Ser., 56: 349-376.

Grose, T. J., Johnson, J. A. and Bigg, G. R., 1995. A comparison between the FRAM (Fine Resolution Antarctic Model) results and observations in the Drake Passage. *Deep-Sea Res.*, **42**:365-388.

Grossman, E. L., 1987. Stable isotopes in modern benthic foraminifera: A study of vital effect. *J. Foram. Res.*, **17**: 48-61.

Harland, R., Pudsey, C. J., Howe, J. A., Fitzpatrick, M. E. J., 1998. Recent dinoflagellate cysts in a transect from the Falkland Trough to the Weddell Sea, Antarctica. *Palaeontology*, **41**: 1093-1131.

Harloff, J. and Mackensen, A. 1997. Recent benthic foraminiferal associations and ecology of the Scotia Sea and Argentine Basin. *Mar. Micropal.*, **31**: 1-29.

Hays, J. D., Lozano, J. A., Shackleton, N. J., Irving, G., 1976. Reconstruction of the Atlantic and Western Indian Ocean sectors of the 18,000 BP Antarctic Ocean. In: R. M. Cline and J. D. Hays (Eds.), *Investigation of the Late Quaternary Palaeoceanography and Palaeoclimatology. Geol. Soc. Am. Mem.*, **145**: 337-372.

Herb, R. 1971. Distribution of recent benthonic foraminifera in the Drake Passage. In: L. I. and I. E. Wallens (Eds.), Biology of the Antarctic Seas IV. *Ant. Res. Ser.*, **17**: 251-300.

Herguera, J. C., 1992. Deep-sea benthic foraminifera and biogenic opal: Glacial to postglacial productivity changes in the western equatorial Pacific. *Mar. Micropal.*, **19**: 79-98.

Herguera, J. C. and Berger, W. H., 1991. Paleoproductivity from benthic foraminifera abundance: Glacial to postglacial change in the west-equatorial Pacific. *Geology*, **19**: 1173-1176.

Herguera, J. C. and Berger, W. H., 1994. Glacial to postglacial drop in productivity in the western equatorial Pacific: mixing rate vs. nutrient concentrations. *Geology*, **22**: 629-632.

Heron-Allen, E. and Earland, A., 1922. Protozoa, 2, Foraminifera. British Antarctic (*Terra Nova*) Expedition, 1910. *Nat. Hist. Rept., Zool.*, **6**: 25-268.

Heron-Allen, E. and Earland, A., 1932. Foraminifera, 1, The ice-free area of the Falkland Islands and adjacent seas. *Discovery Rept.*, **4**: 291-460.

Hodell, D. A., Charles, C. D. and Ninnemann, U. S., 2000. Comparison of interglacial stages in the South Atlantic sector of the Southern Ocean for the past 450 kyr: implications f for Marine Isotope Stage (MIS) 11. *Glob. Planet. Change*, **24**: 7-26.

Hoffman, E. E., 1985.The large-scale horizontal structure of the Antarctic Circumpolar Current from FGGE drifters. *J. Geophys. Res.*, **90**: 7087-7097.

Hoffman, E. E. and Whitworth III, T., 1985. A synoptic description of the flow at Drake Passage from year-long measurements. *J. Geophys. Res.*, **90**: 7177-7187.

Honjo, S., Dymond, J., Prell, W. and Ittekkot, V., 1999. Monsoon-controlled export fluxes to the interior of the Arabian Sea. *Deep-Sea Res. II*, **46**: 1859-1902.

Honjo, S., Francois, R., Manganini, S., Dymond, J. and Collier, R., 2000a. Particle fluxes to the interior of the Southern Ocean in the Western Pacific sector along 170°W. *Deep-Sea Res. II*, **47**: 3521-3548.

Honjo, S., Manganini, S., Francois, R., Dymond, J. and Collier, R., 2000b. Export fluxes in t the APFZ and the open Southern Ocean: a sediment trap array investigation along 170°W. *Deep-Sea Res. II*, **47**.

Howard, W. R. and Prell, W. L., 1992. Late Quaternary surface circulation of the Southern Indian Ocean and its relationship to orbital variations. *Paleoceanography*, **7**: 79-118.

Howard, W. R. and Prell, W. L., 1994. Late Quaternary $CaCO_3$ production and preservation in the Southern Ocean: implications for oceanic and atmospheric carbon cycling. *Paleoceanography*, **9**: 453-482.

Howe, J. A., Pudsey, C. J., Cunningham, A. P., 1997. Pliocene-Holocene contourite deposition under the Antarctic Circumpolar Current, Western Falkland Trough, South Atlantic Ocean. *Mar. Geol.*, **138**: 27-50.

Howe, J. A. and Pudsey, C. J., 1999. Antarctic Circumpolar Deep Water: A Quaternary Paleoflow Record from the Northern Scotia Sea, South Atlantic Ocean. *J. Sed. Res.*, **69**: 847-861.

Ikeda, Y., Siedler, G. and Zwierz, M., 1989. On the variability of Southern Ocean front locations between southern Brazil and the Antarctic Peninsula. *J. Geophys. Res.*, **94**: 4757-7462.

Ikehara, M., Kawamurna, K., Ohkouchi, N., Kimoto, K., Murayama, M., Nakamura, T., Oba, T. and Taira, A., 1997. Alkenone sea surface temperature in the Southern Ocean for the last two deglaciations. *Geophys. Res. Letts.*, **24**: 679-682.

Imbrie, J. and Purdy, E. G., 1962. Classification of Bahamian carbonate sediments. *Am. Assoc. Pet. Geol. Mem.*, **7**: 253-272.

Imbrie, J. and Kipp, N., 1971. A new micropaleontological method for quantitative micropaleontology: application to a Late Pleistocene Caribbean core. In: K. K. Turekian (Ed.), *The Late Cenozoic Glacial Ages*. Yale University Press, New Haven, pp. 71-181.

Imbrie, J., Hays, J. D., Martinson, D. G., McIntyre, A., Mix, A. C., Morley, J. J., Pisias, N. G., Prell, W. L. and Shackleton, N. J., 1984. The orbital theory of Pleistocene climate: Support from a revised chronology of the marine $\delta^{18}O$ record. In: A. L. Berger, J. Imbrie, J. D. Hays, G. J. Kukla and B. Satman (Eds.), *Milankovitch and Climate*. Reidel, Dordrecht, pp. 269-305.

Ingólfsson, Ó., Hjort, C., Berkman, P. A., Björk, S., Colhoun, E., *et al.*, 1998. Antarctic glacial history since the Last Glacial Maximum: an overview of the record on land. *Ant. Sci.*, **10**: 326-344.

Ishman, S. E. and Domack, E. W. 1994. Oceanographic controls on benthic foraminifers from the Bellingshausen margin of the Antarctic Peninsula. *Mar. Micropal.*, **24**: 119-155.

Jacobs, S. S., Amos, A. F. and Bruckhausen, P. M., 1970. Ross Sea oceanography and Antarctic Bottom Water formation. *Deep-Sea Res.*, **17**: 935-962.

Jacobs, S. S., Fairbanks, R. and Horibe, Y., 1985. Origin and evolution of water masses near the Antarctic continental margin: Evidence from $H_2{}^{18}O/H_2{}^{16}O$ ratios in seawater. In: Oceanology of the Antarctic Shelf. *Ant. Res. Ser.*, **43**: 59-85.

Jansen, E, and Veum, T., 1990. Evidence for two-step deglaciation and its impact on North Atlantic deep-water circulation. *Nature*, **343**: 612-616.

Johnson, G. C. and Bryden, H. L., 1989. On the size of the Antarctic Circumpolar Current. *Deep-Sea Res.*, **36**: 39-53.

Jones, R. W., 1984. A revised classification of the unilocular Nodosariida and Buliminida (Foraminifera). *Rev. esp. Micropaleont.*, **16**: 91-160.

Jones, R. W., 1994. *The Challenger Foraminifera*. The Natural History Museum, London. Oxford University Press, New York, 149 pp.

Jones, R. W. and Pudsey, C. J, 1994. Recent benthonic foraminifera from the Western Antarctic Ocean. *J. Micropal.*, **13**: 17-23.

Jones, V. J., Hodgson, D. A. and Chepstow-Lusty, A., 2000. Palaeolimnological evidence for marked Holocene environmental changes on Signy Island, Antarctica. *The Holocene*, **10**: 43-60.

Jordan, R. W. and Pudsey, C. J., 1992. High resolution diatom stratigraphy of Quaternary sediments from the Scotia Sea. *Mar. Micropal.*, **19**: 201-237.

Jorissen, F. J., Barmawidjaja, D. M., Puskaric, S. and Van Der Zwaan, G. J., 1992. Vertical distribution of benthic foraminifera in the northern Adriatic: the relation with the organic flux. *Mar. Micropal.*, **19**: 131-146.

Jouzel, J., Lorius, C., Petit, J. R., Genthon, C. K., Barkov, N. I., Kotlyakov, V. M. and Petrov, V. M., 1987b. Vostok ice core: A continuous isotope temperature record over the last climatic cycle (160,000 years). *Nature*, **329**: 403-407.

Jouzel, J., Petit, J. R., Barkov, N. I., Barnola, J. M., Chappellaz, J., Ciais, P., *et al.*, 1992. The last deglaciation in Antarctica: evidence for a "Younger Dryas" type climatic Event. In: E. Bard and W. S. Broecker (Eds.), *Absolute and radiocarbon chronologies*. NATO ASI Series, Springer, Berlin, pp. 229-266.

Jouzel, J., Vaikmae, R., Petit, J. R., Martin, M., Duclos, Y., Stievenard, M., Lorius, C., Toots, M., *et al.*, 1995. The two-step shape and timing of the last deglaciation in Antarctica. *Clim. Dynam.*, **11**: 151-161.

Joyce, T. M., Zenk, W. and Toole, J. M., 1978. The anatomy of the Antarctic Polar Front in the Drake Passage. *J. Geophys. Res.*, **83**: 6093-6113.

Keir, R., 1988. On the late Pleistocene ocean geochemistry and circulation. *Paleoceanography*, **3**: 413-445.

Kellogg, T. B., Osterman, L. E. and Suiver, M., 1979. Late Quaternary sedimentology and benthic foraminiferal paleoecology of the Ross Sea, Antarctica.

Kennett, J. P., 1968. The fauna of the Ross Sea, Part 6 - ecology and distribution of Foraminifera. *New Zealand Dept. of Scientific and Industrial Res. Bull.*, **186**: 1-47.

Kennett, J. P., 1982. *Marine Geology*. Prentice-Hall, Inc., New Jersey, 752 pp.

Killworth, P. D., 1973. A two-dimensional model for the formation of Antarctic Bottom Water. *Deep-Sea Res.*, **20**: 941-971.

Killworth, P. D., 1977. Mixing on the Weddell Sea continental slope. *Deep-Sea Res.*, **24**: 427-448.

King, S. C., Murray, J. W., Kemp, A. E. S., 1998. Palaeoenvironments of deposition of Neogene laminated diatom mat deposits from the eastern equatorial Pacific from studies of benthic foraminifera (sites 844, 849, 851). *Mar. Micropal.*, **35**: 161-177.

Knox, G. A., 1970. Antarctic Marine Ecosystems. In: M. W. Holdgata (Ed.), *Antarctic Ecology, Vol. 1*. Academic Press, London, pp. 69-96.

Knox, G. A., 1994. *The Biology of the Southern Ocean*. Cambridge University Press, 444 pp.

Knox, F. and McElroy, M. B., 1984. Changes in atmospheric CO_2: Influence of the marine biota at high latitude. *J. Geophys. Res.*, **89**: 4629-4637.

Kroopnick, P., 1974. Modelling the O_2 - CO_2 - ^{13}C system in the eastern equatorial Pacific. *Deep-Sea Res.*, **21**: 211-217.

Kroopnick, P., 1980. The distribution of ^{13}C in the Atlantic Ocean. *Earth Planet. Sci. Lett.*, **49**: 469-484.

Kroopnick, P., 1985. The distribution of carbon-13 in the world oceans. *Deep-Sea Res.*, **32**: 57-84.

Kumar, N., Gwaizda, R. and Anderson, R. F., 1993. ^{231}Pa / ^{230}Th ratios in sediments as proxy for past changes in Southern Ocean productivity. *Nature*, **362**: 45-48.

Kumar, N., 1994. *Trace metals and natural radionuclides as tracers of ocean productivity.* PhD dissertation, Columbia University, New York.

Kuramoto, S. and Koyama, K., 1982. Preliminary report of the oceanographic observations on the 22nd Japanese Antarctic Research Expedition (1980-1981). *Memoirs National Institute of Polar research, Special Issue*, **23**:5-12.

Labeyrie, L. D. and Duplessy, J.-C., 1985. Changes in the oceanic ^{13}C / ^{12}C ratio during the last 140,000 years: high-latitude surface water records. *Palaeogeogr., Palaeoclimatol., Palaeoecol.*, **50**: 217-240.

Labeyrie, L. D., Pichon, J. J., Labracherie, M., Ippolito, P., Duprat, J., Duplessy, J. C., 1986. Melting history of Antarctica during the past 60,000 years. *Nature*, **322**: 701-706.

Labeyrie, L. D., Duplessy, J.-C. and Blanc, P. L., 1987. Variations in mode of formation and temperatures of oceanic deep waters over the past 125,000. *Nature.*, **322**: 701-706.

Labracherie, M., Labeyrie, L. D., Duprat, J., Bard, E., Arnold, M., Pichon, J.-J., Duplessy, J.-C., 1989. The last deglaciation in the Southern Ocean. *Paleoceanography*, **4**: 629-638.

LaBrecque, J. L., 1986. Bathymetry, Northeast. In: J. L. LaBrecque (Ed.), *South Atlantic Ocean and adjacent Antarctic continental margin, Atlas 13.* Ocean Margin Drilling Program, Regional Atlas Series: Marine Science International, Woods Hole, MA, sheet 3.

LaBrecque, J. L. and Rabinowitz, P. D., 1977. Magnetic anomalies bordering the continental margin of Argentina. *Map Ser. Cat. 826*, Amer. Assoc. Petrol. Geol., Tulsa, Okla.

LaBrecque, J. L., Rabinowitz, P. D. and Brenner, C., 1981. General Bathymetric chart of the oceans (GEBCO 5:16). Canadian Hydrographic Office, Ottawa.

Lampitt, R. S. and Antia, A. N., 1997. Particle flux in deep seas: regional characteristics and temporal variability. *Deep-Sea Res.*, **44**: 1377-1403.

Landry, M. R., Brown, S. L., Selp, K. E., Abbott, M. R., Letelier, R. M., Christensen, S., Bidigare, R. R. and Casciotti, K. Initiation of the spring phytoplankton increase in the Antarctic Polar Frontal Zone at 170°W. *J. Geophys. Res.*, submitted.

Laubscher, R. K., Perissinotto, R. and McQuaid, C. D., 1983. Phytoplankton production and biomass at frontal zones in the Atlantic sector of the Southern Ocean. *Polar Biol.*, **13**: 471-481.

Lawver, L. A., Gahagan, L. M. and Coffin, M. F., 1992. The development of paleoseaways around Antarctica. In: J. P. Kennett and D. A. Warnke (Eds.), *The Antarctic Paleoenvironment: A Perspective on Global Change.* AGU Ant. Res. Ser., 56: 7-30.

Lazarus, D. and Caule, J. P., 1993. Cenozoic Southern Ocean reconstructions from sedimentologic, radiolarian and other microfossil data. In: J. P. Kennett and P. A. Warnke (Eds.), The Antarctic Paleoenvironment: A Perspective on Global Change II. *Ant. Res. Ser.*, **60**. American Geophysical Union, Washington D.C., pp. 145-174.

Lazier, J. R. N., 1973. The renewal of Labrador Sea water. *Deep-Sea Res.*, **20**: 341-353.

Lea, D., 1995. A trace metal perspective on the evolution of Antarctic Circumpolar Deep Water chemistry. *Paleoceanography*, **10**: 733-748.

Ledbetter, M. T. and Ciesielski, P. F., 1986. Post-Miocene disconformities and paleoceanography in the Atlantic sector of the Southern Ocean. *Palaeogeogr., Palaeoclimatol., Palaeoecol.*, **52**: 185-214.

Ledford-Hoffman, P. A., Demaster, D. J. and Nittrouer, C. C., 1986. Biogenic silica accumulation in the Ross Sea and the importance of the Antarctic continental shelf deposits in the marine silica budget. *Cosmochim. Acta.*, **50**: 2099-2110.

Leventer, A. and Dunbar, R. B., 1988. Recent diatom record of McMurdo Sound, Antarctica: Implications for history of sea ice extent. *Paleoceanography*, **3**: 259-274.

Linke, P. and Lutze, G. H., 1993. Microhabitat preferences of benthic foraminifera – A static concept or dynamic adaptation to optimise food acquisition? *Mar. Micropal.*, **20**: 215-234.

Linke, P., Altenbach, A., Graf, G. and Heeger, T., 1995. Response of deep sea benthic foraminifera to a simulated sedimentation event. *J. Foram. Res.*, **25**: 75-82.

Lisitsin, A. P., 1972. Sedimentation in the World Ocean with emphasis on the nature, distribution and behaviour of marine suspensions. *Soc. Economic Paleontologists and Mineralogists Special Publication*, **17**, 219 pp.

Liss, P. S. and Merlivat, L., 1986. Air-sea gas exchange rates: introduction and synthesis. In: P. Ménard-Buat (Ed.), *The role of air-sea exchange in geochemical cycling*. NATO ASI Series C185, Dordrecht, Boston, pp. 113-127.

Loeblich, A. R. and Tappan, H., 1987. *Foraminiferal genera and their classification*. Van Nostrand Reinhold, New York, 970 pp.

Locarnini, R. A., Whitworth III, T. and Nowlin Jr., W. D., 1993. The importance of the Scotia Sea on the outflow of Weddell Sea Deep Water. *J. Mar. Res.*, **51**: 135-153.

Locarnini, R. A., Heywood, K. J., Watson, A. J., Van Scoy, K. A. and King, B. A., 1996. UK WOCE A23: Oceanographic observations in the Southern Ocean. In: UK Oceanography '96 (abstracts), University of Wales, Bangor, 2-6 September for The Challenger Society for Marine Science.

Loeblich, A. R. and Tappan, H., 1964. Sarcodina, chiefly "Thecamoebians and Foraminiferida". In: R. C. Moore (Ed.), *Treatise on Invertebrate Paleontology, Protista 2, pt. C*. Kansas University Press, 900 pp.

Lohmann, G. P., 1978. Abyssal benthonic foraminifera as hydrographic indicators in the western South Atlantic Ocean. *J. Foram. Res.*, **8**: 6-34.

Lohmann, G. P., 1981. Modern benthic foraminiferal biofacies: Rio Grande Rise. *Transactions of the American Geophysical Union (abs.)*, **62**: 903 pp.

Lorius, C., Merlivat, L., Jouzel, J. and Pourchet, M., 1979. A 30,000-yr isotope climatic record from Antarctic ice. *Nature*, **280**: 644-648.

Loubere, P., 1991. Deep-sea benthic foraminiferal assemblage response to a surface ocean productivity gradient: a test. *Paleoceanography*, **6**: 193-204.

Loubere, P., 1994. Quantitative estimation of surface ocean productivity and bottom water oxygen concentration using benthic foraminifera. *Paleoceanography*, **9**: 723-737.

Loubere, P., 1996. The surface ocean productivity and bottom water oxygen signals in deep water benthic foraminiferal assemblages. *Mar. Micropal.*, **28**: 247-262.

Loubere, P., 1997. Benthic foraminiferal assemblage formation, organic carbon flux and oxygen concentrations on the outer continental shelf and slope. *J. Foram. Res.*, **27**: 93-100.

Loubere, P. and Fariduddin, M., 1999. Benthic foraminifera and the flux of organic carbon to the seabed. In: B. K. Sen Gupta (Ed.), *Modern Foraminifera*. Kluwer, Dordrecht, pp. 181-199.

Lozano, J. A., 1974. Antarctic Sedimentary, Faunal and Sea-Surface Temperature Responses during the last 230,000 Years with Emphasis on Comparison between 18,000 Years Ago and Today. Doctoral dissertation, Columbia University, New York.

Lozano, J. A. and Hays, J. D., 1976. Relationships of radiolarian assemblages to sediment types and physical oceanography in the Atlantic and western Indian sectors of the Antarctic Ocean. In: R. M. Cline and J. D. Hays (Eds.), *Investigation of Late Quaternary Paleoceanography and Paleoclimatology*. Geol. Soc. Am. Mem., 145: 303-336.

Lutjerharms, J. R. E., Walters, N. M. and Allanson, B. R., 1985. Oceanic frontal systems and biological enhancement. In: W. R. Siegfried, P. R. Candy and R. M. Laws (Eds.), *Antarctic Nutrient Cycles and Food Webs*. Spriger-Verlag, pp. 11-21.

Lutze, G.-F. and Coulbourn, W. T., 1984. Recent benthic foraminifera from the continental margin of north-west Africa: Community structure and distribution. *Mar. Micropal.*, **8**: 361-401.

Lutze, G.-F. and Thiel, H., 1987. *Cibicidoides wuellerstorfi* and *Planulina ariminensis*, elevated epibenthic foraminifera. Univ. of Kiel, *Sonderforschungsbereich 313*, **40**: 163-180.

Macdonald, A. M. and Wunsch, C., 1996. An estimate of global ocean circulation and heat fluxes. *Nature*, **382**: 436-439.

Mackensen, A. and Douglas, R. G., 1989. Down-core distribution of live and dead deep-water benthic foraminifera in box cores from the Weddell Sea and California continental borderland. *Deep-Sea Res.*, **36**: 879-900.

Mackensen, A., Grobe, H., Hubberten, H.-W., Spiess, V., Futterer, D.k., 1989. Stable Isotope Stratigraphy from the Antarctic Continental Margin During the Last One Million Years. *Mar. Geol.*, **87**: 315-321.

Mackensen, A., Grobe, H., Kuhn, G., Futterer, D. K., 1990. Benthic foraminiferal assemblages from the eastern Weddell Sea between 68° and 78°S: Distribution, ecology and fossilization potential. *Mar. Micropal.*, **16**: 241-283.

Mackensen, A., Futterer, D. K., Grobe, H., Schmiedl, G., 1993a. Benthic foraminiferal assemblages from the eastern South Atlantic Polar Front region between 35° and 57°S: Distribution, ecology and fossilization potential. *Mar. Micropal.*, **22**: 33-69.

Mackensen, A., Hubberten, H.-W., Bickert, T., Fischer, G. and Fütterer, D. K., 1993b. The $\delta^{13}C$ in benthic foraminiferal tests of *Fontbotia Wuellerstorfi* (Schwager) relative to the $\delta^{13}C$ of dissolved inorganic carbon in Southern Ocean deep water: Implications for glacial ocean circulation models. *Paleoceanography*, **8**: 587-610.

Mackensen, A., Grobe, H., Hubberten, H.-W., Kuhn, G., 1994. Benthic foraminiferal assemblages and the $\delta^{13}C$ signal in the Atlantic sector of the Southern Ocean: glacial-to-interglacial contrasts. In: R. Zahn, *et al.* (Eds.), *Carbon Cycling in the Glacial Ocean: Constraints on the Ocean's Role in Global Change*. NATO ASI Ser., 117: 105-135.

Mackensen, A., Schmiedl, G., Harloff, J., Giese, M., 1995. Deep-sea foraminifera in the South Atlantic Ocean: ecology and assemblage generation. *Micropalaeontology*, **41**: 342-358.

Mackensen, A., Hubberten, H.-W., Scheele, N. and Schlitzer, R., 1996. Decoupling of $\delta^{13}C_{\Sigma CO2}$ and phosphate in Recent Weddell Sea deep and bottom water: Implications for glacial Southern Ocean paleoceanography. *Paleoceanography*, **11**: 203-215.

Mackensen, A. and Bickert, T., 1999. Stable Carbon Isotopes in Benthic Foraminifera: Proxies for Deep and Bottom water Circulation and New Production. In: G. Fischer and G. Wefer (Eds.), *Use of Proxies in Paleoceanography*. Springer-Verlag, Germany, pp. 229-254.

Mackintosh, N. A., 1946. The Antarctic Convergence and the distribution of surface temperatures in Antarctic waters. *Discovery Reports*, **23**: 177-212.

Malmgren, B. A. and Kennett, J. P., 1976b. Principal component analysis of Quaternary planktic foraminifera in the Gulf of Mexico: paleoclimatic applications. *Mar. Micropal.*, **1**: 299-306.

Malmgren, B. A. and Haq, B. U., 1982. Assessment of Quantitative Techniques in Paleobiogeography. *Mar. Micropal.*, **7**: 213-236.

Mantyla, A. W. and Reid, J. L., 1983. Abyssal characteristics of the world ocean waters. *Deep-Sea Res.*, **30**: 805-833.

Martin, J. H., Knauer, G. A., Karl, D. and Broenkow, W., 1987. VERTEX: carbon cycling in the northeast Pacific. *Deep-Sea Res.*, **34**: 267-286.

Martin, J. H., Fitzwater, S. E. and Gordon, R. M., 1990. Iron deficiency limits phyto-plankton growth in the Antarctic waters. *Global Biogeochem. Cycles*, **4**: 5-12.

Martinson, D. G., Pisias, N. G., Hays, J. D., Imbrie, J., Moore Jr., T. C. and Shackleton, N. J., 1987. Age dating and the orbital theory of the Ice Ages: Development of a high resolution 0 to 300,000-years chronostratigraphy. *Quat. Res.*, **27**: 1-29.

Martinson, D. G. and Iannuzzi, R. A., 1998. Antarctic ocean-ice interaction: implications from ocean bulk property distributions in the Weddell Gyre. *Ant. Res. Ser.*, **74**, pp. 243-271.

Maslennikov, V. V. and Solyankin, Ye. V., 1979. Interannual displacements of the zone of interaction of Weddell Sea waters with the Antarctic Circumpolar Current. *Polar Geog. and Geol.*, **5**: 45-50.

McCorkle, D. C., Keigwin, L. D., Corliss, B. H. and Emerson, S. R., 1990. The influence of microhabitats on the carbon isotopic composition of deep-sea benthic foraminifera. *Paleoceanography*, **5**: 161-185.

McKnight, Jr. W. M., 1962. The Distribution of foraminifera off parts of the Antarctic coast. *Bull. Am. Paleont.*, **44**: 65-158.

McManus, J. F., Oppo, D. W. and Cullen, J. L., 1999. A 0.5 million-year record of millenial-scale climate variability in the North Atlantic. *Science*, **283**: 971-975.

Mead, G. A., 1985. Recent benthic foraminifera in the Polar Front region of the Southwest Atlantic. *Micropaleontology*, **31**: 221-248.

Mead, G. A. and Kennett, J. P., 1987. The distribution of recent benthic foraminifera in the Polar Front region, Southwest Atlantic. *Mar. Micropal.*, **11**: 343-360.

Meredith, M. P., Locarnini, R. A., Van Scoy, K. A., Watson, A. J., Heywood, K. J. and King, B. A., 2000.On the sources of Weddell Gyre Antarctic Bottom Water. *J. Geophys. Res.*, **105**: 1093-1104.

Michel, R. L., 1984. Oceanographic structure of the eastern Scotia Sea – Chemical oceanography. *Deep-Sea Res.*, **31**: 1157-1168.

Mikolajewicz, U., 1996. A meltwater induced collapse of the "conveyor belt". *Report of the Max-Planck Inst. fur Meteorol.*, **189**: 1-25.

Milam, R. W. and Anderson, J. B., 1981. Distribution and ecology of recent benthonic foraminifera of the Adelie-George V continental shelf and slope, Antarctica. *Mar. Micropal.*, **6**: 297-325.

Mitchell, B. G., Brody, E. A., Holm-Hansen, O., McClain, C. and Bishop, J., 1991. Light limitation of phytoplankton biomass and macronutrient utilisation in the Southern Ocean. *Limnology and Oceanography*, **36**: 1662-1677.

Mix, A. C., 1987. The oxygen isotope record of glaciation. In: W. F. Ruddiman and H. E. Wright Jr (Eds.), *North America and Adjacent Oceans During the Last Deglaciation, The Geology of North America*. Vol. K-3, Geol. Soc. Am., Boulder, pp. 111-135.

Mix, A. C., 1989. Influence of productivity variations on long term atmospheric CO_2. *Nature*, **337**: 541-544.

Mix, A. C. and Fairbanks, R. G., 1985. North Atlantic surface-ocean control of Pleistocene deep ocean circulation. *Earth Planet. Sci. Letts.*, **73**: 321-243.

Molinelli, E, J,. 1978. Isohaline thermoclines in the southeast Pacific Ocean. *J. Phys. Oceanogr.*, **8**: 1139-1145.

Molinelli, E. J., 1981. The Antarctic influence on Antarctic Intermediate Water. *J. Mar. Res.*, **39**: 267-293.

Moore, J. K., Abbott, M. R., Richman, J. G., Smith, W. O., Cowles, T. J., Coale, K. H., Gardner, W. D. and Barber, R. T., 1999. Sea WiFS satellite ocean color data at the U.S. Southern Ocean JGOFS line along 170°W. *Geophys. Res. Letts.*, **26**: 1465-1468.

Morley, J. J. and Hays, J. D., 1979. Comparison of glacial and interglacial oceanographic conditions in the South Atlantic from variations in calcium carbonate and radiolarian distributions. *Quat. Res.*, **12**: 396-408.

Morley, J. J., 1989. Variations in high-latitude oceanographic fronts in the Southern Indian Ocean: An estimation based on faunal changes. *Paleoceanography*, **4**: 547-554.

Mortlock, R. A., Charles, C. D., Froelich, P. N., Zibello, M. A., Saltzman, J., Hays, J. D., Burckle, L. H., 1991. Evidence for lower productivity in the Antarctic Ocean during the last glaciation. *Nature*, **351**: 220-223.

Mosby, H., 1934. The waters of the Atlantic Antarctic Ocean. *Sci. Results Norw. Antarct. Exped. 1927-1928,* **11**: 1-131.

Mulitza, S., Arz, H., Kemle-von Mücke, S. and Moos, C., Niebler, H.-S., Pätzold, J. and Segl, M., 1999. The South Atlantic Carbon Isotope Record of Planktic Foraminifera. In: G. Fischer and G. Wefer (Eds.), *Use of Proxies in Paleoceanography*. Springer-Verlag, Germany, pp. 427-445.

Mullan, A. B. and Hickman, J. S., 1990. Meteorology. In: G. P. Glasby (Ed.), *Antarctic Sector of the Pacific*. Elsevier Oceanographic Series, **51**. New York, pp. 21-54.

Müller, P. J. and Suess, E., 1979. Productivity, sedimentation rate, and sedimentary organic matter in the oceans – I. Organic carbon preservation. *Deep-Sea Res.*, **26A**: 1347-1362.

Murray, J. W., 1973. *Distribution and ecology of living benthic foraminiferids*. Crane Russac and Co., New York, 27 pp.

Murray, J. W., 1991. *Ecology and Palaeoecology of Benthic Foraminifera*. Longman, Essex, 397 pp.

Nees, S., Altenbach, A. V., Kassens, H. and Thiede, J., 1997. High-resolution record of foraminiferal response to late Quaternary sea-ice retreat in the Norwegian-Greenland Sea. *Geology*, **25**: 659-662.

Nelson, D. M. and Gordon, L. I., 1982. Production and pelagic dissolution of biogenic silica in the Southern Ocean. *Geochim. Cosmochim. Acta*, **46**: 491-501.

Newsom, K. L., Francavillese, L. and Tierney, J., 1965. Oceanography. In: *Operation Deep Freeze 62, 1961-1962, Marine Geophysical Investigations*. TR-118 U.S. Naval Oceanographic Office, Washington D.C., pp. 8-38.

Niebler, H.-S. and Gersonde, R., 1998. A planktic foraminiferal transfer function for the southern South Atlantic Ocean. *Mar. Micropal.*, **34**: 213-234.

Niebler, H.-S., Hubberten, H.-W. and Gersonde, R., 1999. Oxygen Isotope Values of Planktic Foraminifera: A Tool for the Reconstruction of Surface Water Stratification. In: G. Fischer and G. Wefer (Eds.), *Use of Proxies in Paleoceanography*. Springer-Verlag, Germany, pp. 165-189.

Ninnemann, U. S. and Charles, C. D., 1997. Regional differences in Quaternary Subantarctic nutrient cycling: Link to intermediate and deep water ventilation. *Paleoceanography*, **12**: 560-567.

Ninnemann, U. S., Charles, C. D. and Hodell, D. A., 1999. Origin of Global Millennial Scale Climate Events: Constraints from the Southern Ocean Deep Sea Sedimentary Record. In: P. U. Clark, R. S. Webb and L. D. Keigwin (Eds.), *Mechanisms of Global Climate at Millennial Time Scales*. Geophys. Monogr. Ser., 112: 99-112.

Nowlin, W. D., Whitworth III, T. and Pillsbury, R. D., 1977. Structure and transport of the Antarctic Circumpolar Current at Drake Passage from short-term measurements. *J. Phys. Oceanogr.*, **7**: 788-802.

Nowlin Jr., W. D. and Clifford, M., 1982. The kinematic and thermohaline structure of the Antarctic Circumpolar Current at Drake Passage. *J. Mar. Res.*, **40**: 481-507.

Nowlin Jr., W. D. and Klinck, J. M., 1986. The physics of the Antarctic Circumpolar Current. *Rev. Geophys.*, **24**: 469-491.

Nowlin Jr., W. D. and Zenk, W., 1988. Currents along the margin of the South Shetland Island Arc. *Deep-Sea Res.*, **35**: 269-301.

Nürnberg, C. C., Bohrmann, G., Schlüter. M. and Frank, M., 1997. Barium accumulation in the Atlantic sector of the Southern Ocean: Results from 190,000-year records. *Paleoceanography*, **12**: 594-603.

Nyholm, K. G., 1961. Morphogenesis and biology of the foraminifer *Cibicides lobatulus*. *Zoologiska Bidrag Fran Uppsala,* **33**: 157-196.

Olausson, E., 1965. Evidence of Climate Changes in North Atlantic Deep-Sea Cores. In: M. Sears (Ed.), *Progress in Oceanography*. Pergamon Press, New York, pp. 221-254.

Oppo, D. W. and Fairbanks, R. G., 1987. Variability in the deep and intermediate water circulation of the Atlantic Ocean during the past 12,000 years: Northern hemisphere modulation of the Southern Ocean. *Earth Planet. Sci. Letts.*, **86**: 1- 15.

Oppo, D. W., Fairbanks, R. G., Gordon, A. L. and Shackleton, N. J., 1990. Late Pleistocene Southern Ocean $\delta^{13}C$ Variability. *Paleoceanography*, **5**: 43-54.

Orsi, A. H., Whitworth, T. III, Nowlin, W. D. Jr., 1995. On the meridional extent and fronts of the Antarctic Circumpolar Current. *Deep-Sea Res.*, **42**: 641-673.

Ostapoff, F., 1962. On the frictionally induced transverse circulation of the Antarctic Circumpolar Current. *Deutsche Hydrographische Zeitschrift*, **15**: 103-113.

Osterman, L. E. and Kellogg, T. B., 1979. Recent benthic foraminiferal distributions from the Ross Sea, Antarctica: relation to ecologic and oceanographic conditions. *J. Foram. Res.*, **9**: 250-269.

Parker, W. C. and Arnold, J. A., 1999. Quantitative methods of data analysis in foraminiferal ecology. In: B. K. Sen Gupta (Ed.), *Modern Foraminifera*. Kluwer Academic Publishers, U.K., pp. 71-89.

Parr, W. J., 1950. Foraminifera. *Rept. B.A.N.Z. Antarctic Res. Exped., 1929-1931, Ser. B,* **5**: 235-392.

Patterson, S. L. and Sievers, H. A., 1980. The Weddell-Scotia Confluence. *J. Phys. Oceanogr.*, **10**: 1548-1610.

Pederson, T. F., Pickering, M., Vogel, J. S., Southon, J. N. and Nelson, D. E., 1988. The response of benthic foraminifera to productivity cycles in the eastern equatorial Pacific: Faunal and geochemical constraints on glacial bottom water levels. *Paleoceanography*, **3**: 157-168.

Peeken, I., 1997. Photosynthetic pigment fingerprints as indicators of phytoplankton biomass and development in different water masses of the Southern Ocean during austral spring. *Deep-Sea Res. II*, **44**: 261-282.

Peet, R. K., 1974. The measurement of species diversity. *Annual Review Of Ecology and Systematics*, **5**: 285-307.

Peltier, W. R., 1993. *Ice in the climate system.* Proceedings of the NATO Advanced Research Workshop Ice in the climate system. Springer-Verlag, Berlin, 673 pp.

Peterson, R. G., 1992. The boundary currents of the western Argentine Basin. *Deep-Sea Res.*, **39**: 623-644.

Peterson, R. G. and Whitworth III, T., 1989.The Subantarctic and Polar fronts in relation to deep water masses through the southwestern Atlantic. *J. Geophys. Res.*, **94**: 10817-10835.

Peterson, R. G. and Stramma, L., 1991. Upper-level circulation in the South Atlantic Ocean. *Prog. Oceanogr.*, **26**: 1-73.

Pflum, C. E., 1966. The distribution of foraminifera in the Eastern Ross Sea, Amundsen Sea and Bellingshausen Sea, Antarctica. *Bull. Am. Paleont.*, **50**: 146-209.

Phleger, F. B. and Soutar, A., 1973. Production of benthic foraminifera in three east Pacific oxygen minima. *Micropaleontology*, **19**: 110-115.

Phleger, F. B., 1964. Foraminiferal ecology and marine geology. *Mar. Geol.*, **1**: 16-43.

Pielou, E. C., 1974. *Population and Community Ecology: Principles and Methods.* Gordon and Breach Science Publishers, New York, 424 pp.

Pielou, E. C., 1975. *Ecological Diversity.* John Wiley & Sons Inc., New York, 165 pp.

Pielou, E. C., 1979. A quick method of determining the diversity of foraminiferal assemblages. *J. Paleontol.*, **53**: 1237-1242.

Piola, A. R. and Gordon, A. L., 1989. Intermediate waters in the southwest South Atlantic. *Deep-Sea Res.*, **36**: 1-16.

Pisias, N. G., Martinson, D. G., Moore Jr., T. C., Shackleton, N. J., Prell, W. L., Hays, J. D. and Boden, G., 1984. High resolution stratigraphic correlation of benthic oxygen isotopic records spanning the last 300,000 years. *Mar. Geol.*, **56**: 119-136.

Pondaven, P., Ragueneau, O., Tréguer, P., Hauvespre, A., Dezileau, L. and Reyss, J. L., 2000. Resolving the 'opal paradox' in the Southern Ocean. *Nature*, **405**: 168-175.

Prell, W. L., Hutson, W. H., Williams, D. F., Bé, A. W. H., Geitzenaur, K. and Molfino, B., 1980. Surface circulation in the Indian Ocean during the last glacial maximum, approximately 18,000 years B.P., *Quat. Res.*, **14**: 309-336.

Prell, W. L., Garner, J. W., *et al.*, 1982. Init. Rep. DSDP 68.

Prell, W. L., Imbrie, J., Martinson, D. G., Morley, J. J., Pisias, N. G., Shackleton, N. J. and Streeter, H. F., 1986. Graphic correlation of oxygen isotope stratigraphy application to the late Quaternary. *Paleoceanography.*, **1**: 137-162.

Pudsey, C. J., Barker, P. F., Hamilton, N., 1988. Weddell Sea abyssal sediments: a record of Antarctic Bottom Water flow. *Mar. Geol.*, **81**: 289-314.

Pudsey, C. J., 1992. Late Quaternary changes in Antarctic Bottom Water velocity inferred from sediment grain size in the northern Weddell Sea. *Mar. Geol.*, **107**: 9-34.

Pudsey, C. J., 1993. Calibration of a point-counting technique for estimation of biogenic silica in marine sediments. *J. Sed. Petrol.*, **63**: 760-762.

Pudsey, C. J. and Howe, J. A., 1998. Quaternary history of the Antarctic Circumpolar Current: evidence from the Scotia Sea. *Mar. Geol.*, **148**: 83-112.

Pujol, C. and Bourrouilh, R., 1991. Late Miocene to Holocene planktonic foraminifers from t the subantarctic South Atlantic. *Proc. ODP, Sci. Results*, **114**: 217-228.

Purkerson, D. G. and Millero, F. J., 1996. CO_2 and Nutrients in the Southern Ocean. *U.S. JGOFS Newletter, December*, Vol.8, No.1, p.8.

Quéguiner, B., Tréguer, P., Peeken, I. And Scharek, R., 1997. Biogeochemical dynamics and the silicon cycle in the Atlantic sector of the Southern Ocean during austral spring 1992. *Deep-Sea Res. II*, **44**: 69-89.

Ragueneau, O., Tréguer, P., Leynaert, A., Anderson, R. F., Brzezinski, M. A. *et al.*, 2000. A review of the Si cycle in the modern ocean: recent progress and missing gaps in the application of biogenic opal as a paleoproductivity proxy. *Glob. Planet. Change*, **26**: 317-365.

Rathburn, A. E., Pichon, J.-J., Ayress, M. A., De Dekker, P., 1997. Microfossil and stable-isotope evidence for changes in Late Holocene palaeoproductivity and palaeoceanographic conditions in the Prydz Bay region of Antarctica. *Palaeogeog., Palaeoclim., Palaeoecol.*, **131**: 485-510.

Raymo, M. E., Ruddiman, W. F., Shackleton, N. J. and Oppo, D. W., 1990. The evolution of Atlantic-Pacific $\delta^{13}C$ gradients over the last 2.5 myrs: Evidence for decoupling of deep ocean circulation and global ice volume changes. *Earth Planet Sci. Letts.*, **97**: 353-368.

Raymo, M. E., Oppo, D. W. and Curry, W., 1997. The mid-Pleistocene climate transition: A deep sea carbon isotope perspective. *Paleoceanography*, **12**: 546-559.

Reid, J. L., 1989. On the total geostrophic circulation of the South Atlantic Ocean: flow patterns, tracers and transports. *Progress in Oceanography*, **23**: 149-244.

Reid, J. R., 1996. On the Circulation of the South Atlantic Ocean. In: G. Wefer, G. Berger, W. H. Siedler and D. J. Webb (Eds.), *The South Atlantic: Present and Past Circulation*. Springer, Berlin, pp. 13-44.

Rice, A. L., Billett, D. S. M., Fry, J., John, A. W. G., Lampitt, R. S., Mantoura, R. F. C. and Morris, R. J., 1986. Seasonal deposition of phytodetritus to the deep sea floor. *Proc. R. Soc. Edinb.*, **88B**: 265-279.

Riemann, F., 1989. Gelatinous phytoplankton detritus aggregates on the Atlantic deep-sea bed. Structure and mode of formation. *Mar. Biol.*, **100**: 533-539.

Rintoul, S. R., 1998. On the origin and influence of Adélie Land bottom water. In: S. S. Jacobs and R. F. Weiss (Eds.), *Ocean, Ice and Atmosphere. Interactions at the Antarctic Continental Margin*. Ant. Res. Ser., 75, Am. Geophys. Un., Washington, pp. 151-171.

Robinson, S. G., 1990. Applications for whole-core magnetic measurements of deep-sea sediments: Leg 115 results. *Proc. ODP, Sci. Results*, **115**: 737-771.

Saidova, Kh. M., 1961. The Quantitative distribution of bottom foraminifera in Antarctica. *Doklady Akademii Nauk SSSR*, **139**: 967-969.

Sarnthein, M., Pflaumann, U., Ross, R., Thiedemann, R. and Winn, K., 1992. Transfer functions to reconstruct ocean paleoproductivity: a comparison. In: C. P. Summerhays, W. L. Pfell and K.-C. Emeis (Eds.), *Evolution of Upwelling Systems*. Geol. Soc. Lon. Spec. Publ., 64: 411-427.

Sarnthein, M., Winn, K., Jung, S. J. A., Duplessy, J.-C., Labeyrie, L., Erlenkeuser, H. and Ganssen, G., 1994. Changes in east Atlantic deepwater circulation over the last 30,000 years: Eight time slice reconstructions. *Paleoceanography*, **9**: 209-267.

Schmeidl, G. and Mackensen, A., 1997. Late Quaternary paleoproductivity and deep water circulation in the eastern South Atlantic Ocean: Evidence from benthic foraminifera. *Palaeogeogr., Palaeoclimatol., Palaeoecol.*, **130**: 43-80.

Schmeidl, G., Mackensen, A. and Müller, P. J., 1997. Recent benthic foraminifera from the eastern South Atlantic Ocean: Dependence on food supply and water masses. *Mar. Micropal.*, **32**: 231-287.

Schnitker, D., 1974. West Atlantic abyssal circulation during the past 120,000 years. *Nature*, **248**: 385-387.

Schnitker, D., 1979. The deep waters of the western North Atlantic during the past 24,000 years, and the re-initiation of the Western Boundary Undercurrent. *Mar. Micropal.*, **4**: 265-80.

Schnitker, D., 1980. Quaternary deep-sea benthic foraminifers and bottom water masses. *Ann. Rev. Earth Planet. Sci.*, **8**: 343-370.

Schnitker, D., 1994. Deep-sea benthic foraminifera: food and bottom water masses. In: R. Zahn, *et al* (Eds.), *Carbon cycling in the global ocean: constraints on the ocean's role in global change*. Springer-Verlag, NATO ASI Series, 117: 539-554.

Seabroke, J. M., Hufford, G. L. and Elder, R. B., 1971. Formation of Antarctic Bottom Water in the Weddell Sea. *J. Geophys. Res.*, **76**: 2164-2178.

Sen Gupta, B. K., 1999. Introduction to modern Foraminifera. In: B. K. Sen Gupta (Ed.), *Modern Foraminifera*. Kluwer Academic Publishers, Dordrecht, pp. 3-6.

Sen Gupta, B. K. and Machain-Castillo, M. L., 1993. Benthic foraminifera in oxygen-poor habitats. *Mar. Micropal.*, **20**: 183-201.

Shackleton, N. J., 1967. Oxygen isotope analyses and Pleistocene temperature reassessed. *Nature.*, **215**: 15-17.

Shackleton, N. J., 1977. Carbon-13 in *Uvigerina*: tropical rainforest history and the Equatorial Pacific carbonate dissolution cycles. In: N. R. Anderson and A. Malahoff (Eds.), *The Fate of Fossil Fuel CO_2 in the Oceans*. Plenum, New York, pp. 401-427.

Shackleton, N. J. and Opdyke, N. D., 1973. Oxygen isotope and palaeomagnetic stratigraphy of equatorial Pacific core V28-238: Oxygen isotope temperature and ice volumes on a 10,000 year and 100,000 year time scale. *Quat. Res.*, **3**: 39-55.

Shemesh, A., Macko, S. A., Charles, C. D. and Rau, G. H., 1993. Isotopic Evidence for reduced productivity in the Glacial Southern Ocean. *Science*, **262**: 407-410.

Shimmield, G. B., 1992. Can sediment geochemistry record changes in coastal upwelling palaeoproductivity? Evidence from northwest Africa and the Arabian Sea. In: C. P. Summerhays, W. Prell and K. C. Emeis (Eds.), *Upwelling Systems Since the Early Miocene*. Geol. Soc. London, Spec. Publ., 64: 29-46.

Shimmield, G., Derrick, S., Mackensen, A., Grobe, H., Pudsey, C. J., 1994. The history of barium, biogenic silica and organic carbon accumulation in the Weddell Sea and Antarctic Ocean over the last 150,000 years. In: R. Zahn *et al.* (Eds.), *Carbon Cycling in the Glacial Ocean: Constraints on the Ocean's Role in Global Change*. NATO, ASI Ser., 117: 555-574.

Sievers, H. A. and Emery, W. J., 1978. Variability of the Antarctic Polar Frontal Zone in Drake Passage – Summer 1976-1977. *J. Geophys. Res.*, **83**: 3010-3022.

Sievers, H. A. and Nowlin Jr., W. D., 1984. The stratification and water masses at Drake Passage. *J. Geophys. Res.*, **89**: 10489-10514.

Singer, A. J. and Shemesh, A., 1995. Climatically linked carbon isotope variation during the past 430,000 years in Southern Ocean sediments. *Paleoceanography*, **10**: 171-177.

Smart, C. W., King, S. C., Gooday, A. J., Murray, J. W., Thomas, E., 1994. A benthic foraminiferal proxy of pulsed organic matter paleofluxes. *Mar. Micropal.*, **23**: 89-99.

Smetacek, V., De Baar, H. J., Bathmann, U. V., Lochte, K. and Rutgers Van Der Loeff, M. M., 1997. Ecology and biogeochemistry of the Antarctic Circumpolar Current during austral spring: a summary of Southern Ocean JGOFS cruise ANT X/6 of R.V. *Polarstern. Deep-Sea Res. II*, **44**: 1-21.

Smith, N. R., Zhaoqian, D., Kerry, K. R. and Wright, S., 1984. Water masses and circulation in the region of Prydz Bay, Antarctica. *Deep-Sea Res.*, **31**: 1121-1147.

Smith Jr., W. O. and Nelson, D. M., 1985. Phytoplankton biomass near a receding ice-edge in the Ross Sea. In: W. R. Siegfried, P. R. Condy and R. M. Laws (Eds.), *Antarctic Nutrient Cycles and Food Webs*. Springer, New York, pp. 70-77.

Smith Jr, W. O., Anderson, R. F., Moore, J. K., Codispoti, L. A. and Morrison, J. M., 2000. The US Southern Ocean Joint Global Ocean Flux Study: an introduction to AESOPS. *Deep-Sea Res. II*, **47**: 3073-3093.

Stein M. and Heywood, R. B., 1994. Antarctic environment - physical oceanography: The Antarctic Peninsula and Southwest Atlantic region of the Southern Ocean. In: S. Z. El-Sayed (Ed.), *Southern Ocean Ecology: the BIOMASS perspective*. Cambridge University Press, pp. 11-24.

Stommel, H. M. and Arons, A. B., 1960a. On the abyssal circulation of the world ocean. I. Stationary planetry flow patterns on a sphere. *Deep-Sea Res.*, **6**: 140-154.

Stommel, H. M. and Arons, A. B., 1960b. On the abyssal circulation of the world ocean. II. An idealised model of the circulation pattern and amplitude in oceanic basins. *Deep-Sea Res.*, **6**: 217-233.

Stramma, L. and Peterson, G., 1990. The South Atlantic Current. *J. Phys. Oceanogr.*, **20**: 846-859.

Streeter, S. S., 1973. Bottom water and benthonic foraminifera in the North Atlantic – Glacial-interglacial contrasts. *Quat. Res.*, **3**: 131-141.

Streeter, S. S. and Shackleton, N. J., 1979. Paleocirculation of the deep North Atlantic: 150,000 year record of benthic foraminifera and oxygen-18. *Science*, **203**: 168-171.

Suess, E., 1980. Particulate organic carbon flux in the oceans – surface productivity and oxygen utilisation. *Nature*, **288**: 260-263.

Taylor, H. W., Gordon, A. L. and Molinelli, E., 1978. Climatic characteristics of the Antarctic Polar Front Zone. *J. Geophys. Res.*, **83**: 4572-4578.

Tchernia, P., 1980. *Descriptive Regional Oceanography*. Pergamon, Oxford, 252 pp.

Thiel, H., Pfannkuche, O., Shriever, G., Lochte, K., Gooday, A. L., Hemleben, C., *et al.*, 1990. Phytodetritus on the deep-sea floor in a central oceanic region of the northeast Atlantic. *Biol. Oceanogr.*, **6**: 203-239.

Thomas, E., Booth, C., Maslin, M. and Shackleton, N. J., 1992. Northeastern Atlantic benthic foraminifera during the last 30,000 years. In: ICP IV. (Kiel, Germany.) Abstr. Vol.

Thomas, E., Booth, C., Maslin, M., Shackleton, N. J., 1995. Northeastern Atlantic benthic foraminifera during the last 45,000 years: changes in productivity seen from the bottom up. *Paleoceanography*, **10**: 545-562.

Thunell, R. C., 1976. Optimum indices of calcium carbonate dissolution in deep-sea sediments. *Geology*, **4**: 525-528.

Thunell, R. C., Williams, D. F. and Kennett, J. P., 1977. Late Quaternary paleoclimatology, stratigraphy and sapropel histry in eastern Mediterranean deep-sea sediments. *Mar. Micropal.*, **2**: 371-388.

Thurston, M. H., Bett, B. J., Rice, A. L. and Jackson, P. A. B., 1994. Variations in the invertebrate abyssal megafaunas in the North Atlantic Ocean. *Deep-Sea Res.*, **41**: 1321-1348.

Tréguer, P. and Jacques, G., 1992. Dynamics of nutrients and phytoplankton, and fluxes of carbon, nitrogen and silicon in the Antarctic Ocean. *Polar Biol.*, **12**: 149-162.

Uchio, T., 1960. Benthonic foraminifera of the Antarctic Ocean. *Seto Marine Biol. Lab. Spec. Publ.*, **12**: 3-20.

Van der Zwaan, G., 1982. Paleo-oceanographical reconstructions by means of Foraminifera. *Bull. Societe de Geologie ge France*, **24**: 589-596.

Van der Zwaan, G. J. and Jorissen, F. J., 1991. Biofacial patterns in river-induced shelf anoxia. In: R. V. Tyson and T. H. Pearson (Eds.), *Modern and Ancient Continental Shelf Anoxia*. Geol. Soc. Spec. Publ., 58: 65-82.

Verlencar, X. N. and Dhargalkar, V. K., 1992. Primary productivity and nutrients in the Indian sector of the Southern Ocean. *Indian Journal Mar. Sci.*, **21**: 6-12.

Veth, C., Peeken, I. And Scharek, R., 1997. Physical anatomy of fronts and surface waters in the ACC near the 6°W meridian during austral spring 1992. *Deep-Sea Res. II*, **44**: 23-49.

Violanti, D., 1996. Taxonomy and distribution of recent benthic foraminifers from Terra Nova Bay (Ross Sea, Antarctica), Oceanographic campaign 1987/1988. *Palaeontographia Italica*, **83**: 25-71.

Wadhams, P., 2000. *Ice in the Ocean*. Gordon and Breach Science Publishers, Amsterdam, 351pp.

Ward, B. L., Barrett, P. J. and Vella, P., 1987. Distribution and ecology of benthic foraminifera in McMurdo Sound, Antarctica. *Palaeogeog., Palaeoclimatol., Palaeoecol.*, **58**: 139-153.

Warner, M. J. and Weiss, R. F., 1992. Chlorofluoromethanes in South Atlantic Antarctic Intermediate Water. *Deep-Sea Res.*, **32**: 1485-1497.

Warren, B. A., 1981. Deep circulation of the world ocean. In: B. A. Warren and C. Wunsch (Eds.), *Evolution of Physical Oceanography*. The MIT Press, Cambridge, MA: pp. 6-41

Watanabe, K. and Nakajima, Y., 1982. Vertical distribution of chlorophyll a along 45°E in the Southern Ocean, 1981. *Memoirs National Institute of Polar Research, Special Issue*, **23**: 73-86.

Weaver, P. P. E., Neil, H. and Carter, L., 1997. Sea surface temperature estimates from the Southwest Pacific based on planktonic foraminifera and oxygen isotopes. *Palaeogeogr., Palaeoclimatol., Palaeoecol.*, **131**: 241-256.

Weaver, P. P. E., Carter, L., Neil, H. L., 1998. Response of surface water masses and circulation to late Quaternary climate change east of New Zealand. *Paleoceanography*, **13**: 70-83.

Wefer, G. and Fischer, G., 1991. Annual primary productivity and export flux in the Southern Ocean from sediment trap data. *Mar. Chem.*, **35**: 597-613.

Wefer, G., Berger, W. H., Bijma, J. and Fischer, G., 1999. Clues to Ocean History: a Brief Overview of Proxies. In: G. Fischer and G. Wefer (Eds.), *Use of Proxies in Paleoceanography*. Springer-Verlag, Berlin, pp. 1-68.

Weiss, R. F., Ostlund, H. G., Craig, H., 1979. Geochemical studies of the Weddell Sea. *Deep-Sea Res.*, **26A**: 1093-1120.

Weiss, R. F. and Bullister, J. L., 1984. Chlorofluoromethanes in the Southern Ocean: The ventilation of the Weddell Gyre (abstract). *EOS Trans. AGU*, **65**: 915.

Wells, P., Wells, G., Cali, J. and Chivas, A., 1994. Response of deep-sea benthic foraminifera to Late Quaternary climate changes, southeast Indian Ocean, offshore Western Australia. *Mar. Micropal.*, **23**: 185-229.

Wenk, T. and Siegenthaler, U., 1985. The high-latitude ocean as a control of atmospheric CO_2. In: E. Sundquist and W. S. Broecker (Eds.), *The Carbon Cycle and Atmospheric CO_2: Natural Variations Archean to Present.* AGU Geophys. Monogr. Ser., 32: 185-194.

Westal, F. and Fenner, J., 1990. Polar Front fluctuations and the Upper Gauss to Brunhes paleoceanographic record in the southeast Atlantic Ocean. In: U. Bleil and J. Thiede

(Eds.), *Geological History of the Polar Oceans: Arctic Versus Antarctic*. Kluwer Academic Publishers, Netherlands, pp. 761-782.

Weston, J. F. and Murray, J. W., 1984. Benthic foraminifera as deep-sea water mass indicators. In: *Benthos '83, 2nd International Symposium on Benthic Foraminifera, Pau, April 1983*, pp. 605-610.

Weyl, P. K., 1968. The role of the oceans in climate change: a theory of the ice ages. *Meteorolo. Monogr.*, **8**: 37-62.

Whitworth III, T., 1980. Zonation and geostrophic flow of the Antarctic Circumpolar Current at Drake Passage. *Deep-Sea Res.*, **27**: 497-507.

Whitworth III, T., Nowlin Jr., W. D. and Worley, S. J., 1982. The net transport of the Antarctic Circumpolar Current through Drake Passage. *J. Phys. Oceanogr.*, **12**: 960-971.

Whitworth III, T. and Nowlin Jr., W. D., 1987. Water masses and currents of the Southern Ocean at the Greenwich Meridian. *J. Geophys. Res.*, **92**: 6462-6476.

Whitworth III, T., Nowlin Jr, W. D., Orsi, A. H., Locarnini, R. A. and Smith, S. G., 1994. Weddell sea shelf water in the Bransfield Strait and Weddell-Scotia Confluence. *Deep-Sea Res.*, **41**: 629-641.

Whitworth III, T., Orsi, A. H., Kim, S.-J. and Nowlin Jr, W. D., 1998. Water masses and mixing near the Antarctic slope front. In: S. S. Jacobs and R. F. Weiss (Eds.), *Ocean, Ice, and Atmosphere: Interactions at the Antarctic Continental Margin*. AGU Ant. Res. Ser., 75: 1-27.

Williams, D. F., 1976. Late Quaternary fluctuations of the Polar Front and Subtropical convergence in the Southeast Indian Ocean. *Mar. Micropal.*, **1**:363-375.

Williams, D. F. and Keany, J., 1978. Comparison of radiolarian/planktonic paleoceanography of the subantarctic Indian Ocean. *Quat. Res.*, **9**: 71-86.

Williams, D. F., Bé, A. W. H. and Fairbanks, R. G., 1981. Seasonal stable isotopic variations in living planktonic foraminifera from Bermuda plankton tows. *Palaeogeogr., Palaeoclimatol., Palaeoecol.*, **33**: 71-102.

Williams, D. F., Healy-Williams, N. and Leschak, P., 1985. Dissolution and water-mass patterns in the Southeast Indian Ocean, Part I: Evidence from recent to late Holocene f foraminiferal assemblages. *Geol. Soc. Am. Bull.*, **96**: 176-189.

Williams, D. F., Thunell, R. C., Tappa, E., Rio, D. and Raffi, I., 1988. Chronology of the Pleistocene oxygen isotope record: 0-1.88 m.y. B.P. *Palaeogeogr., Palaeoclimatol., Palaeoecol..*, **64**: 221-240.

Wittstock, R.-R. and Zenk, W., 1983. Some current observations and surface T/S distribution from the Scotia Sea and the Bransfield Strait during early austral summer 1980/1981. *Meteor Forschungs-Ergebnisse, Reihe A/B*, **24**: 77-86.

Woodruff, F., Savin, S. M. and Douglas, R. G., 1980. Biological fractionation of oxygen and carbon isotopes by recent benthic foraminifera. *Mar. Micropal.*, **5**: 3-11.

Wüst, G., 1933. Das Bodenwasser und die Gliederung der Atlantischen Tiefsee. In: *Wissenschaftliche Ergebnisse der Deutschen Atlantischen Expedition auf dem Forschungs- und Vermessungsschiff "Meteor" 1925-1927*, **6**, 107pp.

Wüst, G., 1935. Die Stratosphäre. *Wissenschaftliche Ergebnisse der Deutschen Atlantischen Expedition auf dem Vermessungs- und Forschungsschiff "Meteor" 1925-1927*, **6**: 109-288.

Yoder, J. A., Ackleson, S. G., Barber, R. T., Flament, P., Balch, W. M., 1994. A line in the sea. *Nature*, **371**: 689-692.

Young, S. B. and Schofield, E. K., 1973. Pollen evidence for late Quaternary climate changes on Kerguelen Islands. *Nature*, **245**: 311-312.

Yu, E, F., Francois, R. and Bacon, M. P., 1996. Similar rates of modern and last-glacial ocean thermohaline circulation inferred from radiochemical data. *Nature*, **379**: 689-694.

14.0. APPENDICES

1 Duplicate planktonic foraminiferal count for KC097.
2 Sample list for AMS radiocarbon dating.
3 Absolute abundance counts for KC097.
4 Relative abundance counts of benthic foraminifera for KC097.
5 Species diversity values H(S) and α for KC097, GC062, KC099, KC064 and TC036.
6 Calcium carbonate dissolution indices for KC097, GC062, KC099, KC064 and TC036.
7 Sedimentation Rate, SAR and BFAR for KC097, GC062, KC099, KC064.
8 Absolute abundance counts for GC062.
9 Relative abundance counts of benthic foraminifera for GC062.
10 Absolute abundance counts for KC099.
11 Relative abundance counts of benthic foraminifera for KC099.
12 Absolute abundance counts for KC064.
13 Relative abundance counts of benthic foraminifera for KC064.
14 Absolute abundance counts for TC036.
15 Relative abundance counts of benthic foraminifera for TC036.
16 Absolute abundance counts for TC077 and TC078.
17 Relative abundance counts of benthic foraminifera for TC077 and TC078.
18 PCA species data tables for KC097, GC062 and KC064.
19 Presence of certain diatom species in KC097 and KC064.

Appendix 1 Duplicate planktonic foraminiferal count for KC097.

Depth (cm)	No. planktonics counted	No. planktonics counted (check)
1.5-3	3204	2789
5-6	4631	4787
7-8	19698	20665
10-11	4341	
12-13	19152	
15-16	3428	5621
17-18	27930	29415
20-21	3513	
22-23	21000	
25-26	8944	6698
27-28	30282	29334
30-31	4879	
32-33	19362	
35-36	6062	3374
37-38	39480	42915
40-41	8631	
42-43	18942	
45-46	5061	4265
47-48	16148	
50-51	5110	
55-56	8211	9931
60-61	2569	4836
65-66	3220	
70-71	1876	1548
90-91	446	563
100-101	0	0
110-111	0	0
130-131	0	0
150-151	93	56
170-171	289	
190-191	266	347
210-211	392	
230-231	163	
250-251	700	845
270-271	947	
280-281	0	0

Appendix 2 AMS radiocarbon dating sample list

Number	Core - depth	Purpose of analysis
1	KC064 - top	foraminiferal carbonate - to assess the reservoir effect and age of core top
2	KC064 - top	organic carbon - to assess the reservoir effect and age of core top
3	KC064 - 70cm	date after meltwater event
4	KC064 - 75cm	date initiation of glacial meltwater event
5	KC064 - 80cm	date before initiation of meltwater event
6	KC097 - top	foraminiferal carbonate - to assess reservoir effect and age of core top
7	KC097 - top	organic carbon - to assess the reservoir effect and age of core top
8	KC097 - 20cm	date after meltwater event
9	KC097 - 25cm	date initiation of glacial meltwater event
10	KC097 - 30cm	date before initiation of meltwater event
11	KC099 - 15cm	date after meltwater event
12	KC099 - 20cm	date initiation of glacial meltwater event
13	KC099 - 25cm	date before initiation of meltwater event
14	GC062 - 17cm	date after meltwater event
15	GC062 - 22cm	date initiation of glacial meltwater event
16	GC062 - 27cm	date before initiation of meltwater event

Appendix 3 Absolute abundance counts for KC097.

Depth (cm)	Sample wt. (g)	>63 μm fraction wt. (g)	No. planktonics counted	Wt. planktonics counted (g)	No. planktonics in 1g sed.	No. benthics picked	Wt. benthics counted (g)	No. benthics in 1g sed.
1.5-3	2.15	1.18144	3204	0.00625	281699	178	0.06066	1612
5-6	1.59	0.90806	4631	0.00979	270153	194	0.04901	2261
7-8	1.43	0.88799	19698	0.05301	230747	267	0.05301	3128
10-11	2.30	1.26704	4341	0.01053	227104	203	0.04548	2459
12-13	2.33	1.30775	19152	0.07072	151999	283	0.07072	2246
15-16	2.71	1.63244	3428	0.00934	221086	208	0.08182	1531
17-18	2.65	1.53677	27930	0.06844	236659	383	0.06844	3245
20-21	4.08	2.34706	3513	0.00447	452100	233	0.03043	4405
22-23	3.27	1.73863	21000	0.05703	195783	314	0.05703	2927
25-26	3.76	2.10348	8944	0.00718	696880	255	0.02826	5048
27-28	3.92	2.00536	30282	0.08407	184268	368	0.08407	2239
30-31	2.72	1.33407	4879	0.00337	710085	247	0.02558	4736
32-33	3.23	1.71586	19362	0.04363	235746	241	0.04363	2934
35-36	2.33	1.40477	6062	0.01223	298840	193	0.05155	2257
37-38	2.57	1.29445	39480	0.07999	248597	344	0.07999	2311
40-41	2.67	1.60542	8631	0.01491	348065	229	0.0307	4485
42-43	2.21	1.38376	18942	0.05726	207130	235	0.05726	2570
45-46	2.33	1.46733	5061	0.02096	152061	180	0.06169	1838
47-48	2.43	1.46764	16148	0.07463	130683	204	0.07463	1651
50-51	2.49	1.53457	5110	0.01652	190633	209	0.09078	1419
55-56	2.98	1.92670	8211	0.02279	232943	187	0.08094	1494
60-61	2.35	0.58713	2569	0.01594	40266	260	0.03026	2147
65-66	3.65	1.10858	3220	0.02913	33573	262	0.07035	1131
70-71	3.98	0.89145	1876	0.02168	19382	239	0.08409	677
90-91	3.77	0.35585	446	0.2023	208	73	0.20230	34
100-101	1.94	0.37523	0	0	0	1	0.37523	1
110-111	4.35	0.31395	0	0	0	0	0	0
130-131	3.85	0.26519	0	0	0	0	0	0
150-151	3.27	0.27893	93	0.12942	61	5	0.12942	3
170-171	3.83	0.37264	289	0.19673	143	14	0.19673	7
190-191	2.37	0.25885	266	0.16434	177	7	0.16434	5
210-211	2.72	0.29301	392	0.20586	205	18	0.20586	9
230-231	2.36	0.29066	163	0.19747	102	8	0.19747	5
250-251	2.88	0.79469	700	0.24052	803	12	0.24052	14
270-271	2.80	0.62435	947	0.08034	2628	67	0.33101	45
280-281	4.63	1.30122	0	0	0	0	0	0

KC097 Benthics (%)	1.5 - 3 cm	5 - 6 cm	7 - 8 cm	10 - 11 cm	12 - 13 cm	15 - 16 cm	17 - 18 cm	20 - 21 cm	22 - 23 cm	25 - 26 cm	27 - 28 cm	30 - 31 cm	32 - 33 cm	35 - 36 cm	37 - 38 cm	40 - 41 cm	42 - 43 cm	45 - 46 cm	47 - 48 cm	50 - 51 cm	55 - 56 cm	60 - 61 cm	65 - 66 cm	70 - 71 cm	90 - 91 cm	100 - 101 cm	150 - 151 cm	170 - 171 cm	190 - 191 cm	210 - 211 cm	230 - 231 cm	250 - 251 cm	270 - 271 cm
Angulogerina angulosa	2.81	4.12	1.87	1.97	2.47	2.88	2.35	2.16		0.39	2.72	2.02	0.83	1.08	1.45	1.7	1.28	2.15	4.9	1.92	5.88	0.78	1.15	0.84				7.14	14.3	5.56			2.99
Angulogerina angulosa juv.									0.64																								
Astrononion antarcticus				0.49	0.35	0.48			0.64	0.39	0.27		0.83		0.58	0.85			0.49	1.44	0.53												
Astrononion echolsi	0.56			0.49	0.35	2.4	0.26	1.29	0.96	0.78		3.64		2.16	0.29	1.28		0.54	1.47	0.96	0.53		0.76	0.42				7.14					1.49
Bolivina decussata	2.81	1.03	1.5	1.48	1.41	2.4	0.52	0.43	0.32	0.39	0.54	0.81	0.41	1.62		0.85	1.28	0.54	0.49		1.07												
Bolivina earlandi																	0.43																
Bolivina malovensis	5.06	1.03	1.5	1.97	0.71	1.92	1.57	0.43	0.96	1.18	1.63	0.81	0.59	0.54	0.58	0.85	0.85	1.08		1.44		0.78											
Bolivina pseudopunctata		1.03												1.62			0.43		0.49			1.16											
Bolivina spp.								1.72							0.29																		
Bolivina subspinescens	0.56				0.35		0.52	0.43			0.27	1.21			0.29		0.43		0.49											5.56	12.5		2.99
Bolivinita pseudothalmanni	6.18	5.67	2.25	2.96	3.18	1.92	2.09	1.29	0.64	3.14	1.36	2.83	2.07	2.16	0.87	0.85	0.85		1.96	0.96	1.07	1.55	1.15	0.42									
Brizalina pygmaea							0.26																										
Brizalina spathulata			0.37	0.49							0.54					0.43		1.61															
Bulimina aculeata																	0.43																
Bulimina marginata																								0.42									
Bulimina rostrata	1.12	1.03	0.37	1.97	0.71	1.44		0.86		0.39	0.27		0.41	1.62		1.28			0.49	0.96	1.07									5.56			
Bolivinellina translucens	1.69	2.06	0.37	2.46	1.06	0.96	1.31	0.43	0.96	1.18	0.54	0.81	1.66	0.54	0.29	0.85	1.7	0.54	1.96	1.44	0.53	3.49	6.49	4.18			40						1.49
Cassidulina crassa	3.93	5.67	10.5	15.3	6.71	13.9	12.5	6.47	7.96	9.02	8.42	2.43	5.81	4.86	10.2	3.83	7.23	3.76	5.39	6.25	6.42	1.55	2.29	2.51	4.11				14.3			8.33	11.9
Cassidulina laevigata	0.56		0.37		0.71				0.32	0.39			0.41		0.58			0.54	0.98					0.42									
Cassidulina laevigata var. carinata	0.56	1.03	0.37	0.49			0.26			0.39		0.4					0.43		0.49	0.48													
Cibicides grossepunctatus																					0.53												
Cibicides lobatulus	1.12	1.55	0.37		0.71	1.44		0.43	0.32	0.78	1.63	1.21	0.83	1.08	1.45	0.43	2.13	0.54	2.45	0.48	2.67	1.55	0.76	0.84	5.48			7.14					
Cibicides refulgens	0.56											0.4				0.85				1.44	0.53												
Cibicides wuellerstorfi		0.52			1.41							0.4					1.28			0.48		0.39	0.76	0.84								
Cibicides spp.	4.49	1.55		0.49						0.78		1.62		1.62	0.29	0.43			3.43	0.96	4.81	0.78		1.67					14.3	5.56		8.33	2.99
Cribrostomoides subglobosus	0.56																																1.49
Discorbinella bertheloti	0.56	1.03	0.37		0.71			0.86		0.39			0.83	0.54	0.87	0.43	0.43		0.49	0.96	1.07	0.39	0.38										1.49
Eggerella bradyi	0.56		2.25	0.49	2.47	0.96	0.52	0.43	0.64	0.78	1.09	0.4	2.49	1.62	1.45	0.43	2.55	1.08	1.96	4.33	2.14		0.76										
Ehrenbergina glabra	1.12			0.49		0.48					0.27			0.54	0.58			0.54	0.98	0.48	0.53												
Ehrenbergina trigona											0.54		0.41	0.54	0.29	0.43		1.61	1.96	0.96	2.14		0.76	0.42									
Elilohedra weddellensis	16.3	21.1	35.2	20.2	25.1	25.5	32.9	31.9	35.7	38	31.3	34.8	29.5	24.9	30.5	34	30.2	26.3	16.2	23.1	17.6	39.1	29.4	21.3	6.85		60	50	28.6	44.4	37.5	33.3	44.8
Epistominella exigua	3.93	14.9	7.49	5.91	11.3	4.18	13.6	13.8	16.9	14.9	16.3	12.6	12.9	9.19	14	11.9	11.9	5.91	5.88	6.73	3.74		0.38	0.42								16.7	
Eponides tumidulus		0.52												1.08																			
Eponides sp.			0.75			0.96		0.43		1.18		2.43	0.41	0.54		0.43		1.08		0.48	1.6	3.1	1.53	3.35	9.59			7.14		5.56		8.33	7.46
Fissurina spp.	7.3	3.09	1.5	7.39	3.89	3.37	1.57	4.74	2.87	2.35	2.45	2.43	2.07	2.7	1.45	2.55	1.28	3.76	5.88	2.4	1.07	1.16	1.91	1.67	4.11								
Fursenkoina complanta											0.54							0.54		0.96		2.33	3.05	7.11	20.5								
Fursenkoina earlandi								0.43							0.58			0.54	0.98														
Fursenkoina fusiformis	0.56	1.03							0.32			0.4		0.54		0.43					0.53	1.94	2.67	0.42									
Fursenkoina rotunda																		0.54															
Fursenkoina texturata					0.35				0.32				0.41			0.43																	
Globocassidulina subglobosa	3.93	4.64	13.1	6.9	12.4	7.21	9.66	10.8	13.1	6.67	10.3	8.5	4.98	4.86	9.88	7.66	6.81	10.2	8.82	7.21	4.28	4.65	2.67	4.18	4.11					5.56		8.33	2.99
Gyroidinoides spp.	13.5	8.76	12.7	11.8	11	12.5	9.14	9.48	7.32	8.63	8.7	8.1	13.7	11.9	6.4	11.5	11.1	9.14	10.3	11.5	11.2	5.81	6.87	6.28	1.37							8.33	5.97
Haplophragmoides quadratus					0.35						0.27																						
Hormosellenia sp.	0.56					0.48	0.26																										
Lagena spp.	5.62	5.15	1.5	3.45	1.41	1.44	3.39	3.02	1.91	1.18	1.63	2.83	2.9	2.16	2.33	3.83	2.98	7.53	7.35	7.21	9.63	2.33	4.58	4.18	4.11			21.4					2.99
Laticarinata pauperata											0.27																						
Lenticulina sp.																			0.49		0.53			0.84									
Ioeblichopsis sabulosa																										100							
Marginulina obesa													0.83		0.29			0.54					0.38	0.42									
Melonis barleeanum	1.12	0.52											0.41	0.54	0.58		0.43	0.54	0.49	1.92	1.6	3.1	4.58	6.28	6.85								
Melonis zaandanae																			0.49						1.37								1.49
Nodosaria sp.					0.35																				5.48								
Nonionella bradii	0.56	0.52	0.75		0.71	0.48		0.86	0.64	0.39	0.54		0.83	1.08				0.54															
Nonionella iridea		4.12		2.46	2.47	5.77	3.92	2.59	2.87	2.75	3.53	2.43	6.64	5.95	6.98	4.68	5.96	4.3	0.98	3.37	5.35	20.2	19.5	21.3	17.8								1.49
Nuttalides umbonifera	0.56	0.52	0.37		0.35						0.27	0.4			0.29			0.54			0.53												
Oolina spp.	0.56	0.52			0.71	0.48	0.52			0.39	0.54			0.54	0.58				0.49				0.38	0.42									
Oridorsalis tenera	5.06	2.06	0.37	3.45	3.89	1.92	0.78	1.29	0.96	0.78	0.54	1.62	2.9	3.78	1.45	3.83	3.83	5.38	4.9	3.37	4.28	0.78	0.76	1.26	2.74					11.1	25		5.97
Oridorsalis sp.	1.12	0.52	0.37	2.46	0.35		0.26		0.64			1.62	0.41		1.74		0.43	2.15					0.76	0.84	1.37					11.1	12.5		
Patellina antarctica								0.43					0.41		0.58		0.43				0.53		0.38										
Planulina wuellerstorfi				0.49																	0.53												
Portatrochammina antarctica	1.12	0.52																											14.3				
Portatrochammina sp.																																	
Portatrochammina wiesneri		0.52	0.75																														
Pullenia bulloides		1.03	1.12				0.26		0.64	0.39			0.83		0.29			1.08	0.49	0.48	0.53	0.78	0.38	0.84	1.37								
Pullenia simplex				0.49				0.43	0.32	0.78	0.54	0.4			0.29		0.43	2.15	2.94		0.53	0.78	1.15	1.26									
Pullenia subcarinata	0.56	0.52			0.35							0.4								0.48				0.84									
Pyrgo murrhina					0.35					0.39	0.54	0.4	0.41	2.16	0.29	0.43	0.85			1.92			1.15										
Pyrgo spp.	0.56																			0.48	0.53												
Quinqueloculina seminulum	0.56	0.52		2.46		0.48		0.43					0.41	1.08		0.43		1.08			1.6	1.16	1.15	3.35									
Quinqueloculina venusta	0.56						0.26				0.27			0.54			0.43		0.98	0.48		0.39											
Quinqueloculina sp.1						0.48		0.86								0.85			0.49														
Quinqueloculina sp.2					0.35		0.78		0.64		0.54		0.83		0.58				0.49														
Rhecphax fusiformis			0.37																														
Spirosigmoilina pusilla			0.37																														
Spirosigmoilina tenuis		0.52		0.49			0.26	0.43			0.27			1.62	0.29			0.54						0.42	1.37								
Triloculina tricarinata														0.54									0.38										
Uvigerina auberiana					0.35					0.39	0.27												0.38										
Uvigerina brunnensis																			0.49											8.33			
Uvigerina canariensis																		0.54		0.48													
Uvigerina peregrina														0.54							0.53												
Uvigerina sp.																																	
Veleroninoides wiesneri	1.12																																
Unidentified																														12.5			
Cell 1														0.54														14.3					
Cell 6								0.43			0.27						0.43																
Cell 12		0.52					0.26								0.58						0.53												
Cell 16		0.52																		1.44	1.07		0.38		1.37								
Cell 17			0.37	0.49				0.43	0.64	0.39		0.81					0.85																
Cell 19														1.08				0.54															
Cell 20			0.75		0.71											0.43																	
Cell 21													0.41			0.85																	
Cell 24												0.81																					

Appendix 5 Species diversity vales H(S) and alpha for KC097, GC062, KC099, KC064 and TC036.

KC097

Depth (cm)	H(S)	H(S)max	Alpha
1.5	2.03	3.64	15
5	1.82	3.58	13
7	1.23	3.4	9
10	1.67	3.33	9
12	1.29	3.56	10.5
15	1.53	3.26	8
17	0.94	3.3	7
20	1.41	3.43	10
22	1.06	3.3	7
25	1.26	3.43	9.5
27	1.01	3.56	9.5
30	1.38	3.43	9.5
32	1.42	3.5	11
35	1.87	3.61	14
37	1.09	3.61	11.5
40	1.41	3.47	10
42	1.45	3.43	10
45	1.83	3.56	13
47	1.83	3.61	14
50	1.73	3.56	12
55	1.94	3.64	15
60	1.23	3.22	7
65	1.34	3.5	10.5
70	1.48	3.47	10
90	3.01	2.89	
270	2.45	2.77	

GC062

Depth (cm)	H(S)	H(S) max	Alpha
2	0.92	3.33	8.0
12	0.92	3.43	8.0
22	1.28	3.37	8.5
32	1.27	3.5	10.5
44	1.01	3.22	7.0
50	1.09	3.33	8.5
54	1.4	3	6.0
60	1.88	3.26	10.5

KC064

Depth (cm)	H(S)	H(S)max	Alpha
5	1.70	3.53	12
10	1.53	3.66	14
15	1.45	3.37	9
20	1.50	3.37	9
25	1.46	3.09	6
30	1.47	3.53	9
33	1.21	3.09	8
35	1.23	3.04	5.5
38	1.20	3.30	8.5
40	1.25	3.33	8.5
43	1.26	3.18	7
45	1.40	3.26	7.5
48	1.39	3.26	8
50	1.30	3.30	8
53	1.38	3.18	5
55	1.23	3.37	9
58	1.02	2.71	4
60	1.10	2.71	3.5
63	1.13	2.89	5
65	1.09	3.00	5
68	1.49	2.71	4.5
70	1.43	2.48	6
72	1.58	2.94	7
75	1.18	3.26	3.5
78	0.60	2.20	4
80	0.80	2.77	4.5
83	0.83	2.83	4.5
85	0.95	2.83	3.5
88	0.81	2.56	4
90	0.88	2.77	
100	2.10	3.04	

KC099

Depth (cm)	H(S)	H(S)max	Alpha
2	1.42	3.58	11.5
6	1.08	3.58	10.0
10	1.26	3.33	8.5
15	1.02	3.33	7.5
20	0.91	3.56	9.5
25	1.00	3.47	8.5
30	0.99	3.22	6.5
35	1.37	3.56	11.0
40	1.14	3.66	11.5
45	1.10	3.53	10.5
50	1.06	3.37	8.0
55	1.33	3.33	8.5

TC036

Depth (cm)	H(S)	H(S)max	alpha
1	1.15	3.26	8
5	1.22	3.18	6.5
10	1.25	3.53	10.5
15	1.53	3.61	12
21	1.31	3.5	10
25	1.2	3.47	10
30	1.19	3.53	10.5
35	1.21	3.47	10
42	1.18	3.37	8.5
45	1.06	3.14	5.5
50	1.16	3.4	8.5
55	1.17	3.47	9.5
60	0.84	3.64	10.5
65	1.16	3.5	10
70	1.04	3.47	8.5
75	1.29	3.58	11
80	1.49	3.64	13
85	1.6	3.61	13.5
90	1.3	3.58	11
95	1.55	3.37	9.5
105	1.38	3.47	10.5
110	1.46	3.26	8.5
115	1.52	3.5	11
125	1.33	3.3	7.5
130	1.31	3.37	8.5

Appendix 6 Calcium Carbonate dissolution indices for KC097, GC062, KC099, KC064 and TC036.

KC097

Depth (cm)	% planks	% carbonate
1.5	98.04	70.2
5	98.38	70.3
7	98.60	64.1
10	98.43	64.5
12	98.50	57.4
15	98.50	46.1
17	98.30	15.5
20	98.29	12.4
22	98.10	
25	98.33	
27	98.60	
30	98.03	
32	98.70	
35	99.08	
37	99.10	
40	98.09	
42	98.72	
45	98.44	
47	98.66	
50	98.36	
55	98.62	
60	93.38	
65	96.12	
70	95.52	
90	85.93	
110		
130		
150	94.90	
170	95.38	
190	97.44	
210	95.61	
230	95.32	
250	98.31	
270	98.24	

GC062

Depth (cm)	% planks	% Carb
0	98.93	62.60
10	99.05	65.30
20	98.92	60.00
30	98.13	45.20
40	95.16	23.80
50	93.58	10.50
60	92.91	5.90
80	89.43	0.00
100	70.37	0.00
120	91.60	0.00
140	96.56	0.00
160		0.00
180		0.00
200		0.00
220		0.00
240		0.00

TC036

Depth (cm)	% planks	% Carb.
1	95.36	1
5	97.12	11
10	97.23	5
15	99.32	3
21	98.12	4
25	98.49	7
30	98.41	10
35	98.34	7.5
42	96.97	5
45	96.42	10.5
50	96.64	0
55	97.02	0
60	96.84	
65	96.34	
70	97.10	
75	97.38	
80	98.80	
85	99.15	
90	98.23	
95	99.17	
105	98.84	
110	98.47	
115	98.20	
125	98.70	
130	97.27	

KC099

Depth (cm)	% planks	% Carb
2	98.43	52
6	98.40	46
10	97.97	42
15	97.39	
20	97.02	
25	96.51	
30	95.67	
35	96.39	
40	95.70	
45	96.82	
50	95.85	
55	85.47	

KC064

Depth (cm)	% planks	% Carb
5	96.09	6.3
10	94.22	4.6
15	95.13	7.3
20	95.63	7.7
25	96.62	4
30	96.32	1
33	90.47	0.3
35	96.07	0
38	93.18	0
40	94.06	0
43	92.68	0
45	94.60	0
48	93.12	
50	92.27	
53	95.84	
55	93.71	
58	84.79	
60	92.18	
63	82.74	
65	93.00	
67	90.52	
70	82.80	
72	83.29	
75	87.71	
78	43.65	
80	75.61	
83	68.55	
85	74.57	
88	72.18	
90	78.57	
95	0.00	
100	50.78	
120		
140	75.00	
160		
180	40.00	

Appendix 7 Dry Bulk Density (DBD), Sediment Accumulation Rate (SAR) and Benthic Foraminiferal Accumulation Rate (BFAR) for KC097, GC062, KC099 and KC064.

KC097

Depth (cm)	DBD (g/cc)	SAR (cm^2/kyr)	BFAR (BF/cm^2/kyr)
1	1.299	12.86	20730
10	1.352	13.38	32901
20	1.405	13.91	61274
30	1.378	13.64	64599
40	1.458	14.43	64718
50	1.431	14.2	20149
60	1.59	15.74	33793
69	1.484	14.69	9945

GC062

Depth (cm)	DBD (g/cc)	SAR (cm^2/kyr)	BFAR (BF/cm^2/kyr)
0	1.458	9.77	17604
10	1.484	9.94	29262
20	1.484	9.94	18762
30	1.590	10.65	14829
40	1.670	11.19	8403
50	1.590	10.65	4517
60	1.431	9.59	949
80	1.193	7.99	72
100	1.272	8.52	17

KC064

Depth (cm)	DBD (g/cc)	SAR (cm^2/kyr)	BFAR (BF/cm^2/kyr)
5	1.537	16.45	3389
21	1.564	16.73	7278
41	1.59	17.01	8471
61	1.564	16.73	3112
81	1.617	17.30	3529
101	1.643	17.58	598
121	1.749	18.71	0
141	1.749	18.71	262
161	1.696	18.15	0
181	1.696	18.15	54
201	1.749	18.71	0
221	1.723	18.44	0
241	1.776	19.00	0
261	1.776	19.00	0
281	1.776	19.00	0
301	1.802	19.28	0

KC099

Depth (cm)	DBD (g/cc)	SAR (cm^2/kyr)	BFAR (BF/cm^2/kyr)
2	1.537	17.68	30675
6	1.537	17.68	41088
10	1.537	17.68	55515
15	1.537	17.68	55498
20	1.537	17.68	61509
25	1.537	17.68	60024
30	1.537	17.68	62340
35	1.537	17.68	48019
40	1.537	17.68	44483
45	1.537	17.68	27758
50	1.537	17.68	48178
55	1.537	17.68	3147

Appendix 8 Absolute abundance counts for GC062.

Section	Depth (cm)	Depth (cmbsf)	Sample wt. (g)	>63 µm fraction wt. (g)	No. planktonics counted	Wt. planktonics counted (g)	No. planktonics in 1g sed.	No. benthics picked	Wt. benthics counted (g)	No. benthics in 1g sed.
1	2-4	2-4	3.79	1.43267	34356	0.07763	167294	370	0.07763	1802
	12-14	12-14	2.99	1.28387	40163	0.05631	306260	386	0.05631	2943
	17-18	17-18	3.10	0.47701	30598	0.05952	79104			
	22-24	22-24	3.07	1.50799	24066	0.06845	172699	263	0.06845	1887
	27-28	27-28	3.22	0.48757	22994	0.06253	55681			
	32-34	32-34	3.31	1.28723	14238	0.07598	72875	272	0.07598	1392
2	10-12	44-46	3.61	0.46605	4914	0.04297	14764	250	0.04297	751
	16-17	50-51	3.12	0.48195	3792	0.09463	6190	260	0.09463	424
	20-22	54-56	3.03	0.32807	2121	0.15761	1457	162	0.15761	111
	26-27	60-61	3.05	0.34627	863	0.11732	835	102	0.11732	99
	30-32	64-66	2.95	0.31479	76	0.10909	74	32	0.10909	31
	50-52	84-86	2.47	0.24334	120	0.12566	94	11	0.12566	9
	70-72	104-106	2.37	0.26308	28	0.06910	45	1	0.06910	2
	90-92	124-126	2.49	0.32746	2	0.11902	2	0	0.11902	0
	110-112	144-146	3.14	0.22614	0	0.13649	0	0	0.13649	0
	130-132	164-166	2.55	0.20953	0	0.10442	0	0	0.10442	0
3	40-42	224-226	3.77	0.25741	0	0.11565	0	0	0.11565	0

Appendix 9 Relative abundance counts of benthic foraminifera for GC062.

GC062 Benthics (%)	2-4 cm	12-14 cm	22-24 cm	32-34 cm	44-46 cm	50-51 cm	54-56 cm	60-61 cm	84-66 cm	84-86 cm	104-106 cm
Angulogerina angulosa	0.54	0.78	0.38	0.74	1.20	1.54					
Astrononion antarcticus	0.27	0.26			0.40						
Astrononion echolsi			0.76								
Bolivina decussata	0.27			0.37							
Bolivina malovensis	1.35	1.81	1.14	0.74	0.80	0.38					
Bolivina pseudopunctata	0.27		0.38	0.37	0.40	0.77				9.09	
Bolivina subspinescens		0.26				0.38					
Bolivinellina translucens	0.54	1.04	1.52	1.10	1.60	1.15	3.09	3.03	12.50		
Bolivinita pseudothalmanni	1.35	1.55	0.38	2.94		0.38		0.76			
Brizalina spathulata							0.62				
Bulimina rostrata	0.27			0.37							
Cassidulina crassa	11.35	12.44	6.84	8.82	2.40	3.08	1.23	3.79			
Cassidulina laevigata	0.27		0.38	0.37							
Cassidulina laevigata var. carinata	0.54	0.26									
Cibicides lobatulus		0.78		1.47	0.80	1.15		1.52			
Cibicides wuellerstorfi										9.09	
Cibicides spp.	1.08	0.26	0.76					0.76			
Discorbinella bertheloti		0.26									
Eggerella bradyi	1.35	0.52	3.04	2.57		0.77		0.76			
Ehrenbergina pupa				0.37							
Ehrenbergina trigona			0.38	0.74				0.76			
Eilohedra weddellensis	40.81	34.72	36.50	37.13	65.60	58.85	56.79	48.48	21.88	18.18	100.00
Epistominella exigua	12.70	15.54	9.13	7.72		5.00	0.62	2.27			
Eponides sp.	0.54	1.04	0.38	2.21	2.00	1.92		1.52			
Eponides tumidulus						0.77		0.76			
Fissurina spp.	1.62	2.07	4.56	3.31	4.80	2.31	3.09	2.27		18.18	
Fursenkoina complanata			0.38		0.40		5.56	3.79	43.75		
Fursenkoina earlandi					0.80						
Fursenkoina fusiformis	0.27				0.40	0.38	2.47				
Globocassidulina subglobosa	8.92	9.07	7.98	5.15	2.80	3.85	1.23	2.27			
Gyroidinoides spp.	9.19	9.84	10.27	11.40	2.40	3.08	1.23	2.27		9.09	
Lagena spp.	0.81	1.55	2.66	2.57	1.60	1.54	1.85	3.03		9.09	
Laticarinata pauperata	0.27										
Lenticulina sp.					0.40						
Loeblichopsis sabulosa				0.37							
Marginulina obesa		0.26									
Melonis barleeanum				0.74	0.80	1.54	3.09	3.03	3.13	9.09	
Nonionella bradii		0.52		0.37	0.40			0.76	3.13		
Nonionella iridea	1.35	2.33	1.90	1.47	6.00	5.00	9.88	9.09	12.50		
Nuttalides umbonifera			0.38	0.74							
Oolina spp.				0.74		0.38		0.76			
Oridorsalis tener	1.62	0.52	3.04	2.21	0.80	1.92	4.32	3.03	3.13		
Patellina antarctica					0.40						
Planulina wuellerstorfi		0.26	0.38	0.37							
Pullenia bulloides		0.26	1.90				0.62	0.76		9.09	
Pullenia simplex	1.35	0.26	1.90	0.74	2.00	1.54	1.85	2.27		9.09	
Pullenia subcarinata	0.27	0.26		0.74		0.38	0.62	0.76			
Pyrgo murrhina		0.26	1.14			0.38					
Pyrgo spp.			0.76								
Pyrulina angusta							0.62	0.76			
Quinqueloculina seminulum					0.40		0.62				
Quinqueloculina spp.	0.54	0.26				0.38					
Quinqueloculina sp.1				0.37							
Spirosigmoilina tenuis	0.27	0.26	0.38								
Trochammina glabra			0.38								
Uvigerina canariensis				0.37		0.38					
Unidentified Cell 18		0.52		0.37	0.40	0.77	0.62	0.76			

Appendix 10 Absolute abundance counts for KC099.

Depth (cm)	Sample wt. (g)	>63 µm fraction wt. (g)	No. planktonics counted	Wt. Planktonics counted (g)	No. planktonics in 1g sed.	No. benthics picked	Wt. Benthics picked (g)	No. benthics in 1g sed.
2-3	3.98	1.29254	10759	0.02824	123728	248	0.04642	1735
6-7	5.63	1.84992	9002	0.02526	117098	350	0.04948	2324
10-11	6.12	2.12309	12887	0.02784	160583	252	0.02784	3140
15-16	6.55	2.27589	13769	0.03752	127512	339	0.03752	3139
20-21	6.71	1.90047	14266	0.03256	124096	400	0.03256	3479
25-26	4.98	1.29665	9996	0.02669	97515	348	0.02669	3395
30-31	6.25	1.85874	7777	0.02834	81611	336	0.02834	3526
35-36	9.39	3.20308	7070	0.03203	75295	255	0.03203	2716
40-41	9.30	2.82124	8078	0.04087	59959	339	0.04087	2516
45-46	13.11	3.53885	6643	0.03539	50669	264	0.04538	1570
50-51	10.06	2.48499	7672	0.02864	66170	316	0.02864	2725
55-56	8.95	0.59014	588	0.03987	972	242	0.08944	178
59-60								

KC099 Benthics (%)	2-3 cm	6-7 cm	10-11 cm	15-16 cm	20-21 cm	25-26 cm	30-31 cm	35-36 cm	40-41 cm	45-46 cm	50-51 cm	55-56 cm
Angulogerina angulosa	3.63	3.14	0.40	0.88	1.00	1.44	1.19	2.35	1.77	1.52	0.63	0.41
Astrononion antarcticus			0.40	0.29	0.25				0.59			
Astrononion echolsi						0.29						
Bolivina decussata									0.29			
Bolivina malovensis	1.21	2.29	0.79	2.36	3.26	1.72	0.89	1.57	1.77	2.65	1.90	
Bolivina pseudoplicata										0.38		
Bolivina pseudopunctata					0.25							
Bolivina spp.					0.50	0.57	0.30	0.78	2.36	0.38		0.41
Bolivina subspinescens	0.81							0.78		0.38	0.32	
Bolivinita pseudothalmanni	3.23	2.57	2.38	1.47	0.50	2.59		0.78	1.18	0.76	0.63	
Brizalina spathulata					0.50		1.19	1.96	0.29	0.38	0.95	0.41
Bulimina aculeata	0.40					0.29						
Bulimina rostrata	0.40	0.29			0.25							
Bolivinellina translucens	0.81	1.14	0.40	0.88	0.25	1.15	1.79	0.78	1.77	2.27	1.27	2.90
Cassidulina laevigata		0.29			0.25	0.29	0.30					
Cassidulina laevigata var. carinata	1.21			0.59	0.25	0.57	0.60	0.78		1.14	0.32	
Cassidulina crassa	17.34	14.00	17.46	12.39	13.53	6.03	10.42	7.45	9.14	10.61	11.08	5.81
Cibicides lobatulus	0.40	0.29	0.79		0.75			0.39	1.18	0.38	0.63	
Cibicides wuellerstorfi		0.57		0.29	0.25							0.41
Cibicides spp.	1.21		1.59	2.06	0.25	0.57	0.60	1.57	1.18	2.27	1.58	0.83
Cribrostomoides subglobosus	0.40											
Discorbinella bertheloti	0.40	0.57	0.40		0.50	0.57	0.30	1.18	0.29	0.76	0.32	
Eggerella bradyi	1.21	0.29	1.19		0.25	0.86	0.89	0.39	1.18	1.14	0.32	0.41
Ehrenbergina glabra	0.40											
Ehrenbergina pupa						0.29						
Ehrenbergina trigona	0.40								0.29			
Eilohedra weddellensis	22.98	22.57	32.54	35.10	32.08	38.22	32.44	27.84	24.48	25.38	36.39	32.37
Epistominella exigua	12.90	20.00	14.29	15.34	19.30	18.68	23.51	17.25	10.62	10.23	13.92	1.66
Eponides sp.	0.40			0.29		0.29	0.30	0.39		1.52	0.32	0.41
Fissurina spp.	1.61	1.71	2.38	0.88	0.50	0.57	0.89	1.57	0.29	2.27	0.32	2.90
Fursenkoina complanta		0.29				0.29			0.88	1.14	0.63	2.07
Fursenkoina earlandi				0.59	0.50	1.15	0.30	0.78	2.06	3.41	1.58	2.49
Fursenkoina fusiformis	0.40	0.57	0.40	0.29	0.50	0.29	0.30	0.78		0.38	0.32	1.66
Fursenkoina sp.					0.25							
Fursenkoina texturata			0.40									
Globocassidulina subglobosa	6.85	6.57	10.32	9.14	8.27	4.60	5.95	5.88	4.13	4.92	7.59	1.66
Glomospira gordialis	0.40											
Gyroidinoides spp.	10.08	5.71	3.57	5.90	5.26	5.75	2.98	6.27	4.13	6.82	6.96	3.73
Heronallenia sp.				0.29				0.39				
Hoeglundia elegans	0.40										0.32	
Lagena spp.	1.21	2.57	1.98	1.18	0.75	2.01	1.19	1.18	2.36	1.89		3.32
Laticarinina pauperata		0.57	0.40		0.25							
Lenticulina sp.			0.40					0.78	0.29			
Marginulina obesa	0.40				0.25							
Melonis barleeanum			0.40	0.29		0.57		0.39	0.59	1.14		0.41
Melonis zaandanae	0.81											
Neolenticulina variabilis								0.39				
Nonionella bradii	0.40	1.43		0.59	0.75	0.86	2.08	0.39	0.29	0.38		
Nonionella iridea	3.63	6.29	3.17	5.01	6.52	7.47	10.42	10.59	18.88	10.98	8.86	22.82
Nonionella sp.			0.40									
Nuttalides umbonifera		0.29										
Oolina spp.									0.29		0.32	
Oridorsalis juv.									0.59	0.76		
Oridorsalis sp.		0.57		0.29						0.38		0.83
Oridorsalis tener		0.29		0.29	0.25		0.30		0.29			7.47
Patellina antarctica			0.79					0.39				
Planulina wuellerstorfi		0.29	0.79								0.32	
Pullenia bulloides	0.81	0.57			0.50	0.57			0.59	0.38		
Pullenia osloensis		0.29										
Pullenia simplex	0.81	1.71		1.18	0.75			1.96	1.47	1.89		1.66
Pullenia subcarinata			1.19			0.29		0.39	0.29			
Pullenia sp.							0.30					
Pyrgo laevis								0.39				
Pyrgo murrhina		0.29	0.40			0.29			0.29			
Pyrgo serrata											0.63	
Pyrgo spp.		0.29						0.39	0.29			
Quinqueloculina seminulum	0.81	0.29		1.47	0.25	0.29	0.60	0.39	0.29	0.38	0.32	0.83
Quinqueloculina sp.		0.29	0.40	0.29								
Quinqueloculina venusta									0.59			
Siphouvigerina asperula								0.39				
Tosaia hanzawai												0.83
Uvigerina auberiana					0.25					0.38		
Uvigerina peregrina	0.81	0.29				0.57			0.59			
Uvigerina sp.		0.57								0.38	0.32	0.41
Unidentified												
Cell 5	0.40											0.41
Cell 9												
Cell 15											0.95	
Cell 17	0.40											
Cell 18		0.29										
Cell 19												0.41
Cell 21				0.29								
Cell 23									0.29			

Appendix 12 Absolute abundance counts for KC064.

Depth (cm)	Sample wt. (g)	>63 µm fraction wt. (g)	No. planktonics counted	Wt. planktonics counted (g)	No. planktonics in 1g sed.	No. benthics picked	Wt benthics counted (g)	No. benthics in 1g sed.
Top 10	6.87	1.42409	861	0.02151	8297	212	0.21359	206
10-11	5.30	1.11759	945	0.02351	8476	236	0.19977	249
15-16	5.39	1.06356	938	0.02217	8348	227	0.15352	292
20-21	4.73	0.98638	1554	0.02455	13200	231	0.11073	435
25-26	3.81	0.69610	1400	0.01346	19002	213	0.09388	415
30-31	5.10	1.06106	1834	0.02292	16648	240	0.10746	465
33-34	4.39	0.91283	2289	0.08397	5668	220	0.08397	545
35-36	5.40	0.90749	2373	0.03068	12998	236	0.08408	472
38-39	6.13	1.11749	3551	0.07812	8287	257	0.07812	600
40-41	3.89	0.68805	1694	0.03006	9968	242	0.08602	498
43-44	3.23	0.54346	3101	0.07062	7388	226	0.07062	538
45-46	4.06	0.69906	1946	0.02688	12465	228	0.08086	486
48-49	3.61	0.54434	2898	0.05226	8362	202	0.05226	583
50-51	3.09	0.44111	1253	0.01893	9449	220	0.07034	446
53-54	3.24	0.67008	5320	0.06183	17795	215	0.06183	719
55-56	3.55	0.41921	1162	0.02810	4883	231	0.10501	260
58-59	3.15	0.33857	602	0.06147	1053	191	0.12057	170
60-61	3.56	0.32731	707	0.02284	2846	216	0.10666	186
63-64	2.50	0.23330	532	0.07311	679	203	0.13053	145
65-66	3.65	0.41738	1540	0.03161	5571	244	0.06747	414
67-68	4.37	1.18405	611	0.07935	2086	109	0.16190	182
70-71	3.60	0.37810	77	0.02567	315	96	0.37810	27
72-73	2.82	0.91316	329	0.07551	1411	133	0.14332	300
75-76	3.94	0.39664	735	0.02999	2467	243	0.08167	300
78-79	3.07	0.28849	134	0.07926	159	218	0.10265	200
80-81	4.34	0.42515	217	0.02850	746	235	0.11293	204
83-84	2.89	0.32249	547	0.07126	857	242	0.07126	379
85-86	3.62	0.36154	651	0.03515	1850	244	0.04118	592
88-89	2.40	0.34630	532	0.0843	911	202	0.08430	346
90-91	3.01	0.27463	308	0.03434	818	246	0.12160	185
95-96	2.93	0.33037	0	0.15476	0	57	0.15476	42
100-101	3.41	0.42359	98	0.34599	35	95	0.34599	34
120-121	4.01	0.57270	0	0	0	0	0	0
140-141	4.46	0.59714	51	0.20593	33	17	0.20593	12
160-161	4.94	0.47758	0	0	0	0	0	0
180-181	5.02	0.48626	4	0.18026	2	6	0.18026	3
200-201	5.84	0.58664	0	0	0	0	0	0
220-221	4.49	0.38279	0	0	0	0	0	0
240-241	5.72	0.51261	0	0	0	0	0	0
260-261	4.15	0.37884	0	0	0	0	0	0
280-281	4.41	0.43475	0	0	0	0	0	0
299-300	4.83	0.45639	0	0	0	0	0	0

KC064 Benthics (%)	Top 10 cm	10 - 11 cm	15 - 16 cm	20 - 21 cm	25 - 26 cm	30 - 31 cm	33 - 34 cm	35 - 36 cm	38 - 39 cm	40 - 41 cm	43 - 44 cm	45 - 46 cm	48 - 49 cm	50 - 51 cm	53 - 54 cm	55 - 56 cm	58 - 59 cm	60 - 61 cm	63 - 64 cm	65 - 66 cm	67 - 68 cm	70 - 71 cm	72 - 73 cm	75 - 76 cm	78 - 79 cm	80 - 81 cm	83 - 84 cm	85 - 86 cm	88 - 89 cm	90 - 91 cm	95 - 96 cm	100 - 101 cm	141 - 141 cm	180 - 181 cm
Adercotryma glomeratum	1.42	0.42	0.44																															
Ammobaculites agglutinans	3.77	0.85				0.42																												
Ammobaculites sp.	0.47																																	
Ammodiscus angullae		0.42																																
Ammodiscus tenuis		0.42																		1.23	0.92			0.82										
Angulogerina angulosa	0.47	0.85		0.87	2.35	1.25	1.36	0.85	0.78	0.41	0.88	1.32	1.98	1.36	0.93	0.43																		
Astrononion echolsi		0.42																														1.05		
Bolivina decussata		0.42																						0.82										
Bolivina malovensis																0.43																		
Bolivina pseudopunctata						0.83				0.41																						1.05		
Bolivina sp.A									0.39				0.5																			2.11		
Bolivina spp.																								0.41										
Bolivinella folia																					0.92		0.75	0.41				0.41						16.7
Bolivinellina translucens							0.45																											
Bolivinita pseudothalmanni			0.88											0.45																		1.05		
Brizalina semicostata															3.26																			
Brizalina spathulata																														0.41				
Bulimina elongata																																1.05		
Bulimina marginata																0.43																		
Bulimina rostrata	0.94	1.69	1.32			1.25		0.85		0.41			0.5	0.45					0.99	1.23				4.12	0.92		0.41	0.5	0.41			5.88	
Cassidulina crassa			1.32						1.17	0.83	1.33	0.88	0.5	1.36	0.47																			
Cassidulina laevigata				0.43																														
Cibicides lobatulus	0.47			1.73	1.41			0.85	0.78		0.44		1.98	0.45	1.4			1.39		2.05			1.5		1.83		0.82							
Cibicides grossepunctatus						0.83																												
Cibicides refulgens										0.83																							23.5	
Cibicides wuellerstorfi		0.85	0.44												0.47							2.08	0.75	0.41		0.85								
Cibicides spp.	0.47																																	
Cribrostomoides subglobosus	0.47	1.27																																
Dentalina adventa							0.45					0.44																				1.05		
Discorbinella bertheloti			0.88			0.42	0.45								0.93					0.41		1.04		0.41										
Eggerella bradyi				0.43							0.44				0.93																			
Ehrenbergina trigona	1.89	2.12	2.2	2.16	4.23	0.83	0.45	2.12	0.39	0.41	0.88	2.19	0.99	1.82	0.93	1.3	1.05	1.39	1.48	1.23														
Elphedra weddellensis	23.6	30.5	34.4	29	37.1	31.3	51.4	46.2	47.9	43.8	43.8	38.6	47.5	49.1	45.1	51.9	70.7	60.2	63.5	59	61.5	64.6	56.4	55.1	84.4	78.7	75.6	66.8	80.7	72	87.7	51.6		16.7
Elphidium sp.														0.91																				
Epistominella exigua	3.77	8.9	5.29	3.9	1.88	3.33	2.27	1.69	1.95	0.41	1.33	2.19	1.49	0.91	2.33	0.87	1.05		0.49				4.51	5.35	0.92	1.28		0.82		0.41		5.26		
Eponides sp.	0.94		1.32	2.16	1.88	2.5	2.27	2.97	2.33	2.48	2.21	4.82	4.46	1.82	3.72	2.6	1.57	4.63	1.97	2.46	0.92	2.08	2.26	0.82	0.92	0.43	0.41	2.05		1.22	1.75		5.88	
Fissurina spp.	2.83	2.54	0.88	0.43	1.41	2.08	0.91	1.27	3.89	1.65	2.21	1.75	1.49	2.73	2.33	2.6	1.05	0.93	0.49	2.05			0.75				0.41	0.41						
Fursenkoina complanta	0.47	1.27	0.88	0.43	1.41	0.83	0.45	0.85	1.56	0.83		3.51	0.99	0.91		0.43	0.52	0.46		1.23	0.92		0.75		0.46		0.41	1.49	0.81		3.16		
Fursenkoina earlandi																																1.05		
Fursenkoina fusiformis								0.42		0.41	0.44		0.5			0.43						1.04		1.65										
Fursenkoina texturata		0.85		0.43																														
Globocassidulina subglobosa	3.3	2.54	7.05	1.3	6.1	3.33	11.8	8.9	10.9	6.2	19	8.33	11.9	3.64	11.2	3.46	2.62	1.39	3.94	2.05	0.92		2.26	0.41	3.21	5.11	3.72	2.46	1.49	2.03			11.8	33.3
Glomospira gordialis		0.85	0.88			0.42																												
Globotrochamminopsis sp.	1.89	0.85					0.45		0.39																									
Gyroidinoides spp.	6.6	1.69	7.49	7.79	10.8	12.1	8.64	12.7	3.89	15.7	4.87	10.1	8.42	12.3	5.12	8.23	2.09	4.17	4.43	5.74	1.83	6.25	6.02	4.53		1.28	2.07	4.1	2.97	5.28		4.21	5.88	
Haplophragmoides canariensis	0.47																																	
Haplophragmoides sp.		0.85	0.44			0.42																												
Heronallenia sp.												0.44	0.5																					16.7
Karrerulina conversa	0.94	0.42																																
Lagena spp.	13.7	12.7	14.5	16.5	7.04	5	4.55	5.51	4.67	8.26	3.98	5.26	3.96	6.82	3.72	8.23	5.24	5.56	4.93	5.33	9.17	8.33	3.01	3.7	1.38	0.85	2.89	1.64	0.99	2.85		5.26	5.88	
Lagenammina difflugiformis		0.85																									0.41							
Lenticulina sp.									0.78																									
Lenticulina sp. juv.		0.85	0.44	0.43																														
Loeblichopsis sabulosa						0.42				0.41						0.43																1.05		
Melonis barleeanum	2.83	2.54	3.52	6.49	5.63	6.67	0.91	0.85	0.78	1.24	1.77	3.07	1.49	1.36	0.47	0.43	3.14	1.39	1.97	3.28	6.42	4.17	3.76	3.29	0.46	2.13	1.65	2.46	1.98	1.63				
Melonis pompilioides	1.42	1.69		0.43		0.42				0.41					0.47	0.43											0.41			0.81				
Melonis zaandanae										0.41									0.49	0.82														
Nodosaria sp.										0.41	0.44		0.5														0.41							
Nonionella bradii											0.44				0.47				0.49											0.41				
Nonionella iridea									0.39			0.44		1.36									0.75	3.7										
Nuttalides umbonifera	8.02	2.12	2.64	6.49	6.57	7.08	4.09	4.66	2.72	2.07	2.21	2.63	1.49	0.91	3.26	1.73	4.71	6.02	3.45	1.23	0.92	4.17	0.75	2.06		2.13	3.31	1.64	0.99		1.75		5.88	
Oolina spp.			0.88			0.42	0.45		0.39		0.44	0.88	0.5			0.87							1.5	0.41		0.43	0.83							
Oridorsalis juv.									0.78																									
Oridorsalis tener	0.47	1.27	0.88	3.9	4.23	3.33	2.73	2.54	3.5	3.31	1.77	5.7	2.97	4.09	3.26	5.63	1.05	7.87	3.94	4.92	4.59	1.04	7.52	1.65		2.55	3.31	5.33	1.98	2.85				
Oridorsalis sp.	2.36			3.03		5		3.39	0.39	3.31	1.33	1.75	0.5	0.45		0.43			0.99	0.41	0.92	4.17	0.75	2.47		2.13	0.41	6.97	0.99	4.47		1.05		
Patellina antarctica																																		
Portatrochammina bipolaris			0.44																															
Portatrochammina wiesneri		0.85																								0.85	0.41				1.75			
Pullenia bulloides		0.85	0.88	1.3		0.42			0.39	2.07			0.5				0.52							1.23		0.43								
Pullenia simplex	0.47	0.42		0.87	0.47		0.45	1.27	1.17	1.24	1.77	1.32		0.45				1.39	0.49	0.82	0.92													
Pullenia subcarinata	0.94	2.54	1.76	3.46	0.94	2.5	0.91	0.85	2.72	0.83	3.98	2.19	2.97	3.18	3.72	3.9		2.31	3.94	4.1	4.59		4.51	2.47		0.43	1.24	2.87	3.96	4.07	5.26	2.11		
Pyrulina angusta				0.43	0.94	0.42						0.44			0.47	0.87				0.41		1.04												
Quinqueloculina seminulum														0.91		0.43								1.65				0.41			6.32		
Quinqueloculina sp.2														0.91			0.52														2.11		
Quinqueloculina venusta														0.45																			
Repmanina charoides	2.83	2.54	3.08	0.87	0.47	1.25																												
Sphaeroidina bulloides	0.94			0.87	0.47		4.09		4.67		3.54	0.44	0.99		4.19	1.3	4.19	0.93	1.97		4.59		1.5	1.23			1.65		1.49		1.75	3.16	5.88	
Siphotextularia catenata		0.85																																
Spirolocammina tenuis						0.42																												
Spiroplectammina biformis	1.42																															2.11	5.88	
Spirosigmoilina tenuis																																		
Trochammina discorbis						0.42																												
Trochammina glabra	4.72	4.66	3.52	1.3	2.82	1.67	0.45																											
Trochammina heronalleni	0.94																																	
Trochammina sp.	0.47	0.42																								0.43								
Uvigerina auberiana	3.3	2.97		1.3	0.94	0.83		0.42		0.83		0.44		0.45		0.43																		
Uvigerina canariensis													0.5																					
Uvigerina peregrina		0.85	0.88	1.3	0.94	1.25		0.85	0.39	0.41	0.44	0.44			0.93	0.43																		
Unidentified																																	11.8	
Cell 1																																	5.88	
Cell 2																																	5.88	16.7
Cell 4																																0.5		
Cell 5																								0.41										
Cell 6			0.44																												0.41			
Cell 12																0.43																2.11		
Cell 16																																2.11		
Cell 17												0.44																						
Cell 18														0.45		0.43																		
Cell 19																0.43																		
Cell 21						0.42																		0.41										
Cell 22																																		

Appendix 14 Absolute abundance counts for TC036.

Depth (cm)	Sample wt. (g)	>63 µm fraction wt. (g)	No. planktonics counted	Wt. planktonics counted (g)	No. planktonics in 1g sed.	No. benthics picked	Wt. benthics counted (g)	No. benthics in 1g sed.
1-2	1.68	0.22625	5628	0.03307	22919	255	0.03307	1038
5-6	1.93	0.32920	9114	0.04129	37650	254	0.04129	1049
10-11	2.11	0.31961	10353	0.02980	52624	272	0.02980	1383
15-16	1.91	0.45820	20748	0.04614	107875	251	0.08068	746
21-22	3.00	0.59463	15708	0.03888	80079	280	0.03888	1427
25-26	2.78	0.54799	19026	0.04281	87605	280	0.04281	1289
30-31	2.28	0.56274	20118	0.04779	103901	306	0.04779	1580
35-36	1.91	0.29681	11214	0.03429	50820	287	0.05851	762
42-43	2.10	0.40150	9576	0.03985	45943	265	0.03985	1271
45-46	3.15	0.46020	9492	0.03698	37500	321	0.03698	1268
50-51	1.96	0.39620	9072	0.04358	42080	288	0.04358	1336
55-56	2.23	0.33220	9828	0.0519	28209	289	0.05190	830
60-61	1.46	0.24920	13314	0.0502	45269	448	0.0502	1523
65-66	2.93	0.47497	8274	0.05281	25398	299	0.05281	918
70-71	2.17	0.35983	12306	0.0457	44652	359	0.04570	1303
75-76	2.29	0.39816	10878	0.04793	39461	280	0.04793	1016
80-81	1.70	0.41534	21336	0.071	73419	251	0.07100	864
85-86	2.60	0.65656	19068	0.06812	70686	229	0.11557	500
90-91	1.80	0.30053	16128	0.07247	37157	286	0.07247	659
95-96	2.48	0.56967	25830	0.08548	69412	212	0.08548	570
105-106	2.50	0.42643	14616	0.05607	44464	247	0.09414	448
110-111	1.96	0.34520	12138	0.06112	34977	200	0.08678	406
115-116	2.28	0.39067	8568	0.06338	23163	217	0.09124	408
125-126	2.56	0.35900	13230	0.06213	29862	245	0.07899	435
130-131	3.81	0.63382	9576	0.07408	21504	264	0.07408	593

TC036 Benthics (%)	1-2 cm	5-6 cm	10-11cm	15-16 cm	21-22 cm	25-26 cm	30-31 cm	35-36 cm	42-43cm	45-46cm	50-51cm	55-56 cm	60-61 cm	65-66cm	70-71 cm	75-76 cm	80-81 cm	85-86 cm	90-91 cm	95-96 cm	105-106 c	110-111 c	115-116 c	125-126 c	130-131 c
Angulogerina angulosa			0.74	0.40	0.71				0.38	0.62	0.35	0.35	0.45	0.33	0.56	0.71	1.20	0.87	1.05	0.94	0.40			1.22	0.38
Angulogerina angulosa juv.								0.70									0.80					0.50			
Astrononion antarcticus				0.40		0.36								0.33		0.36	0.40	0.44					0.46		
Astrononion echolsi																							0.46		
Bolivina decussata	0.39		0.37	0.40		0.36	0.33				0.35	0.35				0.36	0.80	0.44		0.47		0.50			
Bolivina malovensis	0.78	0.39	0.74	0.40		0.36	0.98	1.05	0.38		0.35		0.89	0.33		0.36									
Bolivina pseudopunctata						0.36			0.38		0.35	1.04	0.46		0.28	0.71	0.80	1.31	0.35			0.50	0.92		0.76
Bolivina subspinescens																				0.47					
Bolivinellina translucens	0.39	1.57	1.47	1.59	1.79	0.36	0.65	0.70				0.35		1.34	0.28	0.36	0.80	0.87	0.35		1.21	0.50	0.46	2.04	0.76
Bolivinita pseudothalmanni		0.39	1.10		1.79	0.36	0.98	0.35	0.75	1.25		0.35	0.45	1.00	1.11	0.71	2.79	0.87	1.40	1.42		0.50	0.46	1.63	2.27
Brizalina spathulata			0.37	0.40		0.36							0.45												
Bulimina aculeata			0.37										0.22				0.40								
Bulimina elongata	0.39																								
Bulimina rostrata				0.80	0.71	0.36		0.35					0.22	0.33		0.36	0.40	0.87	0.35	0.47		0.50			
Cassidulina crassa	5.49	4.33	3.31	3.19	5.36	6.07	6.21	9.76	9.43	9.35	11.81	3.46	4.02	4.69	4.46	6.07	4.78	1.75	2.45	5.19	5.26	8.50	3.23	6.12	6.44
Cassidulina laevigata					0.36	0.36	0.33				0.69		0.22			0.36	0.40				0.40		0.46		
Cassidulina laevigata var. carinata		0.39						0.35			0.35							0.44	0.35						
Cibicides lobatulus	0.39		1.10	0.40	1.43	0.71	0.33	0.35	0.75	0.62		0.35	1.12	0.33	0.84	1.07	0.40	0.87	1.40	2.36	1.62	0.50	0.46		
Cibicides wuellerstorfi																								0.41	
Cibicides spp.	0.78					0.36					0.35						1.59	0.87			0.40			0.41	
Dentalina sp.			0.37																						
Discorbinella bertheloti	0.39		0.37	0.40	0.36	0.36							0.45				0.40	1.31	0.35		0.81	0.50	0.92	0.41	
Eggerella bradyi	0.39	0.39		2.79	1.43	0.71	0.65	1.05	0.75	1.56	1.04	1.38	0.89	1.34	0.84	1.79	2.39	3.06	0.70	3.77	2.02	1.00	1.84	1.22	1.52
Ehrenbergina glabra			0.37						0.38				0.22												
Ehrenbergina trigona			0.37	1.20	1.07	0.36	0.65	0.35	0.38	0.62	0.35	1.04	0.45		0.28	0.36	0.80	0.87	0.70		0.40		0.46	0.82	
Eilohedra weddellensis	50.20	42.13	41.18	22.31	31.07	39.29	30.39	29.97	40.38	33.96	36.81	40.83	42.19	38.13	37.88	33.21	28.69	26.20	32.17	31.13	25.91	34.00	32.26	25.71	32.56
Epistominella exigua	8.63	5.91	3.68	5.18	8.21	5.71	7.52	6.97	7.55	11.21	7.64	6.23	5.58	6.69	8.64	7.14	3.19	9.61	6.99	9.91	8.10	10.50	6.45	11.02	6.44
Eponides sp.	1.57	2.36	0.74	2.79	0.71	2.14	0.33		0.38		1.74	0.69	2.23	0.67	2.51	2.14	2.39	0.87	1.75	0.47	0.81	1.00		0.82	1.89
Fissurina spp.	1.18	2.36	2.57	2.39	3.93	1.43	2.29	1.05	1.51	1.25	1.74	1.04	0.45	1.34	2.79	1.79	2.39	3.06	3.85	1.89	0.81	0.50	1.38	0.82	1.14
Fursenkoina complanata	1.18	1.97	3.31	2.79	1.43	1.79	0.98	0.35	0.75	0.93	0.69	1.38	1.79	2.34	0.84	2.86	1.20	0.87	2.45	0.94	0.40	0.50	2.30	0.41	1.89
Fursenkoina earlandi												0.35													
Fursenkoina fusiformis				0.40	0.36	0.36					0.69		0.22	0.33	0.28	0.36			1.05		0.40		0.46		
Fursenkoina texturata				0.40					0.38												0.40				
Globocassidulina subglobosa	5.49	9.45	8.09	6.77	8.21	10.00	9.80	13.24	8.68	7.79	9.38	6.92	9.82	7.69	7.24	9.64	7.57	7.42	8.74	10.38	6.88	10.00	6.45	8.98	12.88
Globotrochamminopsis sp.											1.04													0.41	0.38
Gyroidinoides spp.	5.88	8.27	10.66	14.34	8.93	6.79	12.09	5.92	6.79	7.17	7.64	10.73	11.38	10.03	7.80	7.86	10.36	10.04	8.39	8.96	9.72	8.50	7.37	6.53	7.20
Haplophragmoides sp.																									0.38
Lagena spp.	1.18	1.57	1.47	4.38	2.14	3.57	2.29	2.09	1.89	2.49	0.69	0.69	1.79	1.34	1.95	4.64	2.79	1.75	2.10	1.89	4.05	0.50	3.23	2.04	1.89
Lenticulina sp.					0.36		0.33					0.35													
Marginulina obesa													0.22												
Melonis barleeanum	0.78	0.39	1.47	2.79		1.07	3.59		0.38	0.62		1.04	0.67	0.67	1.11		0.80	2.18	0.70	0.94		0.50	1.38	0.41	
Melonis pompilioides				3.98	1.07		0.33	0.70	0.38	0.31	1.04	1.04	0.45	0.67		0.71	1.20	2.18	1.40	0.47	2.93	0.50	0.92	0.41	1.52
Melonis sp. juv.								1.39		1.87		0.69	0.45	0.33	1.67	0.71			0.70	0.94			0.46	1.63	1.14
Melonis zaandanae				0.80																					
Nodosaria sp.															0.28										
Nonionella bradii		0.39												0.33		0.36									
Nonionella iridea	7.45	9.06	4.78	4.78	7.86	9.29	9.48	13.94	12.45	13.40	9.72	7.61	5.58	10.37	7.80	5.00	8.37	6.99	8.39	7.55	18.62	12.50	16.59	22.86	9.09
Nuttalides umbonifera		0.79	1.47	1.20	1.07		0.33	0.35	0.75	0.31	1.04	0.35	0.22	0.33	0.56	0.36	1.20	1.31	1.05		1.21		0.92		0.38
Oolina spp.			0.74	0.40		0.36									0.28									0.41	
Oridorsalis juv.	1.18	1.57	0.74		0.36		0.65					0.35	0.22	0.33	0.28	0.36	0.80		0.70						
Oridorsalis tener	2.75	3.94	1.84	1.99	1.43	2.50	1.31	0.70	0.75		0.69	5.19	1.34	2.68	3.06	3.21	2.79	3.06	3.15	2.83	1.62	2.00	1.84	0.82	2.27
Oridorsalis sp.	0.78		0.74	0.80	1.79	1.43	0.65	2.09	1.13	1.87	1.39	0.35	2.23	1.67	0.84	0.71	0.80	1.31	0.35	0.47	0.40		0.46	0.82	
Patellina antarctica	0.39								0.38						0.56						0.40		0.46		
Planulina wuellerstorfi																		0.44	0.35	0.47	0.40				
Pullenia bulloides		0.39	1.10	1.99	0.71		1.31	0.35	0.38	1.25		2.08	0.67	1.00	0.84	0.36	0.80	0.87	1.40	0.94	0.40		0.92		1.14
Pullenia simplex	0.39	0.79	2.57	2.39	1.07	0.71	0.98	0.70	0.38	0.93		1.04		1.00	1.67	3.21	1.59	2.18	0.70	1.42	0.81	2.50	1.84	0.82	1.14
Pullenia subcarinata			0.37	1.99		0.71	1.63	1.39			0.69	1.04	0.45	1.00	1.39	0.71	1.99	1.75	1.40	1.42	1.21	1.50	1.38	0.82	1.52
Pyrgo murrhina	0.39				0.36	0.36						0.35		0.33			0.80	0.44			0.40				0.38
Pyrgo spp.																		0.44							
Pyrulina angusta							0.33	0.35																	
Quinqueloculina seminulum			0.37	0.40	1.07						0.35		0.22			0.36				0.47	0.81				
Quinqueloculina spp.							0.33							0.33			0.40	0.44	1.05				0.46		0.76
Quinqueloculina sp.1							0.33								0.28		0.40		0.70				0.46		
Quinqueloculina sp.2							0.33	1.05	0.38	0.31			0.22						0.70						
Quinqueloculina venusta								0.35																	
Repmanina charoides																									0.38
Sphaeroidina bulloides	0.78	0.39		1.20	1.79	0.71	0.65	0.70	0.75	0.31	0.35	1.04	0.22	0.33	0.84	0.36		0.87	0.35	0.94	0.40	0.50	1.84		0.76
Spirolocammina tenuis																				0.47					
Spirosigmoilina tenuis			0.37					0.70										0.44				0.50			
Triloculina sp.					0.71												0.40								
Trochammina sp.											0.35														
Uvigerina canariensis			0.37	0.80			0.33	0.35								0.36									
Uvigerina peregrina				0.40	0.36						0.35		0.45												
Uvigerina peregrina juv.																									0.76
Unidentified																									
Cell 18	0.39	0.79	0.37					0.35					0.45					0.44			0.40	0.50			
Cell 20							0.33																		

Appendix 16 Absolute abundance counts for TC077 and TC078.

TC077

Depth (cm)	Sample wt. (g)	>63 µm fraction wt (g)	No. planktonics counted	Wt. counted (planktonics) (g)	No. planktonics in 1g sed.	No. benthics picked	Wt. picked (benthics) (g)	No. benthics in 1g sed.
2-3	2.54	0.27116	3598	0.06723	5713	220	0.16977	138
7-8	3.37	0.27002	1932	0.05843	2649	222	0.14674	121
11-12	2.67	0.15525	931	0.05768	939	90	0.15525	34
18-19	3.29	0.10519	93	0.02965	100	1	0.02965	1

TC078

Depth (cm)	Sample wt. (g)	>63 µm fraction wt (g)	No. planktonics counted	Wt. counted (planktonics) (g)	No. planktonics in 1g sed.	No. benthics picked	Wt. picked (benthics) (g)	No. benthics in 1g sed.
1-2	1.83	0.10136	504	0.10136	275	10	0.10136	5
5-6	1.54	0.07419	277	0.07419	180	2	0.07419	1
14-15	1.96	0.13513	86	0.05745	103	8	0.05745	10
19-20	2.31	0.13689	0	0.08288	0	1	0.08288	1

Appendix 17 Relative abundance counts of benthic foraminifera for TC077 and TC078.

TC077 Benthics (%)	2 - 3 cm	7 - 8 cm	11 - 12 cm	18 - 19 cm
Ammobaculites sp.			1.11	
Angulogerina angulosa			1.11	
Bolivinita pseudothalmanni	0.91			
Bulimina rostrata	1.36	0.45		
Cassidulina crassa		0.45	1.11	
Cibicides wuellerstorfi	0.45	1.8		
Dentalina adventa		0.45		
Eggerella bradyi			1.11	
Ehrenbergina trigona		0.45		
Eilohedra weddellensis	40.9	42.8	36.7	
Epistominella exigua	5.45	14.9	10	
Eponides sp.	0.91		1.11	
Eponides tumidulus	1.82			
Fissurina spp.			1.11	
Fursenkoina complanata	1.36	0.45	1.11	
Fursenkoina texturata		0.45		
Globocassidulina subglobosa	2.73	0.9	3.33	
Globotrochamminopsis sp.	0.45	0.9		
Gyroidinoides spp.	13.2	7.21	8.89	
Lagena spp.	5	1.35	2.22	
Lenticulina sp.			1.11	
Loeblichopsis sabulosa	0.45			100
Melonis barleeanum	0.45		1.11	
Melonis pompilioides			1.11	
Melonis zaandanae			2.22	
Nonionella iridea	1.36	0.9		
Nuttalides umbonifera	6.36	5.41	5.56	
Oridorsalis tener	5.91	6.76	2.22	
Oridorsalis sp.	0.45	1.8	2.22	
Pullenia bulloides	0.45	0.9	1.11	
Pullenia simplex	1.82	0.45		
Pullenia subcarinata	2.73	1.8	2.22	
Pyrgo murrhina	0.45		1.11	
Quinqueloculina seminulum		0.45		
Quinqueloculina sp.2		0.45		
Repmanina charoides	0.45	0.45		
Sphaeroidina bulloides	0.91	1.35	2.22	
Spirolocammina tenuis	0.45			
Spiroplectammina biformis		3.6		
Trochammina glabra			4.44	
Uvigerina auberiana			1.11	
Uvigerina peregrina	2.27	0.9	3.33	
Unidentified				
Cell 18	0.45			
Cell 19		0.45		
Cell 21		1.35		
Cell 22		0.45		
Cell 26	0.45			

TC078 Benthics (%)	1 - 2 cm	5 - 6 cm	14 - 15 cm	19 - 20 cm
Eilohedra weddellensis			50	
Epistominella exigua			12.5	
Gyroidinoides sp.	10	50	12.5	
Hormosina pilulifera	10			
Lagena spp.	10			
Nuttalides umbonifera	30			
Oridorsalis sp.	10			
Pullenia subcarinata			12.5	
Pyrulina sp.			12.5	
Sphaeroidina bulloides		50		
Uvigerina peregrina	10			
Unidentified				
Cell 5	10			100
Cell 8	10			

KC097	1.5 - 3	5 - 6	7 - 8	10 - 11	12 - 13	15 - 16	17 - 18	20 - 21	22 - 23	25 - 26	27 - 28	30 - 31	32 - 33	35 - 36	37 - 38	40 - 41	42 - 43	45 - 46	47 - 48	50 - 51	55 - 56	60 - 61	65 - 66	70 - 71	90 - 91	270 - 271
Angulogerina angulosa	5	8	5	4	7	6	9	5	0	1	10	5	2	2	5	4	3	4	10	4	11	2	3	2	0	2
Astrononion spp.	1	0	0	2	2	6	1	3	5	3	1	9	2	4	3	5	0	1	4	5	2	0	2	1	0	0
Bolivina spp.	15	6	8	7	7	9	10	4	4	4	8	7	3	7	4	4	8	3	3	3	2	5	0	0	0	1
Bolivinita pseudothalmanni	11	11	6	6	9	4	8	3	2	8	5	7	5	4	3	2	2	0	4	2	2	4	3	1	0	2
Bolivinellina translucens	3	4	1	5	3	2	5	1	3	3	2	2	4	1	1	2	4	1	4	3	1	9	17	10	0	1
Cassidulina crassa	7	11	28	31	19	29	48	15	25	23	31	6	14	9	35	9	17	7	11	13	12	4	6	6	3	8
Cibicides spp.	11	7	1	1	6	3	0	1	1	4	6	9	2	5	6	4	8	1	12	7	16	7	4	8	4	2
Eggerella bradyi	1	0	6	1	7	2	2	1	2	2	4	1	6	3	5	1	6	2	4	9	4	0	2	0	0	1
Epistominella exigua	7	29	20	12	32	16	52	32	53	38	60	31	31	17	48	28	28	11	12	14	7	0	1	1	0	0
Eponides spp.	0	1	2	0	0	2	0	1	0	3	0	6	1	3	0	1	0	2	0	1	3	8	4	8	7	0
Fissurina spp.	13	6	4	15	11	7	6	11	9	6	9	6	5	5	5	6	3	7	12	5	2	3	5	4	3	5
Fursenkoina complanta	0	0	0	0	0	0	0	0	0	0	2	0	0	0	0	0	0	1	0	2	0	6	8	17	15	0
Globocassidulina subglobosa	7	9	35	14	35	15	37	25	41	17	38	21	12	9	34	18	16	19	18	15	8	12	7	10	3	2
Gyroidinoides spp.	24	17	34	24	31	26	35	22	23	22	32	20	33	22	22	27	26	17	21	24	21	15	18	15	1	4
Lagena spp.	10	10	4	7	4	3	13	7	6	3	6	7	7	4	8	9	7	14	15	15	18	6	12	10	3	2
Melonis barleeanum	2	1	0	0	0	0	0	0	0	0	0	0	1	1	2	0	1	1	1	4	3	8	12	15	5	0
Nonionella iridea	0	8	0	5	7	12	15	6	9	7	13	6	16	11	24	11	14	8	2	7	10	52	51	51	13	1
Oridorsalis tener	9	4	1	7	11	4	3	3	3	2	2	4	7	7	5	9	9	10	10	7	8	2	2	3	2	4
Pullenia spp.	1	3	3	1	1	0	1	1	3	3	2	1	2	0	2	0	1	6	7	2	2	4	4	7	1	0
Quinqueloculina spp.	2	1	0	5	1	2	4	3	2	0	3	0	3	3	2	3	1	2	4	1	3	4	3	8	0	0

KC064	Top 10	10 - 11	15 - 16	20 - 21	25 - 26	30 - 31	33 - 34	35 - 36	38 - 39	40 - 41	43 - 44	45 - 46	48 - 49	50 - 51	53 - 54	55 - 56	58 - 59	60 - 61	63 - 64	65 - 66	67 - 68	70 - 71	72 - 73	75 - 76	78 - 79	80 - 81	83 - 84	85 - 86	88 - 89	90 - 91	100 - 101
Ammobaculites agglutinans	8	2	0	0	0	1	0	0	0	0	0	0	0	0	0	0	0	0	0	0	0	0	0	0	0	0	0	0	0	0
Brizalina spathulata	0	0	0	0	0	0	0	0	0	0	0	0	0	0	7	0	0	0	0	0	0	0	0	0	0	0	0	0	0	0
Cassidulina crassa	0	0	3	0	0	0	0	0	3	2	3	2	1	3	1	0	0	0	2	3	0	0	0	10	2	0	0	1	1	1	0
Cibicides spp.	2	2	1	4	3	2	0	2	2	2	1	0	4	1	3	0	0	3	5	0	0	2	0	4	2	0	2	0	0	0	0
Ehrenbergina trigona	4	5	5	5	9	2	1	5	1	1	2	5	2	4	2	3	2	3	3	3	0	0	0	0	0	0	0	0	0	0	0
Epistominella exigua	8	21	12	9	4	8	5	4	5	1	3	5	3	2	5	2	2	0	1	0	0	0	6	13	2	3	0	2	0	1	5
Eponides spp.	2	0	3	5	4	6	5	7	6	6	5	11	9	4	8	6	3	10	4	6	1	2	3	2	2	1	1	5	0	3	0
Fissurina spp.	6	6	2	1	3	5	2	3	10	4	5	4	3	6	5	6	2	2	1	5	0	0	1	0	0	0	1	1	0	0	0
Fursenkoina complanta	1	3	2	1	3	2	1	2	4	2	0	8	2	2	0	1	1	1	0	3	1	0	1	0	1	0	0	1	3	2	3
Globocassidulina subglobosa	7	6	16	3	13	8	26	21	28	15	43	19	24	8	24	8	5	3	8	5	1	0	3	1	7	12	9	6	3	5	0
Gyroidinoides spp.	14	4	17	18	23	29	19	30	10	38	11	23	17	27	11	19	4	9	9	14	2	6	8	11	0	3	5	10	6	13	4
Lagena spp.	29	30	33	38	15	12	10	13	12	20	9	12	8	15	8	19	10	12	10	13	10	8	4	9	3	2	7	4	2	7	5
Melonis spp.	9	10	8	16	12	17	2	2	2	5	4	7	3	3	2	2	6	3	5	10	7	4	5	8	1	5	5	6	4	6	1
Nonionella iridea	0	0	0	0	0	0	0	0	1	0	0	1	0	3	0	0	0	0	0	0	0	0	1	9	0	0	0	0	0	1	0
Nuttalides umbonifera	17	5	6	15	14	17	9	11	7	5	5	6	3	2	7	4	9	13	7	3	1	4	1	5	5	5	8	4	2	0	0
Oridorsalis tener	1	3	2	9	9	8	6	6	9	8	4	13	6	9	7	13	2	17	8	12	5	1	10	4	0	6	8	13	4	7	0
Oridorsalis spp.	5	0	0	7	0	12	0	8	1	8	3	4	1	1	0	1	0	0	2	1	1	4	1	6	1	5	1	17	2	11	0
Pullenia spp.	3	9	6	13	3	7	3	5	11	10	13	8	7	8	8	9	1	8	9	12	6	0	6	9	4	4	4	7	8	10	2
Repmanina charoides	6	6	7	2	1	3	0	0	0	0	0	0	0	0	0	0	0	0	0	0	0	0	0	0	0	0	0	0	0	0	0
Sphaeroidina bulloides	2	0	0	2	1	0	9	0	12	0	8	1	2	0	9	3	8	2	4	0	5	0	2	3	4	0	4	0	3	0	3
Trochammina spp.	13	12	8	3	6	5	1	0	0	0	0	0	0	0	0	0	0	0	0	0	0	0	0	0	0	0	0	0	0	0	0
Uvigerina spp.	7	9	2	6	4	5	0	3	1	3	1	2	1	1	2	2	0	0	0	0	0	0	0	0	0	1	0	0	0	0	0

GC062	2-4	12-14	22-24	32-34	44-46	50-51	54-56	60-61
Bolivinellina translucens	2	4	4	3	4	3	5	4
Bolivinita pseudothalmanni	5	6	1	8	0	1	0	1
Cassidulina crassa	42	48	18	24	6	8	2	5
Eggerella bradyi	5	2	8	7	0	2	0	1
Epistominella exigua	47	60	24	21	0	13	1	3
Fissurina spp.	6	8	12	9	12	6	5	3
Fursenkoina complanata	0	0	1	0	1	0	9	5
Globocassidulina subglobosa	33	35	21	14	7	10	2	3
Gyroidinoides spp.	34	38	27	31	6	8	2	3
Lagena spp.	3	6	7	7	4	4	3	4
Melonis barleeanum	0	0	0	2	2	4	5	4
Nonionella iridea	5	9	5	4	15	13	16	12
Oridorsalis tener	6	2	8	6	2	5	7	4
Pullenia spp.	6	3	10	4	5	5	5	5

KC097

Sample	*N. curta*	*N. cylindrus*	*N. angulata*	*N. kerguelensis*	*T. antarctica*	*Thalassiosira* spp	*E. antarctica*	Notes:
1.5-3			A			C		
5-6			A	C		C		
10-11	R		A	C		C		
15-16			C	R		C		
20-21			C-A			C-A		
25-26			C-A			C-A		
30-31			C	C		C		
35-36	R	R	C			C	R	
40-41			C	C		C		
45-46	R		C			C	R	
50-51	R		A			R	R	
55-56	R		C			R	C	
60-61			C	C		R	C	fewer diatoms
65-66			C	C		R	C	
70-71		R	C			R	C	
75-76			C					much fewer diatoms, less well preserved
90-91	R		C	C			R	more lithogenic particles
100-101			C	C			R	
110-111		R	C	C				
130-131	R	R	C	C			R	
150-151	R		C	C			R	
170-171			C	C			R	
190-191			C	C			C	
210-211			C	C			R	
230-231			C	C			R	
250-251			R	R			R	diatoms rare
270-271			R	R			R	
280-281			R	R			R	

KC064

Sample	*N. curta*	*N. cylindrus*	*N. angulata*	*N. kerguelensis*	*T. antarctica*	*Thalassiosira* spp	*E. antarctica*	Notes:
Top 10cm			A	A		C		
10-11	R		A	A		C		
15-16			A	A		C		
20-21	R		A	A		C		
25-26			A	A		C	R	
30-31			A	A		C	R	
35-36			A	C		C		
40-41	R		A	C		C	R	
45-46	R		A	C		C	R	
50-51	R		A	C		C	R	
55-56	R		C	C	R	R	R	
60-61	R		C	C		R	R	
65-66			C	C		R	R	
70-71	R		C	C		R	R	
75-76			C	C		R	R	fewer diatoms, less well preserved
80-81			C	C		R	R	
85-86			C	C		R	R	
90-91		R	C	C		R	R	
100-101			C	C		R	R	much fewer diatoms
120-121			C	C				more lithogenic particles
140-141			C	C				
160-161			C	C			R	
200-201			C	R	R		R	
240-241			C	R	R		R	
280-281			R	R	R		R-C	
299-300								diatom fragments

A = abundant, C = common, R = rare (blank cell = not present).